



Xanthones from the Leaves of *Garcinia nigrolineata*

Mayuree Kamkaew

Master of Science Thesis in Organic Chemistry


Prince of Songkla University


2002

เลขที่	RD405	MB9	2002	e.2
Bib Key	232517			
	27 LIB. 2547			

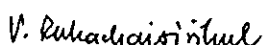
Thesis Title Xanthones from the Leaves of *Garcinia nigrolineata*
Author Miss Mayuree Kamkaew
Major Program Organic Chemistry
Academic Year 2002


Advisory Committee


.....Chairman
(Assoc.Prof.Dr.Vatcharin Rukachaisirikul)


.....Committee
(Asst.Prof.Dr.Chatchanok Karalai)

Examining Committee

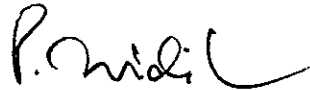
.....Chairman
(Assoc.Prof.Dr.Vatcharin Rukachaisirikul)

.....Committee
(Asst.Prof.Dr.Chatchanok Karalai)

.....Committee
(Dr.Kanda Panthong)

.....Committee
(Dr.Anuchit Plubrukarn)

The Graduate School, Prince of Songkla University, has approved this thesis as partail fulfillment of the requirment for the Master of Science degree in Organic Chemistry.

.....

(Piti Trisdikoon, Ph.D.)

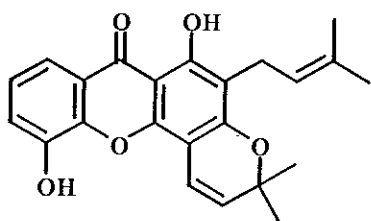
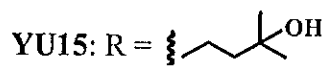
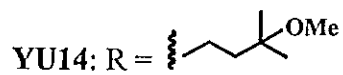
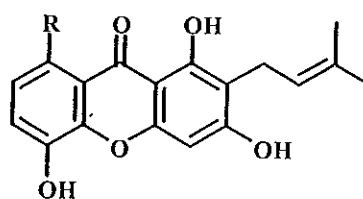
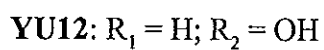
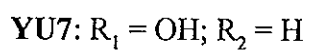
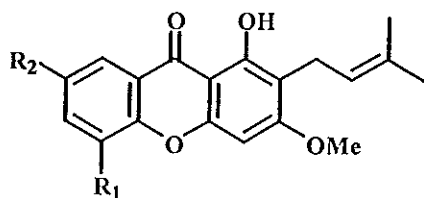
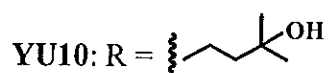
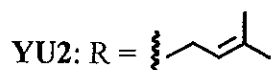
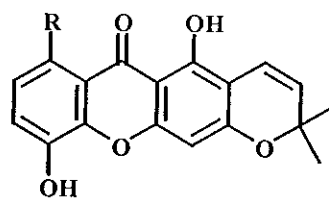
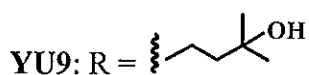
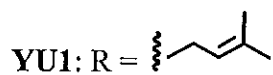
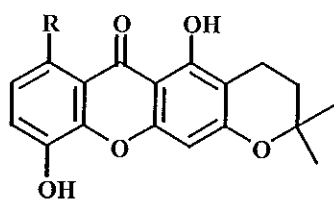
Associate Professor and Dean

Graduate School

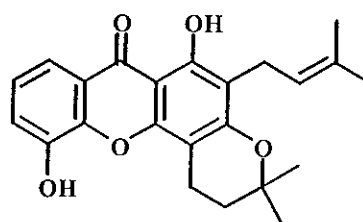
Thesis Title Xanthonenes from the Leaves of *Garcinia nigrolineata*
Author Miss Mayuree Kamkaew
Major Program Organic Chemistry
Academic Year 2002

ABSTRACT

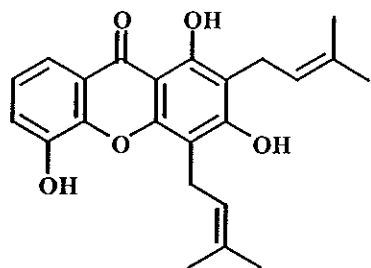
The methanolic extract from the leaves of *Garcinia nigrolineata* was purified by chromatographic techniques to afford twelve new compounds: ten xanthonenes (YU1, YU2, YU6, YU9, YU10, YU11, YU14, YU15, YU16 and YU17), one quinone derivative (YU5) and one isoflavone-like compound (YU13) together with five known compounds: ananixanthone (YU3), 8-desoxygartanin (YU4), 1,5-dihydroxy-3-methoxy-2-(3-methylbut-2-enyl)xanthone (YU7), 1,7-dihydroxy-3-methoxy-2-(3-methylbut-2-enyl)xanthone (YU12) and friedelin (YU8). All structures were determined by 1D and 2D NMR spectroscopic data. Known compounds were also identified by comparison of their spectral data with those reported in the literature.



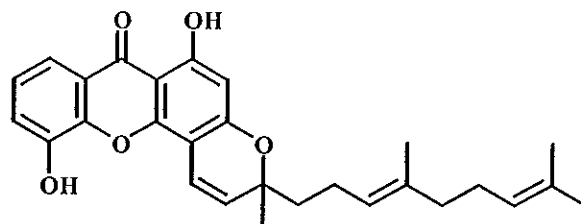
YU3



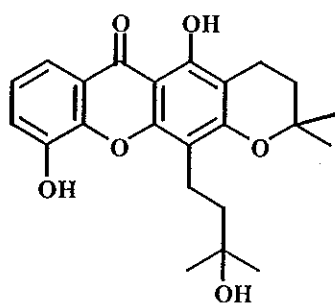
YU6



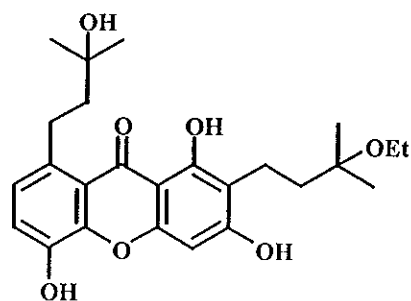
YU4



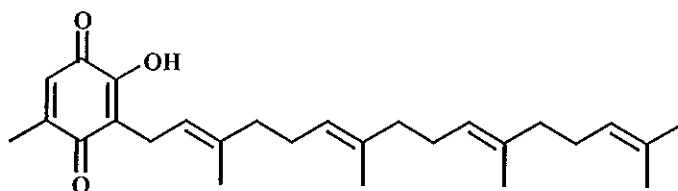
YU11



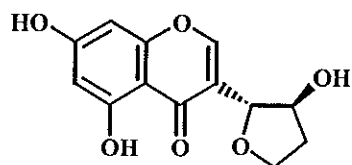
YU16



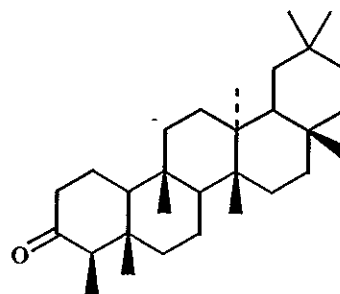
YU17



YU5



YU13

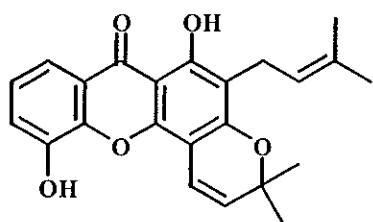
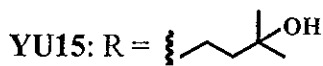
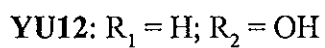
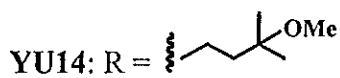
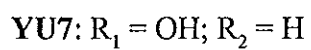
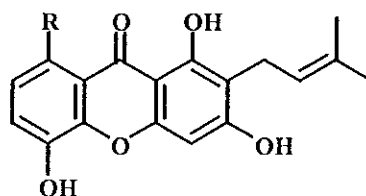
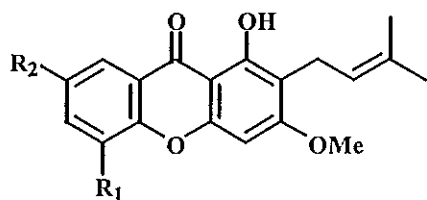
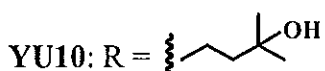
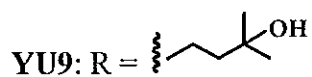
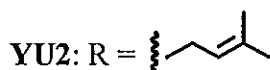
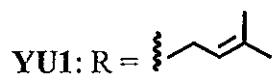
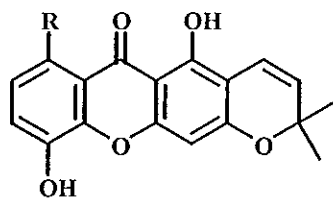
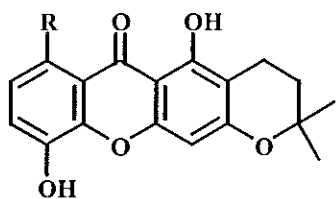


YU8

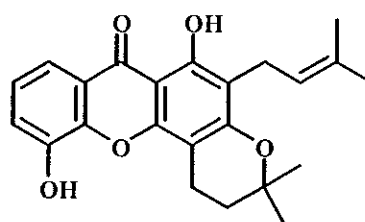
ชื่อวิทยานิพนธ์	แซนโทนจากใบชะมวง (<i>Garcinia nigrolineata</i>)
ผู้เขียน	นางสาวมยุรี คำแก้ว
สาขาวิชา	เคมีอินทรีย์
ปีการศึกษา	2545

บทคัดย่อ

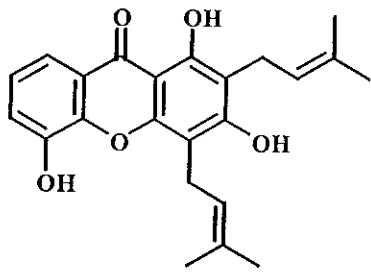
นำส่วนสกัดเมธานอลจากใบชะมวงมาทำการแยกให้บริสุทธิ์ด้วยวิธีทางโครมาโทกราฟี สามารถแยกสารใหม่ได้จำนวน 12 สาร ซึ่งเป็นสารประเภทแซนโทนจำนวน 10 สาร (YU1 YU2 YU6 YU9 YU10 YU11 YU14 YU15 YU16 และ YU17) อนุพันธ์ควิโนน 1 สาร และ สารที่คล้ายไอโซฟลาโวน 1 สาร นอกจากนี้ยังสามารถแยกสารที่มีการรายงานโครงสร้างมาแล้วจำนวน 5 สาร คือ ananixanthone (YU3), 8-desoxygartanin (YU4), 1,5-dihydroxy-3-methoxy-2-(3-methylbut-2-enyl)xanthone (YU7), 1,7-dihydroxy-3-methoxy-2-(3-methylbut-2-enyl)xanthone (YU12) และ friedelin (YU8) ยืนยันโครงสร้างของสารเหล่านี้ด้วยข้อมูล 1D และ 2D NMR สเปกโทรสโกปี สำหรับสารที่มีการรายงานโครงสร้างมาแล้วได้เปรียบเทียบข้อมูลทางสเปกโทรสโกปีกับข้อมูลที่ได้รายงานไว้แล้วด้วย



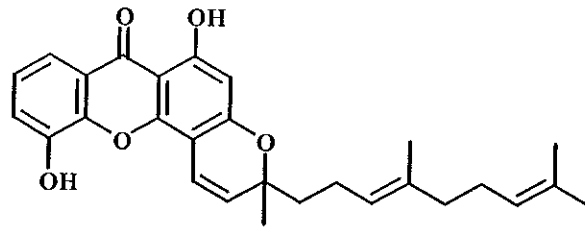
YU3



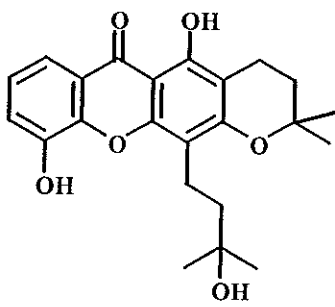
YU6



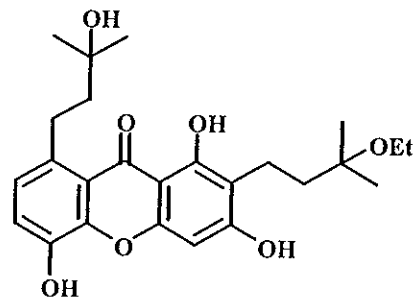
YU4



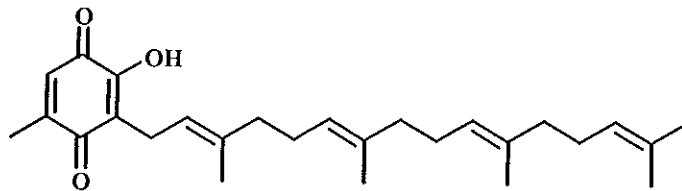
YU11



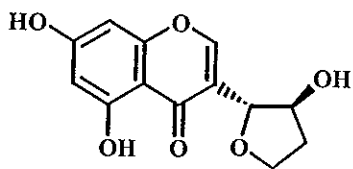
YU16



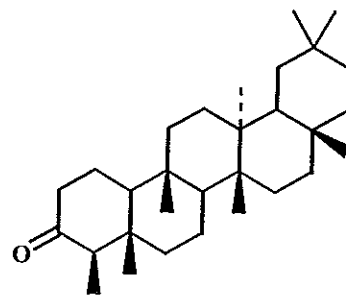
YU17



YU5



YU13



YU8

ACKNOWLEDGEMENTS

I wish to express my deepest gratitude to Associate Professor Dr. Vatcharin Rukachaisirikul, my supervisor, for her guidance and advice throughout my study. I would also like to express my sincere appreciation to her for correction and comments of this thesis.

My sincere thanks are expressed to my co-advisor, Assistant Professor Dr. Chatchanok Karalai, for his kindness and valuable advice. Special thanks are addressed to Professor Dr. Walter C. Taylor, Department of Organic Chemistry, the University of Sydney, Australia, for providing mass spectral data.

I would like to extend my appreciation to the staff of the Department of Chemistry, Faculty of Science, Prince of Songkla University, including the officers for making this thesis possible and to Ms. Dusanee Langjae, the Scientific Equipment Center, Prince of Songkla University, for recording 500 MHz NMR spectra.

This work was made possible by a scholarship from Higher Education Development Project: Postgraduate Education and Research Program in Chemistry, funded by The Royal Thai Government. Additionally, I am grateful to the Graduate School, Prince of Songkla University, for the material support.

Finally, I am totally indebted and thankful to my family, Miss Yaowapa Sukpondma, Miss Thunwadee Ritthiwigrom and friends for their encouragement and support throughout my study.

Mayuree Kamkaew

CONTENTS

	Page
Abstract (in English)	(3)
Abstract (in Thai)	(6)
Acknowledgements	(9)
Contents	(10)
List of Tables	(12)
List of Illustrations	(16)
Abbreviations and Symbols	(23)
Chapter	
1 Introduction	1
1.1 Introduction	1
1.2 Review of literatures	2
1.2.1 Chemical constituents from the genus <i>Garcinia</i>	2
1.2.2 Trioxxygenated xanthenes from the higher plants, quinones and isoflavones from plants of the genus <i>Garcinia</i>	8
1.3 The objectives	33
2 Experimental	34
2.1 Chemicals and instruments	34
2.2 Plant material	35
2.3 Extraction	35
2.4 Chemical investigation of the leaves	35
3 Results and Discussion	109

CONTENTS (Continued)

	Page
3.1 Compound YU1	109
3.2 Compound YU2	113
3.3 Compound YU9	114
3.4 Compound YU10	117
3.5 Compound YU15	120
3.6 Compound YU14	123
3.7 Compound YU17	126
3.8 Compound YU4	129
3.9 Compound YU3	132
3.10 Compound YU6	135
3.11 Compound YU11	138
3.12 Compound YU16	142
3.13 Compound YU7	144
3.14 Compound YU12	147
3.15 Compound YU5	149
3.16 Compound YU13	152
3.17 Compound YU8	154
Bibliography	280
Vitae	291

LIST OF TABLES

Table	Page
1 Compounds from plants of the genus <i>Garcinia</i>	3
2 Trioxygenated xanthones from higher plants	9
3 Quinones and isoflavones from <i>Garcinia</i> plants	19
4 Solubility of the crude extract in various solvents at room temperature	35
5 Fractions obtained from the crude extract of GNT by quick column chromatography	36
6 Subfractions obtained from GNT3 by flash column chromatography	39
7 Subfractions obtained from GNT4 by flash column chromatography	41
8 Subfractions obtained from GNT3.4 and GNT4.2 by flash column chromatography	42
9 Subfractions obtained from C2 by column chromatography over reversed-phase silica gel	43
10 Subfractions obtained from GNT5 by flash column chromatography	48
11 Subfractions obtained from GNT7 by flash column chromatography	50
12 Subfractions obtained from GNT8 by flash column chromatography	55
13 Subfractions obtained from GNT8.3 by column chromatography	56
14 Subfractions obtained from GNT9 by flash column chromatography	57
15 Subfractions obtained from GNT9.4 by column chromatography	58
16 Subfractions obtained from Y4 by column chromatography	59
17 Subfractions obtained from YC2 by flash column chromatography	60
18 Subfractions obtained from GNT10 by column chromatography	62
19 Subfractions obtained from GNT11 by flash column chromatography	63
20 Subfractions obtained from GNT11.4 by flash column chromatography	65

LIST OF TABLES (Continued)

Table	Page
21 Subfractions obtained from GNT12 by column chromatography	68
22 Subfractions obtained from GNT12.2 by column chromatography over reversed-phase silica gel	69
23 Subfractions obtained from S2.2 by flash column chromatography	70
24 Subfractions obtained from GNT13 by column chromatography	74
25 Subfractions obtained from GNT13.2 by column chromatography	75
26 Subfractions obtained from U2 by column chromatography over reversed-phase silica gel	75
27 Subfractions obtained from U2.4 by column chromatography	77
28 Subfractions obtained from U2.5 by column chromatography	78
29 Subfractions obtained from U2.6 by flash column chromatography	80
30 Subfractions obtained from U2.8 by flash column chromatography	81
31 Subfractions obtained from GNT13.3 by column chromatography over reversed-phase silica gel	83
32 Subfractions obtained from F2 by flash column chromatography	85
33 Subfractions obtained from F6 by flash column chromatography	88
34 Subfractions obtained from F6.4 by flash column chromatography	89
35 Subfractions obtained from F6.6 by column chromatography over reversed-phase silica gel	91
36 Subfractions obtained from F8 by flash column chromatography	93
37 Subfractions obtained from F8.2 by flash column chromatography	93
38 Subfractions obtained from F9 by flash column chromatography	95
39 Subfractions obtained from F9.2 by flash column chromatography	96

LIST OF TABLES (Continued)

Table	Page
40 Subfractions obtained from F9.4 by column chromatography over reversed-phase silica gel	98
41 Subfractions obtained from FE4.4 by column chromatography over sephadex LH-20	99
42 Subfractions obtained from FEA4.1 by column chromatography over sephadex LH-20	100
43 Subfractions obtained from F11 by column chromatography over reversed-phase silica gel	102
44 Subfractions obtained from F11.4 by column chromatography over reversed-phase silica gel	103
45 Subfractions obtained from FC4.2 by column chromatography over reversed-phase silica gel	104
46 Subfractions obtained from FCC2.2 by flash column chromatography	105
47 The ^1H and ^{13}C NMR data of compounds YU1 and YU2 in CDCl_3	111
48 Major HMBC correlations of compounds YU1 and YU2	112
49 The ^1H and ^{13}C NMR data of compounds YU1 and YU9 in CDCl_3	116
50 Major HMBC correlations of compounds YU1 and YU9	117
51 The ^1H and ^{13}C NMR data of compounds YU9 and YU10 in CDCl_3	119
52 Major HMBC correlations of compounds YU9 and YU10	120
53 The ^1H and ^{13}C NMR data of compounds YU10 in CDCl_3 and YU15 in Acetone- d_6	122
54 Major HMBC correlations of compounds YU10 and YU15	123

LIST OF TABLES (Continued)

Table	Page
55 The ^1H and ^{13}C NMR data of compounds YU14 in CDCl_3 and YU15 in Acetone- d_6	125
56 Major HMBC correlations of compounds YU14 and YU15	126
57 The ^1H and ^{13}C NMR data of compounds YU15 in Acetone- d_6 and YU17 in CDCl_3	128
58 Major HMBC correlations of compounds YU15 and YU17	129
59 The NMR data of compound YU4 in CDCl_3	131
60 The NMR data of compound YU3 in CDCl_3	134
61 The ^1H and ^{13}C NMR data of compounds YU3 and YU6 in CDCl_3	136
62 Major HMBC correlations of compounds YU3 and YU6	137
63 The ^1H and ^{13}C NMR data of compounds YU3 and YU11 in CDCl_3	140
64 Major HMBC correlations of compounds YU3 and YU11	141
65 The NMR data of compound YU16 in $\text{CDCl}_3/\text{CD}_3\text{OD}$	143
66 The NMR data of compound YU7 in $\text{CDCl}_3/\text{CD}_3\text{OD}$	146
67 The NMR data of compound YU12 in CDCl_3	148
68 The NMR data of compound YU5 in CDCl_3	151
69 The NMR data of compound YU13 in Acetone- d_6	154

LIST OF ILLUSTRATIONS

Figure	Page
1 <i>Garcinia nigrolineata</i>	1
2 UV (MeOH) spectrum of YU1	156
3 FT-IR (neat) spectrum of YU1	156
4 ¹ H NMR (500 MHz) (CDCl ₃) spectrum of YU1	157
5 ¹³ C NMR (125 MHz) (CDCl ₃) spectrum of YU1	158
6 DEPT spectrum of YU1	159
7 NOEDIFF spectrum of YU1 after irradiation at δ_{H} 3.98	160
8 2D HMQC spectrum of YU1	161
9 2D HMBC spectrum of YU1	162
10 Mass spectrum of YU1	163
11 UV (MeOH) spectrum of YU2	164
12 FT-IR (neat) spectrum of YU2	164
13 ¹ H NMR (500 MHz) (CDCl ₃) spectrum of YU2	165
14 ¹³ C NMR (125 MHz) (CDCl ₃) spectrum of YU2	166
15 DEPT spectrum of YU2	167
16 2D HMQC spectrum of YU2	168
17 2D HMBC spectrum of YU2	169
18 Mass spectrum of YU2	170
19 UV (MeOH) spectrum of YU9	171
20 FT-IR (neat) spectrum of YU9	171
21 ¹ H NMR (500 MHz) (CDCl ₃) spectrum of YU9	172
22 ¹³ C NMR (125 MHz) (CDCl ₃) spectrum of YU9	173
23 DEPT spectrum of YU9	174

LIST OF ILLUSTRATIONS (Continued)

Figure	Page
24 2D HMQC spectrum of YU9	175
25 2D HMBC spectrum of YU9	176
26 Mass spectrum of YU9	177
27 UV (MeOH) spectrum of YU10	178
28 FT-IR (neat) spectrum of YU10	178
29 ¹ H NMR (500 MHz) (CDCl ₃) spectrum of YU10	179
30 ¹³ C NMR (125 MHz) (CDCl ₃) spectrum of YU10	180
31 DEPT spectrum of YU10	181
32 2D HMQC spectrum of YU10	182
33 2D HMBC spectrum of YU10	183
34 Mass spectrum of YU10	184
35 UV (MeOH) spectrum of YU15	185
36 FT-IR (neat) spectrum of YU15	185
37 ¹ H NMR (500 MHz) (Acetone- <i>d</i> ₆) spectrum of YU15	186
38 ¹³ C NMR (125 MHz) (Acetone- <i>d</i> ₆) spectrum of YU15	187
39 DEPT spectrum of YU15	188
40 NOEDIFF spectrum of YU15 after irradiation at δ_{H} 5.29	189
41 2D HMQC spectrum of YU15	190
42 2D HMBC spectrum of YU15	191
43 UV (MeOH) spectrum of YU14	192
44 FT-IR (neat) spectrum of YU14	192
45 ¹ H NMR (500 MHz) (CDCl ₃) spectrum of YU14	193
46 ¹³ C NMR (125 MHz) (CDCl ₃) spectrum of YU14	194

LIST OF ILLUSTRATIONS (Continued)

Figure	Page
47 DEPT spectrum of YU14	195
48 NOEDIFF spectrum of YU14 after irradiation at δ_{H} 5.31	196
49 2D HMQC spectrum of YU14	197
50 2D HMBC spectrum of YU14	198
51 UV (MeOH) spectrum of YU17	199
52 FT-IR (neat) spectrum of YU17	199
53 ^1H NMR (500 MHz) (CDCl_3) spectrum of YU17	200
54 ^{13}C NMR (125 MHz) (CDCl_3) spectrum of YU17	201
55 DEPT spectrum of YU17	202
56 2D HMQC spectrum of YU17	203
57 2D HMBC spectrum of YU17	204
58 UV (MeOH) spectrum of YU4	205
59 FT-IR (neat) spectrum of YU4	205
60 ^1H NMR (500 MHz) (CDCl_3) spectrum of YU4	206
61 ^{13}C NMR (125 MHz) (CDCl_3) spectrum of YU4	207
62 DEPT spectrum of YU4	208
63 NOEDIFF spectrum of YU4 after irradiation at δ_{H} 1.76	209
64 NOEDIFF spectrum of YU4 after irradiation at δ_{H} 1.79	210
65 2D HMQC spectrum of YU4	211
66 2D HMBC spectrum of YU4	212
67 Mass spectrum of YU4	213
68 UV (MeOH) spectrum of YU3	214
69 FT-IR (neat) spectrum of YU3	214

LIST OF ILLUSTRATIONS (Continued)

Figure	Page
70 ^1H NMR (500 MHz) (CDCl_3) spectrum of YU3	215
71 ^{13}C NMR (125 MHz) (CDCl_3) spectrum of YU3	216
72 DEPT spectrum of YU3	217
73 NOEDIFF spectrum of YU3 after irradiation at δ_{H} 1.70	218
74 2D HMQC spectrum of YU3	219
75 2D HMBC spectrum of YU3	220
76 Mass spectrum of YU3	221
77 UV (MeOH) spectrum of YU6	222
78 FT-IR (neat) spectrum of YU6	222
79 ^1H NMR (500 MHz) (CDCl_3) spectrum of YU6	223
80 ^{13}C NMR (125 MHz) (CDCl_3) spectrum of YU6	224
81 DEPT spectrum of YU6	225
82 NOEDIFF spectrum of YU6 after irradiation at δ_{H} 5.27	226
83 2D HMQC spectrum of YU6	227
84 2D HMBC spectrum of YU6	228
85 Mass spectrum of YU6	229
86 UV (MeOH) spectrum of YU11	230
87 FT-IR (neat) spectrum of YU11	230
88 ^1H NMR (500 MHz) (CDCl_3) spectrum of YU11	231
89 ^{13}C NMR (125 MHz) (CDCl_3) spectrum of YU11	232
90 DEPT spectrum of YU11	233
91 NOEDIFF spectrum of YU11 after irradiation at δ_{H} 1.58	234
92 NOEDIFF spectrum of YU11 after irradiation at δ_{H} 1.67	235

LIST OF ILLUSTRATIONS (Continued)

Figure	Page
93 2D HMQC spectrum of YU11	236
94 2D HMBC spectrum of YU11	237
95 Mass spectrum of YU11	238
96 UV (MeOH) spectrum of YU16	239
97 FT-IR (neat) spectrum of YU16	239
98 ¹ H NMR (500 MHz) (CDCl ₃ /CD ₃ OD) spectrum of YU16	240
99 ¹³ C NMR (125 MHz) (CDCl ₃ /CD ₃ OD) spectrum of YU16	241
100 DEPT spectrum of YU16	242
101 2D HMQC spectrum of YU16	243
102 2D HMBC spectrum of YU16	244
103 UV (MeOH) spectrum of YU7	245
104 FT-IR (neat) spectrum of YU7	245
105 ¹ H NMR (500 MHz) (CDCl ₃ /CD ₃ OD) spectrum of YU7	246
106 ¹³ C NMR (125 MHz) (CDCl ₃ /CD ₃ OD) spectrum of YU7	247
107 DEPT spectrum of YU7	248
108 NOEDIFF spectrum of YU7 after irradiation at δ_{H} 5.15	249
109 2D HMQC spectrum of YU7	250
110 2D HMBC spectrum of YU7	251
111 UV (MeOH) spectrum of YU12	252
112 FT-IR (neat) spectrum of YU12	252
113 ¹ H NMR (500 MHz) (CDCl ₃) spectrum of YU12	253
114 ¹³ C NMR (125 MHz) (CDCl ₃) spectrum of YU12	254
115 DEPT spectrum of YU12	255

LIST OF ILLUSTRATIONS (Continued)

Figure	Page
116 NOEDIFF spectrum of YU12 after irradiation at δ_{H} 1.69	256
117 2D HMQC spectrum of YU12	257
118 2D HMBC spectrum of YU12	258
119 UV (MeOH) spectrum of YU5	259
120 FT-IR (neat) spectrum of YU5	259
121 ^1H NMR (500 MHz) (CDCl_3) spectrum of YU5	260
122 ^{13}C NMR (125 MHz) (CDCl_3) spectrum of YU5	261
123 DEPT spectrum of YU5	262
124 NOEDIFF spectrum of YU5 after irradiation at δ_{H} 1.71	263
125 2D HMQC spectrum of YU5	264
126 2D HMBC spectrum of YU5	265
127 Mass spectrum of YU5	266
128 UV (MeOH) spectrum of YU13	267
129 FT-IR (neat) spectrum of YU13	267
130 ^1H NMR (500 MHz) (Acetone- d_6) spectrum of YU13	268
131 ^{13}C NMR (125 MHz) (Acetone- d_6) spectrum of YU13	269
132 DEPT spectrum of YU13	270
133 NOEDIFF spectrum of YU13 after irradiation at δ_{H} 4.76	271
134 NOEDIFF spectrum of YU13 after irradiation at δ_{H} 7.95	272
135 2D HMQC spectrum of YU13	273
136 2D HMBC spectrum of YU13	274
137 Mass spectrum of YU13	275
138 FT-IR (neat) spectrum of YU8	276

LIST OF ILLUSTRATIONS (Continued)

Figure	Page
139 ^1H NMR (500 MHz) (CDCl_3) spectrum of YU8	277
140 ^{13}C NMR (125 MHz) (CDCl_3) spectrum of YU8	278
141 Mass spectrum of YU8	279

ABBREVIATIONS AND SYMBOLS

<i>s</i>	=	<i>singlet</i>
<i>d</i>	=	<i>doublet</i>
<i>t</i>	=	<i>triplet</i>
<i>m</i>	=	<i>multiplet</i>
<i>br</i>	=	<i>broad</i>
<i>brs</i>	=	<i>broad singlet</i>
<i>dd</i>	=	<i>doublet of doublet</i>
<i>qt</i>	=	<i>quartet of triplet</i>
<i>dt</i>	=	<i>doublet of triplet</i>
<i>td</i>	=	<i>triplet of doublet</i>
<i>mt</i>	=	<i>multiple of triplet</i>
<i>ddd</i>	=	<i>doublet of doublet of doublet</i>
δ	=	chemical shift relative to TMS
<i>J</i>	=	coupling constant
<i>m/z</i>	=	a value of mass divided by charge
$^{\circ}\text{C}$	=	degree celcius
R_f	=	retention factor
<i>g</i>	=	gram
<i>mg</i>	=	milligram
<i>mL</i>	=	milliliter
cm^{-1}	=	reciprocal centimeter (wavenumber)
<i>nm</i>	=	nanometer
λ_{max}	=	maximum wavelength
ν	=	absorption frequencies

ABBREVIATIONS AND SYMBOLS (Continued)

ϵ	=	Molar extinction coefficient
Hz	=	hertz
MHz	=	megahertz
ppm	=	part per million
rel. int.	=	relative intensity
$[\alpha]_D$	=	specific rotation
c	=	concentration
H-n	=	position of protons
C-n	=	position of carbons
UV	=	Ultraviolet
IR	=	Infrared
NMR	=	Nuclear Magnetic Resonance
1D NMR	=	One Dimensional Nuclear Magnetic Resonance
2D NMR	=	Two Dimensional Nuclear Magnetic Resonance
MS	=	Mass Spectroscopy
HMQC	=	Heteronuclear Multiple Quantum Coherence
HMBC	=	Heteronuclear Multiple Bond Correlation
DEPT	=	Distortionless Enhancement by Polarization transfer
NOE	=	Nuclear Overhauser Effect
NOEDIFF	=	NOE Difference Spectroscopy

ABBREVIATIONS AND SYMBOLS (Continued)

TLC	=	Thin-Layer Chromatography
TMS	=	tetramethylsilane
DMSO	=	dimethylsulphoxide
MeOH	=	methanol
CDCl ₃	=	deuteriochloroform
Acetone- <i>d</i> ₆	=	hexadeuteroacetone
CD ₃ OD	=	tetradeteromethanol
ASA	=	anisaldehyde-sulphuric acid in acetic acid solution

CHAPTER 1

INTRODUCTION

1.1 Introduction

Garcinia nigrolineata, a plant belonging to the Guttiferae family, is distributed throughout Malaya and Burma (Whitemore, 1973). The family Guttiferae contains about 40 genera and over 1000 species. Only 6 genera and 60 species are found in Thailand; i.e., *Calophyllum*, *Cratoxylum*, *Garcinia*, *Mesua*, *Kayea* and *Orchrocarpus* (Panthong, 1999). *G. nigrolineata* is a small to medium tree or very rarely a shrub. Inner bark with scant, bright yellow latex. Differing from *G. parvifolia* in the leaves usually larger, ovate-lanceolate, (9x3)-15x5-(20x6) cm, the black dots and dashes conspicuous; male flowers bigger, 10-13 mm wide, on longer stalks, 9-14 mm, with bigger petals, 8x2-8x3 mm, elongate and reflexed; female with the calyx 10-13 mm wide; the fruits umbonate, faintly ribbed, stigma 2.5-3.5 mm wide; the seeds large, with little pulp (Whitemore, 1973). In Thailand, *G. nigrolineata* is locally named “Cha-Muang (ชะมวง)” (เต็ม, 2523).



Figure 1 *Garcinia nigrolineata*

1.2 Review of literatures

1.2.1 Chemical constituents from the genus *Garcinia*

Species belonging to the genus *Garcinia* (Guttiferae) are a rich source of variety compounds, e.g., xanthenes (Nilar, 2002; Suksamrarn, 2002), benzophenones (Cuesta Rudio, 2001; Huang, 2001; Ali, 2000; Iinuma, 1996f; Spino, 1995; Fukuyama, 1993; Gustafson, 1992; Nyemba, 1990), benzophenone-xanthone dimers (Kosela, 2000, 1999; Iinuma, 1996c, d), biflavonoids (Thoison, 2000; Spino, 1995; Fukuyama, 1993; Goh, 1992; Gunatilaka, 1983), isoflavonoids (Nilar, 2002; Ilyas, 1994) and triterpenes (Nguyen, 2000; Rukachaisirikul, 2000b; Thoison, 2000). Some of these compounds showed interesting biological and pharmacological activities such as cytotoxic (Permana, 2001; Kosela, 2000; Thoison, 2000; Xu, 2000; Cao, 1998a, b), antifungal (Kosela, 2000; Peres, 2000; Gopalakrishnan, 1997), antiinflammatory (Peres, 2000; Chairungsrilerd, 1996; Ilyas, 1994; Parveen, 1991), antiprotozoal (Parveen, 1991), antibacterial (Permana, 2001; Peres, 2000; Rukachaisirikul, 2000a; Ito, 1997; Iinuma, 1996c, f; Parveen, 1991), antiimmunosuppressive (Ilyas, 1994; Parveen, 1991), antitumor (Ito, 1998), antimalarial (Kosela, 2000; Likhitwitayawuid, 1998a, b), anti-HIV (Kosela, 2000; Lin 1997; Gustafson, 1992) activities, antioxidant (Peres, 2001; Kosela, 2000; Iinuma, 1996e; Minami, 1996) and the healing of skin infections and wounds (Ilyas, 1994).

Chemical constituents isolated from *Garcinia* species up to the year 2001 have been reported (Ritthiwigrom, 2002). In the year 2002, there were only two reports on chemical constituents from *G. mangostana* and one unpublished investigation on *G. nigrolineata*, as shown in Table 1.

Table 1 Compounds from plants of the genus *Garcinia*

Scientific name	Investigated part	Compound	Structure	Bibliography
<i>G. mangostana</i>	green fruit hulls	mangostenol	4.2w	Suksumrarn, <i>et al.</i> , 2002
		mangostenone A	4.2bb	
		mangostenone B	4.2aa	
		trapezifolixanthone (toxyloxanthone A)	4.1aaaa	
		tovophyllin B	4.2z	
		α -mangostin	4.2f	
		β -mangostin	4.2g	
		garcinone B	4.2y	
		mangostinone	4.1jjj	
		mangostanol	4.2x	
		(-)-epicatechin	1a	
	heartwood	garciniafuran	4.2cc	Nilar and Harrison, 2002
		1-(OH)-8-(2-(OH)-3- methylbut-3-enyl)- 3,6,7-tri(OMe)-2-(3- methylbut-2-enyl)- xanthone	4.2c	
		mangostanin	4.2l	
		6- <i>O</i> -methyl- mangostanin	4.2m	

Table 1 (Continued)

Scientific name	Investigated part	Compound	Structure	Bibliography
<i>G. mangostana</i>	heartwood	(16 <i>E</i>)-1-(OH)-8-(3-(OH)-3-methylbut-1-enyl)-3,6,7-tri(OMe)-2-(3-methylbut-2-enyl)xanthone	4.2a	Nilar and Harrison, 2002
		1-(OH)-2-(2-(OH)-3-methylbut-3-enyl)-3,6,7-tri(OMe)-8-(3-methylbut-2-enyl)-xanthone	4.2i	
		1,6-di(OH)-2-(2-(OH)-3-methylbut-3-enyl)-3,7-dimethoxy-8-(3-methylbut-2-enyl)xanthone	4.2h	
		(16 <i>E</i>)-1,6-di(OH)-8-(3-(OH)-3-methylbut-1-enyl)-3,7-di(OMe)-2-(3-methylbut-2-enyl)xanthone	4.2b	
		β -mangostin	4.2g	

Table 1 (Continued)

Scientific name	Investigated part	Compound	Structure	Bibliography
<i>G. mangostana</i>	heartwood	1,6-di(OH)-8-(2-(OH)-3-methylbut-3-enyl)-3,7-di(OMe)-2-(3-methylbut-2-enyl)-xanthone	4.2d	Nilar and Harrison, 2002
		1,3-di(OH)-2-(2-(OH)-3-methylbut-3-enyl)-6,7-di(OMe)-8-(3-methylbut-2-enyl)-xanthone	4.2j	
		1,6-di(OH)-3,7-di(OMe)-2-(3-methylbut-2-enyl)-xanthone	4.2k	
		1,6-di(OH)-3,7-di(OMe)-2-(3-methylbut-2-enyl)-8-(2-oxo-3-methylbut-3-enyl)-xanthone	4.2e	
<i>G. nigrolineata</i>	stem bark	1,5-di(OH)-3-(OMe)-4-(2,3-di(OH)-3-methylbutyl)xanthone	4.1vv	Ritthiwigrom, 2002

Table 1 (Continued)

Scientific name	Investigated part	Compound	Structure	Bibliography
<i>G. nigrolineata</i>	stem bark	1,3,5-tri(OH)-4-(3-(OH)-3-methylbutyl)-xanthone	4.1eee	Ritthiwigrom, 2002
		1,5-di(OH)-3-methoxy-4-(3-(OH)-3-methylbutyl)xanthone	4.1uu	
		1,5,6-tri(OH)-3-(OMe)-2-(3-methylbut-2-enyl)-4-(1,1-dimethylallyl)-xanthone	4.2n	
		1,5-di(OH)-6',6'-dimethyldihydropyrano(2',3':3,2)-6'',6''-dimethylpyrano(2'',3'':6,7)xanthone	4.2s	
		1,7-di(OH)-6',6'-dimethylpyrano(2',3':6,5)xanthone	4.1ppp	
		6-deoxyjacareubin	4.1www	
		latisxanthone D	4.2p	

Table 1 (Continued)

Scientific name	Investigated part	Compound	Structure	Bibliography
<i>G. nigrolineata</i>	stem bark	1,5-di(OH)-3-(OMe)-4-(3-(OH)-3-methylbutyl)-6',6'-dimethylpyrano(2',3':6,7)-xanthone	4.2q	Ritthiwigrom, 2002
		1,7-di(OH)-6',6'-dimethylpyrano(2',3':3,4)xanthone	4.1ttt	
		6-deoxyisojacareubin	4.1uuu	
		morusignin C	4.2r	
		1,3,6,7-tetra(OH)-2,5-bis(3-methyl-2-but-enyl)xanthone	4.2o	
		1,3,7-tri(OH)-8-(3-(OH)-3-methylbutyl)-xanthone	4.1ww	
		1,3,7-tri(OH)-2-(3-(OH)-3-methylbutyl)-xanthone	4.1aaa	
		tovoxanthone	4.1nnn	
		brasilixanthone A	4.2u	
		rheediaxanthone A	4.2v	

Table 1 (Continued)

Scientific name	Investigated part	Compound	Structure	Bibliography
<i>G. nigrolineata</i>	stem bark	1,7-di(OH)-6',6'-dimethylpyrano-(2',3':3,2)-6'',6''-dimethylpyrano-(2'',3'':6,5)xanthone	4.2t	Ritthiwigrom, 2002

1.2.2 Trioxxygenated xanthenes from the higher plants, quinones and isoflavones from plants of the genus *Garcinia*

Our examination on the methanol extract from the leaves of *Garcinia nigrolineata* led to the isolation of trioxxygenated xanthenes, major chemical constituents, along with a quinone derivative and an isoflavone-like compound. There has been a review on trioxxygenated xanthenes which were isolated from six families of higher plants, including the genus *Garcinia*, fungal and lichen metabolites during 1821 to 1996 (Peres and Nagem, 1997). In April 2002, additional trioxxygenated xanthenes from only the genus *Garcinia* were summarized (Ritthiwigrom, 2002). Herein, all naturally-occurring trioxxygenated xanthenes, isolated from higher plant families since 1997, were illustrated in Table 2. Quinones and isoflavones isolated from the genus *Garcinia* were also summarized in Table 3.

Table 2 Trioxxygenated xanthenes from higher plants

Scientific name	Investigated part	Compound	Structure	Bibliography
<i>Allanblackia floribunda</i>	stem bark	allanxanthone A	4.1kkk	Nkengfack, <i>et al.</i> , 2002a
<i>Anaxagorea luzonensis</i> A. Gray	heartwood	1,3,5-tri(OH)-4-(3-(OH)-3-methylbutyl)-xanthone	4.1eee	Gonda, <i>et al.</i> , 2000
		1,3,6-tri(OH)-4-prenylxanthone	4.1fff	
		1,3,5-tri(OH)-4-prenylxanthone	4.1ggg	
		1,3,5-tri(OH)-2-prenylxanthone	4.1hhh	
		1,3,7-tri(OH)xanthone (gentisein)	4.1b	
		1,3,5-tri(OH)xanthone	4.1a	
		3,5-di(OH)-1-(OMe)-xanthone	4.1cc	
<i>Calophyllum apetalum</i>	roots	apetalinone A	4.1ffff	Iinuma, <i>et al.</i> , 1997
		apetalinone B	4.1sss	
		apetalinone C	4.1iiii	
		calozeyloxanthone	4.1rrr	
		zeyloxanthone	4.1gggg	
	stem wood	1,3,5-tri(OH)xanthone	4.1a	

Table 2 (Continued)

Scientific name	Investigated part	Compound	Structure	Bibliography
<i>Calophyllum apetalum</i>	stem bark	tomentonone apetalinone D	4.1hhhh 4.1jjjj	Iinuma, <i>et al.</i> , 1997
<i>Calophyllum brasiliensis</i>	stem bark	brasixanthone-B (cudraxanthone Q) brasixanthone-C brasixanthone-D toxyloxanthone A (trapezifolixanthone) 6-deoxyjacareubin 8-desoxygartanin	4.1xxx 4.1yyy 4.1zzz 4.1aaaa 4.1www 4.1lll	Ito, <i>et al.</i> , 2002
<i>Calophyllum caledonicum</i>	trunk bark	2-(OH)-3,4-di(OMe)- xanthone	4.1hh	Morel, <i>et al.</i> , 2000
<i>Calophyllum teysmannii</i> var. <i>inophylloide</i>	wood	1,2,8-tri(OMe)xanthone 3-(OH)-2,4-di(OMe)- xanthone 1,7-di(OH)-3-(OMe)- xanthone (gentisin)	4.1x 4.1ii 4.1f	Kijjoa, <i>et al.</i> , 2000a Kijjoa, <i>et al.</i> , 2000b
<i>Calophyllum thwaitesii</i>	root bark	11,12-dihydrothwaitesi- xanthone thwaitesixanthone 6-deoxy- γ -mangostin	4.1dddd 4.1eeee 4.1zz	Dharmaratne, <i>et al.</i> , 1996

Table 2 (Continued)

Scientific name	Investigated part	Compound	Structure	Bibliography
<i>Calophyllum thwaitesii</i>	root bark	calothwaitesixanthone demethylcalabaxanthone trapezifolixanthone (toxyloxanthone A)	4.1bbbb 4.1cccc 4.1aaaa	Dharmaratne, <i>et al.</i> , 1996
<i>Cratoxylum cochinchinense</i>	stem bark	1,3,7-tri(OH)-2,4-di(3-methylbut-2-enyl)-xanthone 2-geranyl-1,3,7-tri(OH)-4-(3-methylbut-2-enyl)-xanthone 7-geranyloxy-1,3-di(OH)xanthone	4.1ccc 4.1ddd 4.1yy	Nguyen, <i>et al.</i> , 1998
<i>Cratoxylum formosanum</i>	roots	1,4,7-tri(OH)xanthone 1,7-di(OH)-4-(OMe)-xanthone 1,7-di(OH)-8-(OMe)-xanthone	4.1h 4.1g 4.1w	Iinuma, <i>et al.</i> , 1996b
<i>Cratoxylum maingayi</i>	wood	1,7-di(OH)-4-(OMe)-xanthone 1,7-di(OH)-8-(OMe)-xanthone	4.1g 4.1w	Kijjoa, <i>et al.</i> , 1998

Table 2 (Continued)

Scientific name	Investigated part	Compound	Structure	Bibliography
<i>Cratoxylum sumatranum</i>	twigs	cratoxyarborenone F	4.1s	Seo, <i>et al.</i> , 2002
<i>Cudrania cochinchinensis</i>	roots	cudraxanthone Q (brasixanthone-B)	4.1xxx	Hou, <i>et al.</i> , 2001
<i>Garcinia mangostana</i>	green fruit	mangostinone	4.1jjj	Suksumrarn, <i>et al.</i> , 2002
	hulls	trapezifolixanthone (toxyloxanthone A)	4.1aaaa	
<i>Garcinia nigrolineata</i>	stem bark	1,5-di(OH)-3-(OMe)-4-(2,3-di(OH)-3-methylbutyl)xanthone	4.1vv	Ritthiwigrom, 2002
		1,3,5-tri(OH)-4-(3-(OH)-3-methylbutyl)xanthone	4.1eee	
		1,5-di(OH)-3-(OMe)-4-(3-(OH)-3-methylbutyl)xanthone	4.1uu	
		1,7-di(OH)-6',6'-dimethylpyrano-(2',3':6,5)xanthone	4.1ppp	
		6-deoxyjacareubin	4.1www	
		1,7-di(OH)-6',6'-dimethylpyrano-(2',3':3,4)xanthone	4.1ttt	

Table 2 (Continued)

Scientific name	Investigated part	Compound	Structure	Bibliography
<i>Garcinia nigrolineata</i>	stem bark	6-deoxyisojacareubin	4.1uuu	Ritthiwigrom, 2002
		1,3,7-tri(OH)-8-(3-(OH)-3-methylbutyl)xanthone	4.1ww	
		1,3,7-tri(OH)-2-(3-(OH)-3-methylbutyl)xanthone	4.1aaa	
		tovoxanthone	4.1nnn	
<i>Hypericum geminiflorum</i>	leaves	4-(OH)-1,2-di(OMe)-xanthone	4.1ff	Chung, <i>et al.</i> , 1999
<i>Hypericum henryi</i>	stems and leaves	kielcorin	4.1qqq	Wu, <i>et al.</i> , 1998
		1,7-di(OH)-4-(OMe)-xanthone	4.1g	
		1,2,5-tri(OH)xanthone	4.1i	
		1,5-di(OH)-4-(OMe)-xanthone	4.1m	
<i>Hypericum japonicum</i>	aerial parts	6-deoxyisojacareubin	4.1uuu	Wu, <i>et al.</i> , 1998
		1,5-di(OH)xanthone-6- <i>O</i> - β -D-glucoside	4.1u	
		1,5,6-tri(OH)xanthone	4.1t	
<i>Hypericum roeperanum</i>	roots	1,5-di(OH)-2-(OMe)-xanthone	4.1k	Rath, <i>et al.</i> , 1996
<i>Kielmeyera coriacea</i>	leaves and stems	3-(OH)-2,4-di(OMe)-xanthone	4.1ii	Cortez, <i>et al.</i> , 1998

Table 2 (Continued)

Scientific name	Investigated part	Compound	Structure	Bibliography
<i>Kielmeyera coriacea</i>	leaves and stems	4-(OH)-2,3-di(OMe)-xanthone	4.1jj	Cortez, <i>et al.</i> , 1998
		1,3,7-tri(OH)-2-(3-methylbut-2-enyl)-xanthone	4.1bbb	
		1,3,5-tri(OH)-2-(3-methylbut-2-enyl)-xanthone	4.1hhh	
		1,3,7-tri(OH)-2-(3-(OH)-3-methylbutyl)-xanthone	4.1aaa	
		kielcorin	4.1qqq	
<i>Maclura tinctoria</i>	bark	8-desoxygartanin	4.1lll	Groweiss, <i>et al.</i> , 2000
<i>Mammea acuminata</i>	stems	acuminol B	4.1mmm	Inuma, <i>et al.</i> , 1996a
<i>Mammea siamensis</i>	twigs	5-(OH)-1,2-di(OMe)-xanthone	4.1ee	Poobrasert, <i>et al.</i> , 1998
		2,5-di(OH)-1-(OMe)-xanthone	4.1dd	
		1,3,7-tri(OH)xanthone (gentisein)	4.1b	

Table 2 (Continued)

Scientific name	Investigated part	Compound	Structure	Bibliography
<i>Mammea siamensis</i>	twigs	3,5-di(OH)-1-(OMe)-xanthone	4.1cc	Poobrasert, <i>et al.</i> , 1998
		5-(OH)-1,3-di(OMe)-xanthone	4.1gg	
<i>Montrouziera sphaeroidea</i>	stem bark	4-(3',7'-dimethylocta-2',6'-dienyl)-1,3,5-tri-(OH)-9H-xanthen-9-one	4.1iii	Ito, <i>et al.</i> , 2000
<i>Poeciloneuron pauciflorum</i>	stems	1,6-di(OH)-7-(OMe)-xanthone	4.1aa	Tosa, <i>et al.</i> , 1997
		1,6-di(OH)-7-(OMe)-xanthone 6-O- β -D-glucoside	4.1bb	
		1,5-di(OH)-3-(OMe)-xanthone	4.1i	
		1,4,5-tri(OH)xanthone	4.1j	
		1,3,5-tri(OH)xanthone	4.1a	
		1,3,7-tri(OH)xanthone (gentisein)	4.1b	
<i>Polygala caudata</i>	roots	1,2,8-tri(OH)xanthone	4.1v	Li, <i>et al.</i> , 1999
		1,3-di(OH)-2-(OMe)-xanthone	4.1e	

Table 2 (Continued)

Scientific name	Investigated part	Compound	Structure	Bibliography
<i>Polygala caudata</i>	roots	1,3,7-tri(OH)xanthone (gentisein)	4.1b	Li, <i>et al.</i> , 1999
		lancerin	4.1p	
		neolancerin	4.1q	
<i>Polygala cyparissias</i>	aerial parts and roots	1,3-di(OH)-7-(OMe)-xanthone	4.1d	Pinheiro, <i>et al.</i> , 1998
<i>Polygala sibirica</i>	roots	sibricaxanthone A	4.1n	Miyase, <i>et al.</i> , 1999
		sibricaxanthone B	4.1o	
		lancerin	4.1p	
<i>Securidaca inappendiculata</i>	stems	4-(OH)-3,7-di(OMe)-xanthone	4.1kk	Yang, <i>et al.</i> , 2001
		2-(OH)-1,7-di(OMe)-xanthone	4.1y	
		1,7-di(OH)-4-(OMe)-xanthone	4.1g	
		1,3,7-tri(OH)xanthone (gentisein)	4.1b	
		2,7-di(OH)-1-(OMe)-xanthone	4.1z	
<i>Shultesia guianensis</i>	whole plant	1-(OH)-3,7-di(OMe)-xanthone	4.1c	Monte, <i>et al.</i> , 2001

Table 2 (Continued)

Scientific name	Investigated part	Compound	Structure	Bibliography	
<i>Symphonia globulifera</i>	bark	ananixanthone	4.1vvv	Bayma, <i>et al.</i> , 1998	
	root bark	globulixanthone A globulixanthone B	4.1xx 4.1ooo	Nkengfack, <i>et al.</i> , 2002b	
<i>Tovomita brevistaminea</i>	roots	trapezifolixanthone (toxyloxanthone A)	4.1aaaa	Seo, <i>et al.</i> , 1999	
<i>Tovomita krukovii</i>	stem wood- stem bark	3,5-di(OH)-4-(OMe)- xanthone	4.1ll	Zhang, <i>et al.</i> , 2002	
		1,3,5-tri(OH)-8- isoprenylxanthone	4.1mm		
		1,5,7-tri(OH)-8- isoprenylxanthone	4.1nn		
		1,3,7-tri(OH)-2- isoprenylxanthone	4.1bbb		
		1,6-di(OH)-5-(OMe)- xanthone	4.1r		
		1,3,5-tri(OH)xanthone	4.1a		
		1,3,7-tri(OH)xanthone (gentisein)	4.1b		
<i>Vismia guineensis</i>	roots	1,8-di(OH)-3-isoprenyl- oxy-6-methylxanthone	4.1oo	Bilia, <i>et al.</i> , 2000	

Table 2 (Continued)

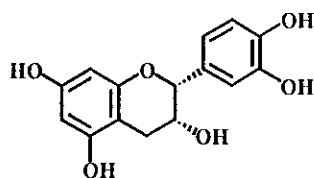
Scientific name	Investigated part	Compound	Structure	Bibliography
<i>Vismia guineensis</i>	roots	1,8-di(OH)-3-(2-(OMe)-3-methylbut-3-enyloxy)-6-methylxanthone	4.1pp	Bilia, <i>et al.</i> , 2000
		1,8-di(OH)-3-(3,7-dimethyl-7-methoxyoct-2-enyloxy)-6-methylxanthone	4.1tt	
		1,8-di(OH)-3-(<i>E</i> -3-(OH)-methylbut-2-enyloxy)-6-methylxanthone	4.1qq	
		1,8-di(OH)-3-geranyloxy-6-methylxanthone	4.1ss	
		1,8-di(OH)-3-(3-(OH)-methyl-4-(OH)but-2-enyloxy)-6-methylxanthone	4.1rr	

Table 3 Quinones and isoflavones from *Garcinia* plants

Scientific name	Investigated part	Compound	Structure	Bibliography
<i>G. atroviridis</i>	roots	atrovirinone	3a	Permana, <i>et al.</i> , 2001
<i>G. nervosa</i>	leaves	4',5,7-tri(OH)-2',3',6'-tri(OMe)isoflavone (nervosin)	2a	Ilyas, <i>et al.</i> , 1994
		3',5,7-tri(OH)-4',5',6'-tri(OMe)isoflavone (irigenin)	2b	
		4',5-di(OH)-6,7-di(OMe)isoflavone (7-methyltectorigenin)	2c	

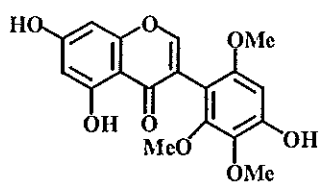
Structure of compounds isolated from higher plants

1. Flavanes

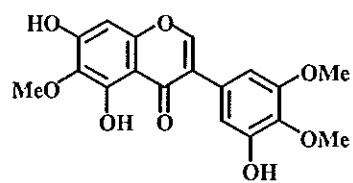


1a: (-)-epicatechin

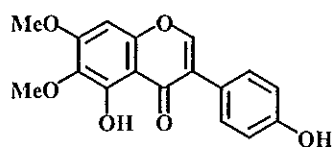
2. Isoflavones



2a: nervosin

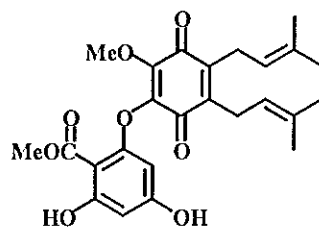


2b: irigenin



2c: 7-methyltectorigenin

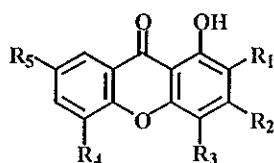
3. Quinones



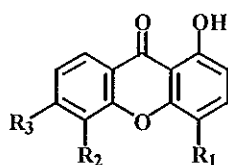
3a: atrovirone

4. Xanthenes

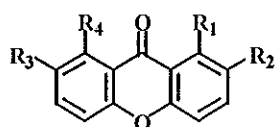
4.1 Trioxygenated xanthenes



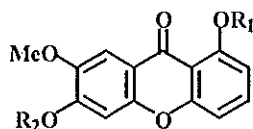
4.1a: $R_1=R_3=R_5=H$; $R_2=R_4=OH$: 1,3,5-tri(OH)xanthone
4.1b: $R_1=R_3=R_4=H$; $R_2=R_5=OH$: 1,3,7-tri(OH)xanthone
4.1c: $R_1=R_3=R_4=H$; $R_2=R_5=OMe$: 1-(OH)-3,7-di(OMe)xanthone
4.1d: $R_1=R_3=R_4=H$; $R_2=OH$; $R_5=OMe$: 1,3-di(OH)-7-(OMe)xanthone
4.1e: $R_1=OMe$; $R_2=OH$; $R_3=R_4=R_5=H$: 1,3-di(OH)-2-(OMe)xanthone
4.1f: $R_1=R_3=R_4=H$; $R_2=OMe$; $R_5=OH$: 1,7-di(OH)-3-(OMe)xanthone
4.1g: $R_1=R_2=R_4=H$; $R_3=OMe$; $R_5=OH$: 1,7-di(OH)-4-(OMe)xanthone
4.1h: $R_1=R_2=R_4=H$; $R_3=R_5=OH$: 1,4,7-tri(OH)xanthone
4.1i: $R_1=R_4=OH$; $R_2=R_3=R_5=H$: 1,2,5-tri(OH)xanthone
4.1j: $R_1=R_2=R_5=H$; $R_3=R_4=OH$: 1,4,5-tri(OH)xanthone
4.1k: $R_1=OMe$; $R_2=R_3=R_5=H$; $R_4=OH$: 1,5-di(OH)-2-(OMe)xanthone
4.1l: $R_1=R_3=R_5=H$; $R_2=OMe$; $R_4=OH$: 1,5-di(OH)-3-(OMe)xanthone
4.1m: $R_1=R_2=R_5=H$; $R_3=OMe$; $R_4=OH$: 1,5-di(OH)-4-(OMe)xanthone
4.1n: $R_1=Glc-^6$ Api; $R_2=R_5=OH$; $R_3=R_4=H$: sibiricaxanthone A
4.1o: $R_1=Glc-^2$ Api; $R_2=R_5=OH$; $R_3=R_4=H$: sibiricaxanthone B
4.1p: $R_1=R_4=H$; $R_2=R_5=OH$; $R_3=Glc$: lancerin
4.1q: $R_1=Glc$; $R_2=R_5=OH$; $R_3=R_4=H$: neolancerin



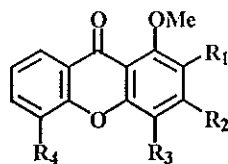
- 4.1r: $R_1=H$; $R_2=OMe$; $R_3=OH$: 1,6-di(OH)-5-(OMe)xanthone
- 4.1s: $R_1=OMe$; $R_2=H$; $R_3=OH$: cratoxyarborenone F
- 4.1t: $R_1=H$; $R_2=R_3=OH$: 1,5,6-tri(OH)xanthone
- 4.1u: $R_1=H$; $R_2=OH$; $R_3=OGlc$: 1,5-di(OH)xanthone-6-*O*- β -D-glucoside



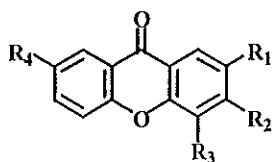
- 4.1v: $R_1=R_2=R_4=OH$; $R_3=H$: 1,2,8-tri(OH)xanthone
- 4.1w: $R_1=R_3=OH$; $R_2=H$; $R_4=OMe$: 1,7-di(OH)-8-(OMe)xanthone
- 4.1x: $R_1=R_2=R_4=OMe$; $R_3=H$: 1,2,8-tri(OMe)xanthone
- 4.1y: $R_1=R_3=OMe$; $R_2=OH$; $R_4=H$: 2-(OH)-1,7-di(OMe)xanthone
- 4.1z: $R_1=OMe$; $R_2=R_3=OH$; $R_4=H$: 2,7-di(OH)-1-(OMe)xanthone



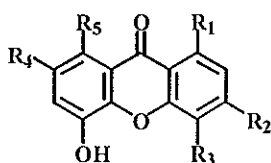
- 4.1aa: $R_1=R_2=H$: 1,6-di(OH)-7-(OMe)xanthone
- 4.1bb: $R_1=H$; $R_2=Glc$: 1,6-di(OH)-7-(OMe)xanthone-6-*O*- β -D-glucoside

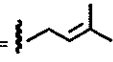
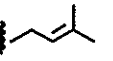


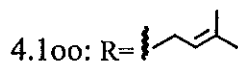
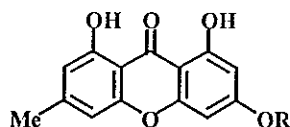
- 4.1cc: $R_1=R_3=H$; $R_2=R_4=OH$: 3,5-di(OH)-1-(OMe)xanthone
 4.1dd: $R_1=R_4=OH$; $R_2=R_3=H$: 2,5-di(OH)-1-(OMe)xanthone
 4.1ee: $R_1=OMe$; $R_2=R_3=H$; $R_4=OH$: 5-(OH)-1,2-di(OMe)xanthone
 4.1ff: $R_1=OMe$; $R_2=R_4=H$; $R_3=OH$: 4-(OH)-1,2-di(OMe)xanthone
 4.1gg: $R_1=R_3=H$; $R_2=OMe$; $R_4=OH$: 5-(OH)-1,3-di(OMe)xanthone



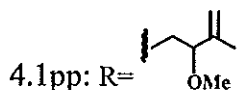
- 4.1hh: $R_1=OH$; $R_2=R_3=OMe$; $R_4=H$: 2-(OH)-3,4-di(OMe)xanthone
 4.1ii: $R_1=R_3=OMe$; $R_2=OH$; $R_4=H$: 3-(OH)-2,4-di(OMe)xanthone
 4.1jj: $R_1=R_2=OMe$; $R_3=OH$; $R_4=H$: 4-(OH)-2,3-di(OMe)xanthone
 4.1kk: $R_1=H$; $R_2=R_4=OMe$; $R_3=OH$: 4-(OH)-3,7-di(OMe)xanthone



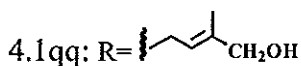
- 4.1ll: $R_1=R_4=R_5=H$; $R_2=OH$; $R_3=OMe$: 3,5-di(OH)-4-(OMe)xanthone
 4.1mm: $R_1=R_2=OH$; $R_3=R_4=H$; $R_5=$  : 1,3,5-tri(OH)-8-isoprenylxanthone
 4.1nn: $R_1=R_4=OH$; $R_2=R_3=H$; $R_5=$  : 1,5,7-tri(OH)-8-isoprenylxanthone



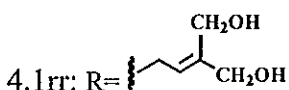
: 1,8-di(OH)-3-isoprenyloxy-6-methylxanthone



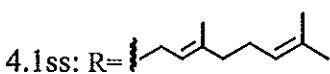
: 1,8-di(OH)-3-(2-(OMe)-3-methylbut-3-enyloxy)-6-methylxanthone



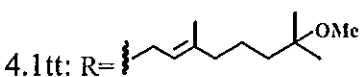
: 1,8-di(OH)-3-(*E*-3-(OH)methylbut-2-enyloxy)-6-methylxanthone



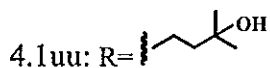
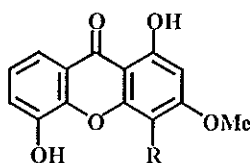
: 1,8-di(OH)-3-(3-(OH)methyl-4-(OH)but-2-enyloxy)-6-methylxanthone



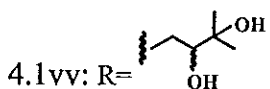
: 1,8-di(OH)-3-geranyloxy-6-methylxanthone



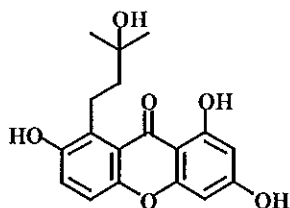
: 1,8-di(OH)-3-(3,7-dimethyl-7-methoxyoct-2-enyloxy)-6-methylxanthone



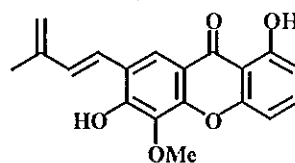
: 1,5-di(OH)-3-(OMe)-4-(3-(OH)-3-methylbutyl)-xanthone



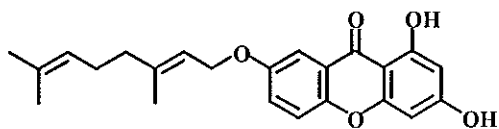
: 1,5-di(OH)-3-(OMe)-4-(2,3-di(OH)-3-methylbutyl)-xanthone



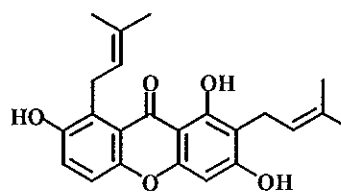
4.1ww: 1,3,7-tri(OH)-8-(3-(OH)-3-methylbutyl)-
xanthone



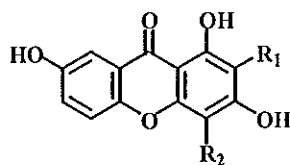
4.1xx: globulixanthone A

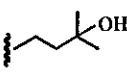


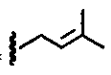
4.1yy: 7-geranyloxy-1,3-di(OH)xanthone

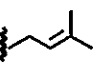


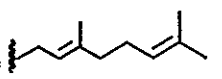
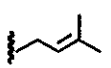
4.1zz: 6-deoxy- γ -mangostin

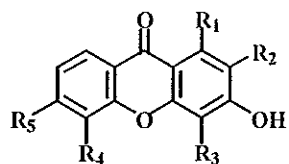


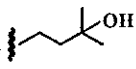
4.1aaa: $R_1 =$  ; $R_2 = H$: 1,3,7-tri(OH)-2-(3-(OH)-3-methylbutyl)xanthone

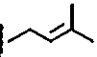
4.1bbb: $R_1 =$  ; $R_2 = H$: 1,3,7-tri(OH)-2-(3-methylbut-2-enyl)xanthone

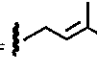
4.1ccc: $R_1 = R_2 =$  : 1,3,7-tri(OH)-2,4-di(3-methylbut-2-enyl)xanthone

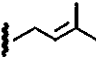
4.1ddd: $R_1 =$  ; $R_2 =$  : 2-geranyl-1,3,7-tri(OH)-4-(3-methylbut-2-enyl)-
xanthone

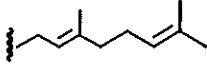


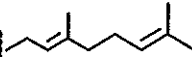
4.1eee: $R_1=R_4=OH$; $R_2=R_5=H$; $R_3=$  : 1,3,5-tri(OH)-4-(3-(OH)-3-methylbutyl)xanthone

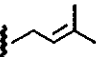

4.1fff: $R_1=R_5=OH$; $R_2=R_4=H$; $R_3=$  : 1,3,6-tri(OH)-4-prenylxanthone

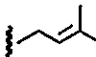
4.1ggg: $R_1=R_4=OH$; $R_2=R_5=H$; $R_3=$  : 1,3,5-tri(OH)-4-prenylxanthone

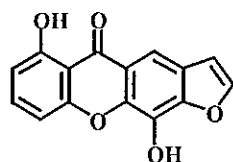
4.1hhh: $R_1=R_4=OH$; $R_2=$  ; $R_3=R_5=H$: 1,3,5-tri(OH)-2-prenylxanthone

4.1iii: $R_1=R_4=OH$; $R_2=R_5=H$; $R_3=$  : 4-(3',7'-dimethylocta-2',6'-dienyl)-1,3,5-tri(OH)-9H-xanthen-9-one

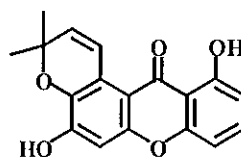
4.1jjj: $R_1=R_4=OH$; $R_2=$  ; $R_3=R_5=H$: mangostinone

4.1kkk: $R_1=R_4=OH$; $R_2=$  ; $R_5=H$; $R_3=$  : allanxanthone A

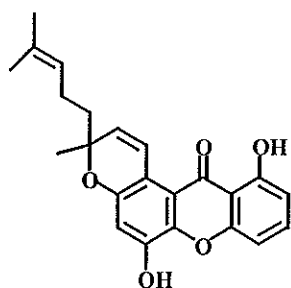
4.1lll: $R_1=R_4=OH$; $R_2=R_3=$  ; $R_5=H$: 8-desoxygartanin



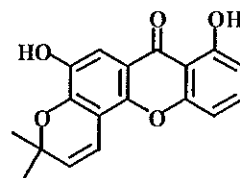
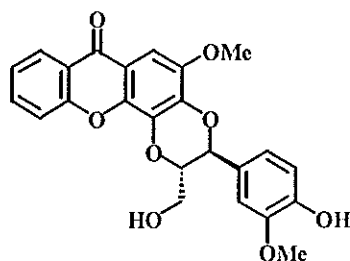
4.1mmm: acuminol B



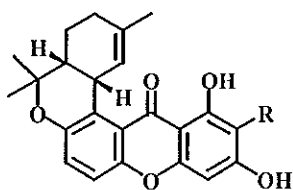
4.1nnn: tovoxanthone



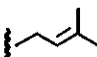
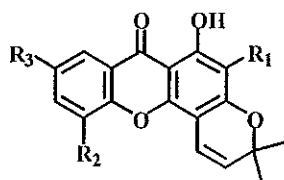
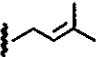
4.1ooo: globulixanthone B

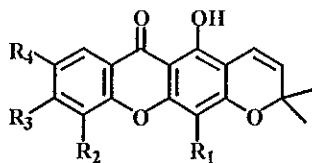
4.1ppp: 1,7-di(OH)-6,6'-dimethylpyrano-
(2',3':6,5)xanthone

4.1qqq: kielcorin

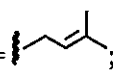


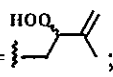
4.1rrr: R=H : calozeyloxanthone

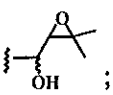
4.1sss: R= : apetalinone B4.1ttt: R₁=R₂=H; R₃=OH : 1,7-di(OH)-6,6'-dimethylpyrano(2',3':3,4)xanthone4.1uuu: R₁=R₃=H; R₂=OH : 6-deoxyisojacareubin4.1vvv: R₁=; R₂=OH; R₃=H : ananixanthone

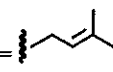


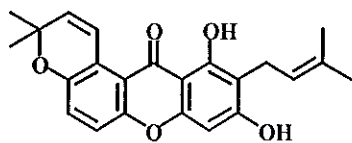
4.1www: $R_1=R_3=R_4=H$; $R_2=OH$: 6-deoxyjacareubin

4.1xxx: $R_1=$ ; $R_2=R_3=H$; $R_4=OH$: brasixanthone-B (cudraxanthone Q)

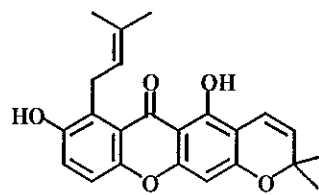
4.1yyy: $R_1=$ ; $R_2=R_3=H$; $R_4=OH$: brasixanthone-C

4.1zzz: $R_1=$ ; $R_2=R_3=H$; $R_4=OH$: brasixanthone-D

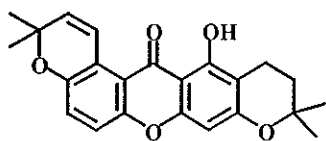
4.1aaaa: $R_1=$ ; $R_2=OH$; $R_3=R_4=H$: toxyloxanthone A (trapezifolixanthone)



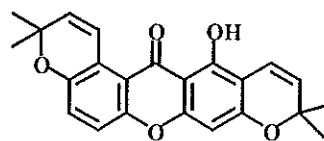
4.1bbbb: calothwaitesixanthone



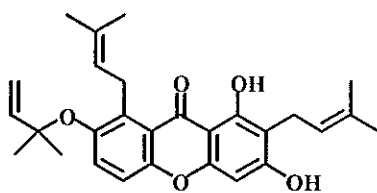
4.1cccc: demethylcalabaxanthone



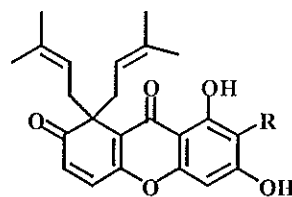
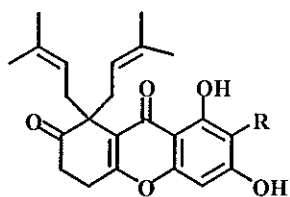
4.1dddd: 11,12-dihydrothwaitesixanthone



4.1eeee: thwaitesixanthone



4.1ffff: apetalinone A



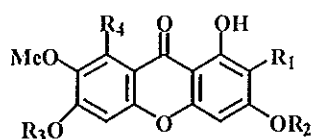
4.1gggg: R = : zeyloxanthone

4.1iiii: R = : apetalinone C

4.1hhhh: R = H : tomentonone

4.1jjjj: R = H : apetalinone D

4.2 Tetraoxygenated xanthenes

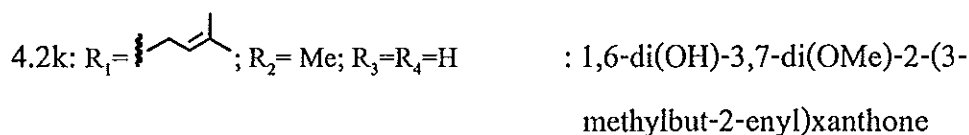
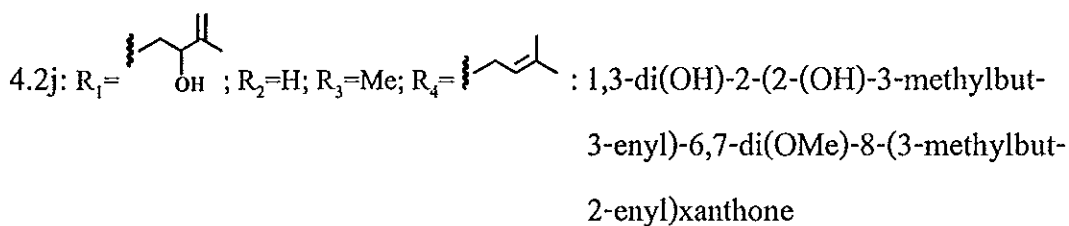
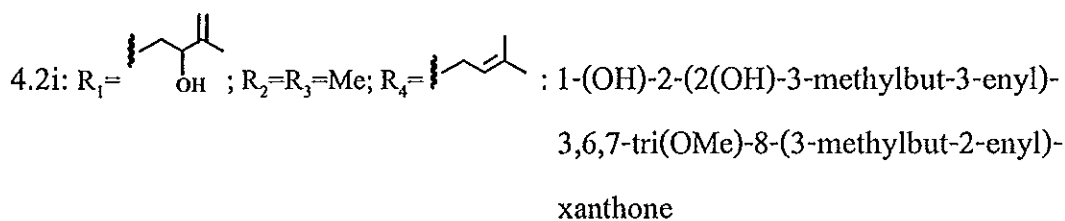
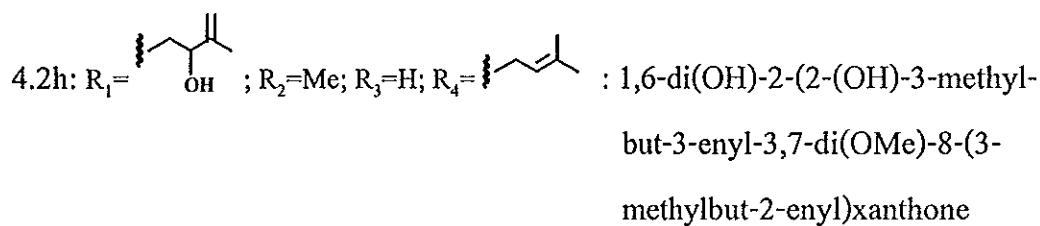
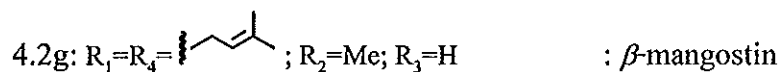
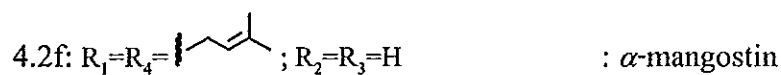
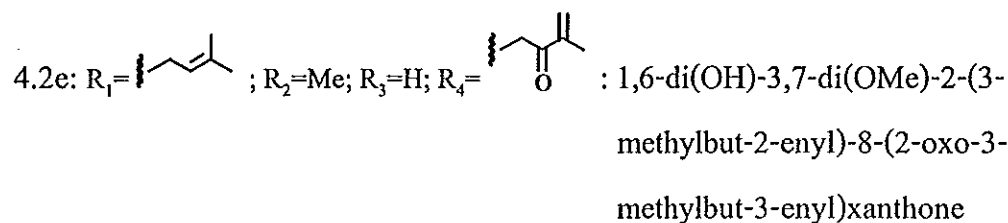
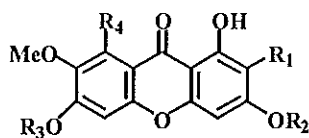


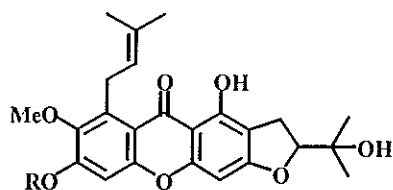
4.2a: R₁ = ; R₂=R₃=Me; R₄ = : (16*E*)-1-(OH)-8-(3-(OH)-3-methylbut-1-enyl)-3,6,7-tri-(OMe)-2-(3-methylbut-2-enyl)-xanthone

4.2b: R₁ = ; R₂=Me; R₃=H; R₄ = : (16*E*)-1,6-di(OH)-8-(3-(OH)-3-methylbut-1-enyl)-3,7-di(OMe)-2-(3-methylbut-2-enyl)xanthone

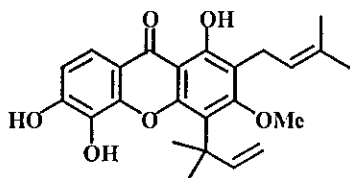
4.2c: R₁ = ; R₂=R₃=Me; R₄ = : 1-(OH)-8-(2-(OH)-3-methylbut-3-enyl)-3,6,7-tri(OMe)-2-(3-methylbut-2-enyl)xanthone

4.2d: R₁ = ; R₂=Me; R₃=H; R₄ = : 1,6-di(OH)-8-(2-(OH)-3-methylbut-3-enyl)-3,7-di(OMe)-2-(3-methylbut-2-enyl)xanthone

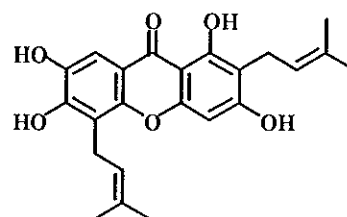




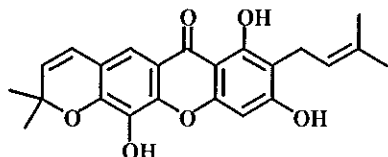
4.2l: R=H : mangostanin

4.2m: R=Me : 6-*O*-methylmangostanin

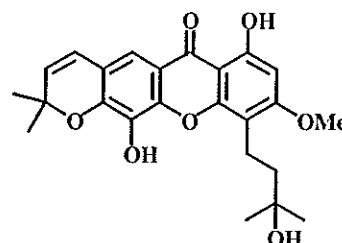
4.2n: 1,5,6-tri(OH)-3-(OMe)-2-(3-methylbut-2-enyl)-4-(1,1-dimethylallyl)xanthone



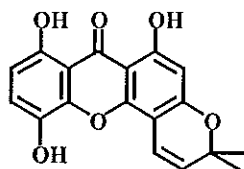
4.2o: 1,3,6,7-tetra(OH)-2,5-bis(3-methyl-2-butenyl)xanthone



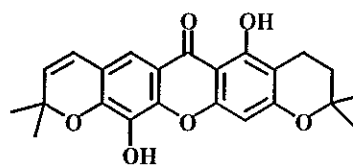
4.2p: latisxanthone D



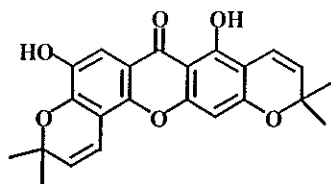
4.2q: 1,5-di(OH)-3-(OMe)-4-(3-(OH)-3-methylbutyl)-6',6'-dimethylpyrano(2',3':6,7)xanthone



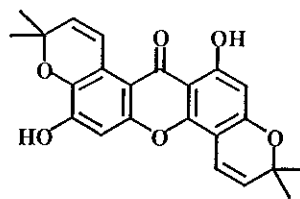
4.2r: morusignin C



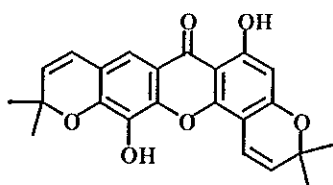
4.2s: 1,5-di(OH)-6',6'-dimethyldihydropyrano(2',3':3,2)-6'',6''-dimethylpyrano(2'',3'':6,7)xanthone



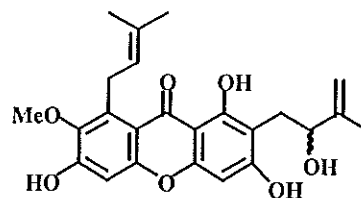
4.2t: 1,7-di(OH)-6',6'-dimethylpyrano-
(2',3':3,2)-6'',6''-dimethylpyrano-
(2'',3'':6,5)xanthone



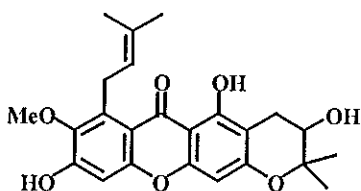
4.2u: brasilixanthone A



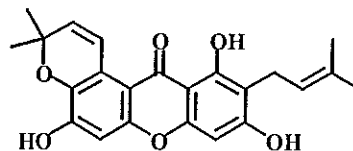
4.2v: rheediaxanthone A



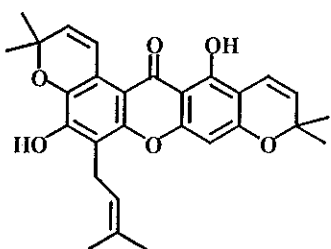
4.2w: mangostenol



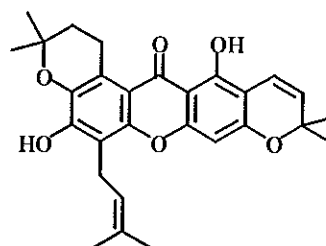
4.2x: mangostanol



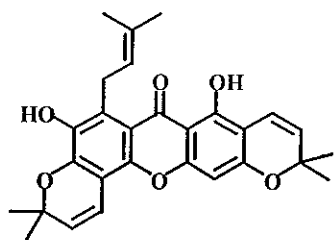
4.2y garcinone B



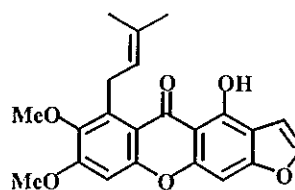
4.2z: tovophyllin B



4.2aa: mangostenone B



4.2bb: mangostenone A



4.2cc: garciniafuran

1.3 The objectives

Based on NAPRALERT database, phytochemical examination on *G. nigrolineata* has not yet been reported. However, investigation on the stem bark of *G. nigrolineata* in our laboratory led to the isolation of ten new xanthenes together with nine known xanthenes. These results prompted us to investigate chemical constituents in other parts of the plant in order to provide additional chemical information. This research involved isolation, purification and structural determination of compounds isolated from the leaves of *G. nigrolineata*, which were collected at the Ton Nga-Chang Wildlife Sanctuary.

CHAPTER 2

EXPERIMENTAL

2.1 Chemicals and instruments

Melting points were determined on an electrothermal melting point apparatus (Electrothermal 9100) and reported without correction. Infrared spectra (IR) were obtained on a FTS165 FT-IR spectrometer and Perkin Elmer Spectrum GX FT-IR system and recorded on wavenumber (cm^{-1}). ^1H and ^{13}C -Nuclear magnetic resonance spectra (^1H and ^{13}C) were recorded on a FTNMR, Varian UNITY INOVA 500 MHz using a solution in deuteriochloroform, deuteromethanol or deuterioacetone with tetramethylsilane (TMS) as an internal standard. Spectra were recorded as chemical shift parameter (δ) value in ppm down field from TMS ($\delta 0.00$). Ultraviolet spectra (UV) were measured with Specord S100 spectrophotometer (Analytik Jena AG). Principle bands (λ_{max}) were recorded as wavelengths (nm) and $\log \epsilon$ in methanol solution. Optical rotation was measured in methanol solution with sodium D line (590 nm) on an AUTOPOL^RII automatic polarimeter. Quick column chromatography, thin-layer chromatography (TLC) and precoated thin-layer chromatography were performed on silica gel 60 GF₂₅₄ (Merck) or reversed-phase C-18. Column chromatography was performed on silica gel (Merck) type (70-230 Mesh ASTM), sephadex LH-20 or reversed-phase C-18. The solvents for extraction and chromatography were distilled at their boiling point ranges prior to use except for petroleum ether (bp. 40-60^oC), diethyl ether and ethyl acetate which were analytical grade reagent.

2.2 Plant material

The leaves of *Garcinia nigrolineata* were collected at the Ton Nga-Chang Wildlife Sanctuary in Hat Yai, Songkhla, Thailand in June 2000 and identified by Ajarn Prakart Sawangchote, Department of Biology, Faculty of Science, Prince of Songkla University. A voucher specimen was deposited at the Prince of Songkla University herbarium.

2.3 Extraction

The dried and ground leaves of *Garcinia nigrolineata* (5.25 kg) were extracted with methanol (15 L) over the period of 5 days at room temperature. The methanol solution was filtered and evaporated under reduced pressure to yield a dark-green residue (300 g).

2.4 Chemical investigation of the leaves

The crude methanol extract from the leaves of *G. nigrolineata* (GNT) was tested for solubility in various solvents at room temperature. The results were show in Table 4.

Table 4 Solubility of the crude extract in various solvents at room temperature

Solvent	Solubility	Physical appearance
Petroleum ether	+	Yellow solution and dark-brown solid
CH ₂ Cl ₂	++	Brown solution and dark-brown solid

Table 4 (Continued)

Solvent	Solubility	Physical appearance
Ether	++	Pale brown solution and dark-brown solid
CHCl ₃	++	Brown solution and dark-brown solid
EtOAc	++	Green-brown solution and dark-brown solid
MeOH	+++	Brown solution
10 % NaHCO ₃	++	Red-brown solution and dark-brown solid
10 % NaOH	++	Brown solution and dark-brown solid

+ partially soluble ++ moderately soluble +++ well-soluble

From the above results, the chemical constituents of crude extract were polar and acidic as it was well soluble in methanol and aqueous basic solution.

The crude methanol extract of GNT (300 g) was separated by quick column chromatography using a stepwise gradient system (chloroform-petroleum ether and methanol-chloroform) and finally with pure methanol. Fractions with the similar chromatogram were combined and evaporated to dryness under reduced pressure to afford sixteen fractions as shown in Table 5.

Table 5 Fractions obtained from the crude extract of GNT by quick column chromatography

Fraction	Weight (g)	Physical appearance
GNT 1	0.9903	Red-brown liquid and white solid
GNT 2	0.1173	Red-brown gum

Table 5 (Continued)

Fraction	Weight (g)	Physical appearance
GNT 3	0.3131	Red-brown gum
GNT 4	0.2175	Red-brown gum
GNT 5	0.1017	Red-brown gum
GNT 6	0.0739	Red-brown gum
GNT 7	0.1096	Red-brown gum
GNT 8	0.4313	Yellow-brown gum
GNT 9	2.8792	Dark-brown gum
GNT 10	2.1161	Dark-brown gum
GNT 11	0.5689	Red-brown gum
GNT 12	4.7044	Green-brown gum
GNT 13	33.1566	Dark-brown gum
GNT 14	25.9400	Dark-brown gum
GNT 15	73.8500	Dark-brown gum
GNT 16	50.150	Dark-brown gum

Fraction GNT1 Chromatogram on normal phase TLC using 40% chloroform-petroleum ether as a mobile phase (2 runs) showed UV-active spots with the R_f values of 0.36, 0.46, 0.56, 0.86 and two other spots near baseline. It was further recrystallized in petroleum ether to give white solid (GNT1S) and the filtrate (GNT1L).

Subfraction GNT1S (YU8) was a white solid (29.6 mg), melting at 251.2-252.4 °C. Chromatogram on normal phase TLC with 50% chloroform-petroleum ether showed one purple spot with the R_f value of 0.46 after dipping the TLC plate in ASA reagent and subsequently heating.

$[\alpha]_D^{29}$	= + 17.0° (c = 9.5 x 10 ⁻² g/100 cm ³ , MeOH)
IR (KBr) $\nu_{cm^{-1}}$	2927, 2863 (C-H stretching), 1716 (C=O stretching)
¹ H NMR (CDCl ₃)(δ ppm) (500 MHz)	2.40 (<i>ddd</i> , <i>J</i> = 13.5, 5.0 and 2.0 Hz, 1H), 2.31 (<i>dd</i> , <i>J</i> = 13.5 and 7.0 Hz, 1H), 2.25 (<i>q</i> , <i>J</i> = 7.0 Hz, 1H), 1.99-1.94 (<i>m</i> , 1H), 1.75 (<i>md</i> , <i>J</i> = 12.5 Hz, 1H), 1.69 (<i>dq</i> , <i>J</i> = 12.5 and 5.0 Hz, 1H), 1.58-1.20 (<i>m</i> , 20H), 1.18 (<i>s</i> , 3H), 1.05 (<i>s</i> , 3H), 1.01 (<i>s</i> , 3H), 1.00 (<i>s</i> , 3H), 0.95 (<i>s</i> , 3H), 0.88 (<i>d</i> , <i>J</i> = 7.2 Hz, 3H), 0.87 (<i>s</i> , 3H), 0.72 (<i>s</i> , 3H)
¹³ C NMR (CDCl ₃)(δ ppm) (125 MHz)	213.29, 59.46, 58.22, 53.09, 42.77, 42.15, 41.53, 41.28, 39.69, 39.25, 38.29, 37.43, 36.00, 35.62, 35.33, 35.03, 32.76, 32.41, 32.09, 31.78, 30.50, 29.99, 28.17, 22.28, 20.26, 18.67, 18.23, 17.95, 14.65, 6.83
EIMS (<i>m/z</i>)(% rel. int.)	426 (22), 411 (15), 302 (26), 273 (47), 246 (29), 231 (40), 218 (48), 205 (56), 193 (30), 191 (50), 179 (54), 163 (58), 161 (49), 149 (50), 137 (62), 135 (55), 124 (60), 123 (75), 121 (62), 119 (47), 111 (60), 109 (73), 108 (46), 107 (64), 97 (60), 96 (73), 95 (76), 93 (64), 91 (56), 83 (72), 82 (71), 81 (80), 79 (64), 69 (91), 68 (64), 67 (77), 57 (69), 55 (100), 53 (66), 43 (89), 41 (88), 39 (47), 29 (77), 28 (64)

Subfraction GNT1L was an orange-yellow gum (960.7 mg). Chromatogram on normal phase TLC using 40% chloroform-petroleum ether as a mobile phase (2 runs) showed four UV-active spots with the *R_f* values of 0.36, 0.46, 0.56 and 0.86 and two other spots near baseline. No further purification was carried out.

Fraction GNT2 Chromatogram on normal phase TLC using 40% chloroform-petroleum ether as a mobile phase (2 runs) showed four major UV-active spots with the R_f values of 0.27, 0.38, 0.43 and 0.51. No further purification was carried out.

Fraction GNT3 Chromatogram on normal phase TLC using 40% chloroform-petroleum ether as a mobile phase (2 runs) showed five major UV-active spots with the R_f values of 0.11, 0.15, 0.19, 0.25 and 0.34. Further separation by flash column chromatography over silica gel was performed. Elution was conducted with a stepwise gradient system (chloroform-petroleum ether and ethyl acetate-chloroform) and finally with pure ethyl acetate. Fractions with the similar chromatogram were combined and evaporated to dryness under reduced pressure to afford eight subfractions, as shown in Table 6.

Table 6 Subfractions obtained from GNT3 by flash column chromatography

Subfraction	Weight (g)	Physical appearance
GNT 3.1	0.0379	Yellow gum
GNT 3.2	0.0355	Orange gum and white solid
GNT 3.3	0.0871	Orange gum
GNT 3.4	0.1096	Orange-yellow gum
GNT 3.5	0.0293	Orange-yellow gum
GNT 3.6	0.0435	Orange-brown gum
GNT 3.7	0.0148	Yellow gum
GNT 3.8	0.0437	Yellow-brown gum

Subfraction GNT3.1 Chromatogram on normal phase TLC with 50% chloroform-petroleum ether (2 runs) showed no major UV-active spots. Therefore, it was not further investigated.

Subfraction GNT3.2 Chromatogram on normal phase TLC with 50% chloroform-petroleum ether (2 runs) showed one major and one pale UV-active spots with the R_f values of 0.57 and 0.11, respectively. Further chromatography on precoated TLC with 50% chloroform-petroleum ether as a mobile phase (2 runs) afforded two bands in low quantity. Further purification was not then attempted.

Subfraction GNT3.3 Chromatogram on normal phase TLC with 50% chloroform-petroleum ether (2 runs) showed many UV-active spots. Therefore, it was not further investigated.

Subfraction GNT3.4 Chromatogram on normal phase TLC with 50% chloroform-petroleum ether (2 runs) showed two overlapping spot with the R_f value of 0.46 and two pale UV-active spots with the R_f values of 0.23 and 0.33. It was then combined with **subfraction GNT4.2** as they showed similar chromatograms.

Subfraction GNT3.5 Chromatogram on normal phase TLC with 50% chloroform-petroleum ether (2 runs) showed two major UV-active spots with the R_f values of 0.21 and 0.45 and one pale UV-active spot with the R_f value of 0.33. It was not further investigated.

Subfraction GNT3.6 Chromatogram on normal phase TLC with 80% chloroform-petroleum ether (2 runs) showed three major UV-active spots with the R_f values of 0.28, 0.33 and 0.58. Further separation on precoated TLC with 80% chloroform-petroleum ether (3 runs) afforded a yellow gum in 4.1 mg. Chromatogram on normal phase TLC with 80% chloroform-petroleum ether (2 runs) showed one major UV-active spot with the R_f value of 0.37 and one pale UV-active spot with the R_f value of 0.32. It was then combined with **band GNT4.4A** as they showed similar major spot.

Subfraction GNT3.7 Chromatogram on normal phase TLC with 80% chloroform-petroleum ether (2 runs) showed one major UV-active spot with the R_f value of 0.11 together with many unseparable spots. Therefore, further purification was not performed.

Subfraction GNT3.8 Chromatogram on normal phase TLC with 80% chloroform-petroleum ether (2 runs) showed none of major UV-active spots. Therefore, it was not further investigated.

Fraction GNT4 Chromatogram on normal phase TLC using 40% chloroform-petroleum ether as a mobile phase (2 runs) showed four major UV-active spots with the R_f values of 0.15, 0.20, 0.28 and 0.38. Further separation by flash column chromatography over silica gel. Elution was conducted with a stepwise gradient system (chloroform-petroleum ether and ethyl acetate-chloroform) and finally with pure ethyl acetate. All fractions were examined by TLC, combined on the basis of their chromatogram and then evaporated to dryness under reduced pressure to afford five subfractions, as shown in Table 7.

Table 7 Subfractions obtained from GNT4 by flash column chromatography

Subfraction	Weight (g)	Physical appearance
GNT4.1	0.0391	Orange gum
GNT4.2	0.0646	Orange gum
GNT4.3	0.0878	Orange-brown gum
GNT4.4	0.0591	Orange-yellow gum
GNT4.5	0.0592	Orange-yellow gum

Subfraction GNT4.1 Chromatogram on normal phase TLC with 50% chloroform-petroleum ether (2 runs) showed many UV-active spots. Therefore, it was not further investigated.

Subfraction GNT4.2 Chromatogram on normal phase TLC with 50% chloroform-petroleum ether (2 runs) showed one major UV-active spot with the R_f value of 0.52 and two pale UV-active spots with the R_f values of 0.24 and 0.40. It was further combined with **subfraction GNT3.4** and then separated by flash column chromatography over silica gel. Elution was conducted with pure petroleum ether, a stepwise gradient system (chloroform-petroleum ether and ethyl acetate-chloroform) and finally with pure ethyl acetate. Fractions with the similar chromatogram were combined and evaporated to dryness under reduced pressure to afford five subfractions, as shown in Table 8.

Table 8 Subfractions obtained from **GNT3.4** and **GNT4.2** by flash column chromatography

Subfraction	Weight (g)	Physical appearance
C1	0.0241	Orange-yellow gum
C2	0.0800	Orange-yellow gum
C3	0.0048	Orange-yellow gum
C4	0.0331	Yellow-brown gum
C5	0.0085	Yellow-brown gum

Subfraction C1 contained many spots, none of which were major components. Therefore, it was not further investigated.

Subfraction C2 Chromatogram on normal phase TLC using 60% chloroform-petroleum ether (2 runs) showed three major UV-active spots with the R_f values of 0.30, 0.41 and 0.48. Further separation by flash column chromatography over reversed-phase silica gel was performed. Elution was conducted initially with 90% methanol in water, followed by decreasing amount of water and finally with pure methanol. Fractions with the similar chromatogram were combined and evaporated to dryness under reduced pressure to afford three subfractions, as shown in Table 9.

Table 9 Subfractions obtained from C2 by column chromatography over reversed-phase silica gel

Subfraction	Weight (g)	Physical appearance
CC1	0.0064	Orange-yellow gum
CC2	0.0697	Orange-yellow gum
CC3	0.0014	Orange-yellow gum

Subfraction CC1 contained many UV-active spots. Therefore, it was not further investigated.

Subfraction CC2 Chromatogram on normal phase TLC with 60% chloroform-petroleum ether (2 runs) showed overlapping UV-active spots with the R_f value of 0.43 and two pale UV-active spots with the R_f values of 0.17 and 0.28. Further separation on precoated TLC with 60% chloroform-petroleum ether as a mobile phase afforded YU5 as an orange-red gum (5.0 mg). Its chromatogram showed one UV-active spot on normal phase TLC with 60% chloroform-petroleum ether (2 runs) with the R_f value of 0.59.

UV (MeOH) λ_{\max} nm (log \mathcal{E})	264 (3.87)
FT-IR (neat) $\nu_{\text{cm}^{-1}}$	3380 (O-H stretching) 2915 (C-H stretching) 1642, 1616 (C=O stretching)
^1H NMR (CDCl_3)(δ ppm) (500 MHz)	6.94 (<i>brs</i> , 1H), 6.59 (<i>q</i> , $J = 1.5$ Hz, 1H), 5.17 (<i>mt</i> , $J = 7.5$ Hz, 1H), 5.14 (<i>mt</i> , $J = 7.5$ Hz, 2H), 5.11 (<i>mt</i> , $J = 7.5$ Hz, 1H), 3.19 (<i>d</i> , $J = 7.5$ Hz, 2H), 2.12 (<i>d</i> , $J = 1.5$ Hz, 3H), 2.09 (<i>mt</i> , $J = 7.5$ Hz, 6H), 2.00 (<i>mt</i> , $J = 7.5$ Hz, 6H), 1.78 (<i>s</i> , 3H), 1.71 (<i>d</i> , $J = 1$ Hz, 3H), 1.63 (<i>s</i> , 3H), 1.62 (<i>s</i> , 3H), 1.61 (<i>s</i> , 3H)
^{13}C NMR (CDCl_3)(δ ppm) (125 MHz)	187.41, 183.44, 150.63, 149.07, 137.19, 135.06, 134.92, 131.28, 128.40, 124.43, 124.25, 124.07, 120.58, 119.58, 39.74, 39.72, 26.79, 26.67, 26.51, 25.72, 22.13, 17.71, 16.59, 16.20, 16.04, 16.01
DEPT 135 ⁰	CH ₃ : 25.72, 17.71, 16.59, 16.20, 16.04, 16.01 CH ₂ : 39.74, 39.72, 26.79, 26.67, 26.51, 22.13 CH : 128.40, 124.43, 124.25, 124.07, 119.58
FABMS (m/z)(% rel. int.)	411 (75), 259 (26), 221 (26), 207 (27), 205 (41), 193 (50), 191 (36), 177 (35), 153 (100), 137 (84), 127 (100), 109 (93), 97 (100), 85 (100)

Subfraction CC3 showed three major UV-active spots on normal phase TLC with 60% chloroform-petroleum ether with the R_f values of 0.26, 0.33 and 0.37. It was not further investigated because it was obtained in low quantity.

Subfraction C3 Chromatogram on normal phase TLC with 60% chloroform-petroleum ether (2 runs) showed overlapping UV-active spot with the R_f value of 0.41

and two pale UV-active spots with the R_f values of 0.08 and 0.31 while chromatogram on reversed-phase TLC with 90% methanol-water (2 runs) showed overlapping UV-active spot with the R_f value of 0.59 and three pale UV-active spots with the R_f values of 0.38, 0.46 and 0.75. It was not further investigated because it was obtained in low quantity.

Subfraction C4 Chromatogram on normal phase TLC with 60% chloroform-petroleum ether (2 runs) showed one major UV-active spot with the R_f value of 0.41 and two pale UV-active spots with the R_f values of 0.08 and 0.31 while chromatogram on reversed-phase TLC with 90% methanol-water (2 runs) showed one major UV-active spot with the R_f value of 0.59 and one pale UV-active spot with the R_f value of 0.46. It was further separated by column chromatography over reversed-phase silica gel, eluting with 90% methanol-water. Fractions with the similar chromatogram were combined and evaporated to dryness under reduced pressure to afford four subfractions. Each fraction was obtained in low quantity. Purification was not further performed.

Subfraction C5 Chromatogram on normal phase TLC with 80% chloroform-petroleum ether (2 runs) showed none of major UV-active spots. Therefore, it was not further investigated.

Subfraction GNT4.3 Chromatogram on normal phase TLC with 50% chloroform-petroleum ether (2 runs) showed many UV-active and unseparable spots. Therefore, it was not further investigated.

Subfraction GNT4.4 Chromatogram on normal phase TLC with 80% chloroform-petroleum ether (2 runs) showed two major UV-active spots with the R_f values of 0.28 and 0.32. Further separation on precoated TLC with 80% chloroform-petroleum ether (3 runs) afforded two bands.

Band GNT4.4A was a yellow gum (6.8 mg). It contained the same major spot as **Band GNT3.6A**. Therefore, they were combined and purified on precoated TLC with 80% chloroform-petroleum ether (3 runs) to afford **YU2** as a yellow gum (7.2 mg). Chromatogram on normal phase TLC with 80% chloroform-petroleum ether (2 runs) showed one UV-active spot with the R_f value of 0.36.

UV (MeOH) λ_{\max} nm (log ϵ)	295 (3.77), 322 (3.58), 380 (3.02)
FT-IR (neat) $\nu_{\text{cm}^{-1}}$	3394 (O-H stretching) 2981, 2929 (C-H stretching) 1650 (C=O stretching)
^1H NMR (CDCl_3)(δ ppm) (500 MHz)	13.56 (<i>s</i> , 1H), 7.20 (<i>d</i> , $J = 8.0$ Hz, 1H), 7.04 (<i>d</i> , $J = 8.0$ Hz, 1H), 6.75 (<i>d</i> , $J = 10.0$ Hz, 1H), 6.31 (<i>s</i> , 1H), 5.69 (<i>brs</i> , 1H), 5.60 (<i>d</i> , $J = 10.0$ Hz, 1H), 5.36 (<i>mt</i> , $J = 7.0$ Hz, 1H), 3.98 (<i>d</i> , $J = 7.0$ Hz, 2H), 1.74 (<i>s</i> , 6H), 1.48 (<i>s</i> , 6H)
^{13}C NMR (CDCl_3)(δ ppm) (125 MHz)	182.88, 160.38, 158.18, 155.50, 145.14, 142.46, 135.49, 132.70, 127.45, 125.18, 122.92, 119.42, 118.40, 115.50, 104.87, 104.17, 94.17, 78.26, 33.01, 28.35, 25.87, 17.98
DEPT 135 $^\circ$	CH ₃ : 28.35, 25.87, 17.98 CH ₂ : 33.01 CH : 127.45, 125.18, 122.92, 119.42, 115.50, 94.17
EIMS (m/z)(% rel. int.)	378 (38), 363 (79), 335 (36), 307 (15), 149 (26), 111 (25), 97 (44), 83 (54), 69 (70)

Band GNT4.4B (YU1) was a pale yellow gum (3.0 mg). Chromatogram on normal phase TLC with 80% chloroform-petroleum ether (2 runs) showed one UV-active spot with the R_f value of 0.29.

UV (MeOH) λ_{\max} nm (log \mathcal{E})	321 (3.93), 376 (3.31)
FT-IR (neat) $\nu_{\text{cm}^{-1}}$	3365 (O-H stretching) 2918, 2850 (C-H stretching) 1646 (C=O stretching)
^1H NMR (CDCl_3) (δ ppm) (500 MHz)	13.60 (<i>s</i> , 1H), 7.19 (<i>d</i> , $J = 8.0$ Hz, 1H), 7.02 (<i>d</i> , $J = 8.0$ Hz, 1H), 6.30 (<i>s</i> , 1H), 5.87 (<i>brs</i> , 1H), 5.36 (<i>mt</i> , $J = 7.5$ Hz, 1H), 3.98 (<i>d</i> , $J = 7.5$ Hz, 2H), 2.73 (<i>t</i> , $J = 7.0$ Hz, 2H), 1.85 (<i>t</i> , $J = 7.0$ Hz, 2H), 1.74 (<i>s</i> , 6H), 1.38 (<i>s</i> , 6H)
^{13}C NMR (CDCl_3) (δ ppm) (125 MHz)	182.93, 161.27, 161.03, 154.02, 145.28, 142.53, 135.40, 132.57, 124.85, 123.09, 119.20, 118.43, 104.35, 103.31, 94.10, 76.35, 33.06, 31.78, 26.75, 25.90, 17.99, 16.08
DEPT 135 $^\circ$	CH ₃ : 26.75, 25.90, 17.99 CH ₂ : 33.06, 31.18, 16.08 CH : 124.85, 123.09, 119.20, 94.10
EIMS (m/z) (% rel. int.)	380 (22), 338 (19), 336 (100), 281 (16), 281 (72), 269 (20)

Subfraction GNT4.5 Chromatogram on normal phase TLC with 80% chloroform-petroleum ether showed many UV-active spots. Therefore, it was not further investigated.

Fraction GNT5 Chromatogram on normal phase TLC with 80% chloroform-petroleum ether showed four major UV-active spots with the R_f values of 0.25, 0.34, 0.52 and 0.62. Further separation by flash column chromatography over silica gel was carried out. Elution was conducted with a stepwise gradient system (chloroform-petroleum ether and ethyl acetate-chloroform) and finally with pure ethyl acetate. Fractions with the similar chromatogram were combined and evaporated to dryness under reduced pressure to afford four subfractions, as shown in Table 10.

Table 10 Subfractions obtained from GNT5 by flash column chromatography

Subfraction	Weight (g)	Physical appearance
GNT5.1	0.0295	Yellow gum
GNT5.2	0.0354	Orange-yellow gum
GNT5.3	0.0301	Yellow gum
GNT5.4	0.0103	Yellow-brown gum

Subfraction GNT5.1 Chromatogram on normal phase TLC with 60% chloroform-petroleum ether showed many UV-active spots, none of which were major components. Therefore, it was not further investigated.

Subfraction GNT5.2 Chromatogram on normal phase TLC with 80% chloroform-petroleum ether (2 runs) showed three major UV-active spots with the R_f values of 0.40, 0.58 and 0.65. It was further rechromatographed on precoated TLC with 60% chloroform-petroleum ether (3 runs) to give three bands.

Band MP1 was a pale yellow gum (3.0 mg). Chromatogram on normal phase TLC with pure petroleum ether showed one major UV-active spot with the R_f value of 0.74. It was not further investigated.

Band MP2 was an orange-yellow gum (3.4 mg). Chromatogram on normal phase TLC with 70% chloroform-petroleum ether showed one major UV-active spot with the R_f value of 0.43 and two pale UV-active spots with the R_f values of 0.38 and 0.46. It was then combined with **subfraction GNT7.2**.

Band MP3 was an orange gum (5.5 mg). Chromatogram on normal phase TLC with 70% chloroform-petroleum ether showed many pale UV-active spots. It was not further investigated because it was obtained in low quantity.

Subfraction GNT5.3 Chromatogram on normal phase TLC with 40% chloroform-petroleum ether (2 runs) showed four major UV-active spots with the R_f values of 0.31, 0.35, 0.42 and 0.49 and one pale UV-active spot with the R_f value of 0.17. It was further purified on precoated TLC with 60% chloroform-petroleum ether (3 runs) afforded four bands.

Band MP4 was an orange-yellow gum (3.9 mg). Chromatogram on normal phase TLC with 70% chloroform-petroleum ether showed one major UV-active spot with the R_f value of 0.42 and one pale UV-active spot with the R_f value of 0.38. It was not further investigated because it was obtained in low quantity.

Band MP5 was a yellow gum (5.8 mg). Chromatogram on normal phase TLC with 60% chloroform-petroleum ether (2 runs) showed one major UV-active spot with the R_f value of 0.30. It showed the same major UV-active spot as the **band UP2**. It was then purified together with the **band UP2**.

Band MP6 was a yellow gum (3.6 mg). Chromatogram on normal phase TLC with 70% chloroform-petroleum ether showed one major UV-active spot with the R_f value of 0.28. It was not further investigated.

Band MP7 was a yellow gum (1.2 mg). Chromatogram on normal phase TLC with 70% chloroform-petroleum ether showed one UV-active spot with the R_f value of

0.26. Its chromatogram indicated that it was YU1 which was firstly isolated from GNT4.4B.

Subfraction GNT5.4 Chromatogram on normal phase TLC with 1% ethyl acetate-petroleum ether (2 runs) showed two major UV-active spots with the R_f values of 0.36 and 0.42 together with many unseparable spots. Therefore, further purification was not performed.

Fraction GNT6 Chromatogram on normal phase TLC with 40% chloroform-petroleum ether (2 runs) showed four major UV-active spots with the R_f values of 0.13, 0.20, 0.24 and 0.28 which corresponded to YU3, YU4, YU2 and YU1, respectively.

Fraction GNT7 Chromatogram on normal phase TLC with 40% chloroform-petroleum ether (2 runs) showed three major UV-active spots with the R_f values of 0.13, 0.18 and 0.47. Further separation by flash column chromatography over silica gel was carried out. Elution was conducted with a stepwise gradient system (chloroform-petroleum ether and ethyl acetate-chloroform) and finally with pure ethyl acetate. Fractions with the similar chromatogram were combined and evaporated to dryness under reduced pressure to afford seven subfractions, as shown in Table 11.

Table 11 Subfractions obtained from GNT7 by flash column chromatography

Subfraction	Weight (g)	Physical appearance
GNT7.1	0.0073	Yellow gum
GNT7.2	0.0290	Orange-yellow gum
GNT7.3	0.0309	Yellow gum
GNT7.4	0.0557	Yellow gum

Table 11 (Continued)

Subfraction	Weight (g)	Physical appearance
GNT7.5	0.0306	Yellow gum
GNT7.6	0.0228	Yellow gum
GNT7.7	0.0451	Yellow-brown gum

Subfraction GNT7.1 Chromatogram on normal phase TLC with pure petroleum ether showed one pale UV-active spot with the R_f value of 0.64. Thus, it was not further investigated.

Subfraction GNT7.2 Chromatogram on normal phase TLC with 60% chloroform-petroleum ether (2 runs) showed two major UV-active spots with the R_f values of 0.40 and 0.51. It was then combined with band **MP2** as they showed similar chromatogram. Further purified on precoated TLC with 60% chloroform-petroleum ether (2 runs) afforded two bands in low quantity. Their chromatograms on normal phase TLC with 60% chloroform-petroleum ether (2 runs) showed unseparable spots. Thus, They were not further purified.

Subfraction GNT7.3 Chromatogram on normal phase TLC with 60% chloroform-petroleum ether (2 runs) showed three major UV-active spots with the R_f values of 0.24, 0.28 and 0.51. Further separation on precoated TLC with the same solvent system (3 runs) afforded two bands.

Band UP1 was an orange-yellow gum (1.2 mg). Chromatogram on normal phase TLC with 60% chloroform-petroleum ether (2 runs) showed one major UV-active spot with the R_f value of 0.58. It was not further investigated because it was obtained in low quantity.

Band UP2 was a pale yellow gum (3.4 mg). It was then combined with **band MP5** as they showed similar chromatogram. Further separation on precoated TLC with 40% chloroform-petroleum ether (4 runs) afforded **YU2** as a yellow gum (4.3 mg).

Subfraction GNT 7.4 Chromatogram on normal phase TLC with 60% chloroform-petroleum ether (2 runs) showed three major UV-active spots with the R_f values of 0.20, 0.24 and 0.28. Further separation on precoated TLC with 60% chloroform-petroleum ether (5 runs) afforded two bands.

Band UP3 was a pale yellow gum (6.9 mg). Chromatogram on normal phase TLC with 60% chloroform-petroleum ether (2 runs) showed many pale UV-active spots. It was not further investigated because it was obtained in low quantity.

Band UP4 was a pale yellow gum (4.8 mg). Chromatogram on normal phase TLC with 60% chloroform-petroleum ether (2 runs) showed one UV-active spot with the R_f value of 0.26. Its ^1H NMR spectral data indicated that it was **YU1**.

Subfraction GNT7.5 Chromatogram on normal phase TLC with 90% chloroform-petroleum ether (2 runs) showed three major UV-active spots with the R_f values of 0.32, 0.40 and 0.44. Further separation on precoated TLC with 10% ethyl acetate-petroleum ether (6 runs) afforded three bands.

Band UP8-9A was a yellow gum (2.3 mg). Chromatogram on normal phase TLC with 10% ethyl acetate-petroleum ether showed one yellow spot with the R_f value of 0.26 and one major UV-active spot with the R_f value of 0.53. One additional purple spot with the R_f value of 0.22 was observed after dipping the TLC plate in ASA reagent and subsequently heating. It was not further investigated because it was obtained in low quantity.

Band UP8-9B was a yellow gum (2.0 mg). Chromatogram on normal phase TLC with 10% ethyl acetate-petroleum ether showed one major UV-active spot with the R_f value of 0.36. Its ^1H NMR spectral data indicated that it was YU1.

Band UP8-9C (YU4) was a yellow solid (1.5 mg), melting at 157.0-158.5 °C. Chromatogram on normal phase TLC with 10% ethyl acetate-petroleum ether showed one UV-active spot with the R_f value of 0.21.

UV (MeOH) λ_{max} nm (log \mathcal{E})	319 (3.95), 369 (3.36)
FT-IR (neat) $\nu_{\text{cm}^{-1}}$	3379 (O-H stretching) 2945, 2925 (C-H stretching) 1642 (C=O stretching)
^1H NMR (CDCl_3)(δ ppm) (500 MHz)	13.21 (<i>s</i> , 1H), 7.78 (<i>dd</i> , $J = 8.0$ and 1.5 Hz, 1H), 7.32 (<i>dd</i> , $J = 8.0$ and 1.5 Hz, 1H), 7.25 (<i>t</i> , $J = 8.0$ Hz, 1H), 6.55 (<i>brs</i> , 1H), 5.72 (<i>brs</i> , 1H), 5.30 (<i>mt</i> , $J = 7.0$ Hz, 1H), 5.28 (<i>mt</i> , $J = 7.0$ Hz, 1H), 3.56 (<i>d</i> , $J = 7.0$ Hz, 2H), 3.50 (<i>d</i> , $J = 7.0$ Hz, 2H), 1.88 (<i>s</i> , 3H), 1.86 (<i>s</i> , 3H), 1.79 (<i>s</i> , 3H), 1.76 (<i>s</i> , 3H)
^{13}C NMR (CDCl_3)(δ ppm) (125 MHz)	181.11, 160.91, 158.64, 152.38, 144.38, 144.00, 136.24, 133.53, 123.82, 122.20, 121.16, 120.86, 119.75, 116.90, 109.08, 105.42, 103.30, 25.88, 25.67, 22.06, 21.63, 17.96
DEPT 135°	CH ₃ : 25.88, 25.67, 17.96 CH ₂ : 22.06, 21.63 CH : 123.82, 122.20, 121.16, 119.75, 116.90
EIMS (m/z)(% rel. int.)	380 (32), 363 (15), 341 (16), 337 (24), 325 (70), 309 (62), 282 (15), 281 (52), 269 (100)

Subfraction GNT7.6 Chromatogram on normal phase TLC with 90% chloroform-petroleum ether (2 runs) showed three major UV-active spots with the R_f values of 0.29, 0.32 and 0.40. Further separation on precoated TLC with 60% chloroform-petroleum ether (3 runs) afforded **YU3** as a yellow solid (1.9 mg), melting at 180.0-182.0 °C. Chromatogram on normal phase TLC with 60% chloroform-petroleum ether (2 runs) showed one UV-active spot with the R_f value of 0.15.

UV (MeOH) λ_{\max} nm (log \mathcal{E})	307 (2.98), 326 (2.95), 373 (2.54)
FT-IR (neat) $\nu_{\text{cm}^{-1}}$	3365 (O-H stretching) 2918, 2849 (C-H stretching) 1646 (C=O stretching)
^1H NMR (CDCl_3)(δ ppm) (500 MHz)	13.22 (<i>s</i> , 1H), 7.79 (<i>dd</i> , $J = 8.0$ and 1.5 Hz, 1H), 7.32 (<i>dd</i> , $J = 8.0$ and 1.5 Hz, 1H), 7.25 (<i>t</i> , $J = 8.0$ Hz, 1H), 6.80 (<i>d</i> , $J = 10.0$ Hz, 1H), 5.65 (<i>d</i> , $J = 10.0$ Hz, 1H), 5.26 (<i>mt</i> , $J = 7.5$ Hz, 1H), 3.37 (<i>d</i> , $J = 7.5$ Hz, 2H), 1.82 (<i>s</i> , 3H), 1.70 (<i>s</i> , 3H), 1.50 (<i>s</i> , 6H)
^{13}C NMR (CDCl_3)(δ ppm) (125 MHz)	180.75, 160.53, 158.60, 149.22, 144.25, 144.07, 131.70, 127.40, 124.00, 121.86, 121.16, 120.10, 117.12, 115.00, 112.22, 103.13, 100.64, 78.10, 28.16, 25.81, 21.22, 17.91
DEPT 135°	CH ₃ : 28.16, 25.81, 17.91 CH ₂ : 21.22 CH : 127.40, 124.00, 121.86, 120.10, 117.12, 115.00
EIMS (m/z)(% rel. int.)	378 (36), 363 (100), 335 (28), 323 (45), 307 (44), 247 (21), 149 (28)

Subfraction GNT7.7 Chromatogram on normal phase TLC with 90% chloroform-petroleum ether (2 runs) showed none of major UV-active spots. Therefore, it was further investigated.

Fraction GNT8 Chromatogram on normal phase TLC with 80% chloroform-petroleum ether showed five major UV-active spots with the R_f values of 0.18, 0.24, 0.30, 0.51 and 0.62. Further separation by flash column chromatography over silica gel was performed. Elution was conducted initially with 10% ethyl acetate-hexane, gradually enriched with ethyl acetate, followed by increasing amount of methanol in ethyl acetate and finally with pure methanol. Fractions with the similar chromatogram were combined and evaporated to dryness under reduced pressure to afford four subfractions, as shown in Table 12.

Table 12 Subfractions obtained from GNT8 by flash column chromatography

Subfraction	Weight (g)	Physical appearance
GNT8.1	0.0857	Orange gum
GNT8.2	0.0953	Orange-yellow gum
GNT8.3	0.1019	Orange-yellow gum
GNT8.4	0.1143	Yellow-brown gum

Subfraction GNT8.1 Chromatogram on normal phase TLC with 10% ethyl acetate-petroleum ether (2 runs) contained many UV-active spots without major component. Therefore, it was not further investigated.

Subfraction GNT8.2 Chromatogram on normal phase TLC with 70% dichloromethane-hexane (3 runs) showed three major UV-active spots with the R_f values of 0.51, 0.58 and 0.63 which corresponded to YU3, YU1 and YU2, respectively.

Subfraction GNT8.3 Chromatogram on normal phase TLC with 70% dichloromethane-hexane (3 runs) showed two major UV-active spots with the R_f values of 0.42 and 0.51. It was further separated by column chromatography over silica gel. Elution was conducted initially with 70% dichloromethane-hexane, gradually enriched with dichloromethane, followed by increasing amount of methanol in dichloromethane and finally with 50% methanol-dichloromethane. Fractions with the similar chromatogram were combined and evaporated to dryness under reduced pressure to afford four subfractions, as shown in Table 13.

Table 13 Subfractions obtained from GNT8.3 by column chromatography

Subfraction	Weight (g)	Physical appearance
T1	0.0053	Pale yellow gum
T2	0.0419	Yellow gum
T3	0.0125	Yellow gum
T4	0.0437	Orange-yellow gum

Subfraction T1 Chromatogram on normal phase TLC with 70% dichloromethane-hexane (2 runs) showed no major UV-active spots. Therefore, it was not further investigated.

Subfraction T2 Chromatogram on normal phase TLC with 50% dichloromethane-hexane (6 runs) showed two major UV-active spots with the R_f values of 0.39 and 0.46. Further chromatography on precoated TLC with 10% ethyl acetate-hexane as a mobile phase (14 runs) afforded YU4 as a yellow solid (30.2 mg).

Subfraction T3 Chromatogram on normal phase TLC with 50% dichloromethane-hexane (6 runs) showed three major UV-active spots with the R_f

values of 0.33, 0.39 and 0.46. Further chromatography on precoated TLC with 10% ethyl acetate-hexane as a mobile phase (15 runs) afforded YU4 and YU3 as yellow solid in 3.0 and 7.3 mg, respectively.

Subfraction T4 Chromatogram on normal phase TLC with 50% dichloromethane-hexane (6 runs) showed none of major UV-active spots. Therefore, it was not further investigated.

Subfraction GNT8.4 Chromatogram on normal phase TLC with 10% ethyl acetate-petroleum ether (3 runs) contained many UV-active spots without major component. Therefore it was not further investigated.

Fraction GNT9 Chromatogram on normal phase TLC with 80% chloroform-petroleum ether showed four major UV-active spots with the R_f values of 0.23, 0.32, 0.54, 0.64 and many green spots near baseline. It was further separated by flash column chromatography over silica gel. Elution was conducted initially with 70% chloroform-hexane, gradually enriched with chloroform, followed by increasing amount of methanol in chloroform and finally with pure methanol. Fractions with the similar chromatogram were combined and evaporated to dryness under reduced pressure to afford five subfractions, as shown in Table 14.

Table 14 Subfractions obtained from GNT9 by flash column chromatography

Subfraction	Weight (g)	Physical appearance
GNT9.1	0.2364	Orange-brown liquid
GNT9.2	0.0874	Yellow-brown gum
GNT9.3	0.0666	Yellow-brown gum
GNT9.4	0.0884	Orange-brown solid
GNT9.5	2.1348	Dark-brown gum

Subfraction GNT9.1 Chromatogram on normal phase TLC with 50% chloroform-hexane (2 runs) showed many UV-active spots. Thus, it was not further investigated.

Subfraction GNT9.2 Chromatogram on normal phase TLC with 60% chloroform-hexane (2 runs) showed three major UV-active spots with the R_f values of 0.28, 0.35 and 0.40 which corresponded to YU4, YU1 and YU2, respectively.

Subfraction GNT9.3 Chromatogram on normal phase TLC with 60% chloroform-hexane (2 runs) showed two major UV-active spots with the R_f values of 0.21 and 0.28, indicating the presence of YU3 and YU4.

Subfraction GNT9.4 Chromatogram on normal phase TLC with 70% chloroform-hexane (2 runs) showed three major UV-active spots with the R_f values of 0.41, 0.55 and 0.71. It was further separated by column chromatography over silica gel. Elution was conducted initially with 60% chloroform-hexane, gradually enriched with chloroform, followed by increasing amount of methanol in chloroform and finally with 50% methanol in chloroform. Fractions with the similar chromatogram were combined and evaporated to dryness under reduced pressure to afford five subfractions, as shown in Table 15.

Table 15 Subfractions obtained from GNT9.4 by column chromatography

Subfraction	Weight (g)	Physical appearance
Y1	0.0005	Colorless gum
Y2	0.0098	Yellow gum
Y3	0.0234	Yellow gum
Y4	0.0201	Yellow gum
Y5	0.0341	Orange-brown gum

Subfraction Y1 Chromatogram on normal phase TLC with 60% chloroform-hexane (2 runs) showed many UV-active spots. It was not further investigated because it was obtained in low quantity.

Subfraction Y2 Chromatogram on normal phase TLC with 60% chloroform-hexane (2 runs) showed one major UV-active spot with the R_f value of 0.30, indicating the presence of YU4.

Subfraction Y3 Chromatogram on normal phase TLC with 60% chloroform-hexane (2 runs) showed one major UV-active spot with the R_f value of 0.31 which corresponded to YU3.

Subfraction Y4 Chromatogram on normal phase TLC with 60% chloroform-hexane (2 runs) showed one major UV-active spot with the R_f value of 0.25 and two pale UV-active spots with the R_f values of 0.30 and 0.37. It was further separated by column chromatography over silica gel. Elution was conducted initially with 60% chloroform-hexane, gradually enriched with chloroform, followed by increasing amount of methanol in chloroform and finally with 20% methanol in chloroform. Fractions with the similar chromatogram were combined and evaporated to dryness under reduced pressure to afford three subfractions, as shown in Table 16.

Table 16 Subfractions obtained from Y4 by column chromatography

Subfraction	Weight (g)	Physical appearance
YC1	0.0097	Yellow gum
YC2	0.0137	Yellow solid
YC3	0.0010	Pale orange gum

Subfraction YC1 Chromatogram on normal phase TLC with 60% chloroform-hexane (2 runs) showed many UV-active spots. It was not further investigated because it was obtained in low quantity.

Subfraction YC2 Chromatogram on normal phase TLC with 60% chloroform-hexane (2 runs) showed one major UV-active spot with the R_f value of 0.27 and one pale UV-active spot with the R_f value of 0.32. It was further separated by flash column chromatography over silica gel. Elution was conducted initially with 50% chloroform-hexane, gradually enriched with chloroform, followed by increasing amount of methanol in chloroform and finally with pure methanol. Fractions with the similar chromatogram were combined and evaporated to dryness under reduced pressure to afford three subfractions, as shown in Table 17.

Table 17 Subfractions obtained from YC2 by flash column chromatography

Subfraction	Weight (g)	Physical appearance
YC2.1	0.0033	Yellow gum
YC2.2	0.0047	Yellow solid
YC2.3	0.0047	Orange-yellow gum

Subfraction YC2.1 Chromatogram on normal phase TLC with 60% chloroform-hexane (2 runs) showed two major UV-active spots with the R_f values of 0.29 and 0.36. It was not further investigated because it was obtained in low quantity.

Subfraction YC2.2 (YU7) Chromatogram on normal phase TLC with 60% chloroform-hexane (2 runs) showed one UV-active spot with the R_f value of 0.27. It melted at 241.2-243.0 °C.

UV (MeOH) λ_{\max} nm (log ϵ)	310 (3.88), 363 (3.25)
FT-IR (neat) $\nu_{\text{cm}^{-1}}$	3402 (O-H stretching) 2918, 2849 (C-H stretching) 1649 (C=O stretching)
^1H NMR ($\text{CDCl}_3 + \text{CD}_3\text{OD}$) (δ ppm) (500 MHz)	12.86 (<i>s</i> , 1H), 7.63 (<i>dd</i> , $J = 8.0$ and 1.5 Hz, 1H), 7.19 (<i>dd</i> , $J = 8.0$ and 1.5 Hz, 1H), 7.13 (<i>t</i> , $J = 8.0$ Hz, 1H), 6.57 (<i>s</i> , 1H), 5.15 (<i>mt</i> , $J = 7.5$ Hz, 1H), 3.87 (<i>s</i> , 3H), 3.29 (<i>d</i> , $J = 7.5$ Hz, 2H), 1.72 (<i>s</i> , 3H), 1.60 (<i>s</i> , 3H)
^{13}C NMR (CDCl_3) (δ ppm) (125 MHz)	181.00, 164.37, 158.83, 155.85, 145.45, 145.11, 131.65, 123.49, 121.70, 121.29, 119.78, 115.42, 111.59, 103.37, 89.89, 55.69, 25.36, 21.00, 17.35
DEPT 135 $^\circ$	CH ₃ : 55.69, 25.36, 17.35 CH ₂ : 21.00 CH : 123.49, 121.70, 119.78, 115.42, 89.89

Subfraction YC2.3 Chromatogram on normal phase TLC with 60% chloroform-hexane (2 runs) showed one major UV-active spot with the R_f value of 0.27, indicating the presence of YU7.

Subfraction YC3 Chromatogram on normal phase TLC with 60% chloroform-hexane (2 runs) showed none of major UV-active spots. Thus, it was not further investigated.

Subfraction Y5 Chromatogram on normal phase TLC with 80% chloroform-hexane (2 runs) showed YU7 as a major spot and two pale UV-active spots with the R_f values of 0.31 and 0.38.

Subfraction GNT9.5 Chromatogram on normal phase TLC with 70% chloroform-hexane (2 runs) showed none of major UV-active spots. Thus, it was not further investigated.

Fraction GNT10 Chromatogram on normal phase TLC with 80% chloroform-petroleum ether showed two pale UV-active spots with the R_f values of 0.31 and 0.45 and many green spots near baseline. Further separation by column chromatography over silica gel was performed. Elution was conducted with 70% chloroform-hexane, gradually enriched with chloroform, followed by increasing amount of methanol in chloroform and finally with pure methanol. Fractions with the similar chromatogram were combined and evaporated to dryness under reduced pressure to afford five subfractions, as shown in Table 18.

Table 18 Subfractions obtained from **GNT10** by column chromatography

Subfraction	Weight (g)	Physical appearance
GNT 10.1	0.0488	Brown solid
GNT 10.2	0.0986	Orange-brown gum
GNT 10.3	0.0203	Yellow gum
GNT 10.4	0.0130	Orange-brown gum
GNT 10.5	2.7320	Dark brown gum

Subfraction GNT10.1 Chromatogram on normal phase TLC with 40% chloroform-hexane (2 runs) showed no major UV-active spots. Therefore, it was not further investigated.

Subfraction GNT10.2 Chromatogram on normal phase TLC with 40% chloroform-hexane (2 runs) showed four major UV-active spots with the R_f values of 0.11, 0.17, 0.21 and 0.25 which corresponded to YU3, YU4, YU2 and YU1, respectively.

Subfraction GNT10.3 Chromatogram on normal phase TLC with 60% chloroform-hexane (2 runs) showed two major UV-active spots with the R_f values of 0.26, and 0.35 which corresponded to YU7 and YU3, respectively.

Subfraction GNT10.4 Chromatogram on normal phase TLC with 60% chloroform-hexane (2 runs) showed one major UV-active spot with the R_f value of 0.26 which corresponded to YU7.

Subfraction GNT10.5 Chromatogram on normal phase TLC with pure chloroform showed many UV-active spots without major component. Therefore, it was not further investigated.

Fraction GNT11 Chromatogram on normal phase TLC with 80% chloroform-petroleum ether showed six UV-active spots with the R_f values of 0.14, 0.19, 0.27, 0.31, 0.52 and 0.62. Further separation by flash column chromatography over silica gel was performed. Elution was conducted with 30% chloroform-petroleum ether, gradually enriched with chloroform, followed by increasing amount of methanol in chloroform and finally with pure methanol. Fractions with the similar chromatogram were combined and evaporated to dryness under reduced pressure to afford six subfractions, as shown in Table 19.

Table 19 Subfractions obtained from GNT11 by flash column chromatography

Subfraction	Weight (g)	Physical appearance
GNT11.1	0.1516	Yellow-brown gum
GNT11.2	0.0278	Yellow solid
GNT11.3	0.0354	Orange-yellow gum
GNT11.4	0.0913	Orange-brown gum

Table 19 (Continued)

Subfraction	Weight (g)	Physical appearance
GNT11.5	0.0808	Orange gum
GNT11.6	0.2495	Dark brown gum

Subfraction GNT11.1 Chromatogram on normal phase TLC with 40% chloroform-petroleum ether (3 runs) showed no major UV-active spots. Therefore, it was not further investigated.

Subfraction GNT11.2 Chromatogram on normal phase TLC with 60% chloroform-petroleum ether (3 runs) showed one major UV-active spot with the R_f value of 0.26. Further separation on precoated TLC with 60% chloroform-petroleum ether (6 runs) afforded YU4 in 8.1 mg.

Subfraction GNT11.3 Chromatogram on normal phase TLC with 60% chloroform-petroleum ether (3 runs) showed many UV-active spots without major component. Therefore, it was not further investigated.

Subfraction GNT11.4 Chromatogram on normal phase TLC with 80% chloroform-petroleum ether (5 runs) showed four major UV-active spots with the R_f values of 0.27, 0.35, 0.38 and 0.41. It was further separated by flash column chromatography over silica gel. Elution was conducted initially with 10% ethyl acetate-petroleum ether, gradually enriched with ethyl acetate and finally with 30% ethyl acetate-petroleum ether. Fractions with the similar chromatogram were combined and evaporated to dryness under reduced pressure to afford five subfractions, as shown in Table 20.

Table 20 Subfractions obtained from GNT11.4 by flash column chromatography

Subfraction	Weight (g)	Physical appearance
M1	0.0410	Orange-brown gum
M2	0.0088	Yellow gum
M3	0.0067	Yellow gum
M4	0.0320	Yellow solid
M5	0.0092	Yellow -brown gum

Subfraction M1 Chromatogram on normal phase TLC with 10% ethyl acetate-petroleum ether (4 runs) showed no major UV-active spots. Therefore, it was not further investigated.

Subfraction M2 Chromatogram on normal phase TLC with 0.5% methanol-chloroform showed one major UV-active spot with the R_f value of 0.47. Further separation on precoated TLC with 0.5% methanol-chloroform (2 runs) afforded YU11 as a yellow gum (5.2 mg). Its chromatogram showed one UV-active spot with the R_f value of 0.47.

$[\alpha]_D^{29}$	= + 58.8 ⁰ ($c = 1.7 \times 10^{-2}$ g/100 cm ³ , MeOH)
UV (MeOH) λ_{\max} nm (log \mathcal{E})	294 (3.67), 310 (3.77), 329 (3.78), 376 (3.26)
FT-IR (neat) $\nu_{\text{cm}^{-1}}$	3418 (O-H stretching) 2927, 2849 (C-H stretching) 1647 (C=O stretching)
¹ H NMR (CDCl ₃) (δ ppm) (500 MHz)	13.00 (<i>s</i> , 1H), 7.79 (<i>dd</i> , $J = 8$ and 1.5 Hz, 1H), 7.34 (<i>dd</i> , $J = 8$ and 1.5 Hz, 1H), 7.27 (<i>t</i> , $J = 8.0$ Hz, 1H), 6.83 (<i>dd</i> , $J = 10.0$ and 0.5 Hz, 1H), 6.30 (<i>d</i> , $J = 0.5$ Hz, 1H), 5.67 (<i>brs</i> , 1H), 5.61 (<i>d</i> , $J = 10.0$, 1H), 5.11 (<i>mt</i> , J = 7.5 Hz, 1H), 5.08 (<i>mt</i> , $J = 7.5$ Hz, 1H), 2.16-2.11 (<i>m</i> ,

	2H), 2.08-2.00 (<i>m</i> , 2H), 1.98-1.94 (<i>m</i> , 2H), 1.86-1.78 (<i>m</i> , 1H), 1.73-1.68 (<i>m</i> , 1H), 1.67 (<i>d</i> , <i>J</i> = 1.0 Hz, 3H), 1.59 (<i>s</i> , 3H), 1.58 (<i>s</i> , 3H), 1.47 (<i>s</i> , 3H)
¹³ C NMR (CDCl ₃)(δ ppm) (125 MHz)	180.67, 163.41, 161.36, 150.91, 144.27, 144.12, 135.76, 131.40, 126.62, 124.22, 124.19, 123.37, 121.17, 120.36, 117.14, 115.04, 103.46, 100.81, 99.58, 80.86, 41.57, 39.63, 27.10, 26.63, 25.70, 22.50, 17.67, 16.00
DEPT 135 ^o	CH ₃ : 27.10, 25.70, 17.67, 16.00 CH ₂ : 41.57, 39.63, 26.63, 22.50 CH : 126.62, 124.22, 124.19, 123.37, 120.36, 117.14, 115.04, 99.58
FABMS (<i>m/z</i>)(% rel. int.)	447 (37), 295 (100), 257 (6)

Subfraction M3 Chromatogram on normal phase TLC with 10% ethyl acetate-petroleum ether (4 runs) showed two major UV-active spots with the *R_f* values of 0.26 and 0.32 which corresponded to YU3 and YU11, respectively.

Subfraction M4 Chromatogram on normal phase TLC with 10% ethyl acetate-petroleum ether (4 runs) showed one major UV-active spot with the *R_f* value of 0.26 which corresponded to YU3.

Subfraction M5 Chromatogram on normal phase TLC with 10% ethyl acetate-petroleum ether (4 runs) showed two major UV-active spots with the *R_f* values of 0.19 and 0.26. It was further rechromatographed on precoated TLC with 10% ethyl acetate-petroleum ether (10 runs) to afford two bands.

Band M5A was a yellow gum (1.5 mg). Chromatogram on normal phase TLC with 10% ethyl acetate-petroleum ether (2 runs) showed one UV-active spot with the *R_f* value of 0.26 which corresponded to YU3.

Band M5B (YU6) was a yellow gum (2.6 mg). Chromatogram on normal phase TLC with 10% ethyl acetate-petroleum ether (2 runs) showed one UV-active spot with the R_f value of 0.20.

UV (MeOH) λ_{\max} nm (log \mathcal{E})	320 (3.89), 374 (3.22)
FT-IR (neat) $\nu_{\text{cm}^{-1}}$	3424 (O-H stretching) 2915, 2863 (C-H stretching) 1642 (C=O stretching)
^1H NMR (CDCl_3)(δ ppm) (500 MHz)	12.86 (<i>s</i> , 1H), 7.80 (<i>dd</i> , $J = 8.0$ and 1.5 Hz, 1H), 7.31 (<i>dd</i> , $J = 8.0$ and 1.5 Hz), 7.26 (<i>t</i> , $J = 8.0$ Hz, 1H), 5.66 (<i>brs</i> , 1H), 5.27 (<i>mt</i> , $J = 7.5$ Hz, 1H), 3.36 (<i>d</i> , $J = 7.5$ Hz, 2H), 2.90 (<i>t</i> , $J = 7.0$ Hz, 2H), 1.91 (<i>t</i> , $J = 7.0$ Hz, 2H), 1.82 (<i>s</i> , 3H), 1.68 (<i>s</i> , 3H), 1.41 (<i>s</i> , 6H)
^{13}C NMR (CDCl_3)(δ ppm) (125 MHz)	180.65, 159.37, 158.07, 151.90, 144.25, 144.08, 131.47, 123.81, 122.11, 121.25, 119.57, 117.08, 112.06, 103.03, 98.96, 76.07, 31.49, 26.79, 25.84, 21.38, 17.93, 16.48
DEPT 135 ^o	CH ₃ : 26.79, 25.84, 17.93 CH ₂ : 31.49, 21.38, 16.48 CH : 123.81, 122.11, 119.57, 117.08
EIMS (m/z)(% rel. int.)	380 (18), 337 (37), 325 (100), 309 (53), 281 (45), 269 (95)

Subfraction GNT11.5 Chromatogram on normal phase TLC with 80% chloroform-petroleum ether (5 runs) showed three major UV-active spots with the R_f values of 0.26, 0.30 and 0.38. It was further separated by flash column chromatography over silica gel. Elution was conducted initially with 10% ethyl acetate-petroleum ether,

gradually enriched with ethyl acetate, followed by increasing amount of methanol in ethyl acetate and finally with pure methanol. Fractions with the similar chromatogram were combined and evaporated to dryness under reduced pressure to afford six subfractions. Chromatogram on normal phase TLC with 8% ethyl acetate-petroleum ether (5 runs) showed many UV-active spots. Each fraction was obtained in low quantity. Further purification was not then performed.

Subfraction GNT11.6 Chromatogram on normal phase TLC with 5% methanol-chloroform showed none of major UV-active spots. Therefore, it was not further investigated.

Fraction GNT12 Chromatogram on normal phase TLC with 80% chloroform-petroleum ether showed six pale UV-active spots with the R_f values of 0.17, 0.21, 0.30, 0.35, 0.52 and 0.61 and many green spots near baseline. Further separation by column chromatography over silica gel was performed. Elution was initially with 1% methanol-chloroform, followed by increasing amount of methanol and finally with pure methanol. Fractions with the similar chromatogram were combined and evaporated to dryness under reduced pressure to afford four subfractions, as shown in Table 21.

Table 21 Subfractions obtained from GNT12 by column chromatography

Subfraction	Weight (g)	Physical appearance
GNT12.1	0.1069	Orange gum
GNT12.2	2.1712	Dark brown gum
GNT12.3	0.5289	Dark brown gum
GNT12.4	1.2490	Green brown gum

Subfraction GNT12.1 Chromatogram on normal phase TLC with 50% chloroform-petroleum ether showed none of major UV-active spots. Therefore, it was not further investigated.

Subfraction GNT12.2 Chromatogram on normal phase TLC with 5% methanol-chloroform showed many UV-active spots and green spots. It was further separated by column chromatography over reversed-phase silica gel, eluting with 50% methanol-water, followed by decreasing amount of water in methanol and finally with pure methanol. Fractions with the similar chromatogram were combined and evaporated to dryness under reduced pressure to afford six subfractions, as shown in Table 22.

Table 22 Subfractions obtained from GNT12.2 by column chromatography over reversed-phase silica gel

Subfraction	Weight (g)	Physical appearance
S2.1	1.7745	Orange-yellow gum
S2.2	0.0317	Orange-brown gum
S2.3	0.0251	Orange-brown gum
S2.4	0.0167	Orange-brown gum
S2.5	0.0896	Green-brown gum
S2.6	0.1867	Dark-green gum

Subfraction S2.1 Chromatogram on normal phase TLC with 1% methanol-chloroform showed no major UV-active spots. Therefore, it was not further investigated.

Subfraction S2.2 Chromatogram on normal phase TLC with 1% methanol-chloroform showed two major UV-active spots with the R_f values of 0.16 and 0.24. It was further separated by flash column chromatography over silica gel. Elution was

conducted initially with pure chloroform, followed by increasing amount of methanol and finally with pure methanol. Fractions with the similar chromatogram were combined and evaporated to dryness under reduced pressure to afford three subfractions, as shown in Table 23.

Table 23 Subfractions obtained from S2.2 by flash column chromatography

Subfraction	Weight(g)	Physical appearance
SA2.1	0.0067	Pale yellow gum
SA2.2	0.0154	Pale yellow gum
SA2.3	0.0113	Orange yellow gum

Subfractions SA2.1 Chromatogram on normal phase TLC with 100% chloroform showed many UV-active spots, none of which were major components. Therefore, it was not further investigated.

Subfractions SA2.2 Chromatogram on normal phase TLC with 1% methanol-chloroform (2 runs) showed two major UV-active spots with the R_f values of 0.37 and 0.42. Further chromatography on precoated TLC with 1% methanol-chloroform (10 runs) afforded two bands.

Band SA2.2A (YU9) was a yellow gum (5.0 mg). Chromatogram on normal phase TLC with 1% methanol-chloroform (3 runs) showed one UV-active spot with the R_f value of 0.57.

UV (MeOH) λ_{\max} nm (log ϵ)	296 (3.15), 319 (3.33), 373 (2.73)
FT-IR (neat) $\nu_{\text{cm}^{-1}}$	3416 (O-H stretching) 2926, 2848 (C-H stretching) 1646 (C=O stretching)

^1H NMR (CDCl_3)(δ ppm) (500 MHz)	13.48 (<i>s</i> , 1H), 7.20 (<i>d</i> , $J = 8.5$ Hz, 1H), 7.00 (<i>d</i> , $J = 8.5$ Hz, 1H), 6.32 (<i>s</i> , 1H), 3.30-3.26 (<i>m</i> , 2H), 2.72 (<i>t</i> , $J = 6.5$ Hz, 2H), 1.85 (<i>t</i> , $J = 6.5$ Hz, 2H), 1.78-1.75 (<i>m</i> , 2H), 1.38 (<i>s</i> , 6H), 1.31 (<i>s</i> , 6H)
^{13}C NMR (CDCl_3)(δ ppm) (125 MHz)	182.67, 161.48, 161.00, 154.04, 145.45, 142.67, 136.68, 125.70, 119.35, 118.30, 104.46, 103.25, 94.15, 76.45, 70.71, 45.90, 31.73, 29.83, 29.27, 26.73, 16.05
DEPT 135 $^\circ$	CH ₃ : 29.27, 26.73 CH ₂ : 45.90, 31.73, 29.83, 16.05 CH : 125.70, 119.35, 94.15
EIMS (m/z)(% rel. int.)	398 (4), 380 (15), 338 (22), 337 (100), 324 (21), 283 (26), 281 (63), 269 (26)

Band SA2.2B (YU10) was a yellow solid (2.8 mg), melting at 161.0-162.0 $^\circ\text{C}$. Chromatogram on normal phase TLC with 1% methanol-chloroform (3 runs) showed one UV-active spot with the R_f value of 0.53.

UV (MeOH) λ_{max} nm ($\log \epsilon$)	295 (3.94), 316 (3.80), 376 (3.24)
FT-IR (neat) $\nu_{\text{cm}^{-1}}$	3424 (O-H stretching) 2925, 2848 (C-H stretching) 1646 (C=O stretching)
^1H NMR (CDCl_3)(δ ppm) (500 MHz)	13.44 (<i>s</i> , 1H), 7.22 (<i>d</i> , $J = 8.5$ Hz, 1H), 7.02 (<i>d</i> , $J = 8.5$ Hz, 1H), 6.74 (<i>dd</i> , $J = 10.0$ and 0.5 Hz, 1H), 6.33 (<i>d</i> , $J = 0.5$ Hz, 1H), 5.61 (<i>d</i> , $J = 10.0$ Hz, 1H), 3.29-3.26 (<i>m</i> , 2H), 1.78-1.75 (<i>m</i> , 2H), 1.48 (<i>s</i> , 6H), 1.32 (<i>s</i> , 6H)

^{13}C NMR (CDCl_3)(δ ppm) (125 MHz)	182.68, 160.61, 158.15, 155.57, 145.34, 142.65, 136.78, 127.55, 126.06, 119.58, 118.35, 115.44, 104.94, 104.15, 94.23, 78.37, 70.73, 45.86, 29.82, 29.28, 28.38
DEPT 135 ⁰	CH ₃ : 29.28, 28.38 CH ₂ : 45.86, 29.82 CH : 127.55, 126.06, 119.58, 115.44, 94.23
EIMS (m/z)(% rel. int.)	396 (5), 378 (12), 364 (21), 363 (100), 345 (25), 335 (63), 308 (23), 307 (45)

Subfractions SA2.3 Chromatogram on normal phase TLC with 1% methanol-chloroform showed (3 runs) many UV-active spots, none of which were major components. Therefore, it was not further investigated.

Subfraction S2.3 Chromatogram on normal phase TLC with 1% methanol-chloroform showed two major UV-active spots with the R_f values of 0.29 and 0.34 and three pale UV-active spots with the R_f values of 0.13, 0.17 and 0.41. It was further separated by flash column chromatography over silica gel. Elution was conducted initially with pure chloroform, followed by increasing amount of methanol and finally with pure methanol. Fractions with the similar chromatogram were combined and evaporated to dryness under reduced pressure to afford ten subfractions. Chromatogram on normal phase TLC with 1% methanol-chloroform showed many UV-active spots. Each fraction was obtained in low quantity. Further purification was not performed.

Subfraction S2.4 Chromatogram on normal phase TLC with 1% methanol-chloroform showed many UV-active and unseparable spots. Therefore, it was not further investigated.

Subfraction S2.5 Chromatogram on normal phase TLC with 1% methanol-chloroform showed four major UV-active spots with the R_f values of 0.18, 0.30, 0.58 and 0.68. It was further separated by flash column chromatography over silica gel. Elution was conducted initially with 80% chloroform-hexane, gradually enriched with chloroform, followed by increasing amount of methanol in chloroform and finally with pure methanol. Fractions with the similar chromatogram were combined and evaporated to dryness under reduced pressure to afford eight subfractions. Their chromatograms on normal phase TLC with 1% methanol-chloroform showed many UV-active spots. Each fraction was obtained in low quantity. Further purification was not then performed.

Subfraction S2.6 Chromatogram on normal phase TLC with 1% methanol-chloroform showed many UV-active and unseparable spots. Therefore, it was not further investigated.

Subfraction GNT12.3 Chromatogram on normal phase TLC with 5% methanol-chloroform showed many UV-active and unseparable spots. It was further separated by column chromatography over reversed-phase silica gel, eluting with 50% methanol-water, followed by decreasing amount of water in methanol and finally with pure methanol. Fractions with the similar chromatogram were combined and evaporated to dryness under reduced pressure to afford ten subfractions. Each fraction was obtained in low quantity. Further purification was not then performed.

Subfraction GNT12.4 Chromatogram on normal phase TLC with 5% methanol-chloroform showed many UV-active and unseparable spots. It was further separated by column chromatography over reversed-phase silica gel, eluting with 50% methanol-water, followed by decreasing amount of water in methanol and finally with pure methanol. Fractions with the similar chromatogram were combined and evaporated to dryness under reduced pressure to afford three subfractions. Each

fraction showed many unseparable spots on normal phase TLC with 5% methanol-chloroform. Further purification was not then performed.

Fraction GNT13 Chromatogram on normal phase TLC with 10% methanol-chloroform showed four major UV-active spots with the R_f values of 0.46, 0.52, 0.62 and 0.70. Further separation by column chromatography over silica gel was performed. Elution was conducted initially with pure chloroform, followed by increasing amount of methanol in chloroform and finally with pure methanol. Fractions with the similar chromatogram were combined and evaporated to dryness under reduced pressure to afford four subfractions, as shown in Table 24.

Table 24 Subfractions obtained from GNT13 by column chromatography

Subfraction	Weight (g)	Physical appearance
GNT13.1	0.4910	Orange-brown gum
GNT13.2	2.0801	Dark-brown gum
GNT13.3	9.3295	Dark-brown gum
GNT13.4	15.8897	Dark-brown gum

Subfraction GNT13.1 Chromatogram on normal phase TLC with 70% chloroform-petroleum ether showed many pale UV-active spots. Thus, it was not further investigated.

Subfraction GNT13.2 Chromatogram on normal phase TLC with 2% methanol-chloroform showed four major UV-active spots with the R_f values of 0.23, 0.29, 0.63 and 0.65 and unseparable spots near baseline. Further separation by column chromatography over silica gel was performed. Elution was conducted initially with pure chloroform, followed by increasing amount of methanol and finally with pure

methanol. Fractions with the similar chromatogram were combined and evaporated to dryness under reduced pressure to afford three subfractions, as shown in Table 25.

Table 25 Subfractions obtained from GNT13.2 by column chromatography

Subfraction	Weight (g)	Physical appearance
U1	0.0628	Orange-yellow gum
U2	1.7082	Dark-brown gum
U3	0.0817	Dark-brown gum

Subfraction U1 Chromatogram on normal phase TLC with 100% chloroform showed many UV-active spots. Thus, it was not further investigated.

Subfraction U2 Chromatogram on normal phase TLC with 0.5% methanol-chloroform showed two major UV-active spots with the R_f values of 0.19 and 0.26 and unseparable spots near baseline. It was further separated by column chromatography over reversed-phase silica gel, eluting with 65% methanol-water, followed by decreasing amount of water in methanol and finally with pure methanol. Fractions with the similar chromatogram were combined and evaporated to dryness under reduced pressure to afford eleven subfractions, as shown in Table 26.

Table 26 Subfractions obtained from U2 by column chromatography over reversed-phase silica gel

Subfraction	Weight (g)	Physical appearance
U2.1	1.2207	Yellow-brown gum
U2.2	0.0255	Yellow-brown gum

Table 26 (Continued)

Subfraction	Weight (g)	Physical appearance
U2.3	0.0257	Yellow-brown gum
U2.4	0.0222	Yellow-brown gum
U2.5	0.0325	Yellow-brown gum
U2.6	0.0315	Yellow-brown gum
U2.7	0.0137	Yellow-brown gum
U2.8	0.0658	Yellow-brown gum
U2.9	0.0640	Yellow-brown gum
U2.10	0.0558	Brown gum
U2.11	0.1196	Dark-brown gum

Subfraction U2.1 Chromatogram on normal phase TLC with 1% methanol-chloroform (3 runs) showed no major UV-active spots. Therefore, it was not further investigated.

Subfraction U2.2 Chromatogram on normal phase TLC with 1% methanol-chloroform (3 runs) showed three major UV-active spots with the R_f values of 0.23, 0.43 and 0.47. It was further separated by flash column chromatography over silica gel. Elution was conducted initially with 1% methanol-chloroform, followed by increasing amount of methanol and finally with pure methanol. Fractions with the similar chromatogram were combined and evaporated to dryness under reduced pressure to afford nine subfractions. Their chromatograms on normal phase TLC with 1% methanol-chloroform showed many UV-active spots. Each fraction was obtained in low quantity. Further purification was not then performed.

Subfraction U2.3 Chromatogram on normal phase TLC with 1% methanol-chloroform (3 runs) showed many UV-active spots. Therefore, it was not further investigated.

Subfraction U2.4 Chromatogram on normal phase TLC with 1% methanol-chloroform (3 runs) showed five major UV-active spots with the R_f values of 0.12, 0.17, 0.39, 0.43 and 0.50. It was further separated by column chromatography over silica gel. Elution was conducted initially with chloroform, followed by increasing amount of methanol and finally with 50% methanol-chloroform. Fractions with the similar chromatogram were combined and evaporated to dryness under reduced pressure to afford three subfractions, as shown in Table 27.

Table 27 Subfractions obtained from U2.4 by column chromatography

Subfraction	Weight (g)	Physical appearance
UC4.1	0.0026	Pale yellow gum
UC4.2	0.0145	Yellow gum
UC4.3	0.0098	Yellow gum

Subfraction UC4.1 Chromatogram on normal phase TLC with 1% methanol-chloroform (5 runs) showed none of major UV-active spots. Therefore, it was not further investigated.

Subfraction UC4.2 Chromatogram on normal phase TLC with 1% methanol-chloroform (5 runs) showed two major UV-active spots with the R_f values of 0.47 and 0.52. Further chromatography on precoated TLC with 1% methanol-chloroform (7 runs) afforded two bands.

Band UC4.2A was a yellow gum (4.3 mg). Chromatogram on normal phase TLC with 1% methanol-chloroform (6 runs) showed one UV-active spot with the R_f value of 0.57. Its ^1H NMR spectral data indicated that it was **YU9** which was firstly isolated from **subfraction SA2.2**.

Band UC4.2B was a yellow gum (3.3 mg). Chromatogram on normal phase TLC with 1% methanol-chloroform (6 runs) showed two major UV-active spots with the R_f values of 0.52 and 0.57. It was further rechromatographed on precoated TLC with 1% methanol-chloroform (11 runs) to give **YU9** and **YU10** in 1.6 and 1.3 mg, respectively.

Subfraction UC4.3 Chromatogram on normal phase TLC with 1% methanol-chloroform (5 runs) showed many UV-active spots. Therefore, it was not further investigated.

Subfraction U2.5 Chromatogram on normal phase TLC with 1% methanol-chloroform (3 runs) showed six major UV-active spots with the R_f values of 0.12, 0.17, 0.39, 0.43, 0.54 and 0.59. It was further separated by column chromatography over silica gel. Elution was conducted initially with 0.5% methanol-chloroform, followed by increasing amount of methanol and finally with 50% methanol-chloroform. Fractions with the similar chromatogram were combined and evaporated to dryness under reduced pressure to afford three subfractions, as shown in Table 28.

Table 28 Subfractions obtained from **U2.5** by column chromatography

Subfraction	Weight (g)	Physical appearance
UC5.1	0.0043	Pale yellow gum
UC5.2	0.0186	Yellow gum
UC5.3	0.0152	Yellow gum

Subfraction UC5.1 Chromatogram on normal phase TLC with 1% methanol-chloroform (2 runs) showed no major UV-active spots. Therefore, it was not further investigated.

Subfraction UC5.2 Chromatogram on normal phase TLC with 1% methanol-chloroform (2 runs) showed two major UV-active spots with the R_f values of 0.32 and 0.38. Further chromatography on precoated TLC with 1% methanol-chloroform (7 runs) afforded two bands.

Band UC5.2A was a yellow gum (5.9 mg). Chromatogram on normal phase TLC with 1% methanol-chloroform (6 runs) showed one UV-active spot with the R_f value of 0.57. Its chromatogram indicated that it was YU9.

Band UC5.2B was a yellow gum (6.3 mg). Chromatogram on normal phase TLC with 1% methanol-chloroform (6 runs) showed two major UV-active spots with the R_f values of 0.52 and 0.57. It was further rechromatographed on precoated TLC with 1% methanol-chloroform (11 runs) to give YU9 and YU10 in 1.5 and 4.6 mg, respectively.

Subfraction UC5.3 Chromatogram on normal phase TLC with 1% methanol-chloroform (2 runs) showed none of major UV-active spots. Therefore, it was not further investigated.

Subfraction U2.6 Chromatogram on normal phase TLC with 1% methanol-chloroform (2 runs) showed three major UV-active spots with the R_f values of 0.12, 0.17 and 0.46. It was further separated by flash column chromatography over silica gel. Elution was conducted initially with 0.5% methanol-chloroform, followed by increasing amount of methanol and finally with 20% methanol-chloroform. Fractions with the similar chromatogram were combined and evaporated to dryness under reduced pressure to afford three subfractions, as shown in Table 29.

Table 29 Subfractions obtained from U2.6 by flash column chromatography

Subfraction	Weight (g)	Physical appearance
UC6.1	0.0043	Pale yellow gum
UC6.2	0.0024	Yellow solid
UC6.3	0.0190	Orange-brown gum

Subfraction UC6.1 Chromatogram on normal phase TLC with 0.5% methanol-chloroform (3 runs) showed many UV-active spots, none of which were major components. Therefore, it was not further investigated.

Subfraction UC6.2 (YU12) Chromatogram on normal phase TLC with 0.5% methanol-chloroform (3 runs) showed one UV-active spot with the R_f value of 0.44, melting at 201.5-203.2 °C.

UV (MeOH) λ_{\max} nm (log \mathcal{E})	230 (4.42), 240 (4.37), 263 (4.36), 307 (4.06), 373 (3.65)
FT-IR (neat) $\nu_{\text{cm}^{-1}}$	3298 (O-H stretching) 2925, 2856 (C-H stretching) 1651 (C=O stretching)
^1H NMR (CDCl_3)(δ ppm) (500 MHz)	12.87 (<i>s</i> , 1H), 7.62 (<i>d</i> , $J = 3.5$ Hz, 1H), 7.36 (<i>d</i> , $J = 8.5$ Hz, 1H), 7.26 (<i>dd</i> , $J = 8.5$ and 3.5 Hz, 1H), 6.43 (<i>s</i> , 1H), 5.66 (<i>brs</i> , 1H), 5.24 (<i>mt</i> , $J = 7.0$ Hz, 1H), 3.94 (<i>s</i> , 3H), 3.38 (<i>d</i> , $J = 7.0$ Hz, 2H), 1.80 (<i>s</i> , 3H), 1.69 (<i>s</i> , 3H)
^{13}C NMR (CDCl_3)(δ ppm) (125 MHz)	180.41, 164.45, 159.39, 156.32, 151.97, 150.52, 131.96, 123.73, 122.02, 121.20, 118.98, 111.72, 109.23, 103.95, 89.57, 55.95, 25.81, 21.32, 17.80

DEPT 135⁰ CH₃ : 55.95, 25.81, 17.80
 CH₂ : 21.32
 CH : 123.73, 122.02, 118.98, 109.23, 89.57

Subfraction UC6.3 Chromatogram on normal phase TLC with 0.5% methanol-chloroform (3 runs) showed many UV-active and unseparable spots. Therefore, it was not further investigated.

Subfraction U2.7 Chromatogram on normal phase TLC with 1% methanol-chloroform (3 runs) showed unseparable spots. Further purification was not then performed.

Subfraction U2.8 Chromatogram on normal phase TLC with 1% methanol-chloroform (3 runs) showed one major UV-active spot with the R_f value of 0.73 and unseparable spots. It was further separated by flash column chromatography over silica gel. Elution was conducted initially with 1% methanol-chloroform, followed by increasing amount of methanol and finally with 30% methanol-chloroform. Fractions with the similar chromatogram were combined and evaporated to dryness under reduced pressure to afford three subfractions, as shown in Table 30.

Table 30 Subfractions obtained from U2.8 by flash column chromatography

Subfraction	Weight (g)	Physical appearance
UC8.1	0.0040	Pale yellow gum
UC8.2	0.0110	Yellow gum
UC8.3	0.0387	Orange-yellow gum

Subfraction UC8.1 Chromatogram on normal phase TLC with 1% methanol-chloroform (3 runs) showed no major UV-active spots. Therefore, it was not further investigated.

Subfraction UC8.2 Chromatogram on normal phase TLC with 1% methanol-chloroform (5 runs) showed two major UV-active spots with the R_f values of 0.47 and 0.52. It was further rechromatographed on precoated TLC with 1% methanol-chloroform (11 runs) to give YU9 and YU10 in 2.4 and 2.9 mg, respectively.

Subfraction UC8.3 Chromatogram on normal phase TLC with 1% methanol-chloroform (5 runs) showed many UV-active spots. Therefore, it was not further investigated.

Subfraction U2.9 Chromatogram on normal phase TLC with 1% methanol-chloroform (3 runs) showed two major UV-active spots with the R_f values of 0.46 and 0.80 and unseparable UV-active spots. It was further separated by flash column chromatography over silica gel. Elution was conducted initially with 0.5% methanol-chloroform, followed by increasing amount of methanol and finally with 20% methanol-chloroform. Fractions with the similar chromatogram were combined and evaporated to dryness under reduced pressure to afford eleven subfractions. Their chromatograms on normal phase TLC with 1% methanol-chloroform (3 runs) showed many UV-active spots. Each fraction was obtained in low quantity. Further purification was not then performed.

Subfraction U2.10 Chromatogram on normal phase TLC with 1% methanol-chloroform (3 runs) showed two major UV-active spots with the R_f values of 0.43 and 0.47 and unseparable UV-active spots. It was further separated by flash column chromatography over silica gel. Elution was conducted initially with 0.5% methanol-chloroform, followed by increasing amount of methanol and finally with 20% methanol-chloroform. Fractions with the similar chromatogram were combined and

evaporated to dryness under reduced pressure to afford four subfractions. Their chromatograms on normal phase TLC with 1% methanol-chloroform (3 runs) showed many UV-active spots. Each fraction was obtained in low quantity. Further purification was not then performed.

Subfraction U2.11 Chromatogram on normal phase TLC with 1% methanol-chloroform (3 runs) showed many unseparable UV-active spots. Therefore, it was not further investigated.

Subfraction U3 Chromatogram on normal phase TLC with 3% methanol-chloroform showed unseparable spots. Thus, it was not further investigated.

Subfraction GNT13.3 Chromatogram on normal phase TLC with 2% methanol-chloroform showed unseparable UV-active spots. It was further separated by column chromatography over reversed-phase silica gel, eluting with 40% methanol-water, followed by decreasing amount of water in methanol and finally with pure methanol. Fractions with the similar chromatogram were combined and evaporated to dryness under reduced pressure to afford fourteen subfractions, as shown in Table 31.

Table 31 Subfractions obtained from GNT13.3 by column chromatography over reversed-phase silica gel

Subfraction	Weight (g)	Physical appearance
F1	0.5370	Orange-brown gum
F2	0.1362	Orange-brown gum
F3	0.0272	Yellow-brown gum
F4	0.1044	Orange gum
F5	0.2300	Yellow-brown gum

Table 31 (Continued)

Subfraction	Weight (g)	Physical appearance
F6	0.1683	Orange-brown gum
F7	0.0175	Orange-brown gum
F8	0.1249	Orange-brown gum
F9	0.3865	Orange-brown gum
F10	0.1890	Yellow-brown gum
F11	0.3458	Yellow-brown gum
F12	0.0282	Yellow-brown gum
F13	1.5629	Brown gum
F14	1.6321	Dark-brown gum

Subfraction F1 Chromatogram on normal phase TLC with 2% methanol-chloroform (2 runs) showed no major UV-active spots. Therefore, it was not further investigated.

Subfraction F2 Chromatogram on normal phase TLC with 2% methanol-chloroform (2 runs) showed three major UV-active spots with the R_f values of 0.08, 0.09 and 0.20. It was further separated by flash column chromatography over silica gel. Elution was conducted initially with 0.5% methanol-chloroform, followed by increasing amount of methanol and finally with pure methanol. Fractions with the similar chromatogram were combined and evaporated to dryness under reduced pressure to afford seven subfractions, as shown in Table 32.

Table 32 Subfractions obtained from **F2** by flash column chromatography

Subfraction	Weight (g)	Physical appearance
F2.1	0.0390	Pale yellow gum
F2.2	0.0061	Pale yellow gum
F2.3	0.0074	Pale yellow crystals
F2.4	0.0062	Pale yellow crystals
F2.5	0.0018	Pale yellow gum
F2.6	0.0104	Pale yellow gum
F2.7	0.0039	Yellow gum

Subfraction F2.1 Chromatogram on normal phase TLC with 2% methanol-chloroform (2 runs) showed many UV-active spots. Therefore, it was not further investigated.

Subfraction F2.2 Chromatogram on normal phase TLC with 2% methanol-chloroform (2 runs) showed one major UV-active spot with the R_f value of 0.22 which corresponded to YU13.

Subfraction F2.3 (YU13) Chromatogram on normal phase TLC with 2% methanol-chloroform (2 runs) showed one UV-active spot with the R_f value of 0.22. It melted at 185.6-187.2 °C.

$[\alpha]_D^{29}$	= - 62.5 ⁰ (c = 1.6 x 10 ⁻² g/100 cm ³ , MeOH)
UV (MeOH) λ_{max} nm (log \mathcal{E})	229 (3.77), 251 (3.89), 258 (3.92), 295 (3.47)
FT-IR (neat) ν_{cm-1}	3367 (O-H stretching) 1657 (C=O stretching)
¹ H NMR (Acetone-d ₆) (δ ppm) (500 MHz)	12.61 (s, 1H), 7.95 (d, J = 2.0 Hz, 1H), 6.39 (d, J = 2.0 Hz, 1H), 6.27 (d, J = 2.0 Hz, 1H), 4.76 (dd, J = 2.5 and 2.0 Hz, 1H), 4.42 (brs, 1H), 4.36 (td, J =

	5.5 and 2.5 Hz, 1H), 4.12 (<i>dt</i> , $J = 8.0$ and 3.0 Hz, 1H), 4.02 (<i>ddd</i> , $J = 8.5$, 8.0 and 6.5 Hz, 1H), 2.14-2.05 (<i>m</i> , 1H), 1.91-1.86 (<i>m</i> , 1H)
^{13}C NMR (Acetone- d_6)(δ ppm) (125 MHz)	183.03, 166.19, 164.24, 160.10, 155.11, 124.06, 106.07, 100.35, 95.01, 82.96, 76.76, 68.27, 34.40
DEPT 135 $^\circ$	CH $_2$: 68.27, 34.40 CH : 155.11, 100.35, 95.01, 82.96, 76.76
EIMS (m/z)(% rel. int.)	246 (14), 223 (38), 218 (22), 207 (100), 205 (29), 153 (20)

Subfraction F2.4 Chromatogram on normal phase TLC with 2% methanol-chloroform (2 runs) showed one UV-active spot with the R_f value of 0.22 which corresponded to YU13.

Subfraction F2.5 Chromatogram on normal phase TLC with 2% methanol-chloroform (3 runs) showed three pale UV-active spots with the R_f values of 0.15, 0.19 and 0.23. Therefore, it was not further investigated.

Subfraction F2.6 Chromatogram on normal phase TLC with 2% methanol-chloroform (3 runs) showed three pale UV-active spots with the R_f values of 0.12, 0.16 and 0.21. It was further separated by column chromatography over reversed-phase silica gel, eluting with 30% methanol-water, followed by decreasing amount of water in methanol and finally with pure methanol. Fractions with the similar chromatogram were combined and evaporated to dryness under reduced pressure to afford six subfractions. Each fraction was obtained in low quantity and their chromatograms showed many UV-active spots on normal phase TLC with 30% ethyl acetate-petroleum ether (3 runs). Further purification was not then performed.

Subfraction F2.7 Chromatogram on normal phase TLC with 2% methanol-chloroform (3 runs) showed none of major UV-active spots. Therefore, it was not further investigated.

Subfraction F3 Chromatogram on normal phase TLC with 2% methanol-chloroform (2 runs) showed three pale UV-active spots with the R_f values of 0.10, 0.16 and 0.31. Therefore, it was not further investigated.

Subfraction F4 Chromatogram on normal phase TLC with 2% methanol-chloroform (2 runs) showed four major UV-active spots with the R_f values of 0.08, 0.18, 0.26 and 0.36. It was further separated by column chromatography over silica gel. Elution was conducted with 0.5% methanol-chloroform, followed by increasing amount of methanol and finally with pure methanol. Fractions with the similar chromatogram were combined and evaporated to dryness under reduced pressure to afford sixteen subfractions. Each fraction was obtained in low quantity. Further purification was not then performed.

Subfraction F5 Chromatogram on normal phase TLC with 2% methanol-chloroform (2 runs) showed many UV-active spots. Therefore, it was not further investigated.

Subfraction F6 Chromatogram on normal phase TLC with 2% methanol-chloroform (2 runs) showed three major UV-active spots with the R_f values of 0.08, 0.13 and 0.23. It was further separated by flash column chromatography over silica gel. Elution was conducted initially with 0.5% methanol-chloroform, followed by increasing amount of methanol and finally with 50% methanol-chloroform. Fractions with the similar chromatogram were combined and evaporated to dryness under reduced pressure to afford seven subfractions, as shown in Table 33.

Table 33 Subfractions obtained from **F6** by flash column chromatography

Subfraction	Weight (g)	Physical appearance
F6.1	0.0116	Yellow gum
F6.2	0.0187	Yellow gum
F6.3	0.0081	Yellow gum
F6.4	0.0151	Yellow gum
F6.5	0.0087	Yellow gum
F6.6	0.0277	Yellow gum
F6.7	0.0436	Yellow-brown gum

Subfraction F6.1 Chromatogram on normal phase TLC with 3% methanol-chloroform (3 runs) showed no major UV-active spots. Therefore, it was not further investigated.

Subfraction F6.2 Chromatogram on normal phase TLC with 3% methanol-chloroform (3 runs) showed four major UV-active spots with the R_f values of 0.35, 0.42, 0.50 and 0.58. Further chromatography on precoated TLC with 2% methanol-chloroform (8 runs) afforded two bands in low quantity. Further purification was not then attempted.

Subfraction F6.3 Chromatogram on normal phase TLC with 3% methanol-chloroform (3 runs) showed two major UV-active spots with the R_f values of 0.26 and 0.32. Further chromatography on precoated TLC with 2% methanol-chloroform (11 runs) afforded **F6.3A** as a yellow gum in 4.2 mg. Chromatogram on normal phase TLC with 2% methanol-chloroform (5 runs) showed one major UV-active spot with the R_f value of 0.34 which was also found in **FB4.2A**. It was then combined with band **FB4.2A**.

Subfraction F6.4 Chromatogram on normal phase TLC with 3% methanol-chloroform (3 runs) showed three major UV-active spots with the R_f values of 0.17, 0.23 and 0.30. It was further separated by flash column chromatography over silica gel. Elution was conducted initially with 0.5% methanol-chloroform, followed by increasing amount of methanol and finally with 20% methanol-chloroform. Fractions with the similar chromatogram were combined and evaporated to dryness under reduced pressure to afford five subfractions, as shown in Table 34.

Table 34 Subfractions obtained from F6.4 by flash column chromatography

Subfraction	Weight (g)	Physical appearance
FB4.1	0.0035	Pale yellow gum
FB4.2	0.0031	Yellow gum
FB4.3	0.0008	Pale yellow gum
FB4.4	0.0042	Pale yellow gum
FB4.5	0.0016	Yellow gum

Subfraction FB4.1 Chromatogram on normal phase TLC with 1% methanol-chloroform (9 runs) showed no major UV-active spots. Therefore, it was not further investigated.

Subfraction FB4.2 Chromatogram on normal phase TLC with 1% methanol-chloroform (9 runs) showed two major UV-active spots with the R_f values of 0.18 and 0.22. Further purification on precoated TLC with 2% methanol-chloroform (11 runs) afforded **FB4.2A** as a yellow gum (1.8 mg). It was combined with **F6.3A** as they showed similar chromatogram. Further separation on precoated TLC with 2% methanol-chloroform (5 runs) afforded **YU16** as a yellow gum (2.2 mg).

Its chromatogram with 2% methanol-chloroform (4 runs) showed one UV-active spot with the R_f value of 0.30.

UV (MeOH) λ_{\max} nm (log \mathcal{E})	218 (4.22), 242 (4.19), 258 (4.09), 319 (3.88)
FT-IR (neat) $\nu_{\text{cm}^{-1}}$	3380 (O-H stretching) 2967, 2928 (C-H stretching) 1643 (C=O stretching)
^1H NMR ($\text{CDCl}_3 + \text{CD}_3\text{OD}$) (δ ppm) (500 MHz)	13.00 (<i>s</i> , 1H), 7.72 (<i>dd</i> , $J = 8.0$ and 1.5 Hz, 1H), 7.25 (<i>dd</i> , $J = 8.0$ and 1.5 Hz, 1H), 7.20 (<i>t</i> , $J = 8.0$ Hz, 1H), 3.01-2.98 (<i>m</i> , 2H), 2.79 (<i>t</i> , $J = 7.5$ Hz, 2H), 1.80-1.78 (<i>m</i> , 2H), 1.77 (<i>t</i> , $J = 7.5$ Hz, 2H), 1.32 (<i>s</i> , 6H), 1.30 (<i>s</i> , 6H)
^{13}C NMR ($\text{CDCl}_3 + \text{CD}_3\text{OD}$) (δ ppm) (125 MHz)	181.25, 160.48, 157.69, 152.58, 145.35, 144.95, 123.47, 121.00, 120.05, 115.84, 111.09, 107.86, 102.91, 71.45, 71.33, 41.55, 41.15, 29.17, 29.09, 16.89, 16.59
DEPT 135 ⁰	CH ₃ : 29.17, 29.09 CH ₂ : 41.55, 41.15, 16.89, 16.59 CH : 123.47, 120.05, 115.84

Subfraction FB4.3 Chromatogram on normal phase TLC with 1% methanol-chloroform (9 runs) showed three major UV-active spots with the R_f values of 0.14, 0.18 and 0.22. Therefore, it was not further investigated.

Subfraction FB4.4 Chromatogram on normal phase TLC with 1% methanol-chloroform (9 runs) showed two major UV-active spots with the R_f values of 0.14 and 0.18. Further purification on precoated TLC with 2% methanol-chloroform (11 runs) afforded **FP2** as a yellow gum (2.3 mg). Chromatogram on normal phase TLC with 2% methanol-chloroform (4 runs) showed one UV-active spot

with the R_f value of 0.21. Its ^1H NMR spectrum indicated that **FP2** was a mixture of two xanthenes. Because of low quantity, further purification was then not attempted.

Subfraction FB4.5 Chromatogram on normal phase TLC with 1% methanol-chloroform (9 runs) showed no major UV-active spots. Therefore, it was not further investigated.

Subfraction F6.5 Chromatogram on normal phase TLC with 3% methanol-chloroform (3 runs) showed four major UV-active spots with the R_f values of 0.16, 0.19, 0.25 and 0.30. Therefore, it was not further investigated.

Subfraction F6.6 Chromatogram on normal phase TLC with 3% methanol-chloroform (3 runs) showed three major UV-active spots with the R_f values of 0.12, 0.17 and 0.21. It was further separated by column chromatography over reversed-phase silica gel, eluting with 60% methanol-water, followed by decreasing amount of water in methanol and finally with pure methanol. Fractions with the similar chromatogram were combined and evaporated to dryness under reduced pressure to afford three subfractions, as shown in Table 35.

Table 35 Subfractions obtained from F6.6 by column chromatography over reversed-phase silica gel

Subfraction	Weight (g)	Physical appearance
FB6.1	0.0095	Yellow gum
FB6.2	0.0095	Yellow gum
FB6.3	0.0099	Yellow gum

Subfraction FB6.1 Chromatogram on normal phase TLC with 2% methanol-chloroform (9 runs) showed no major UV-active spots. Therefore, it was not further investigated.

Subfraction FB6.2 Chromatogram on normal phase TLC with 2% methanol-chloroform (9 runs) showed one major UV-active spot with the R_f value of 0.38 and one pale UV-active spot with the R_f value of 0.15. Further purification on precoated TLC with 2% methanol-chloroform (14 runs) afforded YU9 (6.1 mg).

Subfraction FB6.3 Chromatogram on normal phase TLC with 2% methanol-chloroform (9 runs) showed no major UV-active spots. Therefore, it was not further investigated.

Subfraction F6.7 Chromatogram on normal phase TLC with 3% methanol-chloroform (3 runs) showed no major UV-active spots. Therefore, it was not further investigated.

Subfraction F7 Chromatogram on normal phase TLC with 2% methanol-chloroform (2 runs) showed four major UV-active spots with the R_f values of 0.03, 0.09, 0.13 and 0.15. Therefore, it was not further investigated.

Subfraction F8 Chromatogram on normal phase TLC with 2% methanol-chloroform (2 runs) showed four major UV-active spots with the R_f values of 0.10, 0.14, 0.18 and 0.32. It was further separated by flash column chromatography over silica gel. Elution was conducted initially with 0.5% methanol-chloroform, followed by increasing amount of methanol and finally with 30% methanol-chloroform. Fractions with the similar chromatogram were combined and evaporated to dryness under reduced pressure to afford three subfractions, as shown in Table 36.

Table 36 Subfractions obtained from F8 by flash column chromatography

Subfraction	Weight (g)	Physical appearance
F8.1	0.0233	Yellow-brown gum
F8.2	0.0202	Yellow gum
F8.3	0.0597	Orange-brown gum

Subfraction F8.1 Chromatogram on normal phase TLC with 3% methanol-chloroform (2 runs) showed many UV-active spots. Therefore, it was not further investigated.

Subfraction F8.2 Chromatogram on normal phase TLC with 3% methanol-chloroform (2 runs) showed two major UV-active spots with the R_f values of 0.19 and 0.26 and one pale UV-active spot with the R_f value of 0.31. It was further separated by flash column chromatography over silica gel. Elution was conducted initially with 0.5% methanol-chloroform, followed by increasing amount of methanol and finally with 20% methanol-chloroform. Fractions with the similar chromatogram were combined and evaporated to dryness under reduced pressure to afford three subfractions, as shown in Table 37.

Table 37 Subfractions obtained from F8.2 by flash column chromatography

Subfraction	Weight (g)	Physical appearance
FD2.1	0.0029	Pale yellow gum
FD2.2	0.0151	Yellow gum
FD2.3	0.0027	Yellow gum

Subfraction FD2.1 Chromatogram on normal phase TLC with 2% methanol-chloroform (5 runs) showed two pale UV-active spots with the R_f values of 0.18 and 0.31. Therefore, it was not further investigated.

Subfraction FD2.2 Chromatogram on normal phase TLC with 2% methanol-chloroform (5 runs) showed two major UV-active spots with the R_f values of 0.17 and 0.24. It was further rechromatographed on precoated TLC with 2% methanol-chloroform (9 runs) to afford two bands.

Band FD2.2A was a pale yellow gum (1.4 mg). Chromatogram on normal phase TLC with 2% methanol-chloroform (4 runs) showed one major UV-active spot with the R_f value of 0.29. It was not further investigated.

Band FD2.2B was a yellow gum (4.9 mg). Chromatogram on normal phase TLC with 2% methanol-chloroform (4 runs) showed one UV-active spot with the R_f value of 0.21. Its ^1H NMR spectral data indicated that it was YU9 which was firstly isolated from **subfraction SA2.2**.

Subfraction FD2.3 Chromatogram on normal phase TLC with 2% methanol-chloroform (5 runs) showed no major UV-active spots. Therefore, it was not further investigated.

Subfraction F8.3 Chromatogram on normal phase TLC with 3% methanol-chloroform (2 runs) showed no major UV-active spots. Therefore, it was not further investigated.

Subfraction F9 Chromatogram on normal phase TLC with 2% methanol-chloroform (2 runs) showed six major UV-active spots with the R_f values of 0.04, 0.08, 0.13, 0.23, 0.25 and 0.31. It was further separated by flash column chromatography over silica gel. Elution was conducted initially with 0.5% methanol-chloroform, followed by increasing amount of methanol and finally with 50% methanol-chloroform. Fractions with the similar chromatogram were combined and

evaporated to dryness under reduced pressure to afford five subfractions, as shown in Table 38.

Table 38 Subfractions obtained from **F9** by flash column chromatography

Subfraction	Weight (g)	Physical appearance
F9.1	0.0613	Yellow-brown gum
F9.2	0.0204	Yellow-brown gum
F9.3	0.0159	Yellow-brown gum
F9.4	0.0846	Yellow-brown gum
F9.5	0.1902	Brown gum

Subfraction F9.1 Chromatogram on normal phase TLC with 2% methanol-chloroform showed many UV-active spots. It was not further investigated because it was obtained in low quantity.

Subfraction F9.2 Chromatogram on normal phase TLC with 2% methanol-chloroform (3 runs) showed one major UV-active spot with the R_f value of 0.29 and two pale UV-active spot with the R_f value of 0.24 and 0.27. It was further separated by flash column chromatography over silica gel. Elution was conducted initially with 0.5% methanol-chloroform, followed by increasing amount of methanol and finally with 10% methanol-chloroform. Fractions with the similar chromatogram were combined and evaporated to dryness under reduced pressure to afford three subfractions, as shown in Table 39.

Table 39 Subfractions obtained from F9.2 by flash column chromatography

Subfraction	Weight (g)	Physical appearance
FE2.1	0.0003	Yellow gum
FE2.2	0.0100	Yellow gum
FE2.3	0.0059	Yellow gum

Subfraction FE2.1 Chromatogram on normal phase TLC with 2% methanol-chloroform (5 runs) showed none of major UV-active spots. Therefore, it was not further investigated.

Subfraction FE2.2 Chromatogram on normal phase TLC with 2% methanol-chloroform (5 runs) showed two major UV-active spots with the R_f values of 0.20 and 0.25 and one pale UV-active spot with the R_f value of 0.29. It was further rechromatographed on precoated TLC with 2% methanol-chloroform (9 runs) afforded two bands.

Band FE2.2A (YU17) was a pale yellow gum (3.1 mg). Chromatogram on normal phase TLC with 2% methanol-chloroform (4 runs) showed one UV-active spot with the R_f value of 0.40.

UV (MeOH) λ_{\max} nm (log ϵ)	220 (5.34), 243 (5.31), 273 (5.05), 315 (5.04)
FT-IR (neat) $\nu_{\text{cm}^{-1}}$	3374 (O-H stretching) 2967, 2927 (C-H stretching) 1646 (C=O stretching)
^1H NMR (CDCl_3) (δ ppm) (500 MHz)	13.43 (<i>s</i> , 1H), 9.26 (<i>brs</i> , 1H), 7.19 (<i>d</i> , $J = 8.0$ Hz, 1H), 6.98 (<i>d</i> , $J = 8.0$ Hz, 1H), 6.41 (<i>s</i> , 1H), 3.58 (<i>q</i> , $J = 7.0$ Hz, 2H), 3.29-3.26 (<i>m</i> , 2H), 2.77 (<i>t</i> , $J = 6.5$ Hz, 2H), 1.80 (<i>t</i> , $J = 6.5$ Hz, 2H), 1.78-1.75 (<i>m</i> , 2H), 1.31 (<i>t</i> , $J = 7.0$ Hz, 3H), 1.31 (<i>s</i> , 6H), 1.23 (<i>s</i> ,

	6H)
¹³ C NMR (CDCl ₃)(δ ppm)	182.64, 163.26, 160.48, 154.54, 145.43, 142.67,
(125 MHz)	136.60, 125.72, 119.25, 118.33, 112.12, 103.51,
	94.01, 76.30, 70.76, 57.53, 45.89, 41.48, 29.69,
	29.25, 24.51, 15.46, 15.28
DEPT 135 ^o	CH ₃ : 29.25, 24.51, 15.46
	CH ₂ : 57.53, 45.89, 41.48, 29.69, 15.28
	CH : 125.72, 119.25, 94.01

Band FE2.2B was a pale yellow gum (0.7 mg). Chromatogram on normal phase TLC with 2% methanol-chloroform (4 runs) showed one major UV-active spot with the R_f value of 0.22. It was not further investigated.

Subfraction FE2.3 Chromatogram on normal phase TLC with 2% methanol-chloroform (5 runs) showed no major UV-active spots. Therefore, it was not further investigated.

Subfraction F9.3 Chromatogram on normal phase TLC with 2% methanol-chloroform (3 runs) showed many UV-active spots. Therefore, it was not further investigated.

Subfraction F9.4 Chromatogram on normal phase TLC with 2% methanol-chloroform (3 runs) showed one major UV-active spot with the R_f value of 0.16 and two minor UV-active spots with the R_f values of 0.11 and 0.22 while chromatogram on reversed-phase TLC with 80% methanol-water (2 runs) showed overlapping UV-active spots with the R_f value of 0.20 and one UV-active spot with the R_f value of 0.40. It was further separated by column chromatography over reversed-phase silica gel, eluting with 60% methanol-water, followed by decreasing amount of water in methanol and finally with pure methanol. Fractions with the similar chromatogram

were combined and evaporated to dryness under reduced pressure to afford five subfractions, as shown in Table 40.

Table 40 Subfractions obtained from F9.4 by column chromatography over reversed-phase silica gel

Subfraction	Weight (g)	Physical appearance
FE4.1	0.0037	Yellow-brown gum
FE4.2	0.0075	Yellow-brown gum
FE4.3	0.0069	Yellow gum
FE4.4	0.0543	Yellow solid
FE4.5	0.0171	Yellow gum

Subfraction FE4.1 Chromatogram on normal phase TLC with 2% methanol-chloroform (4 runs) showed none of major UV-active spots. Therefore, it was not further investigated.

Subfraction FE4.2 Chromatogram on normal phase TLC with 2% methanol-chloroform (4 runs) showed two major UV-active spots with the R_f values of 0.14 and 0.22. It was further rechromatographed on precoated TLC with 2% methanol-chloroform (11 runs) to afford two bands.

Band FE4.2A was a pale yellow gum (2.2 mg). Chromatogram on normal phase TLC with 2% methanol-chloroform (4 runs) showed one UV-active spot with the R_f value of 0.21. Its ^1H NMR spectrum indicated that compound **FE4.2A** was a mixture of two xanthenes which was also found in **FP2**. Because of low quantity, further purification was then not attempted.

Band FE4.2B was a pale yellow gum (1.6 mg). Chromatogram on normal phase TLC with 2% methanol-chloroform (4 runs) showed one UV-active spot with the R_f value of 0.13. It was not further investigated.

Subfraction FE4.3 Chromatogram on normal phase TLC with 2% methanol-chloroform (4 runs) showed none of major UV-active spots. Therefore, it was not further investigated.

Subfraction FE4.4 Chromatogram on normal phase TLC with 2% methanol-chloroform (4 runs) showed three major UV-active spots with the R_f values of 0.14, 0.21 and 0.25. It was further separated by column chromatography over sephadex LH-20, eluting with pure methanol. Fractions with the similar chromatogram were combined and evaporated to dryness under reduced pressure to afford two subfractions, as shown in Table 41.

Table 41 Subfractions obtained from FE4.4 by column chromatography over sephadex LH-20

Subfraction	Weight (g)	Physical appearance
FEA4.1	0.0417	Yellow-brown solid
FEA4.2	0.0086	Yellow gum

Subfraction FEA4.1 Chromatogram on normal phase TLC with 3% methanol-chloroform (7 runs) showed one major UV-active spot with the R_f value of 0.22 and one pale UV-active spot with the R_f value of 0.17. It was further separated by column chromatography over sephadex LH-20, eluting with pure methanol. Fractions with the similar chromatogram were combined and evaporated to dryness under reduced pressure to afford three subfractions, as shown in Table 42.

Table 42 Subfractions obtained from FEA4.1 by column chromatography over sephadex LH-20

Subfraction	Weight (g)	Physical appearance
FEA4.1.1	0.0015	Yellow gum
FEA4.1.2	0.0378	Yellow solid
FEA4.1.3	0.0017	Yellow gum

Subfraction FEA4.1.1 Chromatogram on normal phase TLC with 3% methanol-chloroform (7 runs) showed none of major UV-active spots. Therefore, it was not further investigated.

Subfraction FEA4.1.2 Chromatogram on normal phase TLC with 3% methanol-chloroform (7 runs) showed one major UV-active spot with the R_f value of 0.22 and one pale UV-active spot with the R_f value of 0.17. It was further rechromatographed on precoated TLC with 2% methanol-chloroform (13 runs) to afford YU15 as a yellow solid (29.4 mg), melting at 199.1-200.2 °C. Chromatogram on normal phase TLC with 2% methanol-chloroform (5 runs) showed one UV-active spot with the R_f value of 0.26.

UV (MeOH) λ_{\max} nm (log \mathcal{E})	220 (4.53), 245 (4.48), 264 (4.28), 273 (4.24), 317 (4.19), 369 (3.66)
FT-IR (neat) $\nu_{\text{cm}^{-1}}$	3409 (O-H stretching) 2966, 2925 (C-H stretching) 1643 (C=O stretching)
^1H NMR (Acetone- d_6) (δ ppm) (500 MHz)	13.65 (s, 1H), 7.25 (d, $J = 8.0$ Hz, 1H), 7.04 (d, $J = 8.0$ Hz, 1H), 6.56 (s, 1H), 5.29 (mt, $J = 7.0$ Hz, 1H), 3.36 (d, $J = 7.0$ Hz, 2H), 3.33-3.29 (m, 2H), 1.79 (s,

	3H), 1.78-1.74 (<i>m</i> , 2H), 1.65 (<i>s</i> , 3H), 1.30 (<i>s</i> , 6H)
¹³ C NMR (Acetone- <i>d</i> ₆)(δ ppm)	183.73, 163.83, 161.50, 155.58, 147.07, 144.95,
(125 MHz)	136.56, 131.35, 126.51, 123.28, 120.64, 119.40,
	111.14, 104.00, 93.45, 70.38, 46.94, 30.69, 29.54,
	25.83, 21.88, 17.83
DEPT 135 ⁰	CH ₃ : 29.54, 25.83, 17.83
	CH ₂ : 46.94, 30.69, 21.88
	CH : 126.51, 123.28, 120.64, 93.45

Subfraction FEA4.1.3 Chromatogram on normal phase TLC with 3% methanol-chloroform (7 runs) showed none of major UV-active spots. Therefore, it was not further investigated.

Subfraction FEA4.2 Chromatogram on normal phase TLC with 3% methanol-chloroform (7 runs) showed no major UV-active spots. Therefore, it was not further investigated.

Subfraction FE4.5 Chromatogram on normal phase TLC with 2% methanol-chloroform (4 runs) showed none of major UV-active spots. Therefore, it was not further investigated.

Subfraction F9.5 Chromatogram on normal phase TLC with 2% methanol-chloroform (3 runs) showed no major UV-active spots. It was not further investigated because it was obtained in low quantity.

Subfraction F10 Chromatogram on normal phase TLC with 2% methanol-chloroform (2 runs) showed five major UV-active spots with the R_f values of 0.05, 0.10 0.13, 0.16 and 0.37. It was further separated by flash column chromatography over silica gel. Elution was conducted with 0.5% methanol-chloroform, followed by increasing amount of methanol and finally with pure methanol. Fractions with the similar chromatogram were combined and evaporated to dryness under reduced

pressure to afford fifteen subfractions. Each fraction was obtained in low quantity. Further purification was not then performed.

Subfraction F11 Chromatogram on normal phase TLC with 2% methanol-chloroform (2 runs) showed four major UV-active spots with the R_f values of 0.06, 0.14, 0.18 and 0.22. It was further separated by column chromatography over reversed-phase silica gel, eluting with 40% methanol-water, followed by decreasing amount of water in methanol and finally with pure methanol. Fractions with the similar chromatogram were combined and evaporated to dryness under reduced pressure to afford five subfractions, as shown in Table 43.

Table 43 Subfractions obtained from F11 by column chromatography over reversed-phase silica gel

Subfraction	Weight (g)	Physical appearance
F11.1	0.0526	Orange-yellow gum
F11.2	0.0514	Orange gum
F11.3	0.6330	Orange-yellow gum
F11.4	0.1704	Orange gum
F11.5	0.0374	Orange-red gum

Subfraction F11.1 Chromatogram on normal phase TLC with 5% methanol-chloroform showed no major UV-active spots. Therefore, it was not further investigated.

Subfraction F11.2 Chromatogram on normal phase TLC with 5% methanol-chloroform showed two unseparable UV-active spots with the R_f values of 0.08 and 0.13 and one pale UV-active spot with the R_f value of 0.38. It was further separated by column chromatography over reversed-phase silica gel, eluting with 50% methanol-

water, followed by decreasing amount of water in methanol and finally with pure methanol. Fractions with the similar chromatogram were combined and evaporated to dryness under reduced pressure to afford seven subfractions. Each fraction was obtained in low quantity. Further purification was not then performed.

Subfraction F11.3 Chromatogram on normal phase TLC with 5% methanol-chloroform showed many UV-active spots. Therefore, it was not further investigated.

Subfraction F11.4 Chromatogram on normal phase TLC with 5% methanol-chloroform showed three unseparable UV-active spots with the R_f values of 0.25, 0.35 and 0.40 and one pale UV-active spot with the R_f value of 0.55. It was further separated by column chromatography over reversed-phase silica gel, eluting with 50% methanol-water, followed by decreasing amount of water in methanol and finally with pure methanol. Fractions with the similar chromatogram were combined and evaporated to dryness under reduced pressure to afford four subfractions, as shown in Table 44.

Table 44 Subfractions obtained from F11.4 by column chromatography over reversed-phase silica gel

Subfraction	Weight (g)	Physical appearance
FC4.1	0.0358	Orange gum
FC4.2	0.0892	Orange gum
FC4.3	0.0408	Yellow gum
FC4.4	0.0129	Red-brown gum

Subfraction FC4.1 Chromatogram on normal phase TLC with 2% methanol-chloroform (3 runs) showed no major UV-active spots. Therefore, it was not further investigated.

Subfraction FC4.2 Chromatogram on normal phase TLC with 2% methanol-chloroform (3 runs) showed three major UV-active spots with the R_f values of 0.11, 0.25 and 0.33. It was further separated by column chromatography over reversed-phase silica gel, eluting with 65% methanol-water, followed by decreasing amount of water in methanol and finally with pure methanol. Fractions with the similar chromatogram were combined and evaporated to dryness under reduced pressure to afford five subfractions, as shown in Table 45.

Table 45 Subfractions obtained from FC4.2 by column chromatography over reversed-phase silica gel

Subfraction	Weight (g)	Physical appearance
FCC2.1	0.0090	Yellow-brown gum
FCC2.2	0.0311	Yellow-brown gum
FCC2.3	0.0163	Yellow-brown gum
FCC2.4	0.0252	Yellow-brown gum
FCC2.5	0.0088	Yellow-brown gum

Subfraction FCC2.1 Chromatogram on normal phase TLC with 3% methanol-chloroform (5 runs) showed no major UV-active spots. Therefore, it was not further investigated.

Subfraction FCC2.2 Chromatogram on normal phase TLC with 3% methanol-chloroform (5 runs) showed one major UV-active spot with the R_f value of 0.43. It was further separated by flash column chromatography over silica gel. Elution

was conducted initially with 0.5% methanol-chloroform, followed by increasing amount of methanol and finally with 30% methanol-chloroform. Fractions with the similar chromatogram were combined and evaporated to dryness under reduced pressure to afford three subfractions, as shown in Table 46.

Table 46 Subfractions obtained from FCC2.2 by flash column chromatography

Subfraction	Weight (g)	Physical appearance
FCCC2.1	0.0049	Pale yellow gum
FCCC2.2	0.0114	Pale yellow gum
FCCC2.3	0.0090	Yellow gum

Subfraction FCCC2.1 Chromatogram on normal phase TLC with 3% methanol-chloroform (2 runs) showed no major UV-active spots. Therefore, it was not further investigated.

Subfraction FCCC2.2 Chromatogram on normal phase TLC with 3% methanol-chloroform (2 runs) showed one major UV-active spot with the R_f value of 0.25 and one pale UV-active spot with the R_f value of 0.18. It was further rechromatographed on precoated TLC with 20% ethyl acetate-petroleum ether (13 runs) to give two bands.

Band P1A (YU14) was a pale yellow gum (4.9 mg). Chromatogram on normal phase TLC with 20% ethyl acetate-petroleum ether (3 runs) showed one UV-active spot with the R_f value of 0.22.

UV (MeOH) λ_{\max} nm (log \mathcal{E}) 220 (3.98), 245 (4.05), 264 (3.85), 273 (3.80),
319 (3.78), 369 (3.32)

FT-IR (neat) $\nu_{\text{cm}^{-1}}$	3421 (O-H stretching) 2925, 2848 (C-H stretching) 1646 (C=O stretching)
^1H NMR (CDCl_3)(δ ppm) (500 MHz)	13.77 (<i>s</i> , 1H), 7.20 (<i>d</i> , $J = 8.0$ Hz, 1H), 7.01 (<i>d</i> , $J = 8.0$ Hz, 1H), 6.38 (<i>s</i> , 1H), 5.31 (<i>mt</i> , $J = 7.5$ Hz, 1H), 3.47 (<i>d</i> , $J = 7.5$ Hz, 2H), 3.29 (<i>s</i> , 3H), 3.24-3.21 (<i>m</i> , 2H), 1.86 (<i>s</i> , 3H), 1.78 (<i>s</i> , 3H), 1.76-1.74 (<i>m</i> , 2H), 1.29 (<i>s</i> , 6H)
^{13}C NMR (CDCl_3)(δ ppm) (125 MHz)	182.65, 162.18, 160.98, 154.33, 145.22, 142.50, 137.07, 135.98, 125.96, 121.18, 119.45, 118.53, 109.05, 103.95, 93.36, 74.92, 49.24, 41.42, 29.75, 29.68, 25.85, 25.14, 21.44, 17.93
DEPT 135 ⁰	CH ₃ : 49.24, 25.85, 25.14, 17.93 CH ₂ : 41.42, 29.75, 21.44 CH : 125.96, 121.18, 119.45, 93.36

Band P1B was a pale yellow gum (0.6 mg). Chromatogram on normal phase TLC with 20% ethyl acetate-petroleum ether (3 runs) showed one UV-active spot with the R_f value of 0.17. Therefore, it was not further investigated.

Subfraction FCCC2.3 Chromatogram on normal phase TLC with 3% methanol-chloroform (2 runs) showed no major UV-active spots. Therefore, it was not further investigated.

Subfraction FCC2.3 Chromatogram on normal phase TLC with 3% methanol-chloroform (5 runs) showed two major UV-active spots with the R_f values of 0.41 and 0.50 and unseparable UV-active spots with the R_f values of 0.20. It was further separated by flash column chromatography over silica gel. Elution was conducted initially with 0.5% methanol-chloroform, followed by increasing amount of methanol and finally with 30% methanol-chloroform. Fractions with the similar

chromatogram were combined and evaporated to dryness under reduced pressure to afford ten subfractions. Each fraction was obtained in low quantity. Further purification was not then performed.

Subfraction FCC2.4 Chromatogram on normal phase TLC with 3% methanol-chloroform (5 runs) showed one major UV-active spot with the R_f value of 0.20 and one pale UV-active spot with the R_f value of 0.50. It was further separated by flash column chromatography over silica gel. Elution was conducted initially with 0.5% methanol-chloroform, followed by increasing amount of methanol and finally with 30% methanol-chloroform. Fractions with the similar chromatogram were combined and evaporated to dryness under reduced pressure to afford six subfractions. Each fraction was obtained in low quantity. Further purification was not then performed.

Subfraction FCC2.5 Chromatogram on normal phase TLC with 3% methanol-chloroform (5 runs) showed no major UV-active spots. Therefore, it was not further investigated.

Subfraction FC4.3 Chromatogram on normal phase TLC with 2% methanol-chloroform (3 runs) showed unseparable UV-active spots with the R_f values of 0.14 and one pale UV-active spot with the R_f value of 0.35. It was further separated by column chromatography over reversed-phase silica gel, eluting with 50% methanol-water, followed by decreasing amount of water in methanol and finally with pure methanol. Fractions with the similar chromatogram were combined and evaporated to dryness under reduced pressure to afford six subfractions. Each fraction was obtained in low quantity. Further purification was not then performed.

Subfraction FC4.4 Chromatogram on normal phase TLC with 2% methanol-chloroform (3 runs) showed no major UV-active spots. Therefore, it was not further investigated.

Subfraction F11.5 Chromatogram on normal phase TLC with 5% methanol-chloroform showed no major UV-active spots. Therefore, it was not further investigated.

Subfraction F12 Chromatogram on normal phase TLC with 2% methanol-chloroform (2 runs) showed unseparable UV-active spots. Therefore, it was not further investigated.

Subfraction F13 Chromatogram on normal phase TLC with 2% methanol-chloroform (2 runs) showed seven major UV-active spots with the R_f values of 0.09, 0.16, 0.18, 0.20, 0.23 and 0.29, 0.33. It was not further investigated because of limitation of time.

Subfraction F14 Chromatogram on normal phase TLC with 2% methanol-chloroform (2 runs) showed no major UV-active spots. Therefore, it was not further investigated.

Subfraction GNT13.4 Chromatogram on normal phase TLC with 7% methanol-chloroform showed unseparable UV-active spots. It was not further investigated because of limitation of time.

Fraction GNT14 Chromatogram on normal phase TLC with 30% methanol-chloroform showed two major UV-active spots with the R_f values of 0.05 and 0.25. It was not further investigated because of limitation of time.

Fraction GNT15 Chromatogram on normal phase TLC with 30% methanol-chloroform showed two major UV-active spots with the R_f values of 0.06 and 0.87 and pale spots with the R_f values of 0.22 and 0.67. It was not further investigated because of limitation of time.

Fraction GNT16 Chromatogram on normal phase TLC with 30% methanol-chloroform showed none of major UV-active spots. Therefore, it was not further investigated.

CHAPTER 3

RESULTS AND DISCUSSION

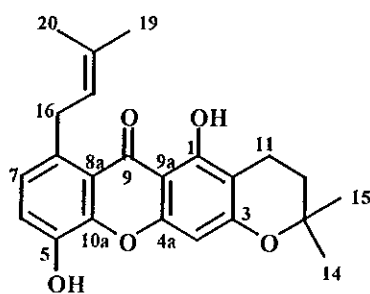
The leaves of *G. nigrolineata* were extracted with MeOH and the resulting dried residue was then separated by various chromatographic techniques to afford ten new xanthenes (YU1, YU2, YU6, YU9, YU10, YU11, YU14, YU15, YU16 and YU17), one new quinone derivative (YU5) and one new isoflavone-like compound (YU13) together with four known xanthenes (YU3, YU4, YU7 and YU12) and friedelin (YU8). All structures were determined by 1D and 2D NMR spectroscopic data. Known compounds were also identified by comparison of their spectral data with those reported in the literature.

3.1 Compound YU1

Compound YU1 was obtained as a pale yellow gum. It showed a molecular ion at m/z 380 (Figure 10), which corresponded to a molecular formula of $C_{23}H_{24}O_5$. The IR spectrum (Figure 3) exhibited absorption bands at 3365 (a hydroxyl group) and 1646 cm^{-1} (a conjugated carbonyl group). The UV spectrum (Figure 2) with absorption bands at 321 and 376 nm indicated that YU1 was a xanthone derivative. The ^1H NMR spectrum (Figure 4) (Table 47) showed the presence of two hydroxyl groups [δ 5.87 (1H, *brs*) and 13.60 (1H, *s*, chelated OH)], two *ortho*-coupled aromatic protons [δ 7.02 and 7.19 (1H each, *d*, $J = 8.0$ Hz)] and one singlet aromatic proton [δ 6.30 (1H, *s*)]. Other signals could be attributed to an isoprenyl group [δ 3.98 (2H, *d*, $J = 7.5$ Hz), 5.36 (1H, *mt*, $J = 7.5$ Hz) and 1.74 (6H, *s*)] and a dimethylchromane ring

$[\delta 2.73$ (2H, *t*, $J = 7.0$ Hz), 1.85 (2H, *t*, $J = 7.0$ Hz), and 1.38 (6H, *s*)]. The ^{13}C NMR spectrum (**Figure 5**) (**Table 47**) showed 22 resonances for 23 carbon atoms: twelve quaternary carbons ($\delta 182.93, 161.27, 161.03, 154.02, 145.28, 142.53, 135.40, 132.57, 118.43, 104.35, 103.31$ and 76.35), four methine carbons ($\delta 124.85, 123.09, 119.20$ and 94.10), three methylene carbons ($\delta 33.06, 31.78$ and 16.08) and four methyl carbons [$\delta 26.75$ (2xC), 25.90 and 17.99]. The appearance of the methylene protons (H-16) of the isoprenyl group at $\delta 3.98$ suggested that this side chain was at a *peri* position to a carbonyl group. These methylene protons showed cross peaks in the HMBC spectrum (**Figure 9**) (**Table 48**) with an aromatic methine carbon ($\delta 124.85$, C-7) and a quaternary aromatic carbon ($\delta 118.43$, C-8a), indicating that the isoprenyl group linked with C-8 ($\delta 135.40$). One of the *ortho*-coupled aromatic proton ($\delta 7.02$, H-7) gave a cross peak in the HMQC spectrum (**Figure 8**) with C-7 and also showed correlations with the methylene carbon ($\delta 33.06$, C-16) of the isoprenyl side chain and an oxygenated aromatic carbon ($\delta 142.53$, C-5) in the HMBC spectrum. Enhancement of the signal of the aromatic proton, H-7, (**Figure 7**) was observed upon irradiation of the methylene protons, H-16, of the isoprenyl group. These confirmed that this aromatic proton and the isoprenyl group were on C-7 and C-8, respectively. The C-5 position was substituted by a hydroxyl group according to the chemical-shift value of C-5. Thus, the other *ortho*-coupled aromatic proton at $\delta 7.19$ was attributed to H-6. The chelated hydroxyl group ($\delta 13.60$, 1-OH) was placed at C-1 because of its formation of an intramolecular hydrogen bond with the carbonyl group. In the HMBC spectrum, this chelated hydroxy proton and the methylene protons ($\delta 1.85$, H-12) of the chromane ring gave cross peaks with the same quaternary aromatic carbon ($\delta 104.35$, C-2), indicating that the dimethylchromane ring was fused to C-2 and C-3 ($\delta 161.27$) of the xanthone nucleus with an ether linkage at C-3. The remaining aromatic proton at $\delta 6.30$ was then assigned to H-4 due to its cross peaks with C-2, C-3, C-4a (154.02), C-9 (182.93) and C-9a (103.31). Therefore, YU1 was assigned as 1,5-dihydroxy-8-(3-

methylbut-2-enyl)-6',6'-dimethyldihydropyrano(2',3':3,2)xanthone (1), a new naturally occurring xanthone.



(1)

Table 47 The ^1H and ^{13}C NMR data of compounds YU1 and YU2 in CDCl_3

Position	δ_{H} (mult., J_{Hz})		δ_{C} (C-Type)	
	YU1	YU2	YU1	YU2
1-OH	13.60 (<i>s</i>)	13.56 (<i>s</i>)	161.03 (C)	158.18 (C)
2			104.35 (C)	104.87 (C)
3			161.27 (C)	160.38 (C)
4	6.30 (<i>s</i>)	6.31 (<i>s</i>)	94.10 (CH)	94.17 (CH)
4a			154.02 (C)	155.50 (C)
5-OH	5.87 (<i>brs</i>)	5.69 (<i>brs</i>)	142.53 (C)	142.46 (C)
6	7.19 (<i>d</i> , 8.0)	7.20 (<i>d</i> , 8.0)	119.20 (CH)	119.42 (CH)
7	7.02 (<i>d</i> , 8.0)	7.04 (<i>d</i> , 8.0)	124.85 (CH)	125.18 (CH)
8			135.40 (C)	135.49 (C)
8a			118.43 (C)	118.40 (C)
9			182.93 (C=O)	182.88 (C=O)
9a			103.31 (C)	104.17 (C)
10a			145.28 (C)	145.14 (C)
11	2.73 (<i>t</i> , 7.0)	6.75 (<i>d</i> , 10.0)	16.08 (CH_2)	115.50 (CH)
12	1.85 (<i>t</i> , 7.0)	5.60 (<i>d</i> , 10.0)	31.78 (CH_2)	127.45 (CH)

Table 47 (Continued)

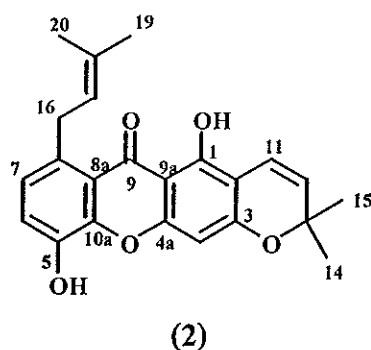
Position	δ_{H} (mult., J_{Hz})		δ_{C} (C-Type)	
	YU1	YU2	YU1	YU2
13			76.35 (C)	78.26 (C)
14, 15	1.38 (s)	1.48 (s)	26.75 (CH ₃)	28.35 (CH ₃)
16	3.98 (d, 7.5)	3.98 (d, 7.0)	33.06 (CH ₂)	33.01 (CH ₂)
17	5.36 (mt, 7.5)	5.36 (mt, 7.0)	123.09 (CH)	122.92 (CH)
18			132.57 (C)	132.70 (C)
19	1.74 (s)	1.74 (s)	25.90 (CH ₃)	25.87 (CH ₃)
20	1.74 (s)	1.74 (s)	17.99 (CH ₃)	17.98 (CH ₃)

Table 48 Major HMBC correlations of compounds YU1 and YU2

Proton	YU1	YU2
1-OH	C-1, C-2, C-9a	C-1, C-2, C-9a
H-4	C-2, C-3, C-4a, C-9, C-9a	C-2, C-3, C-4a, C-9, C-9a
H-6	C-5, C-7, C-8, C-8a, C-10a	C-5, C-7, C-8, C-10a
H-7	C-5, C-6, C-8a, C-16	C-5, C-6, C-8, C-8a, C-9, C-16
H-11	C-1, C-2, C-3, C-12, C-13	C-1, C-3, C-13
H-12	C-2, C-11, C-13, C-14, C-15	C-2, C-13, C-14, C-15
H-14, H-15	C-12, C-13, C-14, C-15	C-11, C-12, C-13, C-14, C-15
H-16	C-7, C-8, C-8a, C-17, C-18	C-7, C-8, C-8a, C-17, C-18
H-17	C-16, C-19, C-20	C-16, C-19, C-20
H-19, H-20	C-17, C-18, C-19, C-20	C-17, C-18, C-19, C-20

3.2 Compound YU2

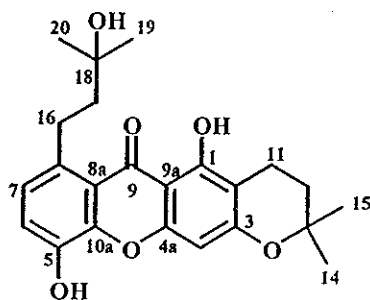
Compound **YU2** was isolated as a yellow gum with a molecular formula of $C_{23}H_{22}O_5$ (m/z 378) determined by EIMS (Figure 18). The IR spectrum (Figure 12) showed absorption bands at 3394 and 1650 cm^{-1} for a hydroxyl group and a conjugated carbonyl functionality, respectively. The UV spectrum (Figure 11) exhibited characteristic absorption bands of a xanthone chromophore at 295, 322 and 380 nm. Its 1H NMR data (Figure 13) (Table 47) were similar to those of **YU1**. It contained two-*ortho* coupled protons [δ 7.20 and 7.04 (1H each, *d*, $J = 8.0$ Hz)], one singlet aromatic proton [δ 6.31 (1H, *s*)], signals for an isoprenyl group [δ 3.98 (2H, *d*, $J = 7.0$ Hz), 5.36 (1H, *mt*, $J = 7.0$ Hz) and 1.74 (6H, *s*)] and two hydroxyl groups [δ 5.69 (1H, *brs*) and 13.56 (1H, *s*, chelated OH)]. The differences in 1H NMR spectrum were two doublets of *cis*-olefinic protons of a dimethylchromene ring [δ 6.75 (1H, *d*, $J = 10.0$ Hz) and 5.60 (1H, *d*, $J = 10.0$ Hz)] which replaced two triplet signals belonging to the methylene protons of the dimethylchromane ring in **YU1**. Important observations from the HMBC experiment (Figure 17) (Table 48) were as follows. The correlations of H-11/C-1 (δ 158.18), H-11/C-3 (δ 160.38) and H-12/C-2 (δ 104.87) suggested that the dimethylchromene ring was fused in a linear fashion to the xanthone nucleus and the oxygen atom of the dimethylchromene ring was attached to C-3. The location of the isoprenyl group at C-8 and the non-chelated hydroxyl group (δ 5.69) at C-5 were found to be identical to that of **YU1** since they showed the same HMBC data. The structure of **YU2** was therefore concluded to be 1,5-dihydroxy-8-(3-methylbut-2-enyl)-6',6'-dimethylpyrano(2',3':3,2)xanthone (**2**), a new trioxygenated xanthone.



3.3 Compound YU9

Compound YU9, obtained as a yellow gum, had a molecular formula of $C_{23}H_{26}O_6$ (m/z 398) as established by EIMS (Figure 26). Its UV spectrum (Figure 19) (λ_{max} 296, 319 and 373) showed the occurrence of a xanthone nucleus. The IR spectrum (Figure 20) showed absorption bands at 3416 and 1646 cm^{-1} for a hydroxyl group and a carbonyl functionality, respectively. Compound YU9 showed similar 1H NMR characteristic signals of a 1-hydroxy-6',6'-dimethyldihydropyrano(2',3':3,2)-xanthone moiety [δ 13.48 (1H, *s*), 2.72 (2H, *t*, $J = 6.5$ Hz), 1.85 (2H, *t*, $J = 6.5$ Hz), 1.38 (6H, *s*) and 6.30 (1H, *s*)] (Figure 21) (Table 49) to those found in YU1. In addition, a multiplet-signal of two methylene protons at δ 1.78-1.75 (*m*, H-17) replaced the olefinic-proton signal of the C-8 isoprenyl group in YU1 while singlets for two methyl groups appeared at higher field (δ 1.31). Comparison of the 1H and ^{13}C NMR (Figure 22) (Table 49) spectra of YU1 and YU9 showed that the differences were due to signals of a five-carbon substituent at C-8. In the ^{13}C NMR spectrum of YU9, there were signals for two methylene carbons at δ 29.83 (C-16) and δ 45.90 (C-17), a quaternary carbon connected to a hydroxyl group at δ 70.71 (C-18), and two methyl carbons at δ 29.27 (C-19 and C-20). These data suggested that YU9 contained a 3-hydroxy-3-methylbutyl moiety [δ 3.30-3.26 (2H, *m*), 1.78-1.75 (2H, *m*) and 1.31 (6H, *s*)], instead of an isoprenyl group. The highly-deshielded position (δ 3.30-3.26) of the

methylene protons (H-16) of the 3-hydroxy-3-methylbutyl unit indicated that this side chain was at C-8, a *peri* position to a carbonyl group. This was confirmed by the following HMBC data (Figure 25) (Table 50). The methylene protons, H-16, showed cross peaks with a methine carbon (δ 125.70, C-7) and a quaternary carbon (δ 118.30, C-8a) while other methylene protons, H-17, showed a cross peak with a quaternary aromatic carbon (δ 136.68, C-8). The aromatic protons at δ 7.20 and 7.00 were then assigned to H-6 and H-7, respectively, based on above data as well as HMQC data (Figure 24). The 3J correlation between H-7 and an oxyaromatic carbon (δ 142.67, C-5) revealed the presence of a hydroxyl group at C-5. The chelated OH proton (δ 13.48) caused cross peaks with two quaternary aromatic carbons at δ 104.46 (C-2) and 103.25 (C-9a), indicating that C-2 position was not substituted by a group possessing an oxygen function. Furthermore, C-2 correlated to methylene protons (δ 1.85, H-12) of the chromane ring in the HMBC spectrum. These data suggested that the chromane ring was fused to C-2 and C-3 (δ 161.48) and formed an ether linkage with C-3, the same position and arrangement as the dimethylchromane ring in the structure of YU1. Therefore, YU9 was assigned as 1,5-dihydroxy-8-(3-hydroxy-3-methylbutyl)-6',6'-dimethyldihydropyrano(2',3':3,2)xanthone (3), a new naturally occurring xanthone which might be derived from YU1 by hydration reaction at the C-8 substituent.



(3)

Table 49 The ^1H and ^{13}C NMR data of compounds YU1 and YU9 in CDCl_3

Position	δ_{H} (mult., J_{Hz})		δ_{C} (C-Type)	
	YU9	YU1	YU9	YU1
1-OH	13.48 (s)	13.60 (s)	161.00 (C)	161.03 (C)
2			104.46 (C)	104.35 (C)
3			161.48 (C)	161.27 (C)
4	6.32 (s)	6.30 (s)	94.15 (CH)	94.10 (CH)
4a			154.04 (C)	154.02 (C)
5-OH		5.87 (brs)	142.67 (C)	142.53 (C)
6	7.20 (d, 8.5)	7.19 (d, 8.0)	119.35 (CH)	119.20 (CH)
7	7.00 (d, 8.5)	7.02 (d, 8.0)	125.70 (CH)	124.85 (CH)
8			136.68 (C)	135.40 (C)
8a			118.30 (C)	118.43 (C)
9			182.67 (C=O)	182.93 (C=O)
9a			103.25 (C)	103.31 (C)
10a			145.45 (C)	145.28 (C)
11	2.72 (t, 6.5)	2.73 (t, 7.0)	16.05 (CH ₂)	16.08 (CH ₂)
12	1.85 (t, 6.5)	1.85 (t, 7.0)	31.73 (CH ₂)	31.78 (CH ₂)
13			76.45 (C)	76.35 (C)
14, 15	1.38 (s)	1.38 (s)	26.73 (CH ₃)	26.75 (CH ₃)
16	3.30-3.26 (m)	3.98 (d, 7.5)	29.83 (CH ₂)	33.06 (CH ₂)
17	1.78-1.75 (m)	5.36 (mt, 7.5)	45.90 (CH ₂)	123.09 (CH)
18			70.71 (C)	132.57 (C)
19	1.31 (s)	1.74 (s)	29.27 (CH ₃)	25.90 (CH ₃)
20	1.31 (s)	1.74 (s)	29.27 (CH ₃)	17.99 (CH ₃)

Table 50 Major HMBC correlations of compounds YU1 and YU9

Proton	YU9	YU1
1-OH	C-1, C-2, C-9a	C-1, C-2, C-9a
H-4	C-2, C-3, C-4a, C-9, C-9a	C-2, C-3, C-4a, C-9, C-9a
H-6	C-5, C-8, C-8a, C-10a	C-5, C-7, C-8, C-8a, C-10a
H-7	C-5, C-8a, C-16	C-5, C-6, C-8a, C-16
H-11	C-1, C-2, C-3, C-12, C-13	C-1, C-2, C-3, C-12, C-13
H-12	C-2, C-11, C-13, C-14, C-15	C-2, C-11, C-13, C-14, C-15
H-14, H-15	C-11, C-12, C-13, C-14, C-15	C-12, C-13, C-14, C-15
H-16	C-7, C-8, C-8a, C-17, C-18	C-7, C-8, C-8a, C-17, C-18
H-17	C-8, C-18, C-19, C-20	C-16, C-19, C-20
H-19, H-20	C-17, C-18, C-19, C-20	C-17, C-18, C-19, C-20

3.4 Compound YU10

Compound **YU10** was obtained as a yellow solid, melting at 161.0-162.0 °C. Its molecular formula was determined as $C_{23}H_{24}O_6$ (m/z 396) by EIMS (Figure 34). Its UV (Figure 27) and IR (Figure 28) data suggested that **YU10** also possesses a xanthone skeleton. The 1H NMR spectrum (Figure 29) (Table 51) consisted of one hydrogen-bonded hydroxyl signal [δ 13.44 (1H, *s*)], two *ortho*-coupled aromatic signals [δ 7.22 and 7.02 (1H each, *d*, $J = 8.5$ Hz)], a doublet of an aromatic proton [δ 6.33 (1H, *d*, $J = 0.5$ Hz)], signals of a 3-hydroxy-3-methylbutyl unit [δ 3.29-3.26 (2H, *m*), 1.78-1.75 (2H, *m*) and 1.32 (6H, *s*)] and characteristic signals of a chromene ring [δ 6.74 (1H, *dd*, $J = 10.0$ and 0.5 Hz), 5.61 (1H, *d*, $J = 10.0$ Hz) and 1.48 (6H, *s*)]. Its 1H NMR data were similar to those of **YU9**. Direct comparison of their 1H NMR spectra indicated that the signals for methylene protons, H-11 and H-12, of **YU9** were replaced, in **YU10**, by two deshielded doublets (δ 6.74 and 5.61) associated with two

cis-olefinic protons ($J = 10.0$ Hz). A small coupling constant ($J = 0.5$ Hz) between the more deshielded chromene hydrogen (H-11) and the aromatic proton at $\delta 6.33$ by a 5J extended W pathway indicated that this aromatic proton was at *ortho* position to the chromene oxygen. Furthermore, the correlations of H-11/C-1 ($\delta 158.15$), H-11/C-3 ($\delta 160.61$) and H-12/C-2 ($\delta 104.94$) in the HMBC spectrum (Figure 33) (Table 52) suggested that the dimethylchromene ring was fused in a linear fashion to the xanthone nucleus and its oxygen atom was attached to C-3. The signal of the chelated hydroxyl group at $\delta 13.44$ and the chemical shift value of C-1 established the substituent at C-1 to be a hydroxyl group. The highly-deshielded position of the methylene protons ($\delta 3.29$ - 3.26 , H-16) of the 3-hydroxy-3-methylbutyl unit suggested that this side chain was at the other *peri* position to carbonyl group. Supported evidence came from HMBC data which also indicated that YU10 possessed the identical left-handed aromatic ring to YU9. Accordingly, the structure of YU10 was determined as 1,5-dihydroxy-8-(3-hydroxy-3-methylbutyl)-6',6'-dimethylpyrano(2',3':3,2)xanthone (4), a new trioxygenated xanthone.

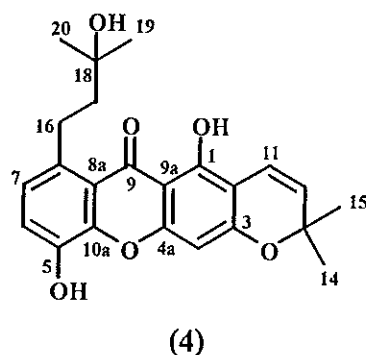


Table 51 The ^1H and ^{13}C NMR data of compounds YU9 and YU10 in CDCl_3

Position	δ_{H} (mult., J_{Hz})		δ_{C} (C-Type)	
	YU10	YU9	YU10	YU9
1-OH	13.44 (s)	13.48 (s)	158.15 (C)	161.00 (C)
2			104.94 (C)	104.46 (C)
3			160.61 (C)	161.48 (C)
4	6.33 (d, 0.5)	6.32 (s)	94.23 (CH)	94.15 (CH)
4a			155.57 (C)	154.04 (C)
5-OH			142.65 (C)	142.67 (C)
6	7.22 (d, 8.5)	7.20 (d, 8.5)	119.58 (CH)	119.35 (CH)
7	7.02 (d, 8.5)	7.00 (d, 8.5)	126.06 (CH)	125.70 (CH)
8			136.78 (C)	136.68 (C)
8a			118.35 (C)	118.30 (C)
9			182.68 (C=O)	182.67 (C=O)
9a			104.15 (C)	103.25 (C)
10a			145.34 (C)	145.45 (C)
11	6.74 (dd, 10.0 and 0.5)	2.72 (t, 6.5)	115.44 (CH)	16.05 (CH ₂)
12	5.61 (d, 10.0)	1.85 (t, 6.5)	127.55 (CH)	31.73 (CH ₂)
13			78.37 (C)	76.45 (C)
14, 15	1.48 (s)	1.38 (s)	28.38 (CH ₃)	26.73 (CH ₃)
16	3.29-3.26 (m)	3.30-3.26 (m)	29.82 (CH ₂)	29.83 (CH ₂)
17	1.78-1.75 (m)	1.78-1.75 (m)	45.86 (CH ₂)	45.90 (CH ₂)
18-OH			70.73 (C)	70.71 (C)
19, 20	1.32 (s)	1.31 (s)	29.28 (CH ₃)	29.27 (CH ₃)

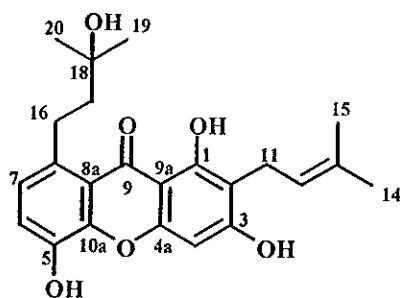
Table 52 Major HMBC correlations of compounds YU9 and YU10

Proton	YU10	YU9
1-OH	C-1, C-2, C-9a	C-1, C-2, C-9a
H-4	C-2, C-3, C-4a, C-9, C-9a	C-2, C-3, C-4a, C-9, C-9a
H-6	C-5, C-8, C-8a, C-10a	C-5, C-8, C-8a, C-10a
H-7	C-5, C-8a, C-16	C-5, C-8a, C-16
H-11	C-1, C-2, C-3, C-13	C-1, C-2, C-3, C-12, C-13
H-12	C-2, C-13, C-14, C-15	C-2, C-11, C-13, C-14, C-15
H-14, H-15	C-11, C-12, C-13, C-14, C-15	C-11, C-12, C-13, C-14, C-15
H-16	C-7, C-8, C-8a, C-17, C-18	C-7, C-8, C-8a, C-17, C-18
H-17	C-8, C-16, C-18, C-19, C-20	C-8, C-18, C-19, C-20
H-19, H-20	C-17, C-18, C-19, C-20	C-17, C-18, C-19, C-20

3.5 Compound YU15

Compound YU15 was obtained as a yellow solid, melting at 199.1-200.2 °C. Its UV (Figure 35) and IR (Figure 36) spectra were indicative of a xanthone derivative. Its ¹H (Figure 37) (Table 53) and ¹³C NMR (Figure 38) (Table 53) spectra were similar to those of YU9 and YU10. The presence of two *ortho*-coupled aromatic proton [δ 7.25 and 7.04 (1H each, *d*, *J* = 8.0 Hz)] and a 3-hydroxy-3-methylbutyl group [δ 3.33-3.29 (2H, *m*), 1.78-1.74 (2H, *m*) and 1.30 (6H, *s*)] suggested that YU15 possessed the same left-handed aromatic ring as YU9 and YU10: a hydroxyl group and the 3-hydroxy-3-methylbutyl group at C-5 and C-8, respectively. Similarity of HMBC data (Figure 42) (Table 54) supported above conclusion. In addition, its ¹H NMR spectrum showed signals for an isoprenyl group [δ 3.36 (2H, *d*, *J* = 7.0 Hz), 5.29 (1H, *mt*, *J* = 7.0 Hz), 1.65 (3H, *s*) and 1.79 (3H, *s*)] and an aromatic proton signal at δ 6.56 (1H, *s*). In the HMBC spectrum, the methylene protons signal at δ 3.36 (H-11) of the

isoprenyl group showed cross peaks with a quaternary aromatic carbon signal at δ 111.14 (C-2) and two oxygenated carbon signals at δ 161.50 (C-1) and 163.83 (C-3), indicating that the isoprenyl unit was located at C-2. The chemical-shift values of C-1 and C-3 together with the presence of the chelated hydroxyl group suggested the substituents at C-1 and C-3 to be hydroxy groups. The NOEDIFF data (Figure 40) showed that the methyl signal at δ 1.65 was *cis* to an olefinic proton, H-12, according to the enhancement of this methyl signal after irradiation of H-12. The aromatic proton signal at δ 6.56 was attributed to H-4 due to 2J correlations with carbon signals at δ 163.83 (C-3) and 155.58 (C-4a) and 3J correlations with carbon signals at δ 111.14 (C-2) and 104.00 (C-9a). Thus, compound YU15 was determined as 1,3,5-trihydroxy-2-(3-methylbut-2-enyl)-8-(3-hydroxy-3-methylbutyl)xanthone (5), a new naturally occurring xanthone. It might be a precursor of the cyclized compounds, YU9 and YU10.



(5)

Table 53 The ^1H and ^{13}C NMR data of compounds YU10 in CDCl_3 and YU15 in Acetone- d_6

Position	δ_{H} (mult., J_{Hz})		δ_{C} (C-Type)	
	YU15	YU10	YU15	YU10
1-OH	13.65 (s)	13.44 (s)	161.50 (C)	158.15 (C)
2			111.14 (C)	104.94 (C)
3			163.83 (C)	160.61 (C)
4	6.56 (s)	6.33 (d, 0.5)	93.45 (CH)	94.23 (CH)
4a			155.58 (C)	155.57 (C)
5-OH			144.95 (C)	142.65 (C)
6	7.25 (d, 8.0)	7.22 (d, 8.5)	120.64 (CH)	119.58 (CH)
7	7.04 (d, 8.0)	7.02 (d, 8.5)	126.51 (CH)	126.06 (CH)
8			136.56 (C)	136.78 (C)
8a			119.40 (C)	118.35 (C)
9			183.73 (C=O)	182.68 (C=O)
9a			104.00 (C)	104.15 (C)
10a			147.07 (C)	145.34 (C)
11	3.36 (d, 7.0)	6.74 (dd, 10.0 and 0.5)	21.88 (CH ₂)	115.44 (CH)
12	5.29 (mt, 7.0)	5.61 (d, 10.0)	123.28 (CH)	127.55 (CH)
13			131.35 (C)	78.37 (C)
14	1.65 (s)	1.48 (s)	25.83 (CH ₃)	28.38 (CH ₃)
15	1.79 (s)	1.48 (s)	17.83 (CH ₃)	28.38 (CH ₃)
16	3.33-3.29 (m)	3.29-3.26 (m)	30.69 (CH ₂)	29.82 (CH ₂)
17	1.78-1.74 (m)	1.78-1.75 (m)	46.94 (CH ₂)	45.86 (CH ₂)
18-OH			70.38 (C)	70.73 (C)
19, 20	1.30 (s)	1.32 (s)	29.54 (CH ₃)	29.28 (CH ₃)

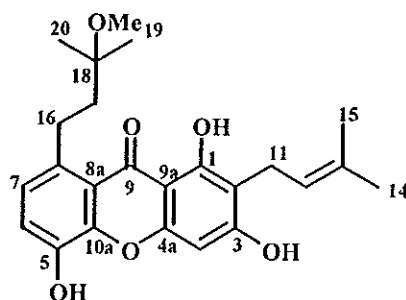
Table 54 Major HMBC correlations of compounds YU10 and YU15

Proton	YU15	YU10
1-OH	C-1, C-2, C-9a	C-1, C-2, C-9a
H-4	C-2, C-3, C-4a, C-9, C-9a	C-2, C-3, C-4a, C-9, C-9a
H-6	C-5, C-7, C-8, C-10a	C-5, C-8, C-8a, C-10a
H-7	C-5, C-6, C-8, C-8a, C-16	C-5, C-8a, C-16
H-11	C-1, C-2, C-3, C-12, C-13	C-1, C-2, C-3, C-13
H-12	C-11, C-14, C-15	C-2, C-13, C-14, C-15
H-14	C-12, C-13, C-15	C-11, C-12, C-13, C-15
H-15	C-12, C-13, C-14	C-11, C-12, C-13, C-14
H-16	C-7, C-8, C-8a, C-17, C-18	C-7, C-8, C-8a, C-17, C-18
H-17	C-8, C-16, C-18, C-19, C-20	C-8, C-16, C-18, C-19, C-20
H-19, H-20	C-17, C-18, C-19, C-20	C-17, C-18, C-19, C-20

3.6 Compound YU14

Compound YU14 was obtained as a pale yellow gum. The IR spectrum (Figure 44) exhibited absorption bands due to a hydroxyl group (3421 cm^{-1}) and a conjugated carbonyl group (1646 cm^{-1}). The UV spectrum (Figure 43) was identical to those of YU15. Its ^1H NMR spectrum (Figure 45) (Table 55) was similar to that of YU15 except for an additional signal of a methoxyl group at $\delta 3.29$. The ^{13}C NMR spectrum (Figure 46) showed the same number of quaternary, methine and methylene carbons as those found in YU15 except for the fact that it contained one more methyl carbon at $\delta 49.24$. This carbon corresponded to a methoxy carbon due to its chemical-shift value. These data supported the presence of the methoxyl group. In the HMBC spectrum (Figure 50) (Table 56), these methoxy protons gave a cross peak with a quaternary carbon ($\delta 74.92$, C-18), indicating the attachment of the methoxyl group at

C-18. Thus, the side chain in YU14 became a 3-methoxy-3-methylbutyl unit [δ 3.24-3.21 (2H, *m*), 1.76-1.74 (2H, *m*), 3.29 (3H, *s*) and 1.29 (6H, *s*)]. The correlations of H-16/C-7 (δ 125.96), H-16/C-8a (δ 118.53) and H-17/C-8 (δ 137.70) suggested that the 3-methoxy-3-methylbutyl unit was attached to C-8. The remaining HMBC correlations were almost identical to those of YU15, indicating that YU14 contained the chelated hydroxyl group at C-1, the isoprenyl group at C-2 and two free hydroxyl groups at C-3 and C-5. The NOEDIFF data observed (Figure 48) for the olefinic H-12 and the methyl protons (δ 1.78, Me-14) suggested that they were *cis*. Thus, YU14 was assigned as 1,3,5-trihydroxy-2-(3-methylbut-2-enyl)-8-(3-methoxy-3-methylbutyl)xanthone (6), the methyl ether of YU15 and a new naturally occurring xanthone.



(6)

Table 55 The ^1H and ^{13}C NMR data of compounds YU14 in CDCl_3 and YU15 in Acetone- d_6

Position	δ_{H} (mult., J_{Hz})		δ_{C} (C-Type)	
	YU14	YU15	YU14	YU15
1-OH	13.77 (<i>s</i>)	13.65 (<i>s</i>)	160.98 (C)	161.50 (C)
2			109.05 (C)	111.14 (C)
3-OH			162.18 (C)	163.83 (C)
4	6.38 (<i>s</i>)	6.56 (<i>s</i>)	93.36 (CH)	93.45 (CH)
4a			154.33 (C)	155.58 (C)
5-OH			142.50 (C)	144.95 (C)
6	7.20 (<i>d</i> , 8.0)	7.25 (<i>d</i> , 8.0)	119.45 (CH)	120.64 (CH)
7	7.01 (<i>d</i> , 8.0)	7.04 (<i>d</i> , 8.0)	125.96 (CH)	126.51 (CH)
8			137.07 (C)	136.56 (C)
8a			118.53 (C)	119.40 (C)
9			182.65 (C=O)	183.73 (C=O)
9a			103.95 (C)	104.00 (C)
10a			145.22 (C)	147.07 (C)
11	3.47 (<i>d</i> , 7.5)	3.36 (<i>d</i> , 7.0)	21.44 (CH ₂)	21.88 (CH ₂)
12	5.31 (<i>mt</i> , 7.5)	5.29 (<i>mt</i> , 7.0)	121.18 (CH)	123.28 (CH)
13			135.98 (C)	131.35 (C)
14	1.78 (<i>s</i>)	1.65 (<i>s</i>)	25.85 (CH ₃)	25.83 (CH ₃)
15	1.86 (<i>s</i>)	1.79 (<i>s</i>)	17.93 (CH ₃)	17.83 (CH ₃)
16	3.24-3.21 (<i>m</i>)	3.33-3.29 (<i>m</i>)	29.75 (CH ₂)	30.69 (CH ₂)
17	1.76-1.74 (<i>m</i>)	1.78-1.74 (<i>m</i>)	41.42 (CH ₂)	46.94 (CH ₂)
18			74.92 (C)	70.38 (C)
18-OMe	3.29 (<i>s</i>)		49.24 (CH ₃)	
19, 20	1.29 (<i>s</i>)	1.30 (<i>s</i>)	25.14 (CH ₃)	29.54 (CH ₃)

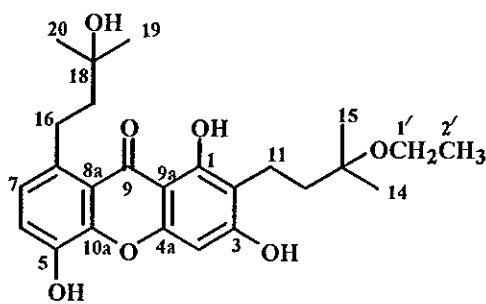
Table 56 Major HMBC correlations of compounds YU14 and YU15

Proton	YU14	YU15
1-OH	C-1, C-2, C-9a	C-1, C-2, C-9a
H-4	C-2, C-3, C-4a, C-9, C-9a	C-2, C-3, C-4a, C-9, C-9a
H-6	C-5, C-8, C-10a	C-5, C-7, C-8, C-10a
H-7	C-5, C-6, C-9, C-16	C-5, C-6, C-8, C-8a, C-16
H-11	C-1, C-2, C-3, C-12, C-13	C-1, C-2, C-3, C-12, C-13
H-12	C-11, C-14, C-15	C-11, C-14, C-15
H-14	C-12, C-13, C-15	C-12, C-13, C-15
H-15	C-12, C-13, C-14	C-12, C-13, C-14
H-16	C-7, C-8, C-8a, C-17	C-7, C-8, C-8a, C-17, C-18
H-17	C-8, C-16, C-18, C-19, C-20	C-8, C-16, C-18, C-19, C-20
MeO-18	C-18	
H-19, H-20	C-17, C-18, C-19, C-20	C-17, C-18, C-19, C-20

3.7 Compound YU17

Compound **YU17** was obtained as a pale yellow gum. The IR spectrum (**Figure 52**) suggested the presence of a hydroxyl group (3374 cm^{-1}) and a conjugated carbonyl group (1646 cm^{-1}). Its UV spectrum (**Figure 51**) (λ_{max} 220, 243, 273 and 315) showed the occurrence of a xanthone nucleus. Its ^1H (**Figure 53**) (**Table 57**) spectrum was similar to that of **YU15**. The presence of two *ortho*-coupled aromatic protons [δ 7.19 and 6.98 (1H each, *d*, $J = 8.0\text{ Hz}$)] and a 3-hydroxy-3-methylbutyl group [δ 3.29-3.26 (2H, *m*), 1.78-1.75 (2H, *m*) and 1.31 (6H, *s*)] suggested that **YU17** possessed the same left-handed aromatic ring as **YU15**: a hydroxyl group and 3-hydroxy-3-methylbutyl group at C-5 and C-8, respectively. Similarity of HMBC data (**Figure 57**) (**Table 58**) supported above conclusion. In addition, signals for an ethoxyl

group [δ 3.58 (2H, *q*, $J = 7.0$ Hz) and 1.31 (3H, *t*, $J = 7.0$ Hz)], two methyl groups [δ 1.23 (6H, *s*)] and four methylene protons [δ 2.77 (2H, *t*, $J = 6.5$ Hz) and 1.80 (2H, *t*, $J = 6.5$ Hz)] replaced signals of the C-2 isoprenyl group in YU15. Comparison of the ^1H and ^{13}C NMR (Figure 54) (Table 57) spectra of YU15 and YU17 confirmed the difference in the structure of C-2 substituent. In the ^{13}C NMR spectrum, the C-2 substituent in YU17 contained signals for two methylene carbons at δ 15.28 (C-11) and 41.48 (C-12), a quaternary carbon at δ 76.30 (C-13), two methyl carbons at δ 24.51 (C-14 and C-15) and ethoxy carbons at δ 57.53 (C-1') and 15.46 (C-2'). In the HMBC spectrum, the methylene protons (H-1') of the ethoxyl group gave a cross peak with the quaternary carbon, C-13, indicating its attachment at C-13. These data suggested that YU17 contained a 3-ethoxy-3-methylbutyl unit. The correlations of H-11/C-1 (160.48), H-11/C-3 (163.26) and H-12/C-2 (112.12) suggested that the 3-ethoxy-3-methylbutyl unit was attached to C-2. The chemical-shift values of C-1 and C-3 together with the presence of the chelated hydroxyl group suggested the substituents at C-1 and C-3 to be hydroxyl groups. The aromatic proton signal at δ 6.41 was attributed to H-4 due to 3J correlations with the ^{13}C signals at δ 112.12 (C-2) and 103.51 (C-9a). Thus, compound YU17 was determined as 1,3,5-trihydroxy-2-(3-ethoxy-3-methylbutyl)-8-(3-hydroxy-3-methylbutyl)xanthone (7), a new naturally occurring xanthone.



(7)

Table 57 The ^1H and ^{13}C NMR data of compounds YU15 in Acetone- d_6 and YU17 in CDCl_3

Position	δ_{H} (mult., J_{Hz})		δ_{C} (C-Type)	
	YU17	YU15	YU17	YU15
1-OH	13.43 (<i>s</i>)	13.65 (<i>s</i>)	160.48 (C)	161.50 (C)
2			112.12 (C)	111.14 (C)
3-OH			163.26 (C)	163.83 (C)
4	6.41 (<i>s</i>)	6.56 (<i>s</i>)	94.01 (CH)	93.45 (CH)
4a			154.54 (C)	155.58 (C)
5-OH			142.67 (C)	144.95 (C)
6	7.19 (<i>d</i> , 8.0)	7.25 (<i>d</i> , 8.0)	119.25 (CH)	120.64 (CH)
7	6.98 (<i>d</i> , 8.0)	7.04 (<i>d</i> , 8.0)	125.72 (CH)	126.51 (CH)
8			136.60 (C)	136.56 (C)
8a			118.33 (C)	119.40 (C)
9			182.64 (C=O)	183.73 (C=O)
9a			103.51 (C)	104.00 (C)
10a			145.43 (C)	147.07 (C)
11	2.77 (<i>t</i> , 6.5)	3.36 (<i>d</i> , 7.0)	15.28 (CH ₂)	21.88 (CH ₂)
12	1.80 (<i>t</i> , 6.5)	5.29 (<i>mt</i> , 7.0)	41.48 (CH ₂)	123.28 (CH)
13			76.30 (C)	131.35 (C)
1'	3.58 (<i>q</i> , 7.0)		57.53 (CH ₂)	
2'	1.31 (<i>t</i> , 7.0)		15.46 (CH ₃)	
14	1.23 (<i>s</i>)	1.65 (<i>s</i>)	24.51 (CH ₃)	25.83 (CH ₃)
15	1.23 (<i>s</i>)	1.79 (<i>s</i>)	24.51 (CH ₃)	17.83 (CH ₃)
16	3.29-3.26 (<i>m</i>)	3.33-3.29 (<i>m</i>)	29.69 (CH ₂)	30.69 (CH ₂)
17	1.78-1.75 (<i>m</i>)	1.78-1.74 (<i>m</i>)	45.89 (CH ₂)	46.94 (CH ₂)
18			70.76 (C)	70.38 (C)
19, 20	1.31 (<i>s</i>)	1.30 (<i>s</i>)	29.25 (CH ₃)	29.54 (CH ₃)

Table 58 Major HMBC correlations of compounds YU15 and YU17

Proton	YU17	YU15
I-OH	C-1, C-2, C-9a	C-1, C-2, C-9a
H-4	C-2, C-3, C-4a, C-9a	C-2, C-3, C-4a, C-9, C-9a
H-6	C-5, C-8, C-10a	C-5, C-7, C-8, C-10a
H-7	C-5, C-8a, C-16	C-5, C-6, C-8, C-8a, C-16
H-11	C-1, C-2, C-3, C-12, C-13	C-1, C-2, C-3, C-12, C-13
H-12	C-2, C-11, C-13, C-14, C-15	C-11, C-14, C-15
H-1'	C-2', C-13	
H-2'	C-1'	
H-14	C-12, C-13, C-15	C-12, C-13, C-15
H-15	C-12, C-13, C-14	C-12, C-13, C-14
H-16	C-7, C-8, C-8a, C-17	C-7, C-8, C-8a, C-17, C-18
H-17	C-16, C-18	C-8, C-16, C-18, C-19, C-20
H-19, H-20	C-17, C-18, C-19, C-20	C-17, C-18, C-19, C-20

3.8 Compound YU4

Compound YU4 was isolated as a yellow solid, melting at 157.0-158.5 °C. It showed a molecular ion at m/z 380 (Figure 67) which corresponded to a molecular formula of $C_{23}H_{24}O_5$. The IR spectrum (Figure 59) exhibited absorption bands at 3379 and 1642 cm^{-1} for a hydroxyl group and a conjugated carbonyl functionality. The absorption bands at λ_{max} 319 and 369 nm in the UV spectrum (Figure 58) indicated that YU4 has a xanthone chromophore. The 1H NMR spectrum (Figure 60) (Table 59) showed characteristic peaks of a 1,2,3-trisubstituted benzene ring in an ABX system [δ 7.78 and 7.32 (1H each, dd $J = 8.0$ and 1.5 Hz) and 7.25 (1H, t , $J = 8.0$ Hz)] and two isoprenyl groups [δ 3.56 (2H, d , $J = 7.0$ Hz), 5.28 (1H, mt , $J = 7.0$ Hz), 1.88 (3H, s)

and 1.76 (3H, *s*); 3.50 (2H, *d*, $J = 7.0$ Hz), 5.30 (1H, *mt*, $J = 7.0$ Hz), 1.86 (3H, *s*) and 1.79 (3H, *s*) in addition to three hydroxyl groups [δ 13.21 (1H, *s*, chelated OH), 6.55 (1H, *brs*) and 5.72 (1H, *brs*)]. The ^{13}C NMR spectrum (Figure 61) (Table 59) showed 22 resonances for 23 carbon atoms: twelve quaternary carbons (δ 181.11, 160.91, 158.64, 152.38, 144.38, 144.00, 136.24, 133.53, 120.86, 109.08, 105.42 and 103.30), five methine carbons (δ 123.82, 122.20, 121.16, 119.75 and 116.90), two methylene carbons (δ 22.06 and 21.63) and four methyl carbons [δ 25.88, 25.67, 17.96 (2xC)]. In the HMBC spectrum (Figure 66) (Table 59), one of aromatic protons in the ABX system, which appeared at the lowest field (δ 7.78, H-8), gave cross peaks with a carbonyl carbon (δ 181.11, C-9), a methine aromatic carbon (δ 119.75, C-6) and an oxygenated aromatic carbon (δ 144.00, C-10a). These results proved that this aromatic proton was located at C-8 (δ 116.90), a *peri* position to the carbonyl group. Based on the values of coupling constant, two remaining aromatic protons at δ 7.32 and 7.25 were then attributed to H-6 and H-7, respectively. They showed a correlation with the same oxyaromatic carbon (δ 144.38, C-5), in the HMBC spectrum, suggesting that the C-5 position was substituted by a hydroxyl group. The chelated hydroxy proton (δ 13.21) caused cross peaks with three aromatic carbons at δ 158.64 (C-1), 109.08 (C-2) and 103.30 (C-9a), indicating that the C-2 position was not substituted by a group possessing an oxygen function. The methylene protons, H-16, of the isoprenyl group correlated to C-1, C-2 and C-3 (δ 160.91) whereas the methylene protons, H-11, of the other isoprenyl group correlated to C-3, C-4 (δ 105.42) and C-4a (δ 152.38). Consequently, two isoprenyl units were located at C-2 and C-4. The hydroxyl group was then assigned to be at C-3 according to the chemical-shift value of C-3. In addition, irradiation of both vinylic methyl protons [Me-14 (δ 1.76) and Me-19 (δ 1.79)], in the NOEDIFF spectra (Figure 63 and 64), enhanced only signals of olefinic protons, H-12 (δ 5.28) and H-17 (δ 5.30), respectively. These indicated that olefinic protons, H-12 and H-17, were *cis* to the vinylic methyl protons. YU4 was then

identified as 8-desoxygartanin (**8**) which was previously isolated from *Garcinia mangostana* (Govindachari, *et al.*, 1971).

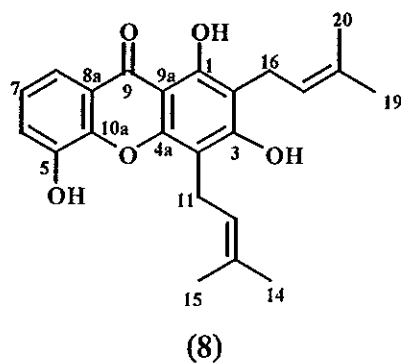


Table 59 The NMR data of compound YU4 in CDCl₃

Position	YU4		HMBC correlation	8-desoxygartanin
	δ_{H} (mult, J_{Hz})	δ_{C} (C-Type)		δ_{H} (mult, $J_{\text{Hz}})^a$
1-OH	13.21 (<i>s</i>)	158.64 (C)	C-1, C-2, C-9a	13.61 (<i>s</i>)
2		109.08 (C)		
3-OH	6.55 (<i>brs</i>)	160.91 (C)	C-2, C-3, C-4	9.75 (<i>s</i>)
4		105.42 (C)		
4a		152.38 (C)		
5-OH	5.72 (<i>brs</i>)	144.38 (C)		9.05(<i>s</i>)
6	7.32 (<i>dd</i> , 8.0 and 1.5)	119.75 (CH)	C-5, C-8, C-10a	7.30-7.05 (<i>m</i>)
7	7.25 (<i>t</i> , 8.0)	123.82 (CH)	C-5, C-8a, C-10a	7.30-7.05 (<i>m</i>)
8	7.78 (<i>dd</i> , 8.0 and 1.5)	116.90 (CH)	C-5, C-6, C-9, C-10a	7.58 (<i>q</i>)
8a		120.86 (C)		
9		181.11 (C=O)		
9a		103.30 (C)		

Table 59 (Continued)

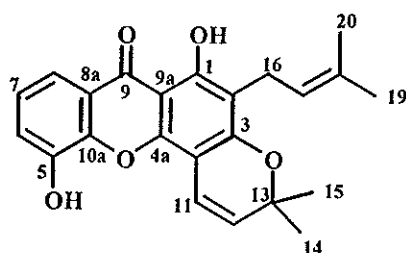
Position	YU4		HMBC correlation	8-desoxygartanin
	δ_{H} (mult., J_{Hz})	δ_{C} (C-Type)		δ_{H} (mult., $J_{\text{Hz}})^{\text{a}}$
10a		144.00 (C)		
11	3.56 (<i>d</i> , 7.0)	22.06 (CH ₂)	C-3, C-4, C-4a, C-12, C-13	3.60-3.40 (<i>br</i>)
12	5.28 (<i>mt</i> , 7.0)	122.20 (CH)	C-15	5.24 (<i>br</i>)
13		133.53 (C)		
14	1.76 (<i>s</i>)	25.67 (CH ₃)	C-12, C-13, C-15	1.66 (<i>s</i>)
15	1.88 (<i>s</i>)	17.96 (CH ₃)	C-12, C-13, C-14	1.82 (<i>s</i>)
16	3.50 (<i>d</i> , 7.0)	21.63 (CH ₂)	C-1, C-2, C-3, C-17, C-18	3.60-3.40 (<i>br</i>)
17	5.30 (<i>mt</i> , 7.0)	121.16 (CH)	C-16, C-19	5.24 (<i>br</i>)
18		136.24 (C)		
19	1.79 (<i>s</i>)	25.88 (CH ₃)	C-17, C-18, C-20	1.66 (<i>s</i>)
20	1.86 (<i>s</i>)	17.96 (CH ₃)	C-18, C-19	1.82 (<i>s</i>)

^a ¹H NMR data of 8-desoxygartanin in CDCl₃/CD₃SOCD₃

3.9 Compound YU3

Compound YU3 was obtained as a yellow solid, melting at 180.0-182.0 °C. The UV absorption (Figure 68) indicated YU3 to be a xanthone derivative. The IR spectrum (Figure 69) showed absorption bands for a hydroxyl group (3365 cm⁻¹) and a conjugated carbonyl group (1646 cm⁻¹). It had a molecular ion at *m/z* 378 in EIMS (Figure 76), corresponding to a molecular formula of C₂₃H₂₂O₅. Its ¹H NMR spectrum (Figure 70) (Table 60) was similar to that of YU4: characteristic peaks of a 1,2,3-trisubstituted benzene ring [δ 7.79 and 7.32 (1H each, *dd*, J = 8.0 and 1.5 Hz) and 7.25 (1H, *t*, J = 8.0 Hz)], an isoprenyl group [δ 5.26 (1H, *mt*, J = 7.5 Hz), 3.37 (2H, *d*, J = 7.5 Hz), 1.82 (3H, *s*) and 1.70 (3H, *s*)] and a chelated hydroxyl group [δ 13.22 (1H, *s*)].

The other signals were attributed to protons of a dimethylchromene ring [δ 6.80 (1H, *d*, $J = 10.0$ Hz), 5.65 (1H, *d*, $J = 10.0$ Hz) and 1.50 (6H, *s*)]. The HMBC data (Figure 75) (Table 60) of all aromatic protons of the 1,2,3-trisubstituted benzene ring were identical to those of YU4, indicating that YU3 contained only a hydroxyl substituent at C-5. The location of the isoprenyl group, the dimethylchromene ring and the chelated-hydroxyl group on the right-handed ring of the xanthone nucleus was established by the following HMBC data. The isoprenyl unit was assigned to be attached at C-2 (δ 112.22) by the correlations between H-16 (δ 3.37) and C-1 (δ 160.53), C-2 and C-3 (δ 158.60). In addition, the enhancement of the signal of an olefinic proton, H-17 (δ 5.26), upon irradiation at δ 1.70 [vinylic methyl proton (Me-19)] in the NOEDIFF spectrum (Figure 73), suggested that this olefinic proton was *cis* to Me-19. The chelated hydroxyl group was definitely attached at C-1. The remaining dimethylchromene ring was found to be fused in an angular form at C-4 (δ 100.64) through an oxygen at C-3 according to the HMBC correlations between the *cis*-olefinic proton (δ 6.80, H-11) and two oxygenated aromatic carbons, C-3 and C-4a. YU3 was then identified as ananixanthone (9) which was previously isolated from *Symphonia globulifera* (Bayma, *et al.*, 1998).



(9)

Table 60 The NMR data of compound YU3 in CDCl₃

Position	YU3		HMBC correlation	ananixanthone	
	δ_{H} (mult., J_{Hz})	δ_{C} (C-Type)		δ_{H} (mult., $J_{\text{Hz}})^{\text{a}}$	δ_{C} (C-Type) ^a
1-OH	13.22 (s)	160.53 (C)	C-1, C-2, C-9a	13.08 (s)	160.90 (C)
2		112.22 (C)			112.60 (C)
3		158.60 (C)			159.00 (C)
4		100.64 (C)			101.10 (C)
4a		149.22 (C)			149.70 (C)
5-OH		144.25 (C)		5.69 (s)	144.80 (C)
6	7.32 (dd, 8.0 and 1.5)	120.10 (CH)	C-5, C-8, C-10a	7.30 (dd, 7.8 and 1.8)	120.60 (CH)
7	7.25 (t, 8.0)	124.00 (CH)	C-5, C-8a, C-10a	7.24 (t, 7.8)	124.30 (CH)
8	7.79 (dd, 8.0 and 1.5)	117.12 (CH)	C-5, C-6, C-9, C-10a	7.75 (dd, 7.8 and 1.8)	117.80 (CH)
8a		121.16 (C)			121.60 (C)
9		180.75 (C=O)			181.20 (C=O)
9a		103.13 (C)			103.60 (C)
10a		144.07 (C)			144.60 (C)
11	6.80 (d, 10.0)	115.00 (CH)	C-3, C-4a, C-13	6.75 (d, 10.0)	115.40 (CH)
12	5.65 (d, 10.0)	127.40 (CH)	C-4, C-13	5.26 (d, 10.0)	127.70 (CH)
13		78.10 (C)			78.50 (C)
14, 15	1.50 (s)	28.16 (CH ₃)	C-12, C-13, C-14, C-15	1.48 (s)	28.60 (CH ₃)
16	3.37 (d, 7.5)	21.22 (CH ₂)	C-1, C-2, C-3, C-17, C-18	3.50 (d, 6.7)	21.60 (CH ₂)
17	5.26 (mt, 7.5)	121.86 (CH)	C-16, C-19, C-20	5.24 (d, 6.7)	122.30 (CH)
18		131.70 (C)			132.10 (C)
19	1.70 (s)	25.81 (CH ₃)	C-17, C-18, C-20	1.87 (s)	26.20 (CH ₃)

Table 60 (Continued)

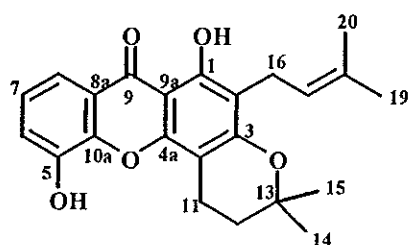
Position	YU3		HMBC correlation	ananixanthone	
	δ_{H} (mult., J_{Hz})	δ_{C} (C-Type)		δ_{H} (mult., $J_{\text{Hz}})^{\text{a}}$	δ_{C} (C-Type) ^a
20	1.82 (s)	17.91 (CH ₃)	C-17, C-18, C-19	1.72 (s)	18.30 (CH ₃)

^a ¹H and ¹³C NMR data of ananixanthone in CDCl₃

3.10 Compound YU6

Compound **YU6** was obtained as a yellow gum. The molecular formula was determined as C₂₃H₂₄O₅ by EIMS (Figure 85). The UV (Figure 77) and IR spectra (Figure 78) suggested that **YU6** was also a xanthone derivative. Its ¹H NMR spectrum (Figure 79) (Table 61) was similar to that of **YU3**: signals for a 1,2,3-trisubstituted benzene ring [δ 7.80 and 7.31 (1H each, *dd*, $J = 8.0$ and 1.5 Hz) and 7.26 (1H, *t*, $J = 8.0$ Hz)], an isoprenyl group [δ 3.36 (2H, *d*, $J = 7.5$ Hz), 5.27 (1H, *mt*, $J = 7.5$ Hz), 1.68 and 1.82 (3H each, *s*)] and a chelated-hydroxyl group [δ 12.86 (1H, *s*)]. However, two doublets belonging to the olefinic protons, H-11 and H-12, of the dimethylchromene residue in **YU3** were replaced by two triplets of the methylene protons, H-11 and H-12, of the dimethylchromane unit in **YU6**. In the HMBC spectrum (Figure 84) (Table 62), both methylene protons (δ 2.90, H-11) of the chromane ring and that (δ 3.36, H-16) of the isoprenyl group gave cross peaks with the same oxyaromatic carbon (δ 159.37, C-3), while the other methylene protons (δ 1.91, H-12) correlated with a quaternary aromatic carbon (δ 98.96, C-4). These data indicated that the dimethylchromane ring was fused to the xanthone nucleus at the same position as the dimethylchromene ring in **YU3**. The isoprenyl group was also attached to the same carbon, C-2. The NOEDIFF data (Figure 82) indicated that the

methyl signal at δ 1.68, Me-19, was *cis* to an olefinic proton, H-17, according to the enhancement of this methyl signal after irradiation of H-17. In addition, the HMBC correlations of three aromatic protons were identical to those of YU3. Thus, YU6 was a dihydropyran derivative of YU3 and assigned as 1,5-dihydroxy-2-(3-methylbut-2-enyl)-6',6'-dimethyldihydropyrano(2',3':3,4)xanthone (10), a new naturally occurring xanthone.



(10)

Table 61 The ^1H and ^{13}C data of compounds YU3 and YU6 in CDCl_3

Position	δ_{H} (mult., J_{Hz})		δ_{C} (C-Type)	
	YU6	YU3	YU6	YU3
1-OH	12.86 (<i>s</i>)	13.22 (<i>s</i>)	158.07 (C)	160.53 (C)
2			112.06 (C)	112.22 (C)
3			159.37 (C)	158.60 (C)
4			98.96 (C)	100.64 (C)
4a			151.90 (C)	149.22 (C)
5-OH	5.66 (<i>brs</i>)		144.08 (C)	144.25 (C)
6	7.31 (<i>dd</i> , 8.0 and 1.5)	7.32 (<i>dd</i> , 8.0 and 1.5)	119.57 (CH)	120.10 (CH)
7	7.26 (<i>t</i> , 8.0)	7.25 (<i>t</i> , 8.0)	123.81 (CH)	124.00 (CH)
8	7.80 (<i>dd</i> , 8.0 and 1.5)	7.79 (<i>dd</i> , 8.0 and 1.5)	117.08 (CH)	117.12 (CH)
8a			121.25 (C)	121.16 (C)

Table 61 (Continued)

Position	δ_{H} (mult., J_{Hz})		δ_{C} (C-Type)	
	YU6	YU3	YU6	YU3
9			180.65 (C=O)	180.75 (C=O)
9a			103.03 (C)	103.13 (C)
10a			144.25 (C)	144.07 (C)
11	2.90 (<i>t</i> , 7.0)	6.80 (<i>d</i> , 10.0)	16.48 (CH ₂)	115.00 (CH)
12	1.91 (<i>t</i> , 7.0)	5.65 (<i>d</i> , 10.0)	31.49 (CH ₂)	127.40 (CH)
13			76.07 (C)	78.10 (C)
14, 15	1.41 (<i>s</i>)	1.50 (<i>s</i>)	26.79 (CH ₃)	28.16 (CH ₃)
16	3.36 (<i>d</i> , 7.5)	3.37 (<i>d</i> , 7.5)	21.38 (CH ₂)	21.22 (CH ₂)
17	5.27 (<i>mt</i> , 7.5)	5.26 (<i>mt</i> , 7.5)	122.11 (CH)	121.86 (CH)
18			131.47 (C)	131.70 (C)
19	1.68 (<i>s</i>)	1.70 (<i>s</i>)	25.84 (CH ₃)	25.81 (CH ₃)
20	1.82 (<i>s</i>)	1.82 (<i>s</i>)	17.93 (CH ₃)	17.91 (CH ₃)

Table 62 Major HMBC correlations of compounds YU3 and YU6

Proton	YU6	YU3
1-OH	C-1, C-2, C-9a	C-1, C-2, C-9a
H-6	C-8, C-10a	C-5, C-8, C-10a
H-7	C-5, C-8a, C-10a	C-5, C-8a, C-10a
H-8	C-6, C-9, C-10a	C-5, C-6, C-9, C-10a
H-11	C-3, C-4, C-4a, C-12, C-13	C-3, C-4a, C-13
H-12	C-4, C-11, C-13, C-14, C-15	C-4, C-13
H-14, H-15	C-12, C-13, C-14, C-15	C-12, C-13, C-14, C-15
H-16	C-1, C-2, C-3, C-17, C-18	C-1, C-2, C-3, C-17, C-18

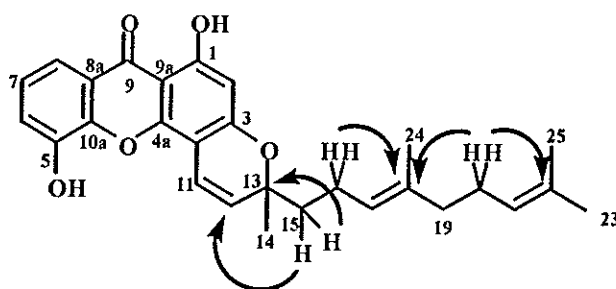
Table 62 (Continued)

Proton	YU6	YU3
H-17	C-16, C-19, C-20	C-16, C-19, C-20
H-19	C-17, C-18, C-20	C-17, C-18, C-20
H-20	C-17, C-18, C-19	C-17, C-18, C-19

3.11 Compound YU11

Compound YU11 was isolated as a yellow gum. The molecular formula of $C_{28}H_{30}O_5$ was determined by its molecular ion at m/z 447 $[M+H]^+$ in the FABMS spectrum (Figure 95). The IR spectrum (Figure 87) suggested the presence of a hydroxyl group (3424 cm^{-1}) and a conjugated carbonyl group (1647 cm^{-1}). Its UV spectrum (Figure 86) (λ_{max} 294, 310, 329 and 376 nm) showed the occurrence of a xanthone nucleus. The ^1H NMR spectrum (Figure 88) (Table 63) showed characteristic signals of a 1,2,3-trisubstituted benzene ring [δ 7.79 and 7.34 (1H each, *dd*, $J = 8.0$ and 1.5 Hz) and 7.27 (1H, *t*, $J = 8.0$ Hz)], a chelated hydroxyl group [δ 13.00 (1H, *s*)] and a methylchromene ring [δ 6.83 (1H, *dd*, $J = 10.0$ and 0.5 Hz), 5.61 (1H, *d*, $J = 10.0$ Hz) and 1.47 (3H, *s*)]. All aromatic protons of the 1,2,3-trisubstituted benzene ring showed identical HMBC correlations (Figure 94) (Table 64) to those in YU3, indicating that both YU11 and YU3 had the same left-handed aromatic ring. A small coupling constant ($J = 0.5$ Hz) between the more deshielded chromene hydrogen and an aromatic proton at δ 6.30, occurred by 5J extended W pathway, suggested that this aromatic proton was *ortho* to the chromene oxygen. It showed 2J cross peaks with two oxyaromatic carbons, δ 163.41 (C-1) and δ 161.36 (C-3), and a 3J cross peak with a quaternary carbon, C-4 (δ 100.81). These data established the location of this aromatic proton at C-2 (δ 99.58). The fusion of the

methylchromene ring at C-3 and C-4 with an ether linkage at C-3 was established by correlations of H-11/C-3 and H-12/C-4. The remaining signals in the ^1H NMR spectrum belonged to a 4,8-dimethylnon-3,7-dienyl group [δ 1.86-1.78 (1H, *m*), 1.73-1.68 (1H, *m*), 2.16-2.11 (2H, *m*), 5.11 (1H, *mt*, $J = 7.5$ Hz), 1.98-1.94 (2H, *m*), 2.08-2.00 (2H, *m*), 5.08 (1H, *mt*, $J = 7.5$ Hz), 1.67 (3H, *d*, $J = 1.0$ Hz), 1.58 (3H, *s*) and 1.59 (3H, *s*)]. The structure of the dienyl moiety was established using HMBC correlations as shown. Cross peaks between the methylene protons, H-15 (δ 1.86-1.78 and 1.73-1.68) with an olefinic carbon, C-12 (δ 126.62) and an oxycarbon, C-13, linked C-15 of the dienyl moiety to C-13 of the methylchromene ring. The *E*-configuration of the C-17/C-18 double bond in the 4,8-dimethylnon-3,7-dienyl side chain was deduced from the NOEDIFF spectrum (Figure 91) since irradiation of Me-24 (δ 1.58) affected only signals of methylene protons, H-16, H-19 and H-20 but did not enhanced the signal of the olefinic proton, H-17. Upon irradiation of Me-23 (δ 1.67), enhancement of the signal of H-21 (δ 5.08) was observed (Figure 92). Therefore, this methyl group was *cis* to H-21. Thus, YU11 was assigned as 1,5-dihydroxy-6'-methyl-6'-(4,8-dimethylnon-3,7-dienyl)pyrano(2',3':3,4)xanthone (11), a new naturally occurring xanthone.



(11)

Table 63 The ^1H and ^{13}C data of compounds YU3 and YU11 in CDCl_3

Position	δ_{H} (mult., J_{Hz})		δ_{C} (C-Type)	
	YU11	YU3	YU11	YU3
1-OH	13.00 (<i>s</i>)	13.22 (<i>s</i>)	163.41 (C)	160.53 (C)
2	6.30 (<i>d</i> , 0.5)		99.58 (CH)	112.22 (C)
3			161.36 (C)	158.60 (C)
4			100.81 (C)	100.64 (C)
4a			150.91 (C)	149.22 (C)
5-OH	5.67 (<i>brs</i>)		144.27 (C)	144.25 (C)
6	7.34 (<i>dd</i> , 8.0 and 1.5)	7.32 (<i>dd</i> , 8.0 and 1.5)	120.36 (CH)	120.10 (CH)
7	7.27 (<i>t</i> , 8.0)	7.25 (<i>t</i> , 8.0)	124.19 (CH)	124.00 (CH)
8	7.79 (<i>dd</i> , 8.0 and 1.5)	7.79 (<i>dd</i> , 8.0 and 1.5)	117.14 (CH)	117.12 (CH)
8a			121.17 (C)	121.16 (C)
9			180.67 (C=O)	180.75 (C=O)
9a			103.46 (C)	103.13 (C)
10a			144.12 (C)	144.07 (C)
11	6.83 (<i>dd</i> , 10.0 and 0.5)	6.80 (<i>d</i> , 10.0)	115.04 (CH)	115.00 (CH)
12	5.61 (<i>d</i> , 10.0)	5.65 (<i>d</i> , 10.0)	126.62 (CH)	127.40 (CH)
13			80.86 (C)	78.10 (C)
14	1.47 (<i>s</i>)	1.50 (<i>s</i>)	27.10 (CH_3)	28.16 (CH_3)
15	1.86-1.78 (<i>m</i>) 1.73-1.68 (<i>m</i>)	1.50 (<i>s</i>)	41.57 (CH_2)	28.16 (CH_3)
16	2.16-2.11 (<i>m</i>)	3.37 (<i>d</i> , 7.5)	22.50 (CH_2)	21.22 (CH_2)
17	5.11 (<i>mt</i> , 7.5)	5.26 (<i>mt</i> , 7.5)	123.37 (CH)	121.86 (CH)
18			135.76 (C)	131.70 (C)
19	1.98-1.94 (<i>m</i>)	1.70 (<i>s</i>)	39.63 (CH_2)	25.81 (CH_3)
20	2.08-2.00 (<i>m</i>)	1.82 (<i>s</i>)	26.63 (CH_2)	17.91 (CH_3)

Table 63 (Continued)

Position	δ_{H} (mult., J_{Hz})		δ_{C} (C-Type)	
	YU11	YU3	YU11	YU3
21	5.08 (<i>mt</i> , 7.5)		124.22 (CH)	
22			131.40 (C)	
23	1.67 (<i>d</i> , 1.0)		25.70 (CH ₂)	
24	1.58 (<i>s</i>)		16.00 (CH ₂)	
25	1.59 (<i>s</i>)		17.67 (CH ₂)	

Table 64 Major HMBC correlations of compounds YU3 and YU11

Proton	YU11	YU3
1-OH	C-1, C-2, C-9a	C-1, C-2, C-9a
H-2	C-1, C-3, C-4, C-9a	
H-6	C-5, C-8, C-10a	C-5, C-8, C-10a
H-7	C-5, C-8a, C-10a	C-5, C-8a, C-10a
H-8	C-5, C-6, C-9, C-10a	C-5, C-6, C-9, C-10a
H-11	C-3, C-4a, C-13	C-3, C-4a, C-13
H-12	C-4, C-13	C-4, C-13
H-14	C-12, C-13, C-15	C-12, C-13, C-14, C-15
H-15	C-12, C-13, C-14, C-16, C-17	C-12, C-13, C-14, C-15
H-16	C-15, C-17, C-18	C-1, C-2, C-3, C-17, C-18
H-17	C-16, C-19, C-24	C-16, C-19, C-20
H-19	C-17, C-18, C-20, C-24	C-17, C-18, C-20
H-20	C-18, C-19, C-21, C-22	C-17, C-18, C-19
H-21	C-23	
H-23	C-21, C-22, C-25	

Table 64 (Continued)

Proton	YU11	YU3
H-24	C-17, C-18, C-19	
H-25	C-21, C-22, C-23	

3.12 Compound YU16

Compound YU16 was obtained as a yellow gum. The IR spectrum (Figure 97) exhibited absorption bands at 3380 (a hydroxyl group) and 1643 cm^{-1} (a conjugated carbonyl group). The UV (Figure 96) spectrum with absorption bands at 218, 242, 258 and 319 nm indicated that it was a xanthone derivative. The ^1H NMR spectrum (Figure 98) (Table 65) showed characteristic peaks of a 1,2,3-trisubstituted benzene ring [δ 7.72 and 7.25 (1H each, *dd*, $J = 8.0$ and 1.5 Hz) and 7.20 (1H, *t*, $J = 8.0$ Hz)], a dimethylchromane ring [δ 2.79 (2H, *t*, $J = 7.5$ Hz), 1.77 (2H, *t*, $J = 7.5$ Hz) and 1.30 (6H, *s*)] and a 3-hydroxy-3-methylbutyl unit [δ 3.01-2.98 (2H, *m*), 1.80-1.78 (2H, *m*) and 1.30 (6H, *s*)] in addition to a chelated hydroxy proton [δ 13.00 (1H, *s*)]. The HMBC data (Figure 102) (Table 65) of all aromatic protons of the 1,2,3-trisubstituted benzene ring were identical to those of YU6, indicating that YU16 contained a hydroxyl substituent at C-5. The location of the dimethylchromane ring, the 3-hydroxy-3-methylbutyl group and the chelated hydroxyl group on the right-handed ring of the xanthone nucleus was established by the following HMBC data. The chelated hydroxyl group which was definitely attached on C-1 showed cross peaks with C-2 (δ 111.09) and C-9a (δ 102.91). The dimethylchromane ring was found to be fused in a linear fashion at C-2 (δ 111.09) through an oxygen at C-3 (δ 160.48) according to the HMBC correlations between the methylene protons (δ 2.79, H-16) and two oxygenated aromatic carbons at δ 157.69 (C-1) and δ 160.48 (C-3) as well as

a correlation between the methylene protons (δ 1.77, H-17) and C-2. The remaining 3-hydroxy-3-methylbutyl unit was assigned to be attached at C-4 (δ 107.86) by the correlations of H-11 (δ 3.01-3.28)/C-3, H-11/C-4a (δ 152.58) and H-12 (δ 1.80-1.78)/C-4. Therefore, YU16 was assigned as 1,5-dihydroxy-4-(3-hydroxy-3-methylbutyl)-6',6'-dimethyldihydropyrano(2',3':3,2)xanthone (12), a new naturally occurring xanthone.

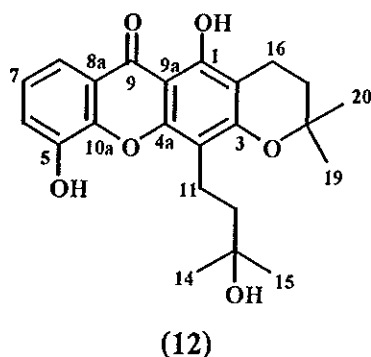


Table 65 The NMR data of compound YU16 in $\text{CDCl}_3/\text{CD}_3\text{OD}$

Position	δ_{H} (mult., J_{Hz})	δ_{C} (C-Type)	HMBC correlation
1-OH	13.00 (s)	157.69 (C)	C-2, C-9a
2		111.09 (C)	
3		160.48 (C)	
4		107.86 (C)	
4a		152.58 (C)	
5-OH		145.35 (C)	
6	7.25 (dd, 8.0 and 1.5)	120.05 (CH)	C-8, C10a
7	7.20 (t, 8.0)	123.47 (CH)	C-5, C-8a
8	7.72 (dd, 8.0 and 1.5)	115.84 (CH)	C-6, C-9, C-10a
8a		121.00 (C)	

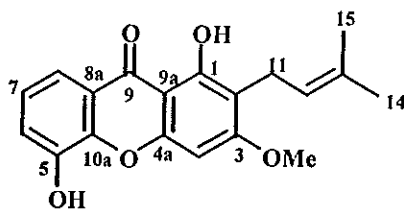
Table 65 (Continued)

Position	$\delta_{\text{H}}(\text{mult.}, J_{\text{Hz}})$	$\delta_{\text{C}}(\text{C-Type})$	HMBC correlation
9		181.25 (C=O)	
9a		102.91 (C)	
10a		144.95 (C)	
11	3.01-3.98 (<i>m</i>)	16.89 (CH ₂)	C-3, C-4, C-4a, C-12, C-13
12	1.80-1.78 (<i>m</i>)	41.55 (CH ₂)	C-4, C-11, C-13, C-14, C-15
13-OH		71.45 (C)	
14, 15	1.32 (<i>s</i>)	29.09 (CH ₃)	C-12, C-13, C-14, C-15
16	2.79 (<i>t</i> , 7.5)	16.59 (CH ₂)	C-1, C-2, C-3, C-17, C-18
17	1.77 (<i>t</i> , 7.5)	41.15 (CH ₂)	C-2, C-16, C-19, C-20
18		71.33 (C)	
19,20	1.30 (<i>s</i>)	29.17 (CH ₃)	C-17, C-18, C-19, C-20

3.13 Compound YU7

Compound YU7 was isolated as a yellow solid, melting at 241.2-243.0 °C. The UV (Figure 103) and IR (Figure 104) spectral data suggested that it was a xanthone derivative. The ¹H NMR spectrum (Figure 105) (Table 66) showed characteristic signals of a 1,2,3-trisubstituted aromatic ring: δ 7.63 and 7.19 (1H each, *dd*, $J = 8.0$ and 1.5 Hz) and 7.13 (1H, *t*, $J = 8.0$ Hz). These data together with HMBC data (Figure 110) (Table 66) indicated that the left-handed aromatic ring of YU7 had the same substitution pattern as YU6. In addition, the ¹H NMR spectrum exhibited a chelated hydroxy proton at δ 12.86 (1H, *s*), a singlet of a methoxyl group at δ 3.87 (3H, *s*), a singlet aromatic proton at δ 6.57 (1H, *s*) and characteristic signals of an isoprenyl group [δ 3.29 (2H, *d*, $J = 7.5$ Hz), 5.15 (1H, *mt*, $J = 7.5$ Hz), 1.72 and 1.60 (3H each, *s*)]. In the HMBC spectrum, the chelated hydroxy proton (δ 12.86) caused cross peaks

with aromatic carbons at δ 158.83 (C-1), 111.59 (C-2) and 103.37 (C-9a). Furthermore, C-1 correlated to methylene protons (δ 3.29, H-11) of the isoprenyl group while these protons correlated to an oxygenated aromatic carbon C-3 (δ 164.37) which showed a correlation to the methoxy protons (δ 3.87). These spectral evidence established the location of the chelated hydroxyl group, the isoprenyl unit and methoxyl group at C-1, C-2 and C-3, respectively. The methyl group of the isoprenyl unit at δ 1.60 was found to be *cis* to the olefinic proton, H-12, due to the enhancement of this methyl signal upon irradiation of H-12 in the NOEDIFF experiment (Figure 108). The remaining aromatic proton (δ 6.57) was then attributed to H-4 based on 3J correlations of H-4/C-2 and H-4/C-9a. Thus, YU7 was identified as 1,5-dihydroxy-3-methoxy-2-(3-methylbut-2-enyl)xanthone (13). It has been previously isolated from *Garcinia mangostana* (Sen, *et al.*, 1981).



(13)

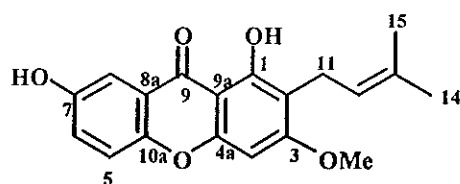
Table 66 The NMR data of compound YU7 in CDCl₃/CD₃OD

Position	YU7		HMBC correlation	YU7 (published data)
	δ_{H} (mult., J_{Hz})	δ_{C} (C-Type)		δ_{H} (mult., $J_{\text{Hz}})^{\text{a}}$
1-OH	12.86 (s)	158.83 (C)	C-1, C-2, C-9a	13.10 (s)
2		111.59 (C)		
3		164.37 (C)		
3-OMe	3.87 (s)	55.69 (CH ₃)	C-3	3.99 (s)
4	6.57 (s)	89.89 (CH)	C-2, C-3, C-4a, C-9, C-9a	6.74 (s)
4a		155.85 (C)		
5-OH		145.45 (C)		
6	7.19 (dd, 8.0 and 1.5)	119.78 (CH)	C-5, C-8, C-8a, C-10a	7.35 (m)
7	7.13 (t, 8.0)	123.49 (CH)	C-5, C-8, C-8a	7.35 (m)
8	7.63 (dd, 8.0 and 1.5)	115.42 (CH)	C-6, C-9, C-10a	7.65 (q)
8a		121.29 (C)		
9		181.00 (C=O)		
9a		103.37 (C)		
10a		145.11 (C)		
11	3.29 (d, 7.5)	21.00 (CH ₂)	C-1, C-2, C-3, C-12, C-13	3.30-3.60 (d, 6.5)
12	5.15 (mt, 7.5)	121.70 (CH)	C-11, C-14	5.20 (t, 6.5)
13		131.65 (C)		
14	1.60 (s)	25.36 (CH ₃)	C-12, C-13, C-15	1.66 (s)
15	1.72 (s)	17.35 (CH ₃)	C-12, C-13, C-14	1.76 (s)

^a ¹H NMR data of 1,5-dihydroxy-3-methoxy-2-(3-methylbut-2-enyl)xanthone in DMSO-*d*₆

3.14 Compound YU12

Compound **YU12** was isolated as a yellow solid, melting at 201.5-203.2 °C. Its IR (Figure 112) and UV (Figure 111) spectral data showed absorption bands of a hydroxylated xanthone. Its ¹H (Figure 113) (Table 67) and ¹³C NMR spectra (Figure 114) (Table 67) were similar to those of **YU7**. Signals of a chelated hydroxyl group [δ 12.87 (1H, *s*)], an isoprenyl group [δ 3.38 (2H, *d*, $J = 7.0$ Hz), 5.24 (1H, *mt*, $J = 7.0$ Hz), 1.80 and 1.69 (3H each, *s*)], a methoxyl group [δ 3.94 (3H, *s*)] and an aromatic proton [δ 6.43 (1H, *s*)] suggested that **YU12** possessed the same right-handed ring as **YU7**. This conclusion was confirmed by HMBC data (Figure 118) (Table 67) which were identical to those of **YU7**. The NOEDIFF data (Figure 116) indicated that the olefinic proton, H-12 (δ 5.24), of the isoprenyl group was *cis* to the methyl protons, Me-14 (δ 1.69), according to the enhancement of this olefinic signal after irradiation of Me-14. In addition, three aromatic protons of a 1,2,4-trisubstituted benzene ring [δ 7.62 (1H, *d*, $J = 3.5$ Hz), 7.36 (1H, *d*, $J = 8.5$ Hz) and 7.26 (1H, *dd*, $J = 8.5$ and 3.5 Hz)] and a hydroxy proton signal at δ 5.66 (1H, *brs*) were observed in the ¹H NMR spectrum. The lowest-field aromatic proton (δ 7.62) of the 1,2,4-trisubstituted benzene ring was attributed to H-8 based on its chemical shift value and a cross peak between this aromatic proton and a carbonyl carbon (δ 180.41, C-9) in the HMBC spectrum. Consequently, other aromatic protons at δ 7.36 and 7.26 were assigned to H-5 and H-6, respectively. The ³*J* correlation between H-5 and an oxyaromatic carbon (δ 151.97, C-7) revealed the substituent at C-7 to be a hydroxyl group. **YU12** was then identified as 1,7-dihydroxy-3-methoxy-2-(3-methylbut-2-enyl)xanthone (**14**) which was previously isolated from *Garcinia mangostana* (Mahabusarakam and Wiriyachitra, 1987).



(14)

Table 67 The NMR data of compound YU12 in CDCl₃

Position	YU12		HMBC correlation	YU12
	δ_{H} (mult., J_{Hz})	δ_{C} (C-Type)		(published data)
				δ_{H} (mult., J_{Hz}) ^a
1-OH	12.87 (s)	159.39 (C)	C-1, C-2, C-9a	13.03 (s)
2		111.72 (C)		
3		164.45 (C)		
3-OMe	3.94 (s)	55.95 (CH ₃)	C-3	3.92 (s)
4	6.43 (s)	89.57 (CH)	C-2, C-3, C-4a, C-9, C-9a	6.41 (s)
4a		156.32 (C)		
5	7.36 (d, 8.5)	118.98 (CH)	C-7, C-8a, C-10a	7.29 (d, 8.0)
6	7.26 (dd, 8.5 and 3.5)	123.73 (CH)	C-8, C-10a	7.26 (dd, 8.0 and 2.0)
7-OH	5.66 (brs)	151.97 (C)		9.25 (s)
8	7.62 (d, 3.5)	109.23 (CH)	C-6, C-9, C-10a	7.64 (d, 2.0)
8a		121.20 (C)		
9		180.41 (C=O)		
9a		103.95 (C)		
10a		150.52 (C)		
11	3.38 (d, 7.0)	21.32 (CH ₂)	C-1, C-2, C-3, C-12, C-13	3.36 (d, 7.0)
12	5.24 (mt, 7.0)	122.02 (CH)	C-11, C-14, C-15	5.23 (brt, 7.0)
13		131.96 (C)		

Table 67 (Continued)

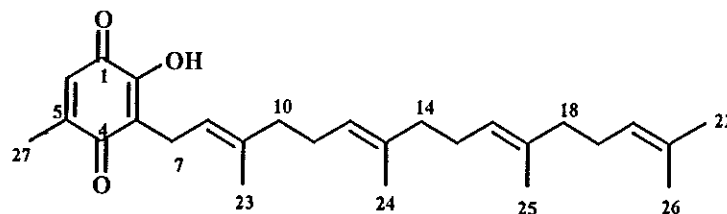
Position	YU12		HMBC correlation	YU12 (published data)
	δ_{H} (mult., J_{Hz})	δ_{C} (C-Type)		δ_{H} (mult., J_{Hz}) ^a
14	1.69 (s)	25.81 (CH ₃)	C-12, C-13, C-15	1.68 (s)
15	1.80 (s)	17.80 (CH ₃)	C-12, C-13, C-14	1.79 (s)

^a ¹H NMR data of 1,7-dihydroxy-3-methoxy-2-(3-methylbut-2-enyl)xanthone in CDCl₃/CD₃SOCD₃

3.15 Compound YU5

Compound YU5 was obtained as an orange-red gum. Its molecular formula was determined as C₂₇H₃₈O₃ (m/z 411 [M+H]⁺) by FABMS (Figure 127). The IR spectrum (Figure 120) exhibited absorption bands at 3380 cm⁻¹ for a hydroxyl group, 1642 and 1616 cm⁻¹ for two carbonyl groups. The UV spectrum (Figure 119) showed an absorption band at 264 nm, indicating the presence of a *p*-benzoquinone moiety (Naito, *et al.*, 1992). The ¹³C NMR spectrum (Figure 122) (Table 68) showed 26 resonances: nine quaternary carbons (δ 187.41, 183.44, 150.63, 149.07, 137.19, 135.06, 134.92, 131.28, 120.58), five methine carbons (δ 128.40, 124.23, 124.25, 124.07, 119.58), seven methylene carbons [δ 39.74 (2xC), 39.72, 26.79, 26.67, 26.51, 22.13] and six methyl carbons (δ 25.72, 17.71, 16.59, 16.20, 16.04, 16.01). The carbon signals at δ 183.44 and 187.41 were attributed to *p*-benzoquinone carbonyl carbons. Its ¹H NMR spectrum (Figure 121) (Table 68) showed a quinonoid methyl signal at δ 2.12 (3H, *d*, J = 1.5 Hz), a quinonoid proton signal at δ 6.59 (1H, *q*, J = 1.5 Hz) and an enolic hydroxyl signal at δ 6.94 (1H, *brs*). In addition, signals of four olefinic-methine protons (δ 5.17, 5.14 and 5.11), seven methylene groups (δ 3.19, 2.09 and 2.00) and

five methyl groups (δ 1.78, 1.71, 1.62 and 1.61) suggested that a substituent of *p*-quinone unit contained four isoprene units. Most of the methyl signals did not show an NOE enhancement to any signal of olefinic protons except for Me-22 (δ 1.71) which enhanced a signal of the olefinic proton, H-20 (δ 5.14) (Figure 124). These indicated that the configuration of internal double bond was all *E* and the methyl group at 1.71, not the methyl group at δ 1.63, was *cis* to H-20. The chemical shifts of all carbons were assigned by comparing these data with those of (2*E*, 6*E*)-farnesol (Naito, *et al.*, 1992) together with the HMBC data (Figure 126) (Table 68). This C₂₀ substituent was assigned to be at C-3 according to HMBC correlations between the methylene protons, H-7 (δ 3.19) of the side chain and quinonoid carbons: C-2 (δ 150.63), C-3 (δ 120.58) and C-4 (δ 187.41). The quinonoid proton (δ 6.59, H-6) showed cross peaks, in the HMBC spectrum, with a carbonyl carbon (C-4), an oxyquinonoid carbon (C-2) and a methyl carbon (δ 16.59, C-27) while the methyl protons (δ 2.12, Me-27) showed cross peaks with the carbonyl carbon (C-4) and a quinonoid-methine carbon (δ 128.40, C-6). These data established the location of the methyl group and the quinonoid proton at C-5 and C-6, respectively. Thus, the C-2 position must be substituted by a hydroxyl group. On the basis of these spectral data, YU5 had the structure 15, a new *p*-benzoquinone.



(15)

Table 68 The NMR data of compound YU5 in CDCl₃

Position	δ_{H} (mult., J_{Hz})	δ_{C} (C-Type)	HMBC correlation
1		183.44 (C=O)	
2-OH	6.94 (<i>brs</i>)	150.63 (C)	
3		120.58 (C)	
4		187.41 (C=O)	
5		149.07 (C)	
6	6.59 (<i>q</i> , 1.5)	128.40 (CH)	C-2, C-4, C-27
7	3.19 (<i>d</i> , 7.5)	22.13 (CH ₂)	C-2, C-3, C-4, C-8, C-9
8	5.17 (<i>mt</i> , 7.5)	119.58 (CH)	C-7, C-23
9		137.19 (C)	
10	2.00 (<i>mt</i> , 7.5)	39.74 (CH ₂)	C-8, C-9, C-11, C-12, C-13
11	2.09 (<i>mt</i> , 7.5)	26.51 (CH ₂)	C-10, C-12, C-13
12	5.11 (<i>mt</i> , 7.5)	124.07 (CH)	C-10, C-11, C-24
13		135.06 (C)	
14	2.00 (<i>mt</i> , 7.5)	39.74 (CH ₂)	C-11, C-12, C-13, C-16, C-17
15	2.09 (<i>mt</i> , 7.5)	26.67 (CH ₂)	C-13, C-16, C-17
16	5.14 (<i>mt</i> , 7.5)	124.25 (CH)	C-25
17		134.92 (C)	
18	2.00 (<i>mt</i> , 7.5)	39.72 (CH ₂)	C-16, C-17, C-20, C-25
19	2.09 (<i>mt</i> , 7.5)	26.79 (CH ₂)	C-17, C-20, C-25
20	5.14 (<i>mt</i> , 7.5)	124.43 (CH)	-
21		131.28 (C)	
22	1.71 (<i>d</i> , 1.0)	25.72 (CH ₃)	C-20, C-21, C-26
23	1.78 (<i>s</i>)	16.04 (CH ₃)	C-8, C-9, C-10
24	1.61 (<i>s</i>)*	16.20 (CH ₃)	C-13, C-16, C-17, C-18, C-20
25	1.62 (<i>s</i>)*	16.01 (CH ₃)	C-13, C-16, C-17, C-18, C-20

Table 68 (Continued)

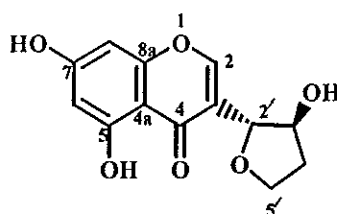
Position	δ_{H} (mult., J_{Hz})	δ_{C} (C-Type)	HMBC correlation
26	1.63 (s)	17.71 (CH ₃)	C-20, C-21, C-22
27	2.12 (d, 1.5)	16.59 (CH ₃)	C-4, C-5, C-6

* interchangeable

3.16 Compound YU13

Compound YU13 was obtained as pale yellow crystals, melting at 185.6-187.2 °C. Its molecular formula was determined as C₁₃H₁₂O₆ by EIMS (Figure 137). Its UV spectrum (Figure 128) showed absorption bands at 229, 251, 258 and 295 nm. The IR spectrum (Figure 129) showed absorption bands at 3367 (a hydroxyl group) and 1657 cm⁻¹ (a carbonyl group). The ¹H NMR spectrum (Figure 130) (Table 69) showed signals of two methine protons at δ 4.76 (1H, *dd*, $J = 2.5$ and 2.0 Hz, H-2') and 4.36 (1H, *td*, $J = 5.5$ and 2.5 Hz, H-3') and two sets of non-equivalent methylene protons: one set at δ 4.12 (1H, *dt*, $J = 8.0$ and 3.0 Hz, H-5') and 4.02 (1H, *ddd*, $J = 8.5$, 8.0 and 6.5 Hz, H-5') and the other set at δ 2.14-2.05 (1H, *m*, H-4') and 1.91-1.86 (1H, *m*, H-4'). The HMQC spectrum (Figure 135) revealed a cross peak between the more deshielded methine proton and an oxycarbon at δ 82.96 (C-2') and that between the other methine proton and an oxycarbon at δ 76.76 (C-3'). Furthermore, the more deshielded methylene protons showed a cross peak in the HMQC spectrum with an oxycarbon at δ 68.28 (C-5') while other methylene protons correlated with a *sp*³ carbon at δ 34.40 (C-4'). The chemical-shift values of H-3' and C-3' suggested the substituent at C-3 to be a hydroxyl group. HMBC correlations (Figure 136) (Table 69) of H-2'/C-5' and H-5'/C-2' established a tetrahydrofuran unit with an ether linkage between C-2' and C-5'. Signals of one chelated hydroxyl group (δ 12.62), one free hydroxyl group

(δ 4.43), two *meta*-coupled aromatic protons [δ 6.39 (1H, *d*, $J = 2.0$ Hz) and 6.27 (1H, *d*, $J = 2.0$ Hz)] and an olefinic proton [δ 7.85 (1H, *d*, $J = 2.0$ Hz)] were also present in ^1H NMR spectrum. The olefinic proton (δ 7.85, H-2) showed correlations in the HMBC spectrum with a carbonyl carbon, δ 188.04, and two oxycarbons at δ 160.11 (C-8a) and δ 82.96 (C-2') of the 3-hydroxytetrahydrofuran unit. These data together with the chemical-shift values of H-2 suggested that YU13 possessed an isoflavone-like structure carrying the 3-hydroxytetrahydrofuran at C-3 instead of a phenyl ring. The chelated hydroxyl group (δ 12.62, 5-OH) was placed at C-5 because it formed an intramolecular hydrogen bond with the carbonyl group. A pair of *meta*-coupled doublets at δ 6.39 ($J = 2.0$ Hz) and δ 6.27 ($J = 2.0$ Hz) were then attributed to H-6 and H-8, respectively. The 2J correlations between the aromatic methine protons, H-6 and H-8, and an oxyaromatic carbon (δ 166.19, C-7) established the substituent at C-7 to be a hydroxyl group. Therefore, YU13 had the new isoflavone-like structure 16. The relative stereochemistry of the 3-hydroxyfuran moiety was established by NOEDIFF data. Irradiation of the olefinic proton, H-2, enhanced signals of the methine proton, H-2', and one of the methylene protons, H-5' β at δ 4.12 (Figure 134) while irradiation of H-2' did not affect the signal of H-3' but enhanced the signal of H-2 (Figure 133). These results indicated that H-2' and H-3' were *trans*.



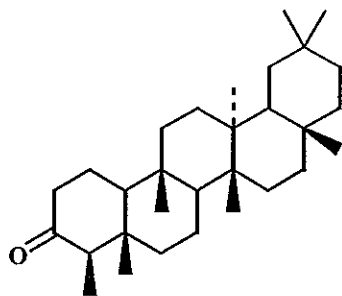
(16)

Table 69 The NMR data of compound YU13 in Acetone- d_6

Position	δ_H (mult., J_{Hz})	δ_C (C-Type)	HMBC correlation
2	7.95 (<i>d</i> , 2.0)	155.11 (CH)	C-2', C-3, C-4, C-8a
3		124.07 (C)	
4		188.04 (C=O)	
4a		106.07 (C)	
5-OH	12.62 (<i>s</i>)	164.24 (C)	C-4a, C-5, C-6, C7
6	6.39 (<i>d</i> , 2.0)	100.36 (CH)	C-4a, C-5, C-7, C-8
7-OH	4.43 (<i>brs</i>)	166.19 (C)	
8	6.27 (<i>d</i> , 2.0)	95.02 (CH)	C-4a, C-6, C-7, C-8a
8a		160.11 (C)	
2'	4.76 (<i>dd</i> , 2.5 and 2.0)	82.96 (CH)	C-2, C-3', C-3, C-5'
3'	4.36 (<i>td</i> , 5.5 and 2.5)	76.76 (CH)	C-5'
4' α	1.91-1.86 (<i>m</i>)	34.40 (CH ₂)	
β	2.14-2.05 (<i>m</i>)		
5' α	4.02 (<i>ddd</i> , 8.5, 8.0 and 6.5)	68.28 (CH ₂)	C-4'
β	4.12 (<i>dt</i> , 8.0 and 3.0)		C-2', C-3'

3.17 Compound YU8

Compound YU8 was obtained as a white solid, melting at 251.2-252.4 °C. The mass spectrum (Figure 141) showed a molecular ion at m/z 426, corresponding to a molecular formula of C₃₀H₅₀O while the IR spectrum (Figure 138) exhibited an absorption band at 1716 cm⁻¹ for a carbonyl group. Its ¹H NMR (Figure 139) and ¹³C NMR (Figure 140) spectral data suggested that YU8 was friedelin (17). Comparison of its melting point and TLC chromatogram with those of authentic friedelin (Kaewnok, 2000) supported this conclusion.



(17)

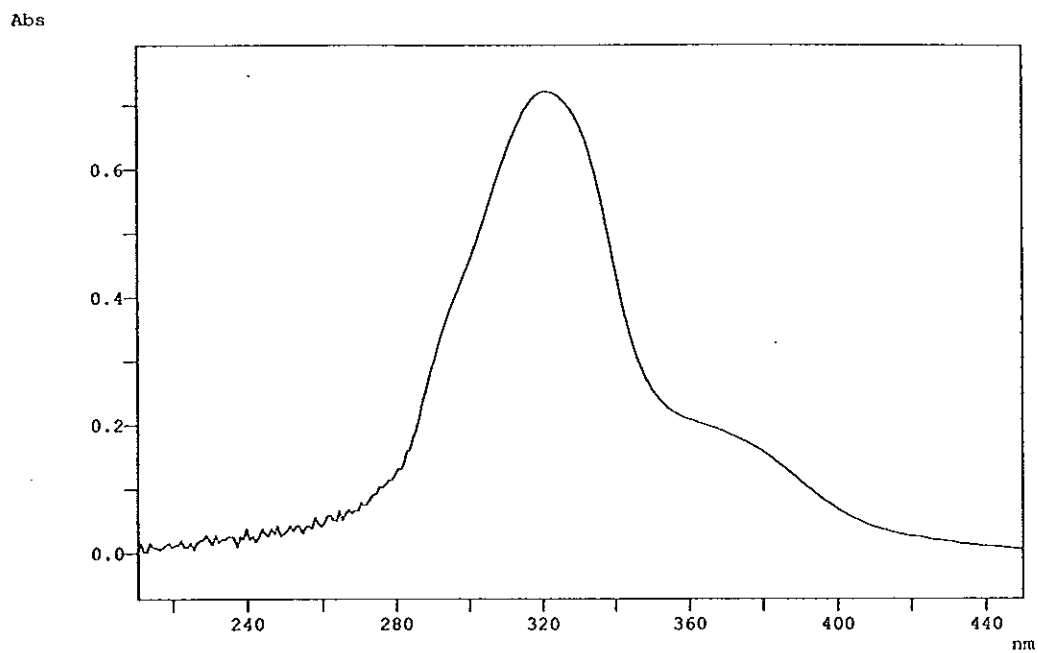


Figure 2 UV (MeOH) spectrum of YU1

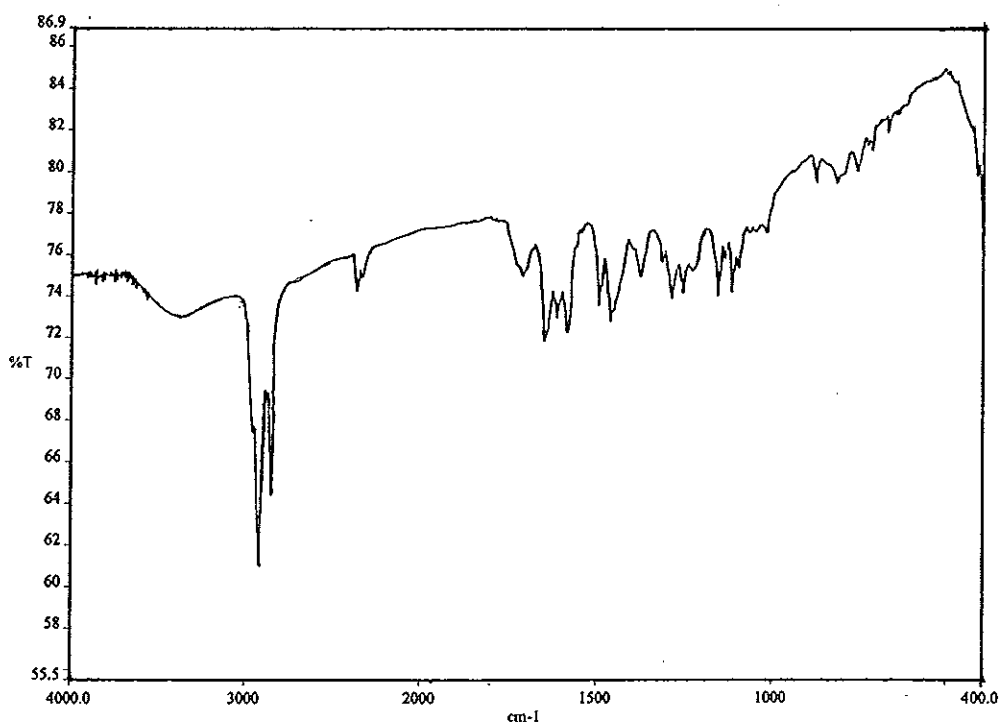


Figure 3 FT-IR (neat) spectrum of YU1

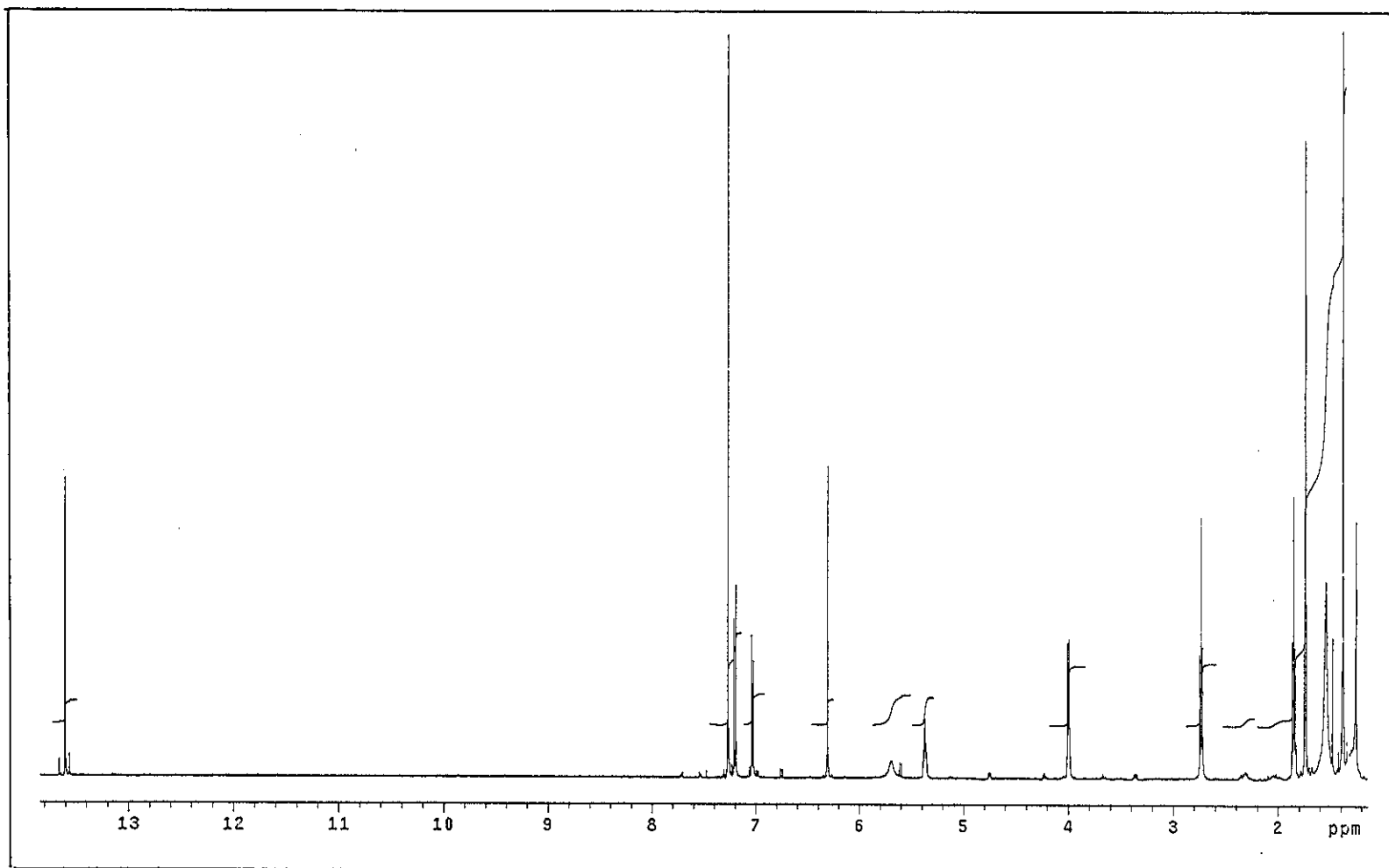


Figure 4 ^1H NMR (500 MHz) (CDCl_3) spectrum of YU1

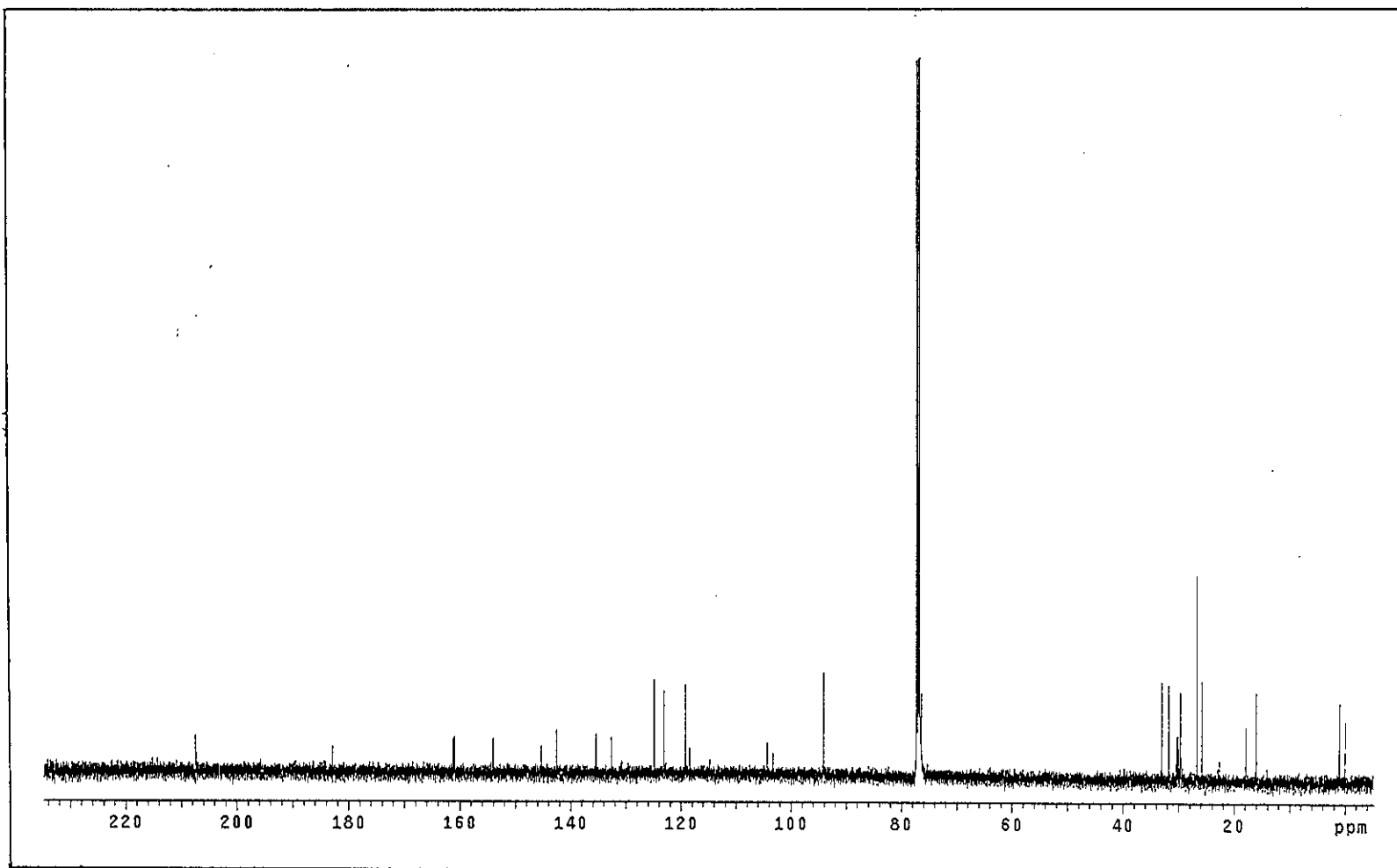


Figure 5 ^{13}C NMR (125 MHz) (CDCl_3) spectrum of YU1

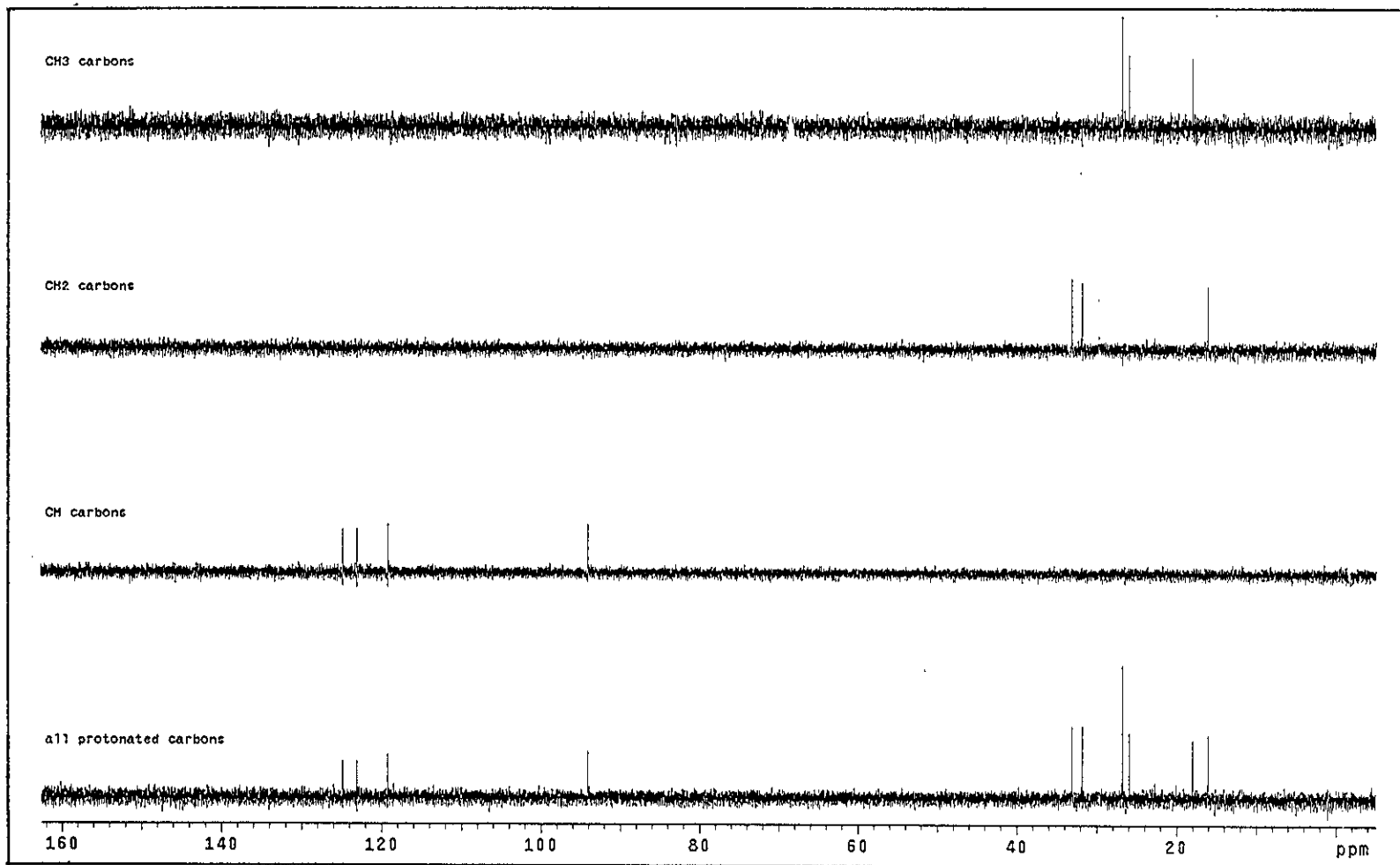


Figure 6 DEPT spectrum of YU1

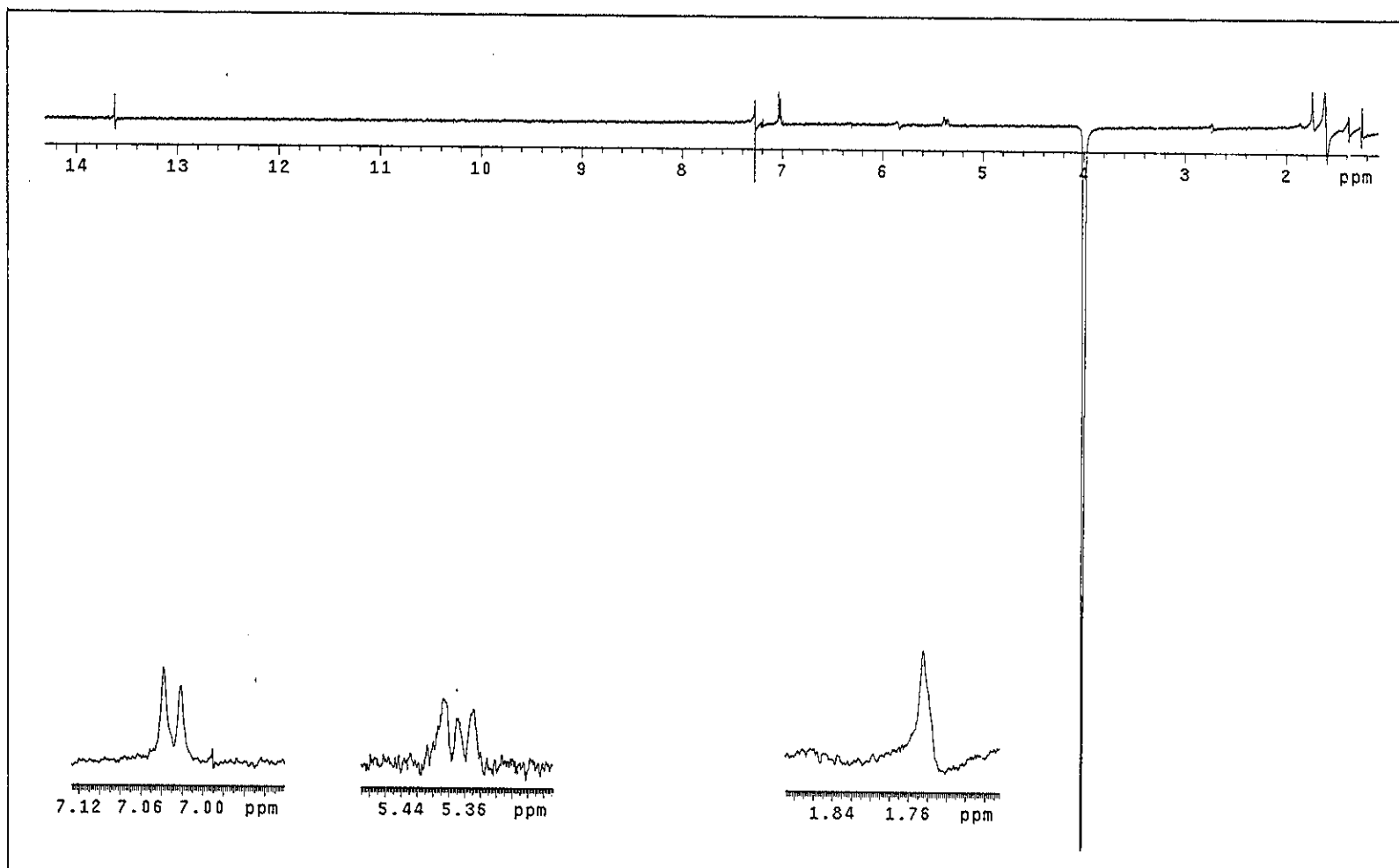


Figure 7 NOEDIFF spectrum of YU1 after irradiation at δ_H 3.98

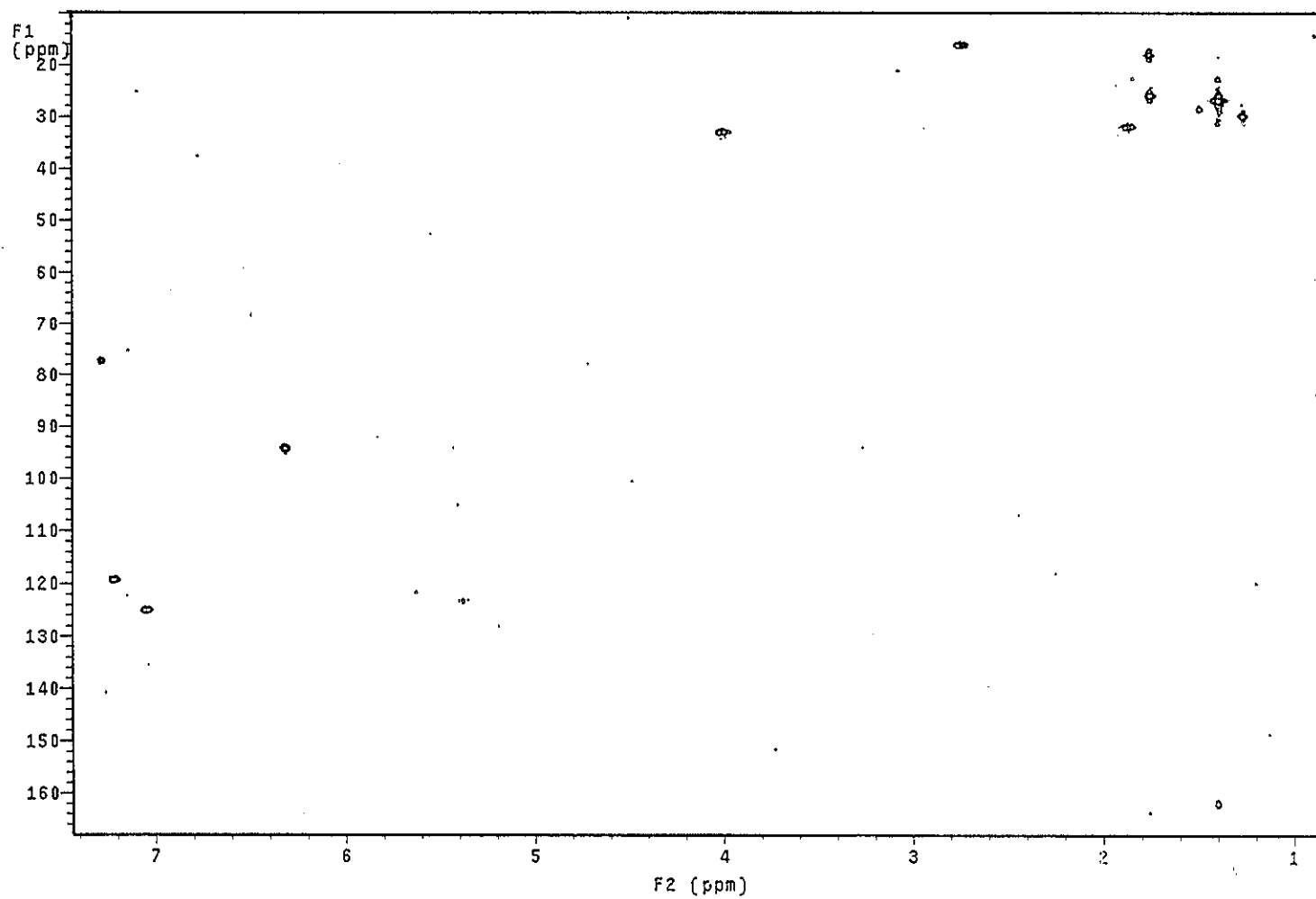


Figure 8 2D HMQC spectrum of YU1

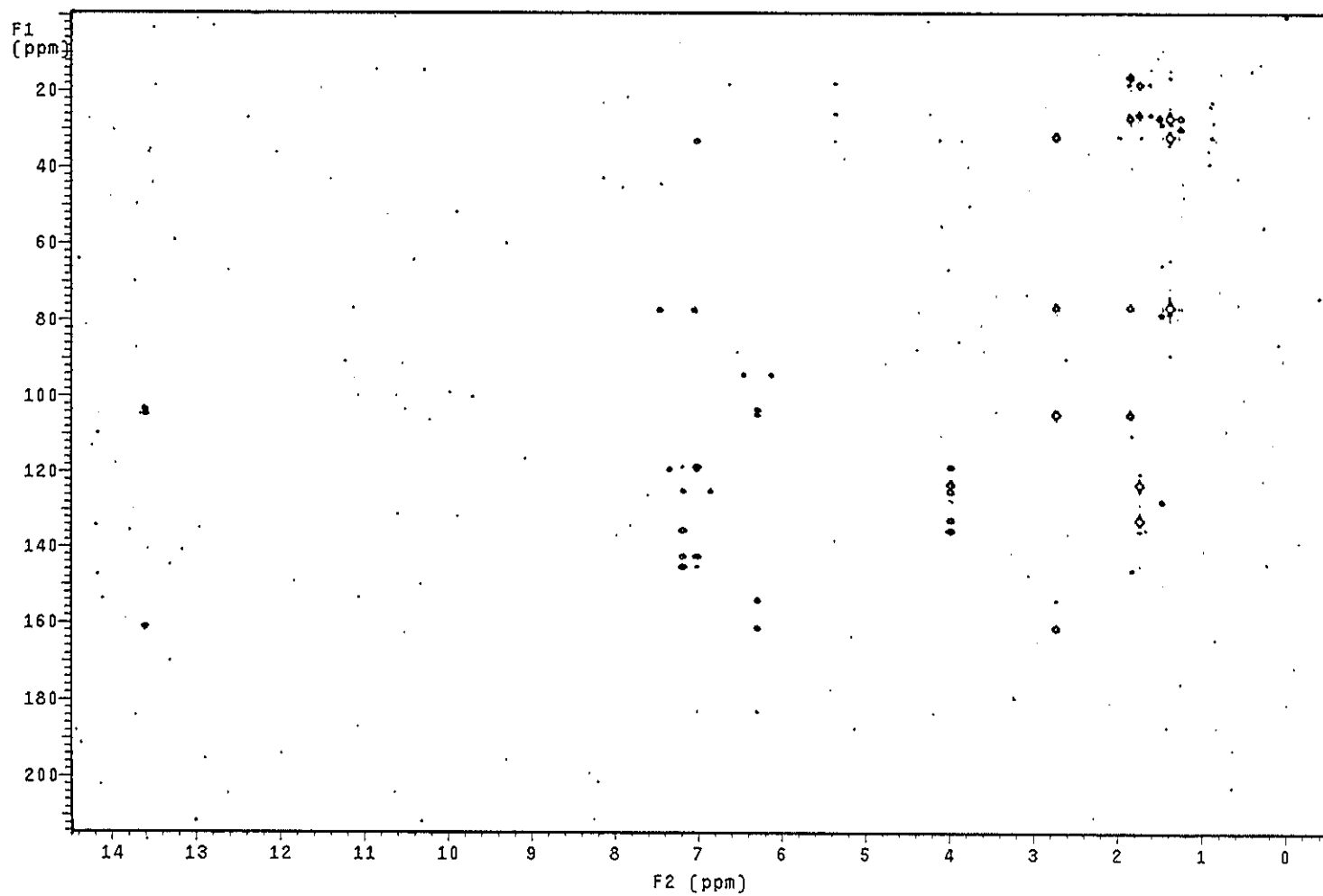


Figure 9 2D HMBC spectrum of YU1

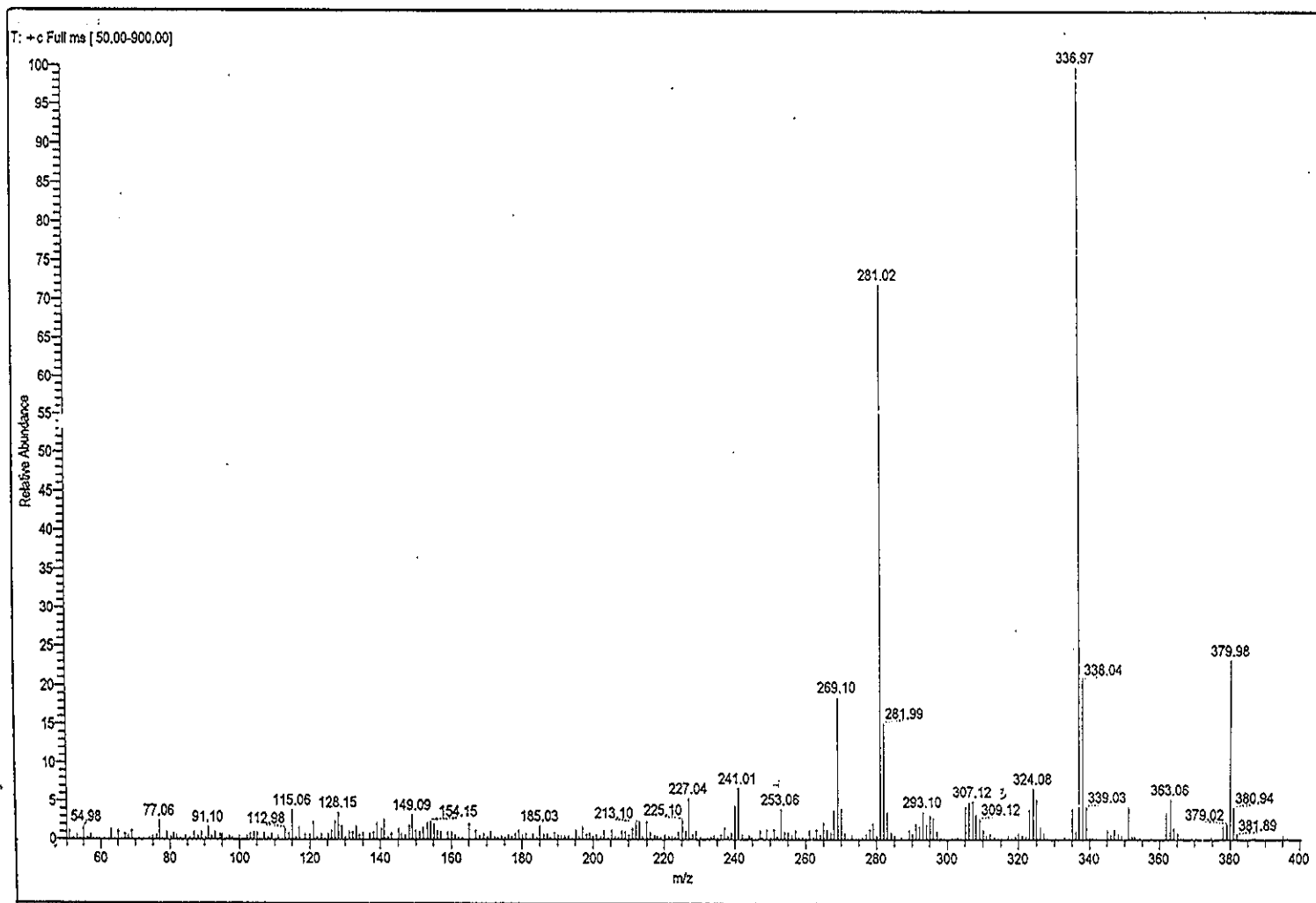


Figure 10 Mass spectrum of YU1

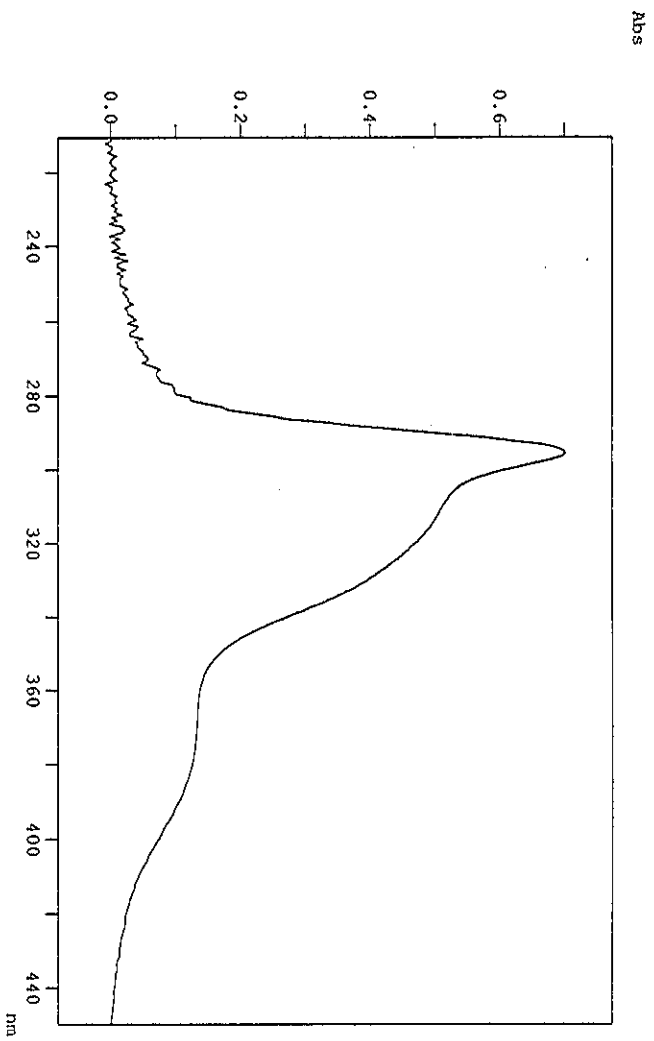


Figure 11 UV (MeOH) spectrum of YU2

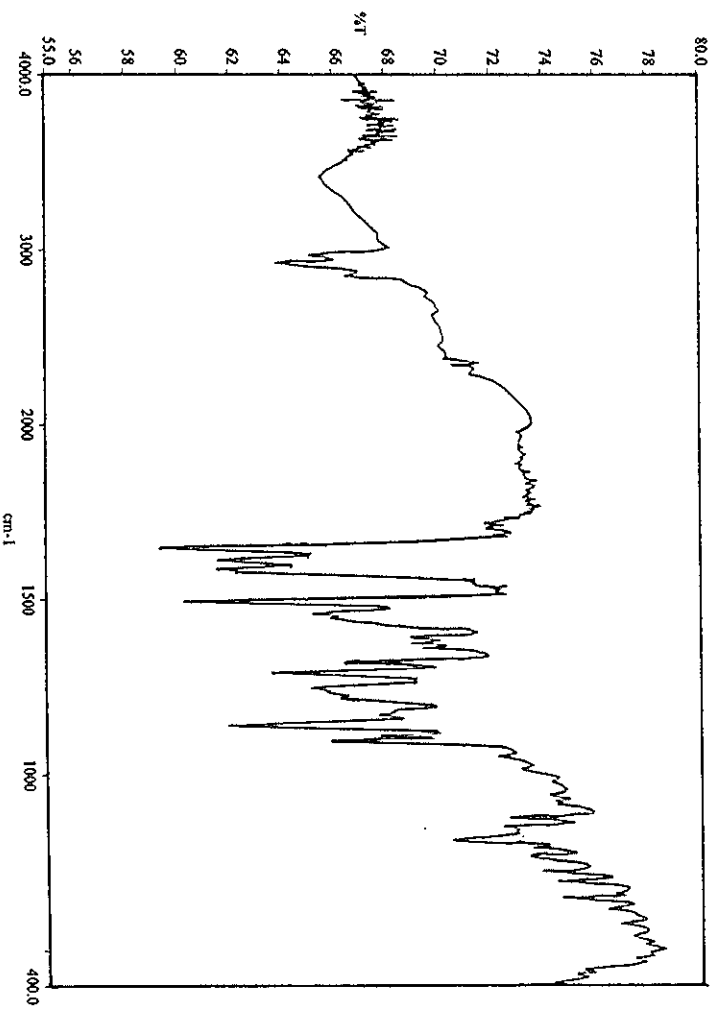


Figure 12 FT-IR (heat) spectrum of YU2

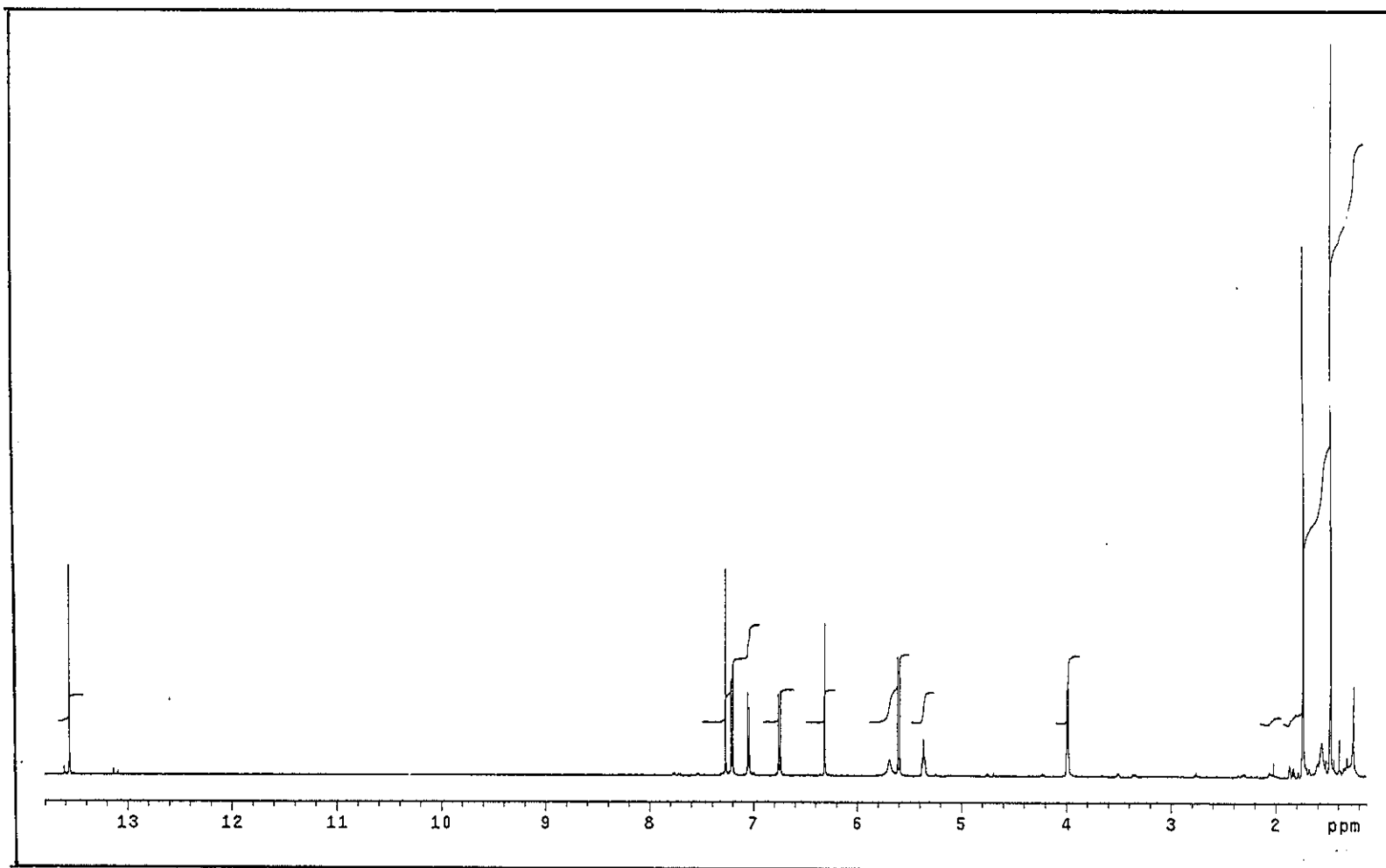


Figure 13 ^1H NMR (500 MHz) (CDCl_3) spectrum of YU2

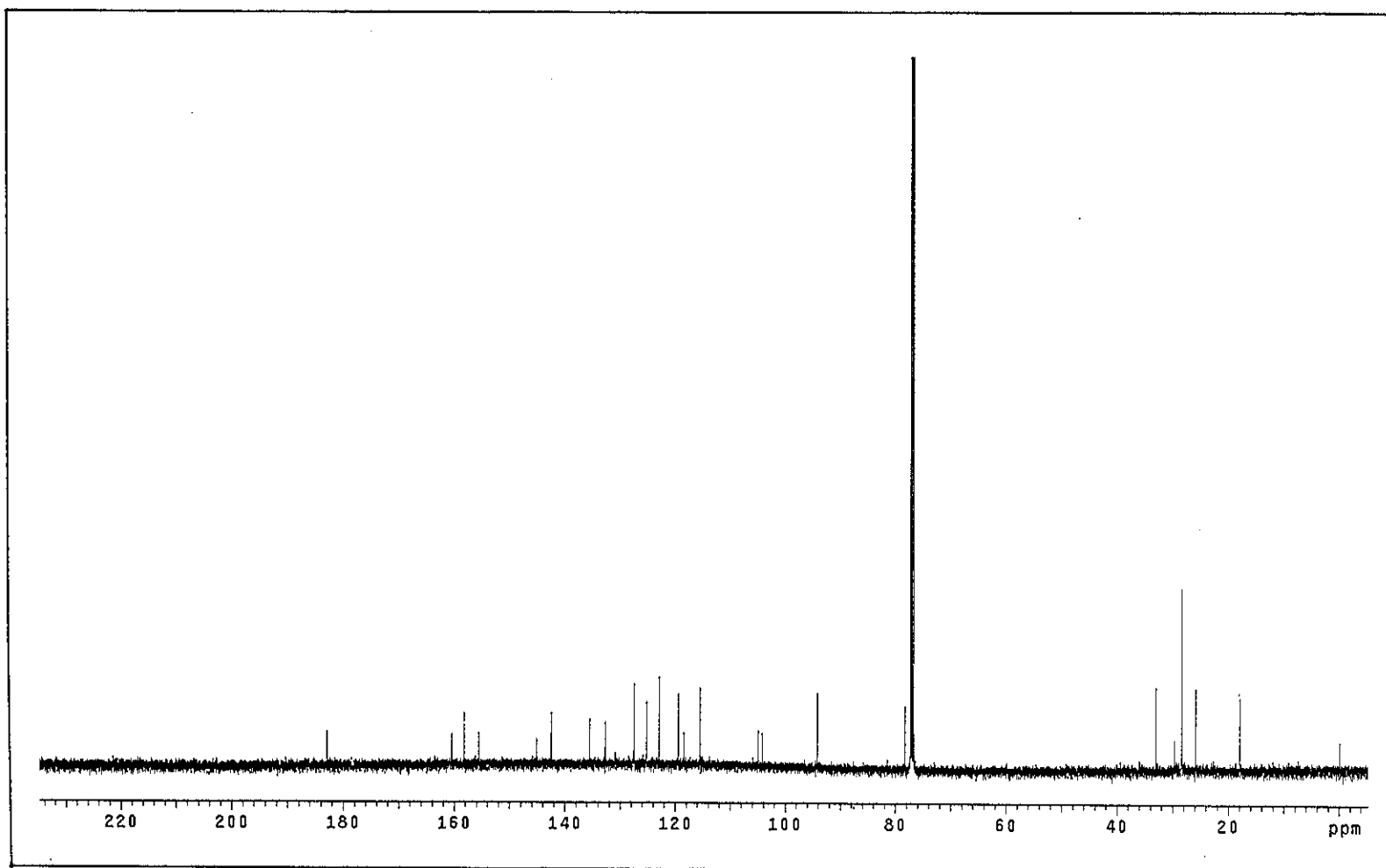


Figure 14 ^{13}C NMR (125 MHz) (CDCl_3) spectrum of YU2

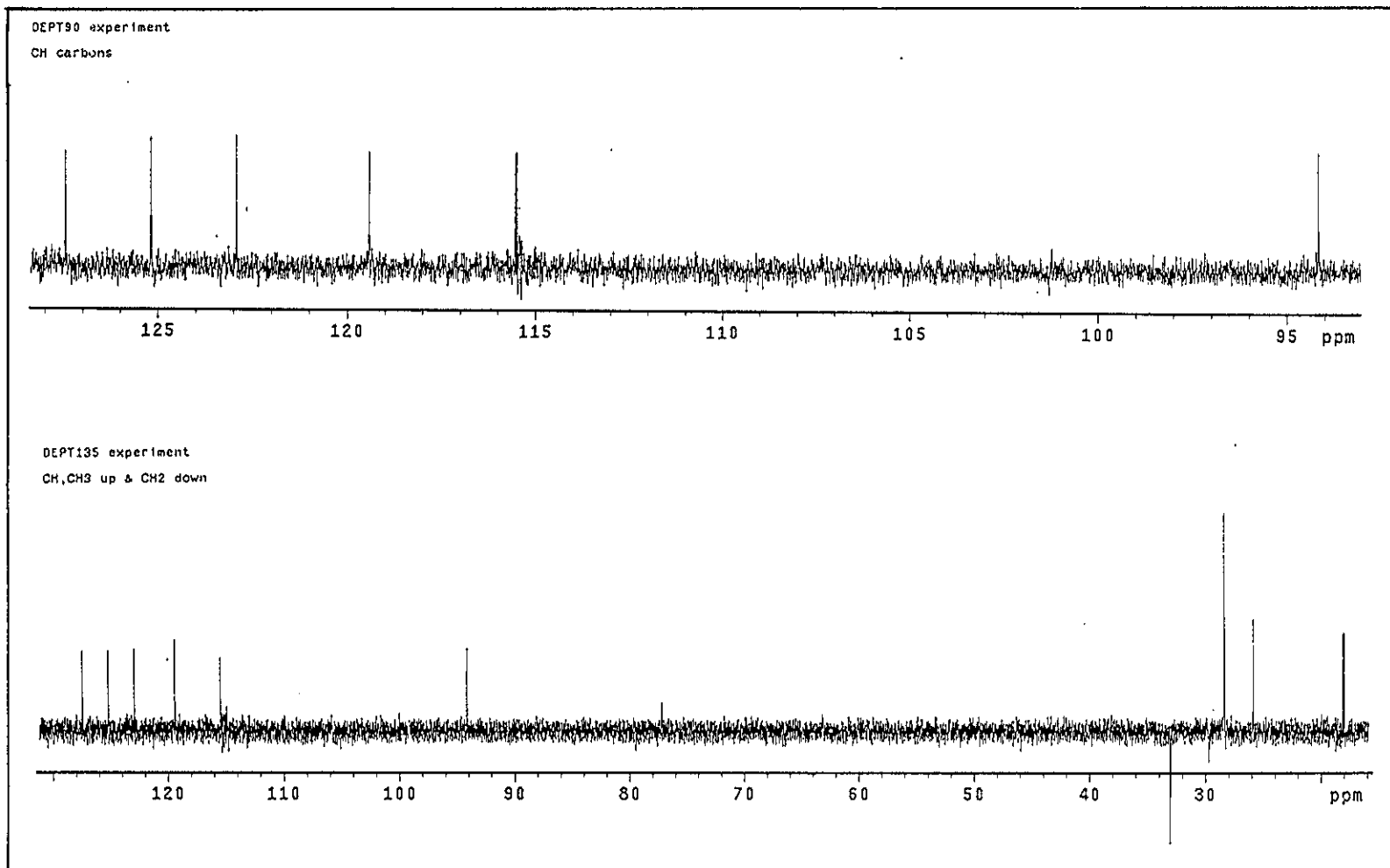


Figure 15 DEPT spectrum of YU2

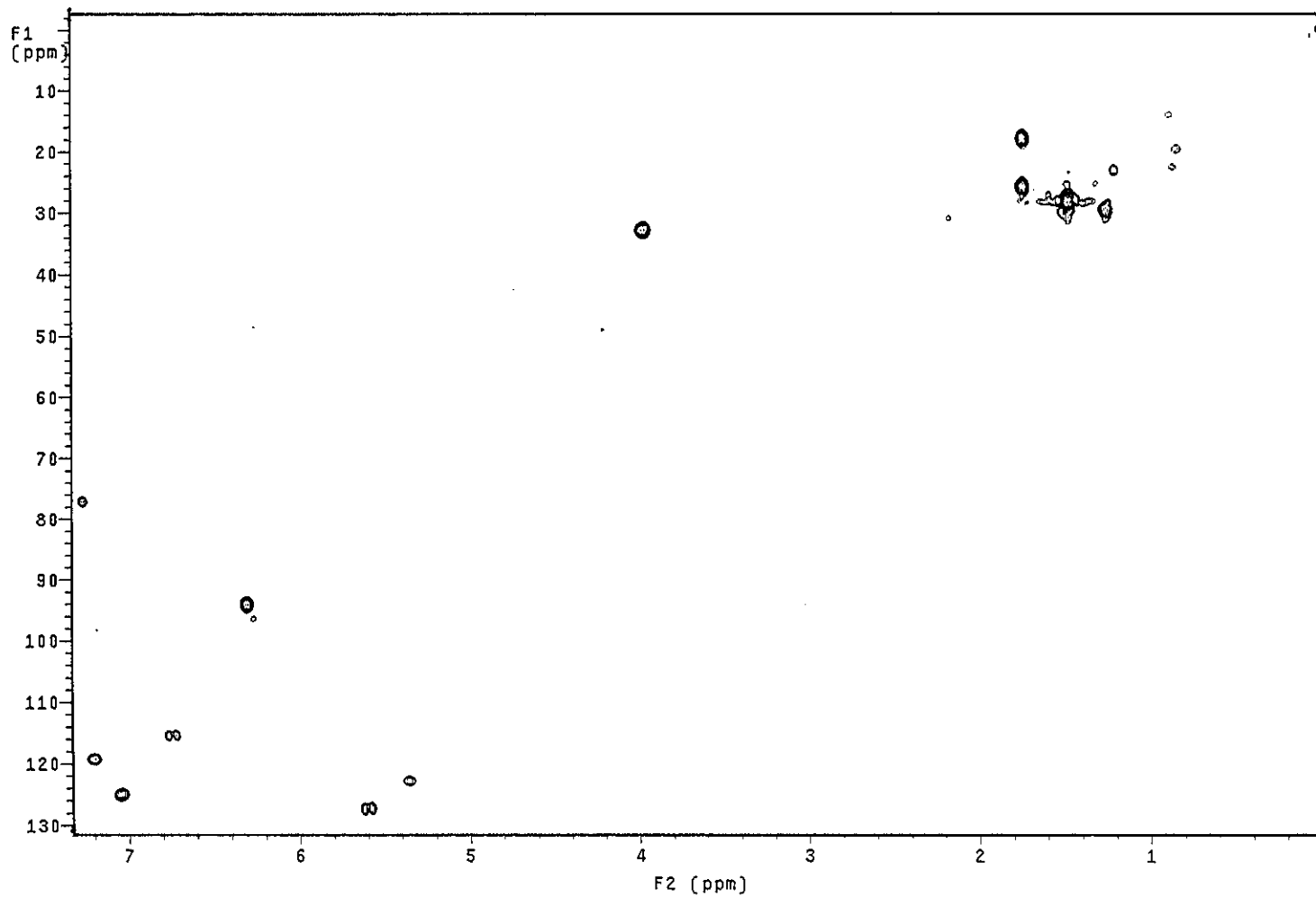


Figure 16 2D HMQC spectrum of YU2

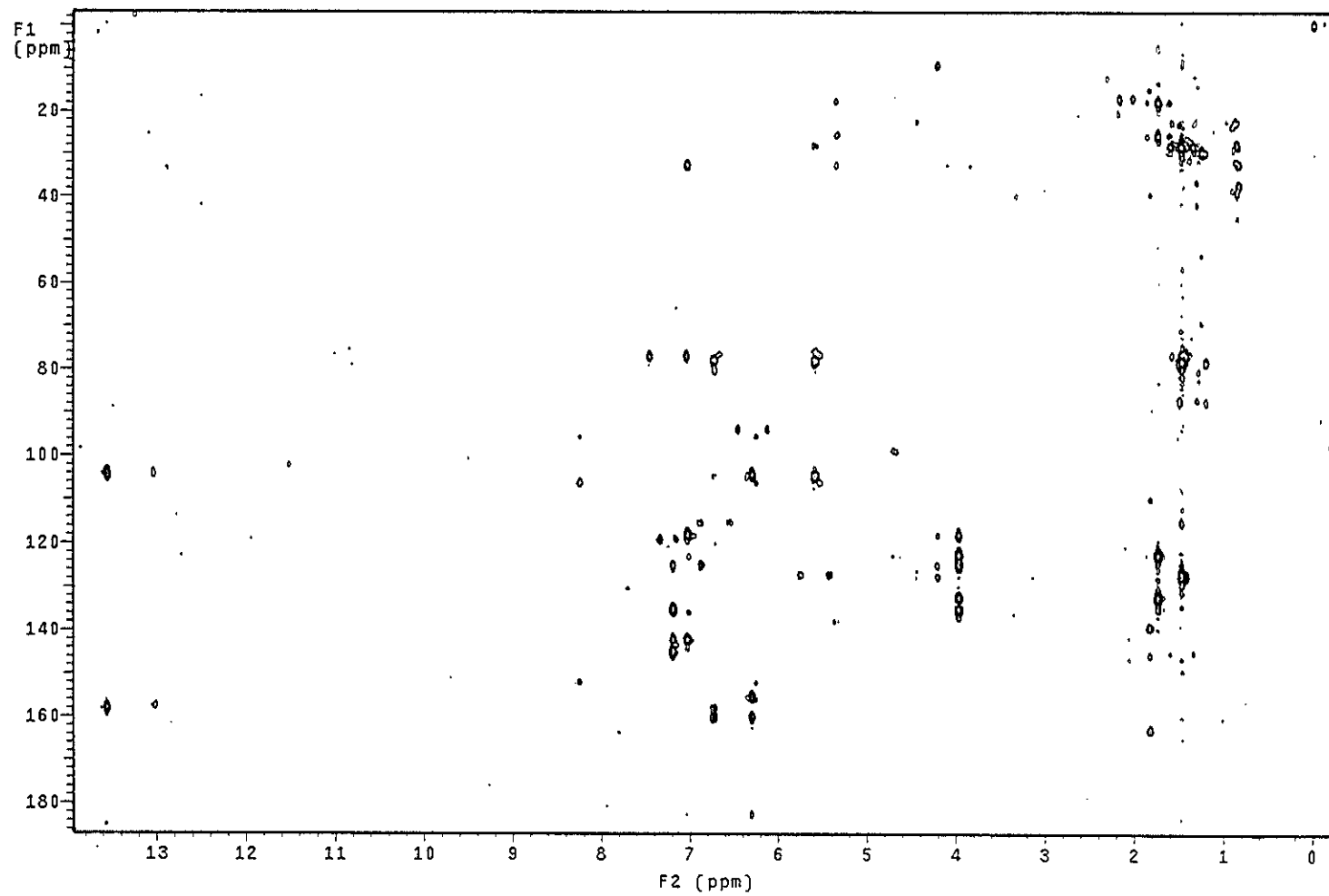


Figure 17 2D HMBC spectrum of YU2

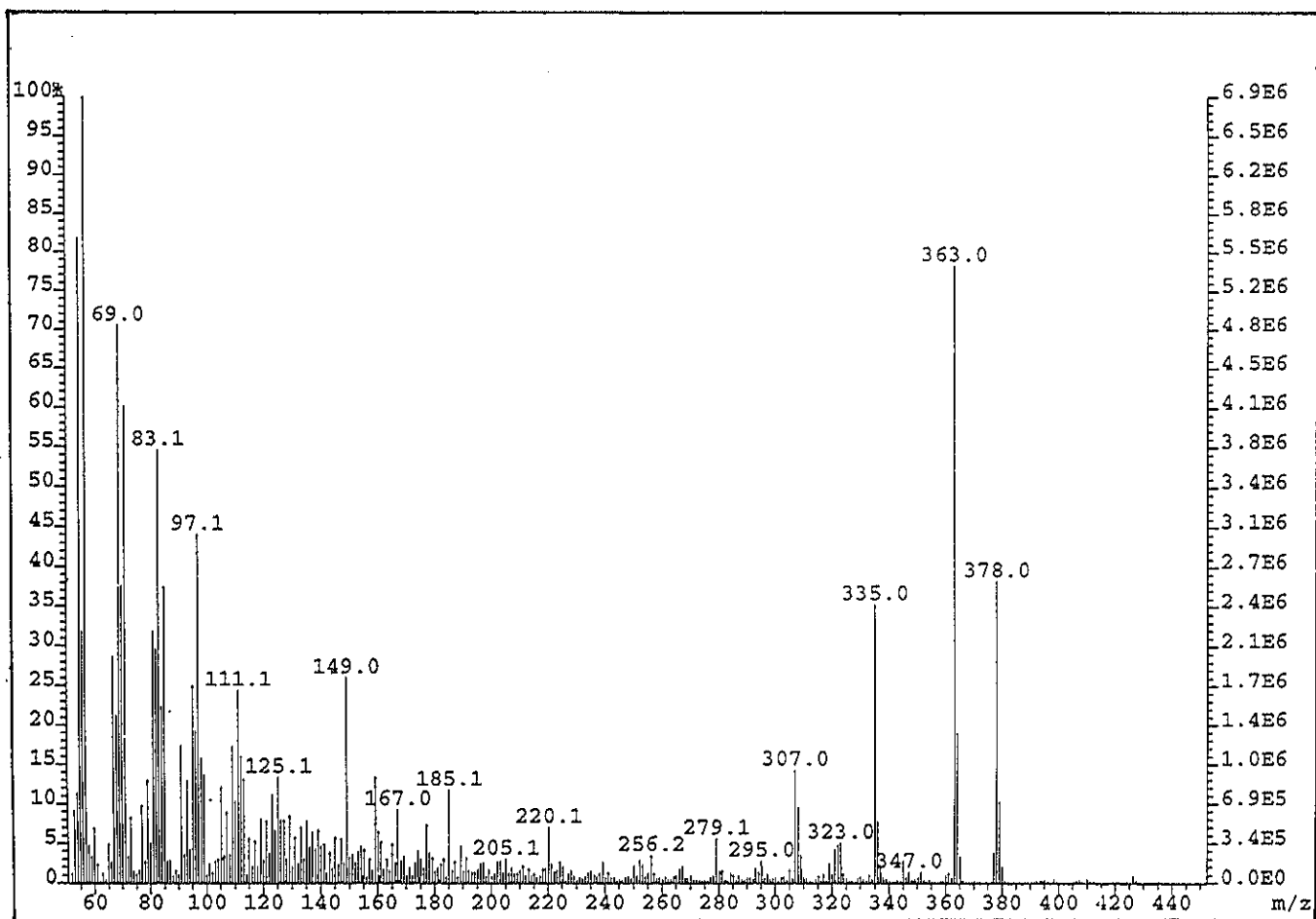


Figure 18 Mass spectrum of YU2

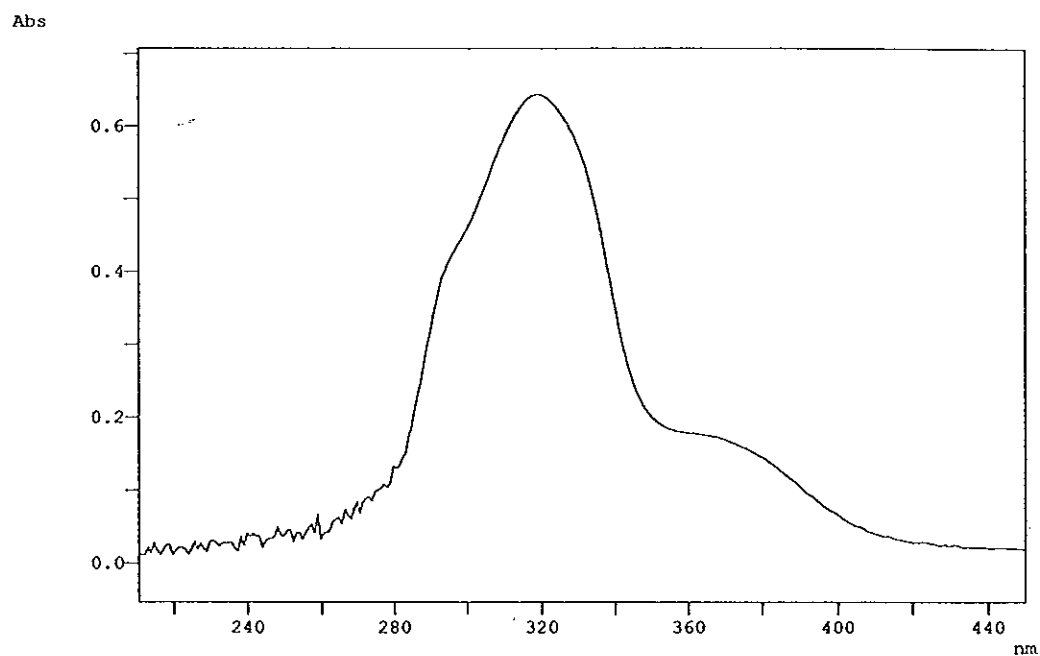


Figure 19 UV (MeOH) spectrum of YU9

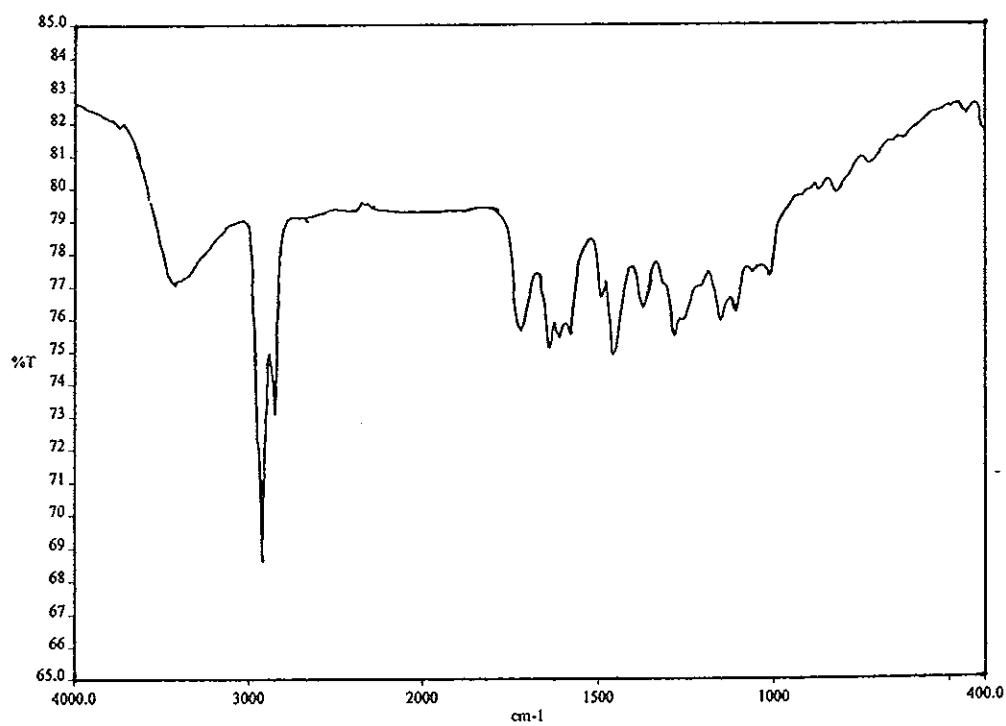


Figure 20 FT-IR (neat) spectrum of YU9

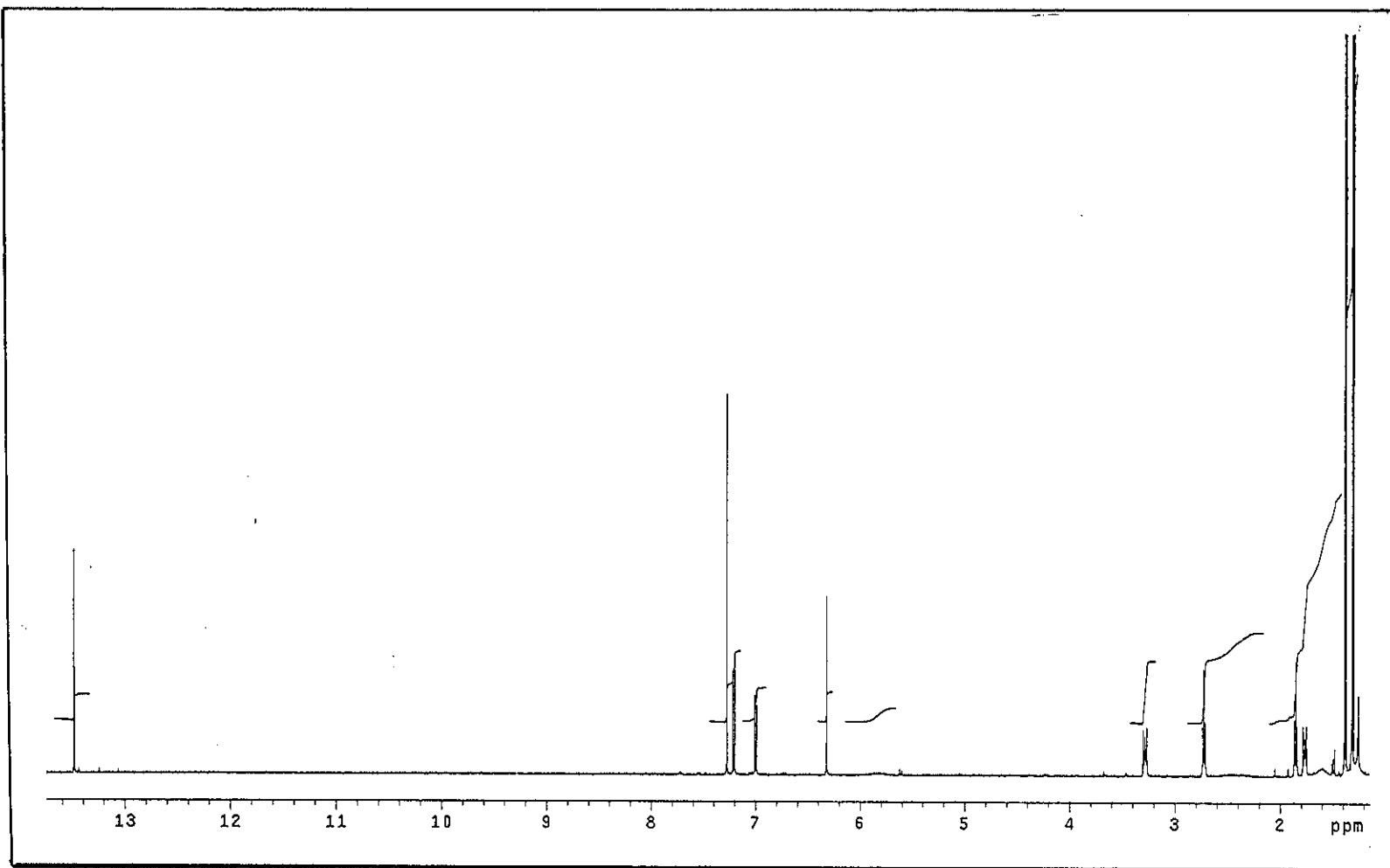


Figure 21 ^1H NMR (500 MHz) (CDCl_3) spectrum of YU9

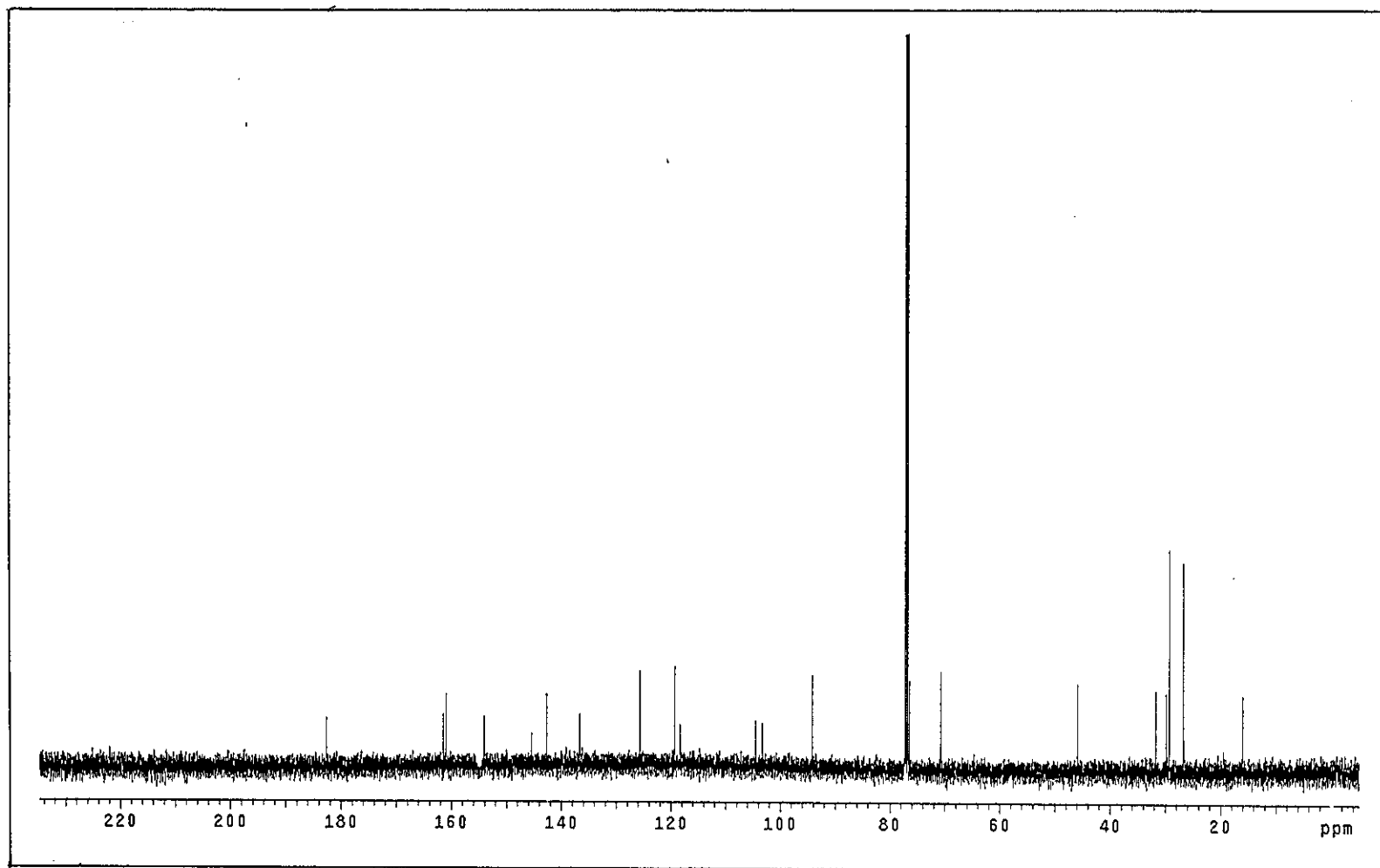


Figure 22 ^{13}C NMR (125 MHz) (CDCl_3) spectrum of YU9

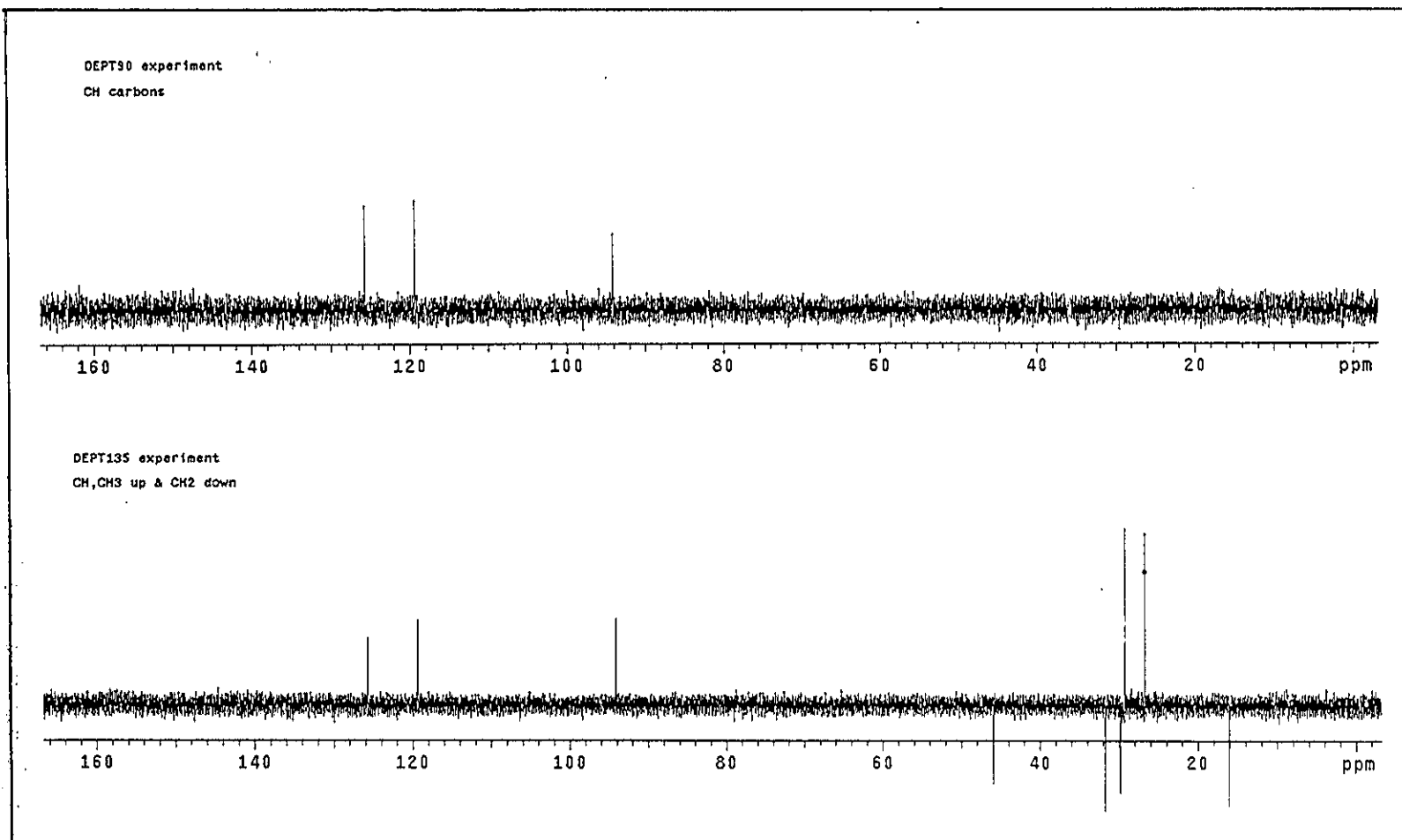


Figure 23 DEPT spectrum of YU9

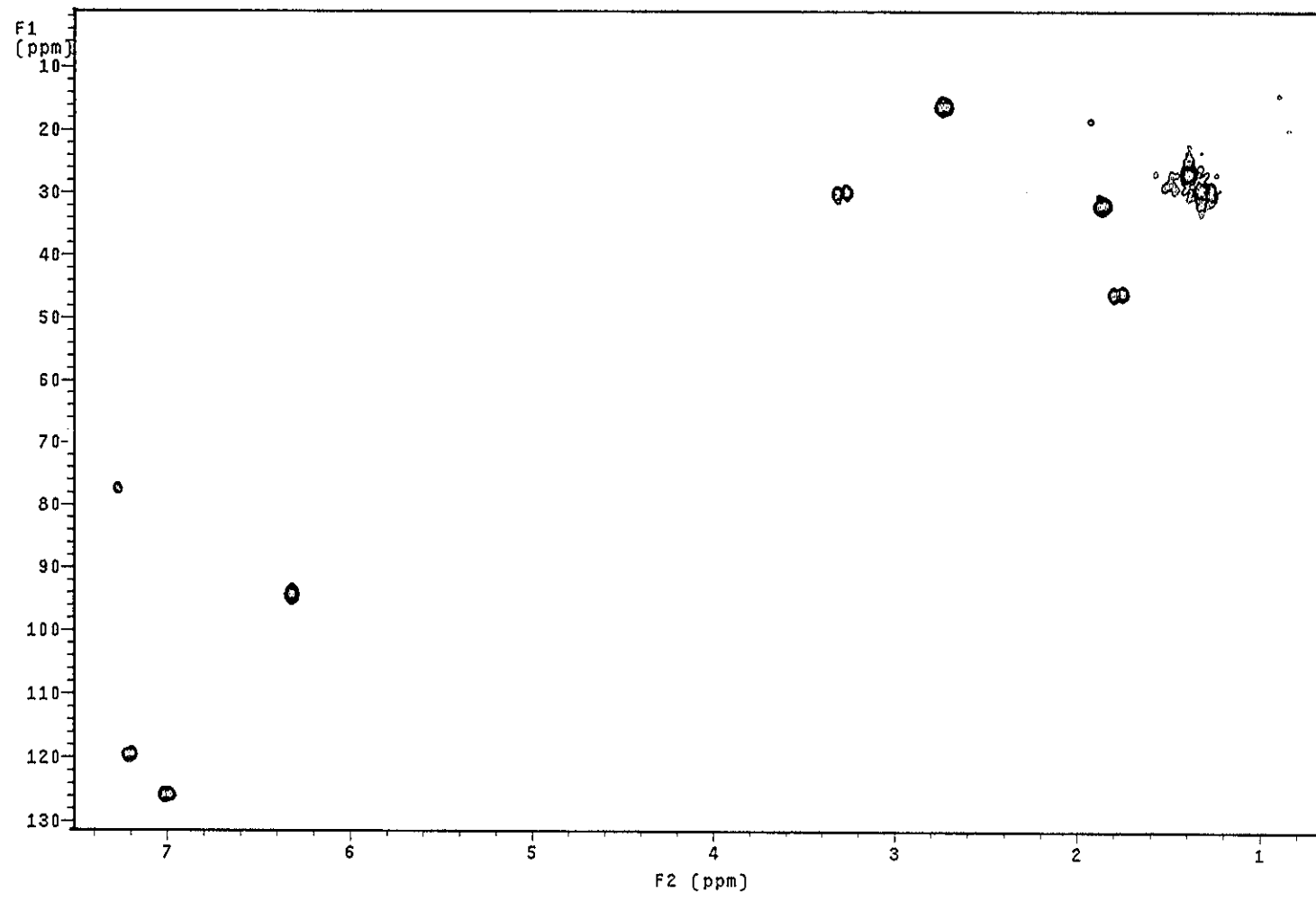


Figure 24 2D HMQC spectrum of YU9

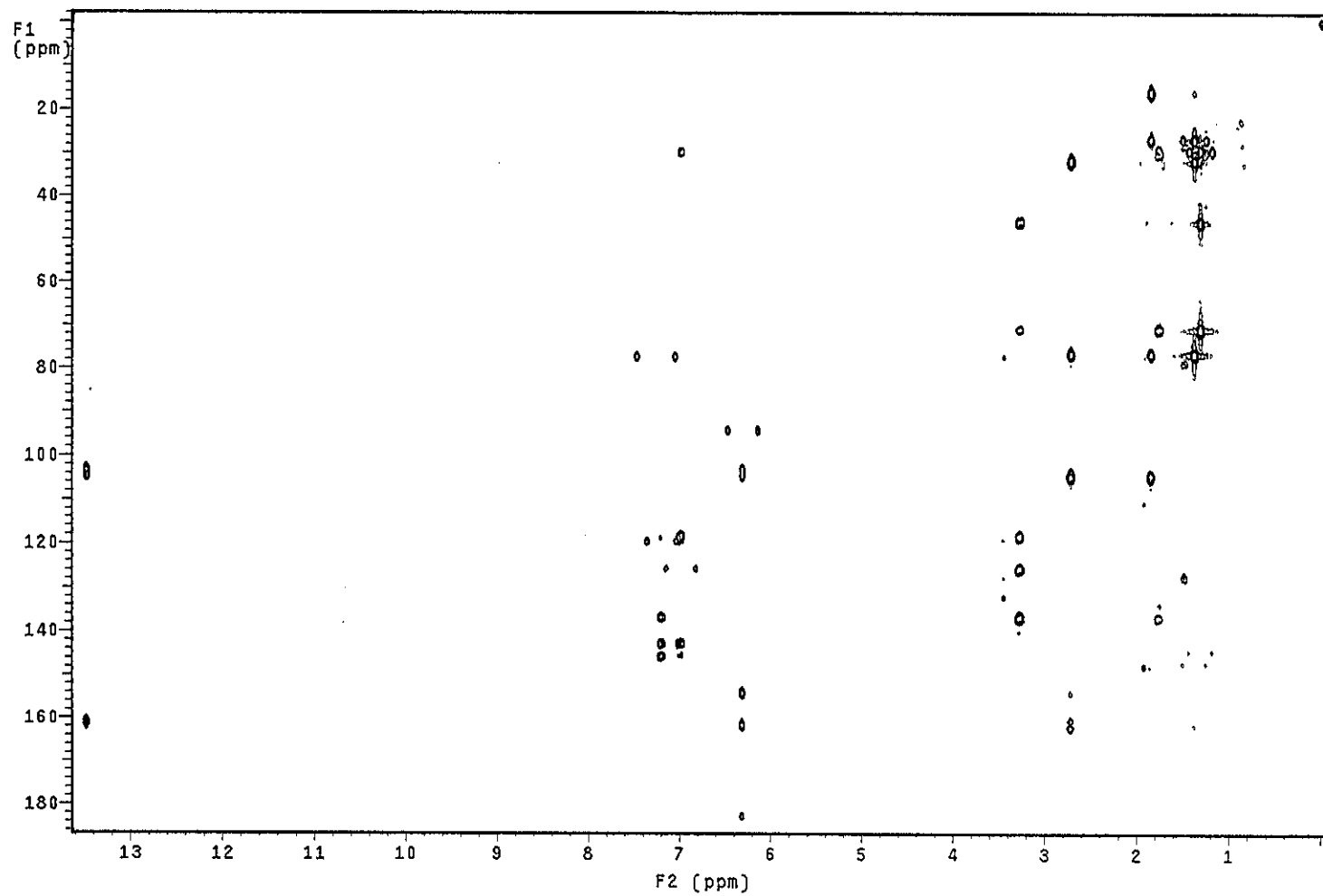


Figure 25 2D HMBC spectrum of YU9

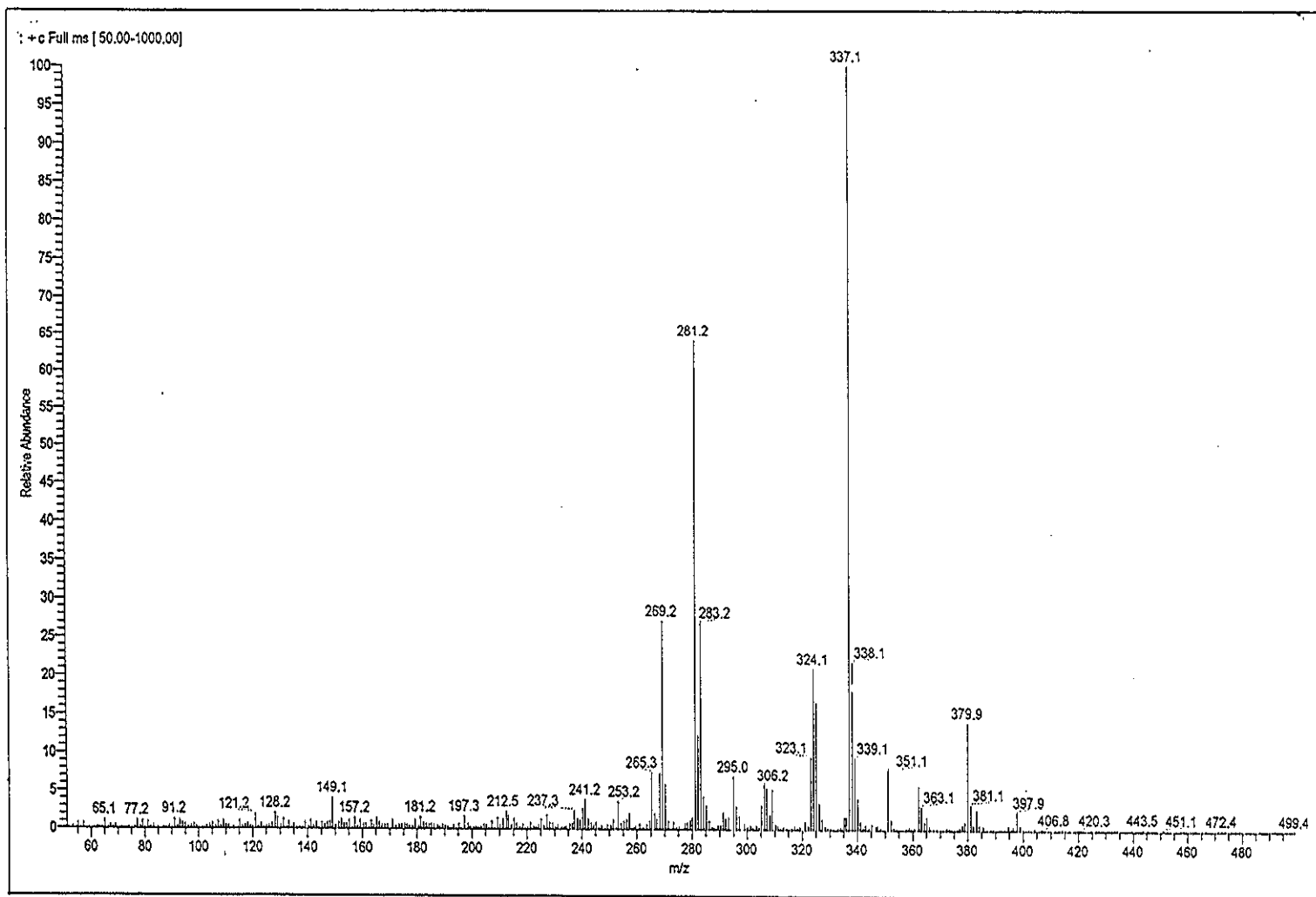


Figure 26 Mass spectrum of YU9

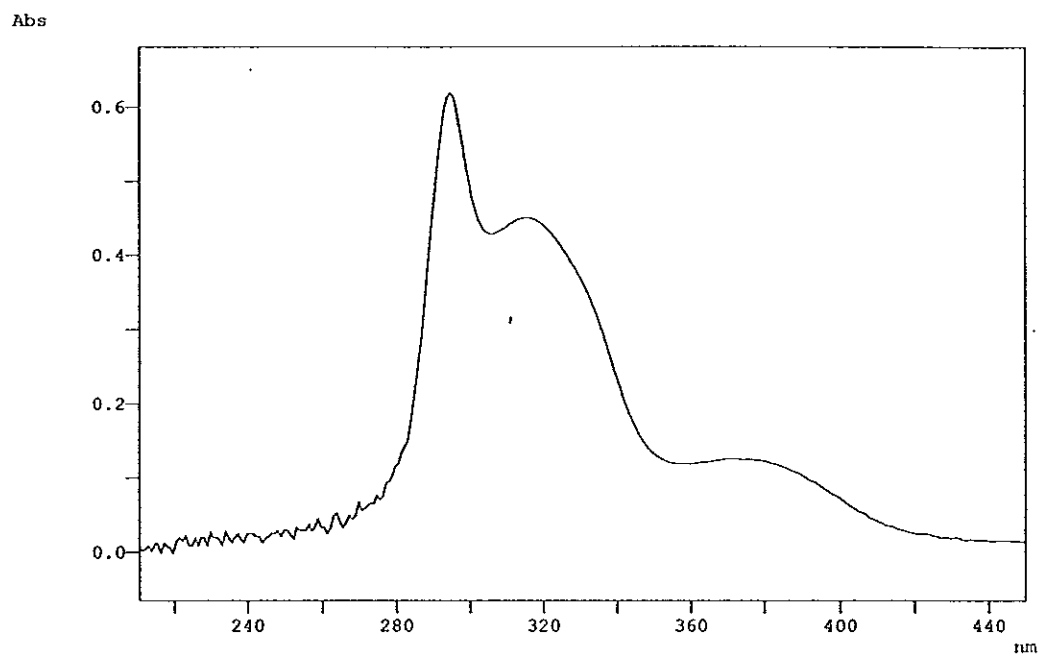


Figure 27 UV (MeOH) spectrum of YU10

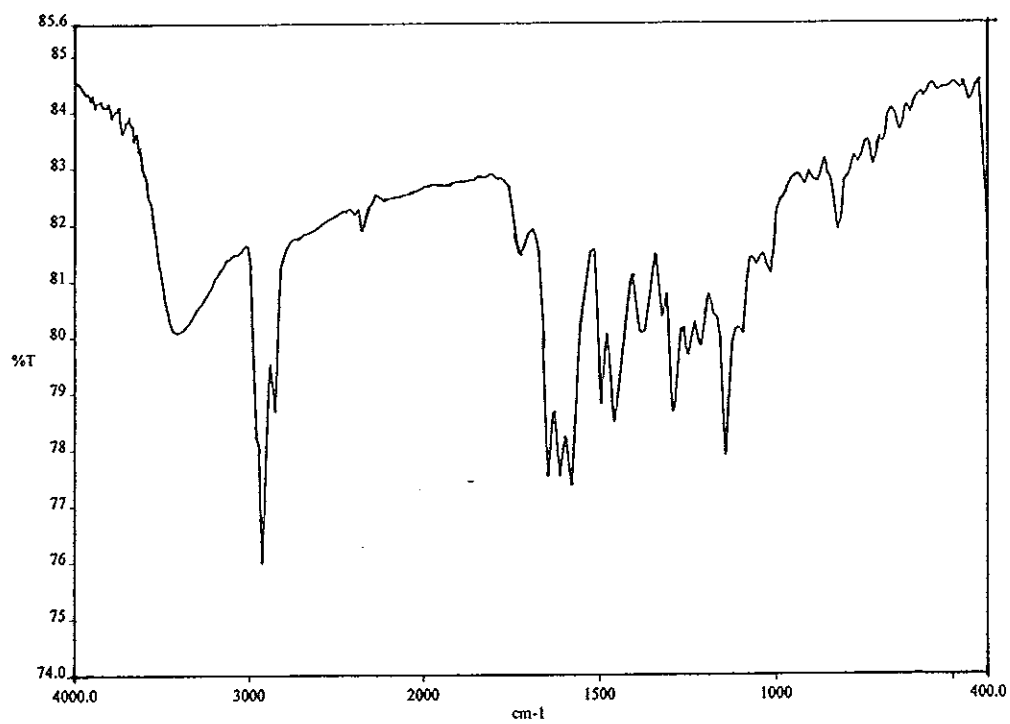


Figure 28 FT-IR (neat) spectrum of YU10

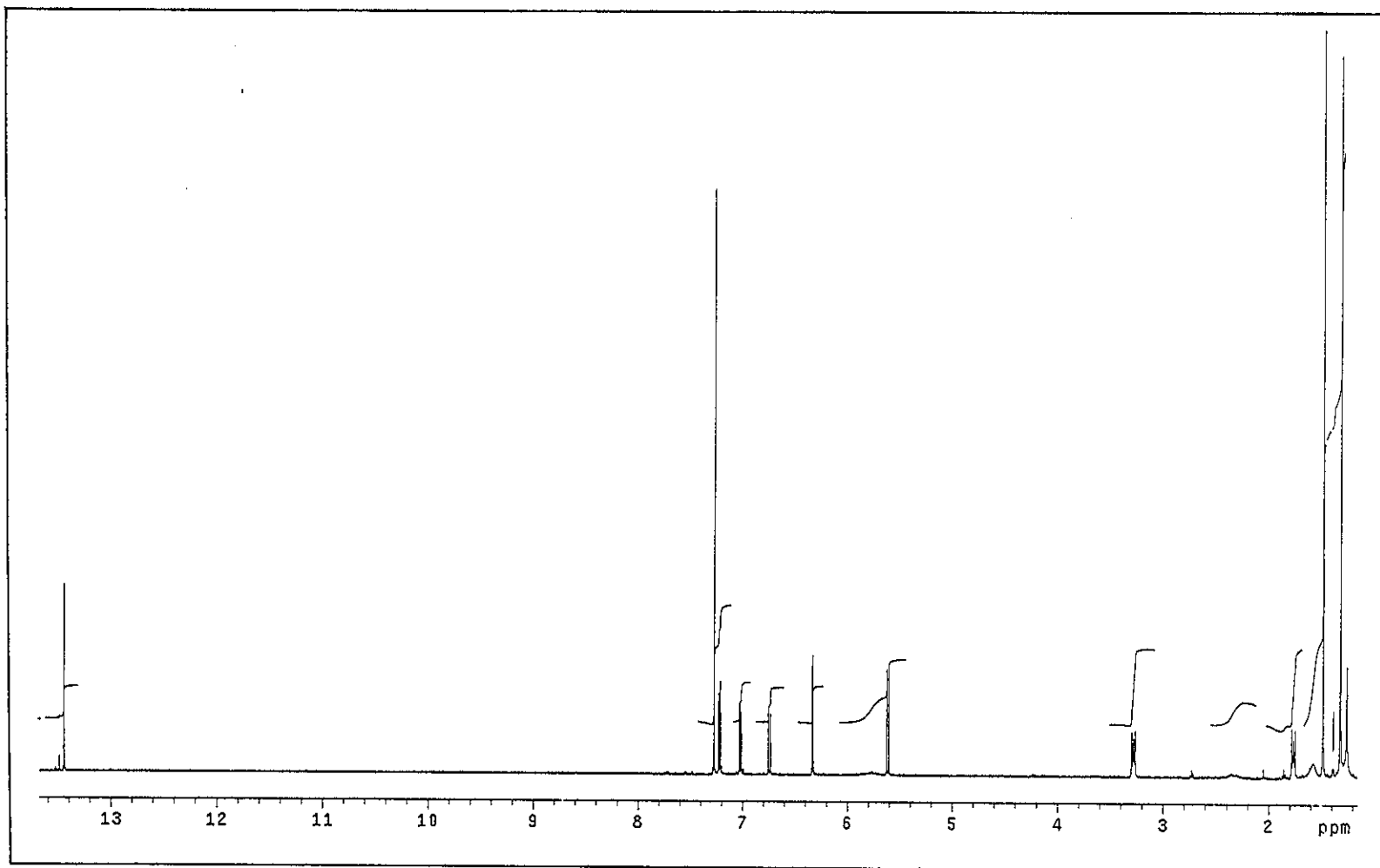


Figure 29 ^1H NMR (500 MHz) (CDCl_3) spectrum of YU10

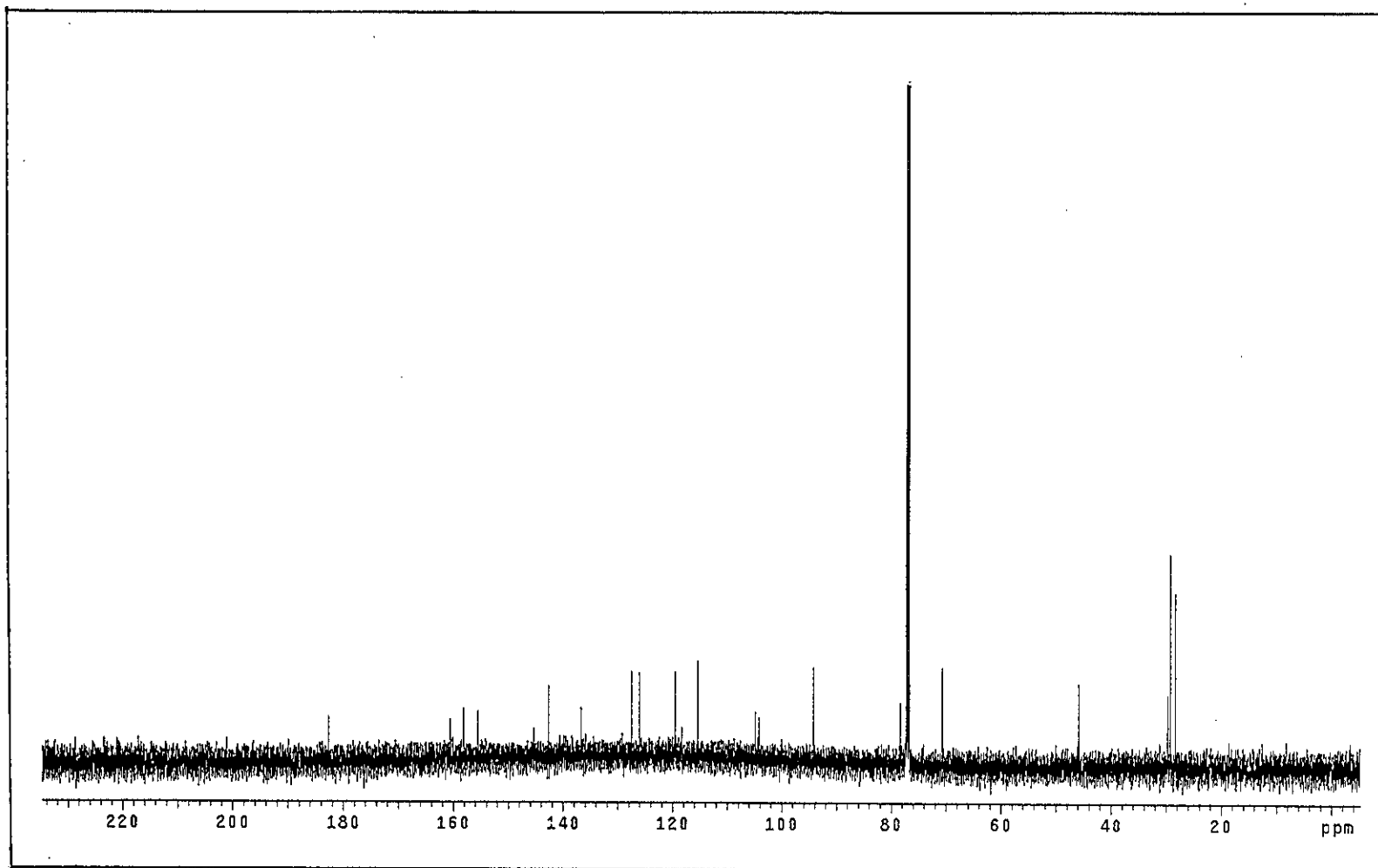


Figure 30 ^{13}C NMR (125 MHz) (CDCl_3) spectrum of YU10

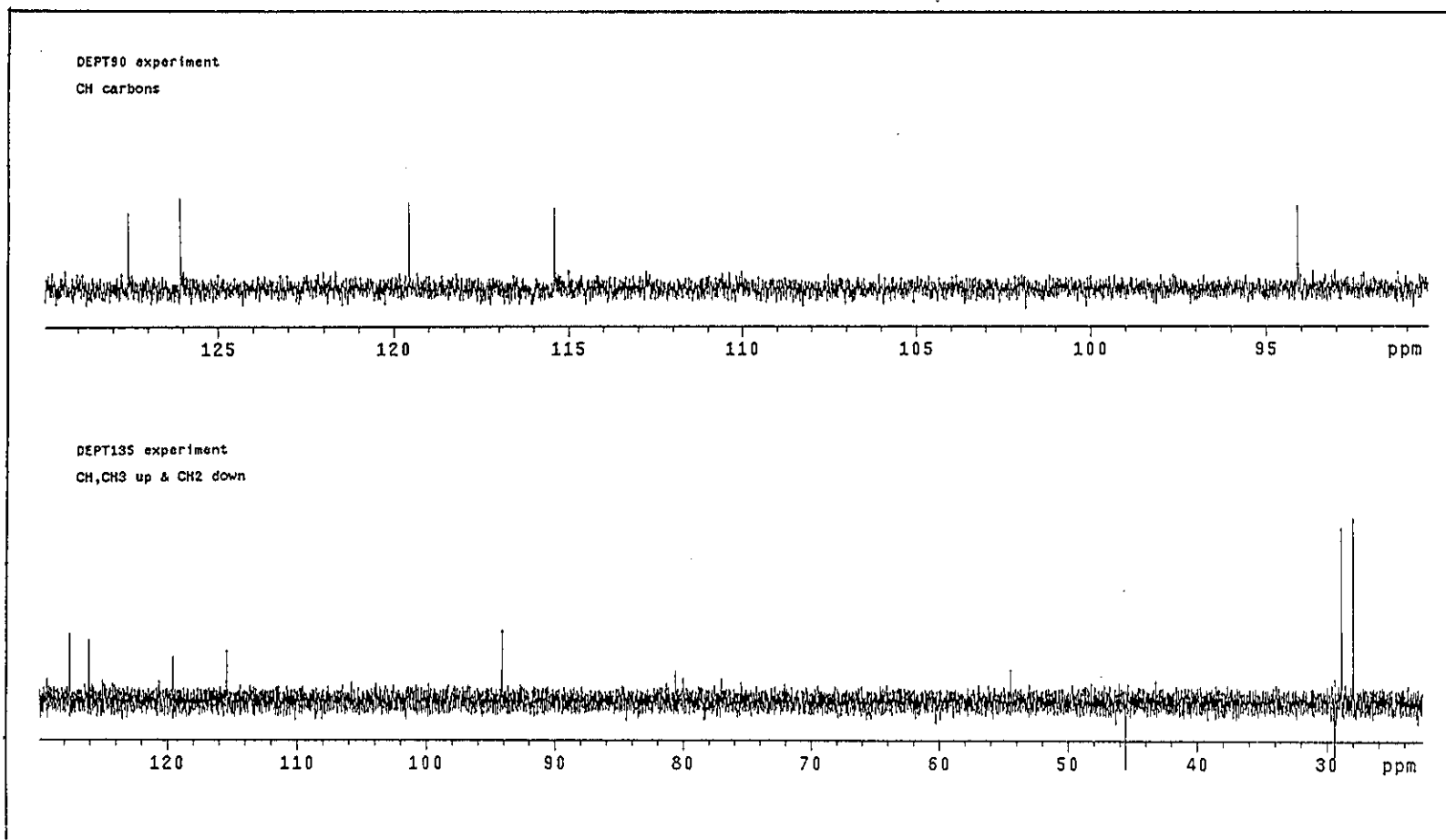


Figure 31 DEPT spectrum of YU10

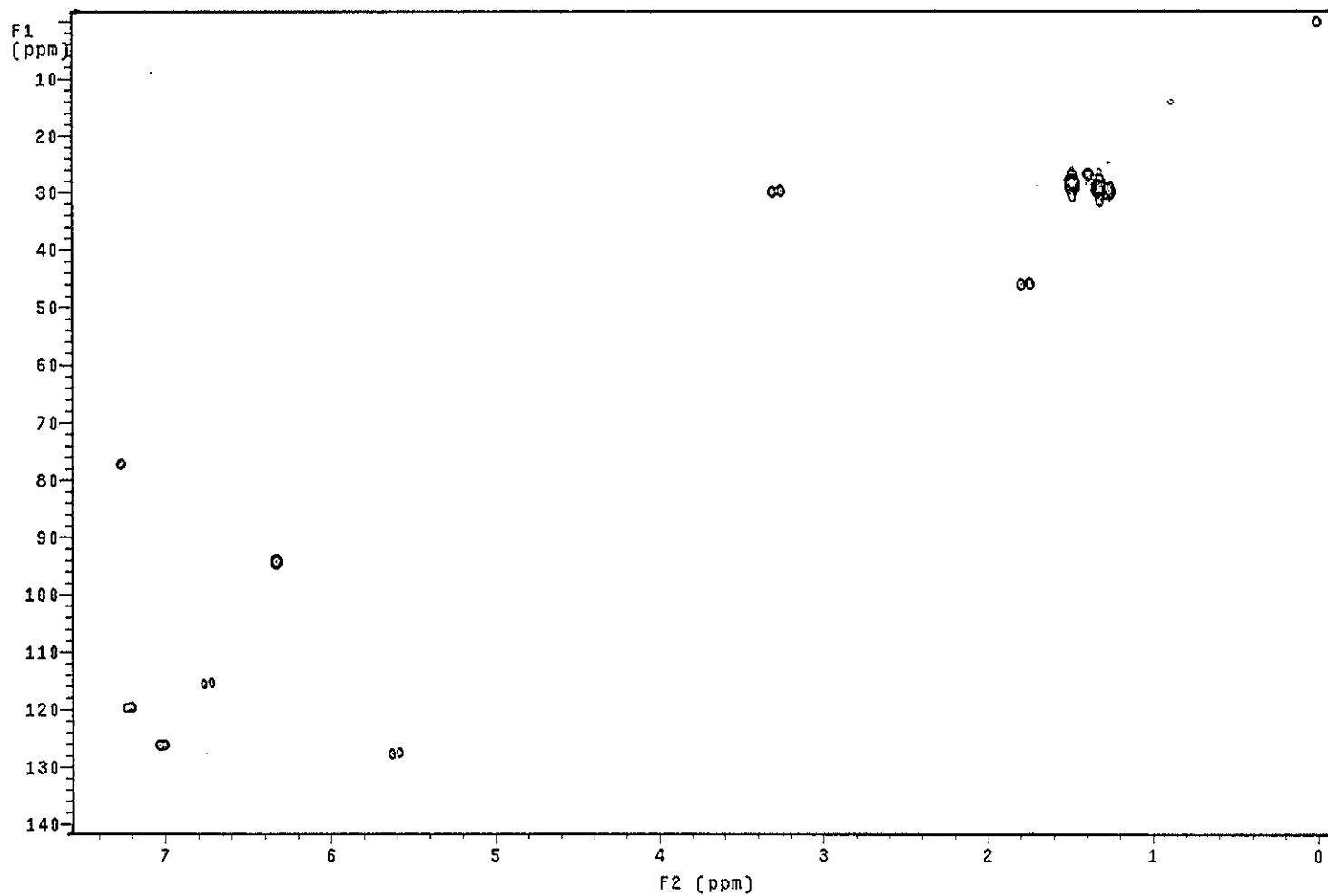


Figure 32 2D HMQC spectrum of YU10

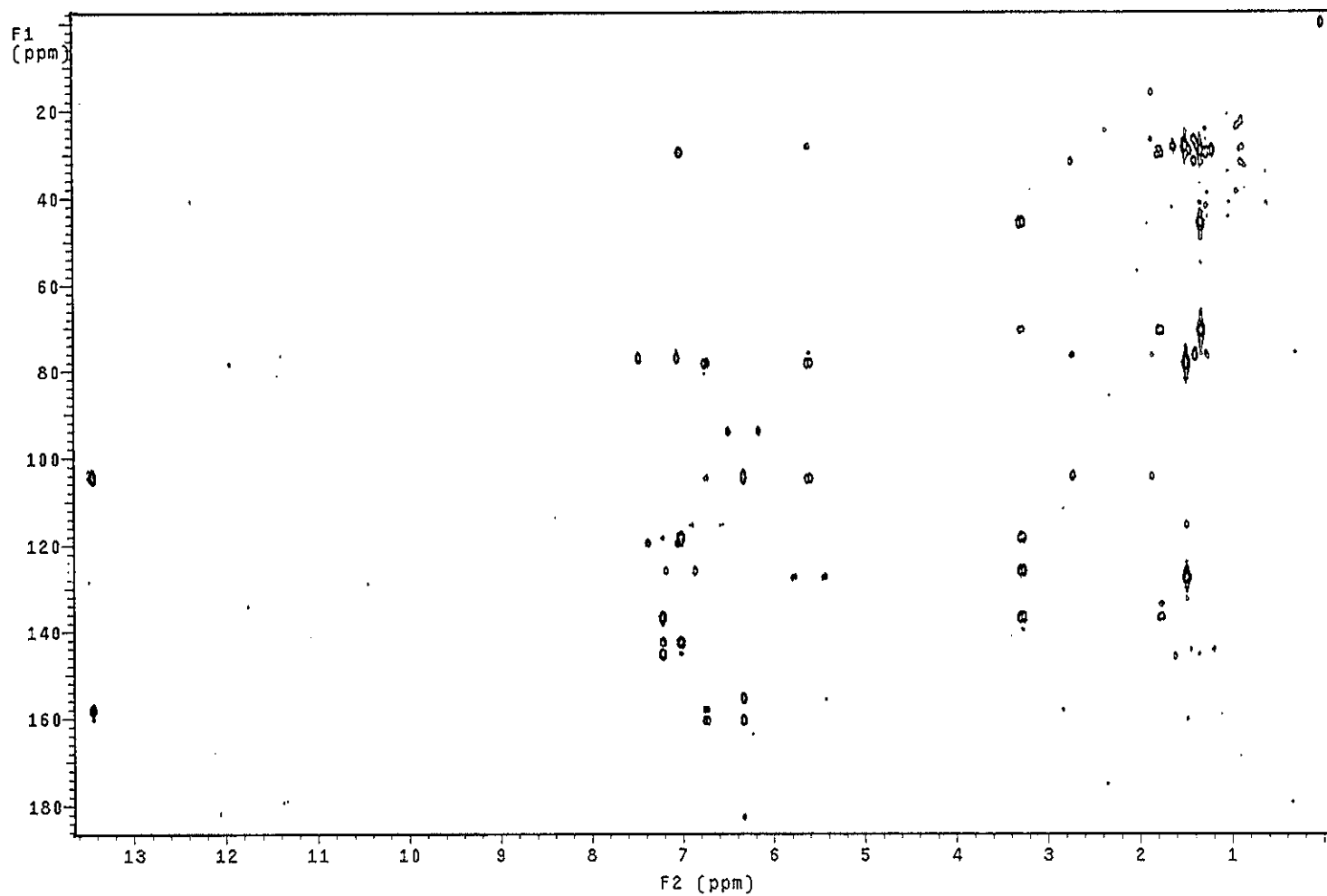


Figure 33 2D HMBC spectrum of YU10

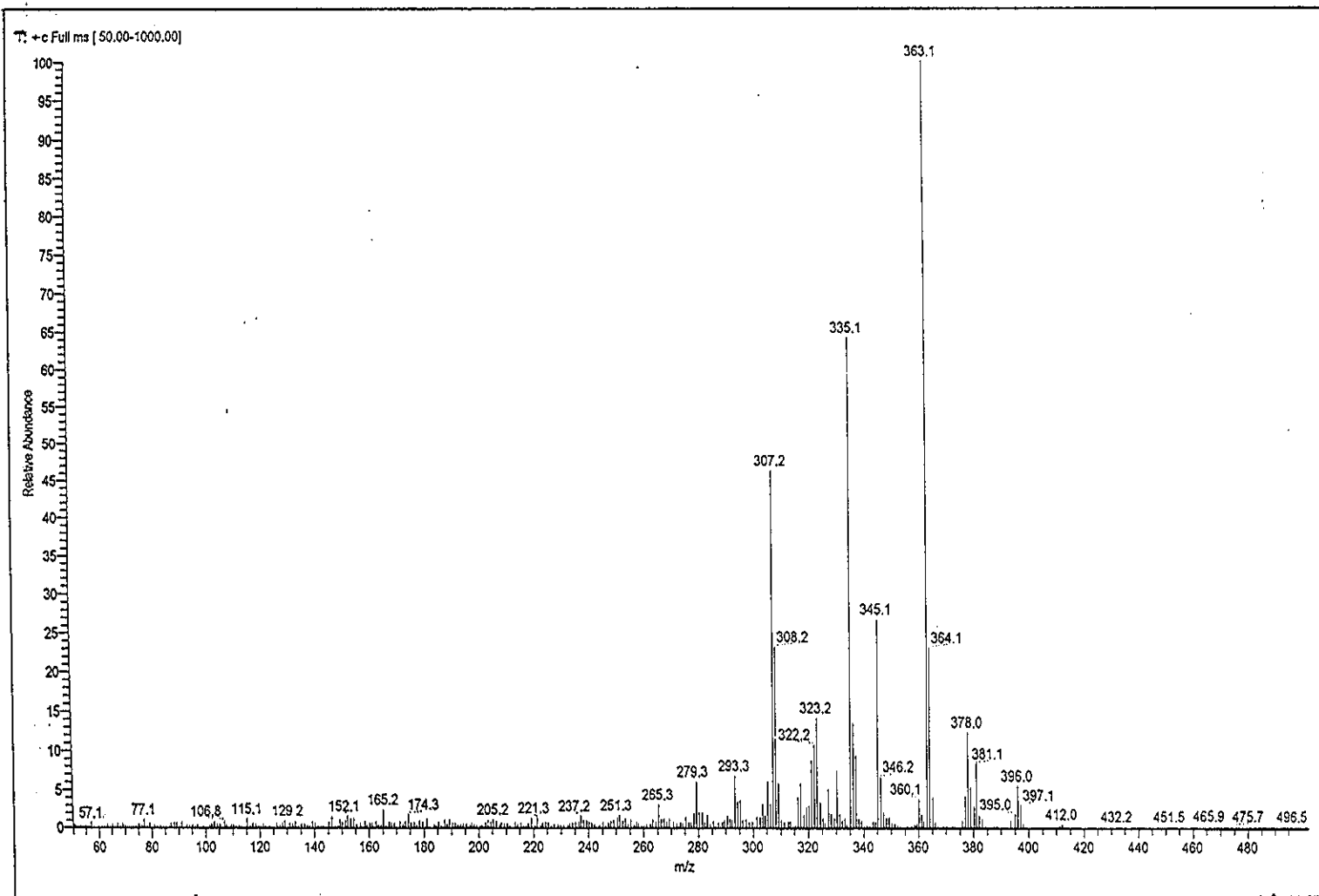


Figure 34 Mass spectrum of YU10

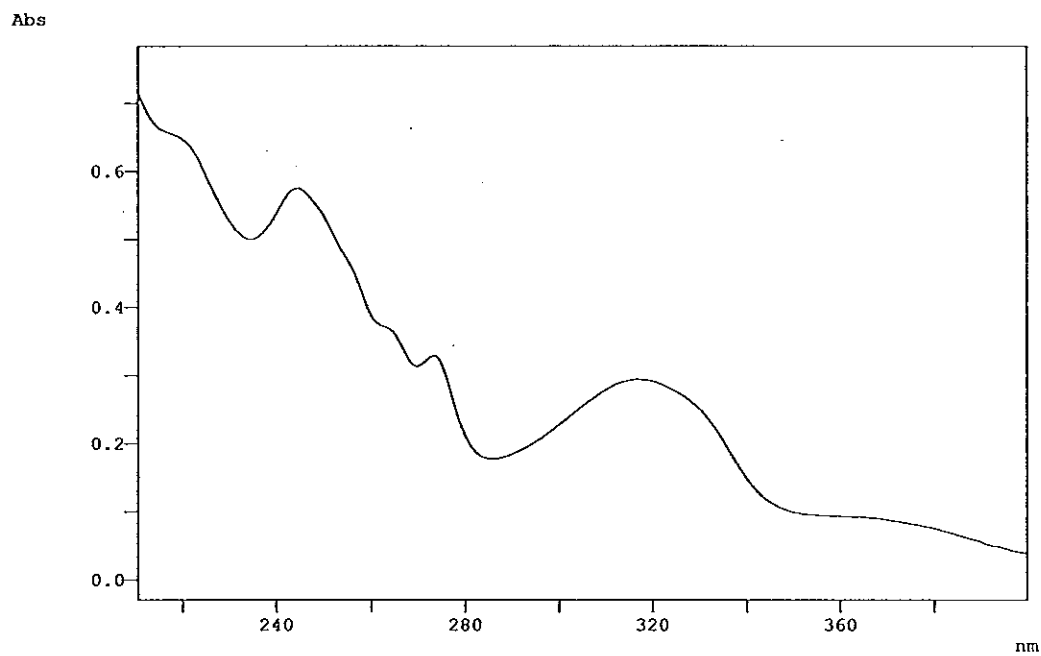


Figure 35 UV (MeOH) spectrum of YU15

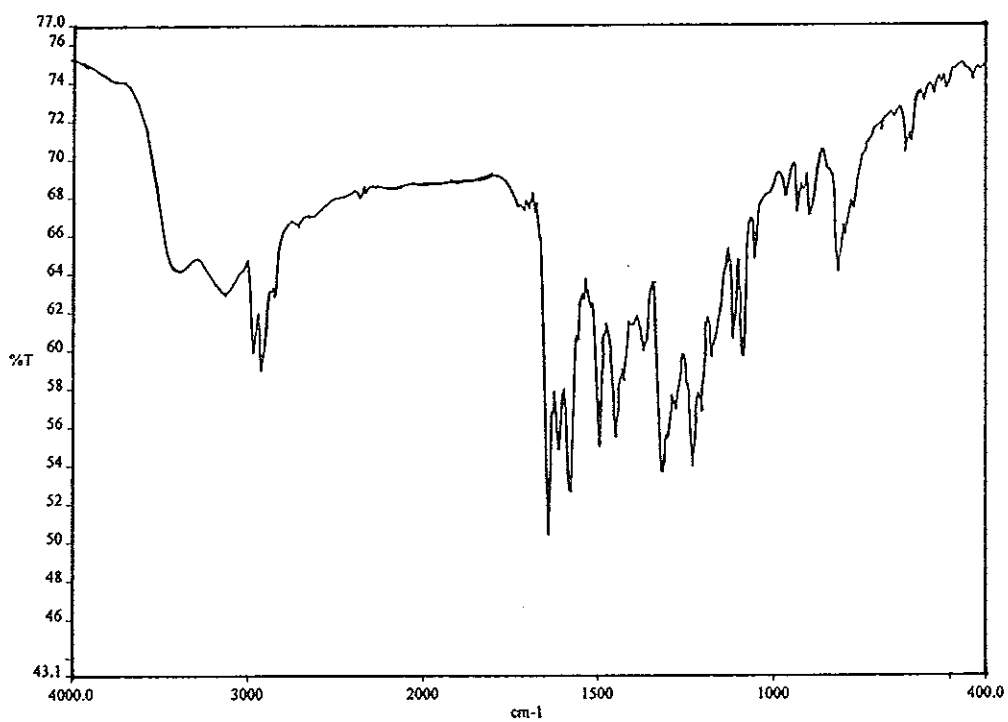


Figure 36 FT-IR (neat) spectrum of YU15

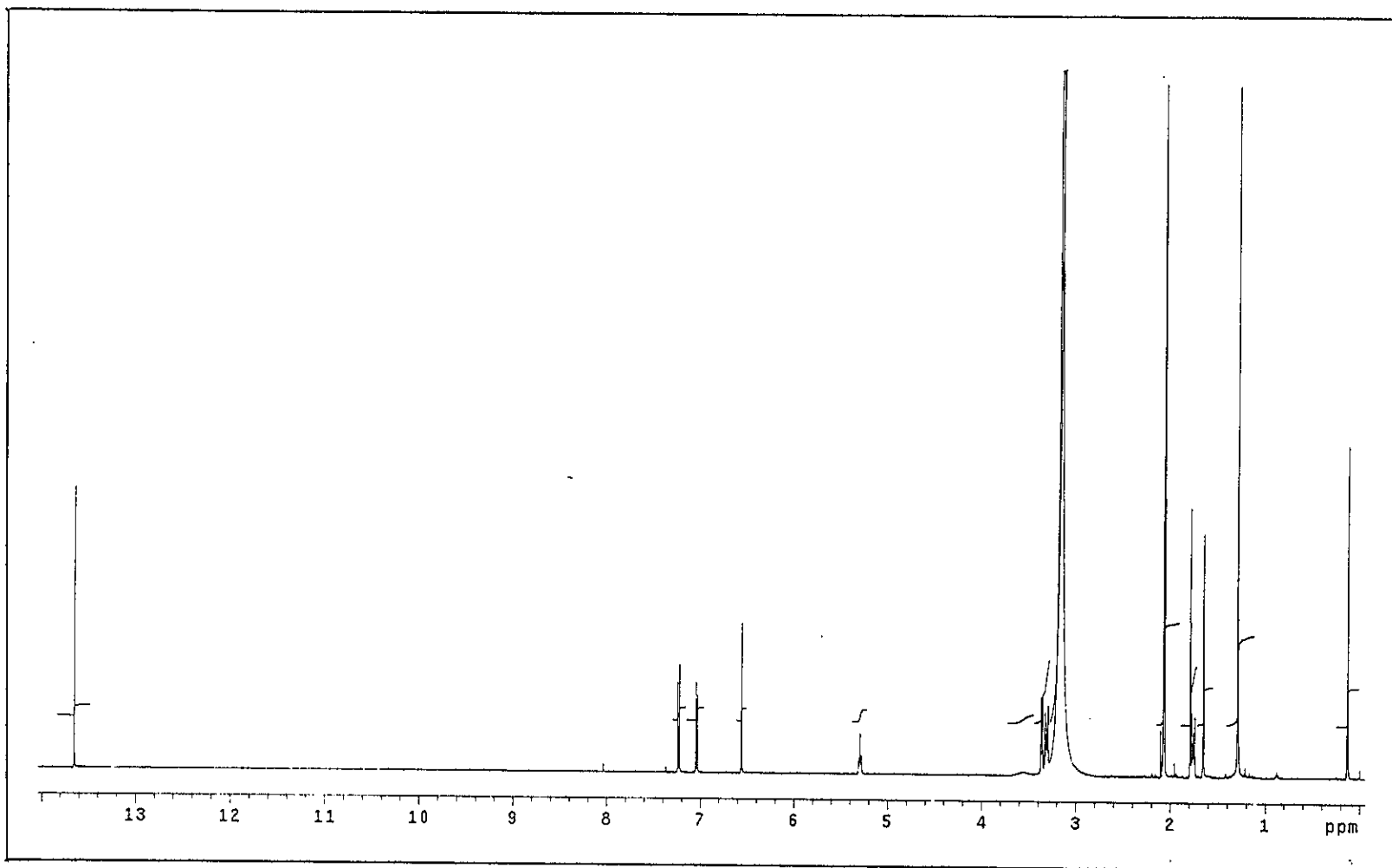


Figure 37 ^1H NMR (500 MHz) (Acetone- d_6) spectrum of YU15

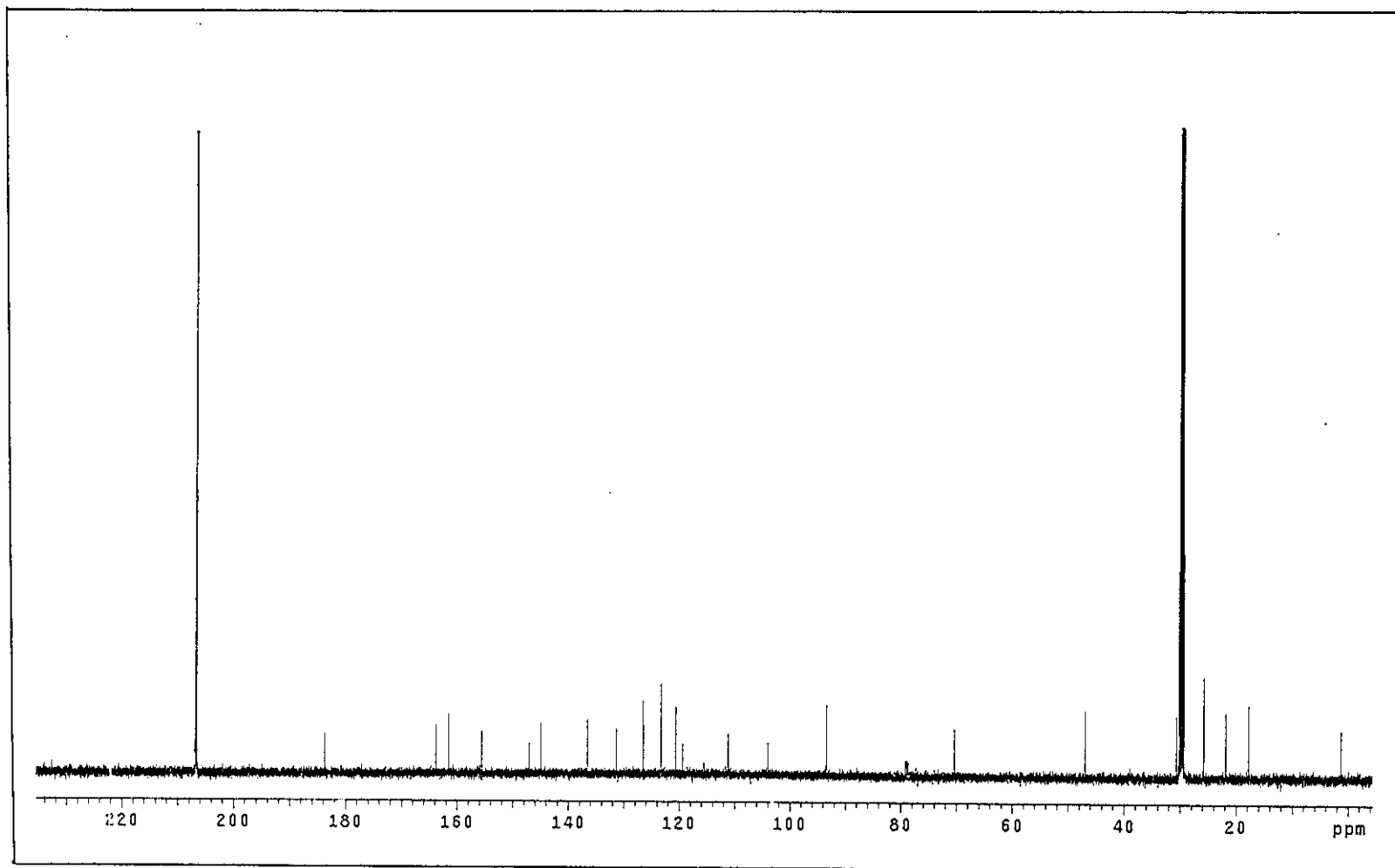


Figure 38 ^{13}C NMR (125 MHz) (Acetone- d_6) spectrum of YU15

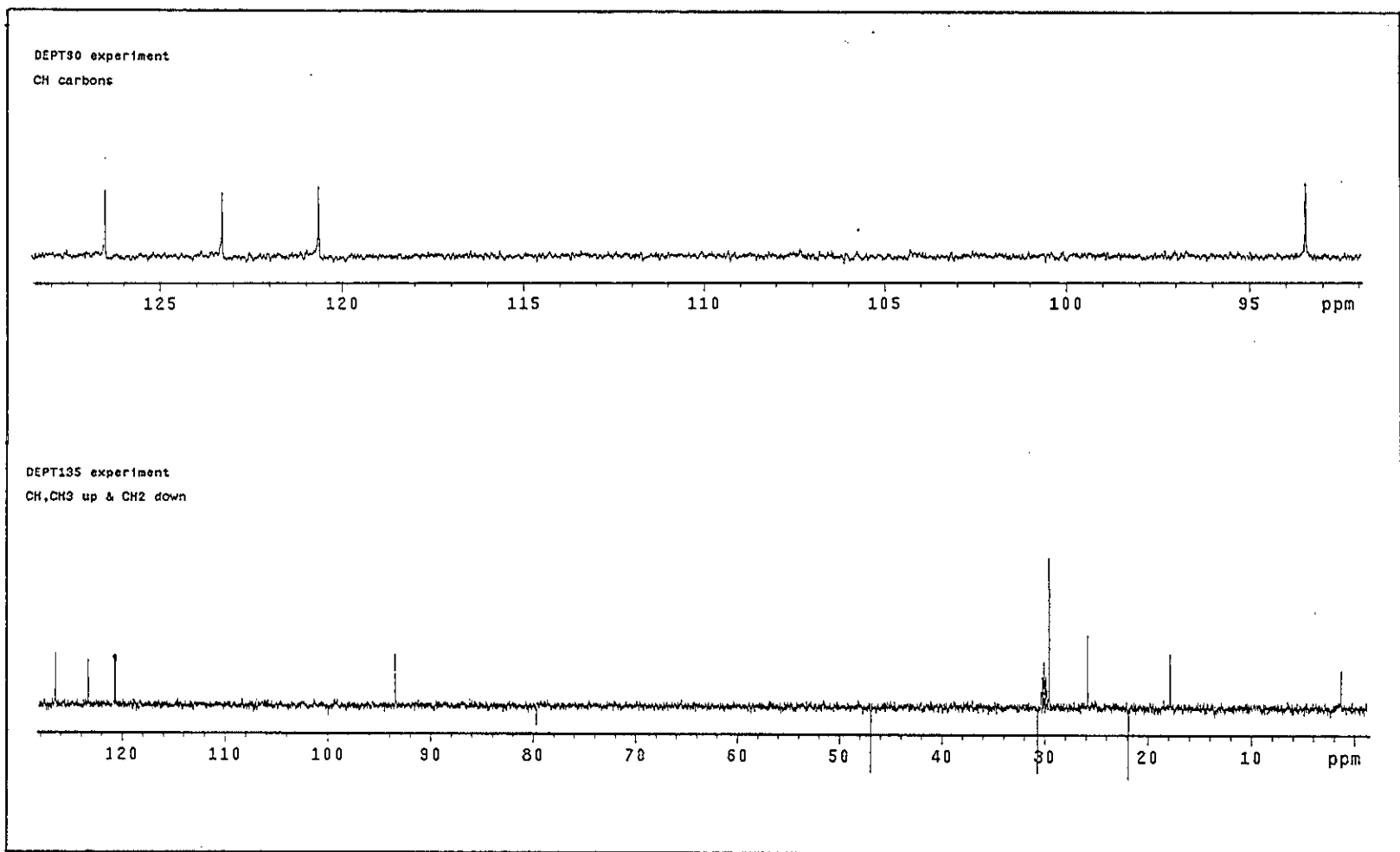


Figure 39 DEPT spectrum of YU15

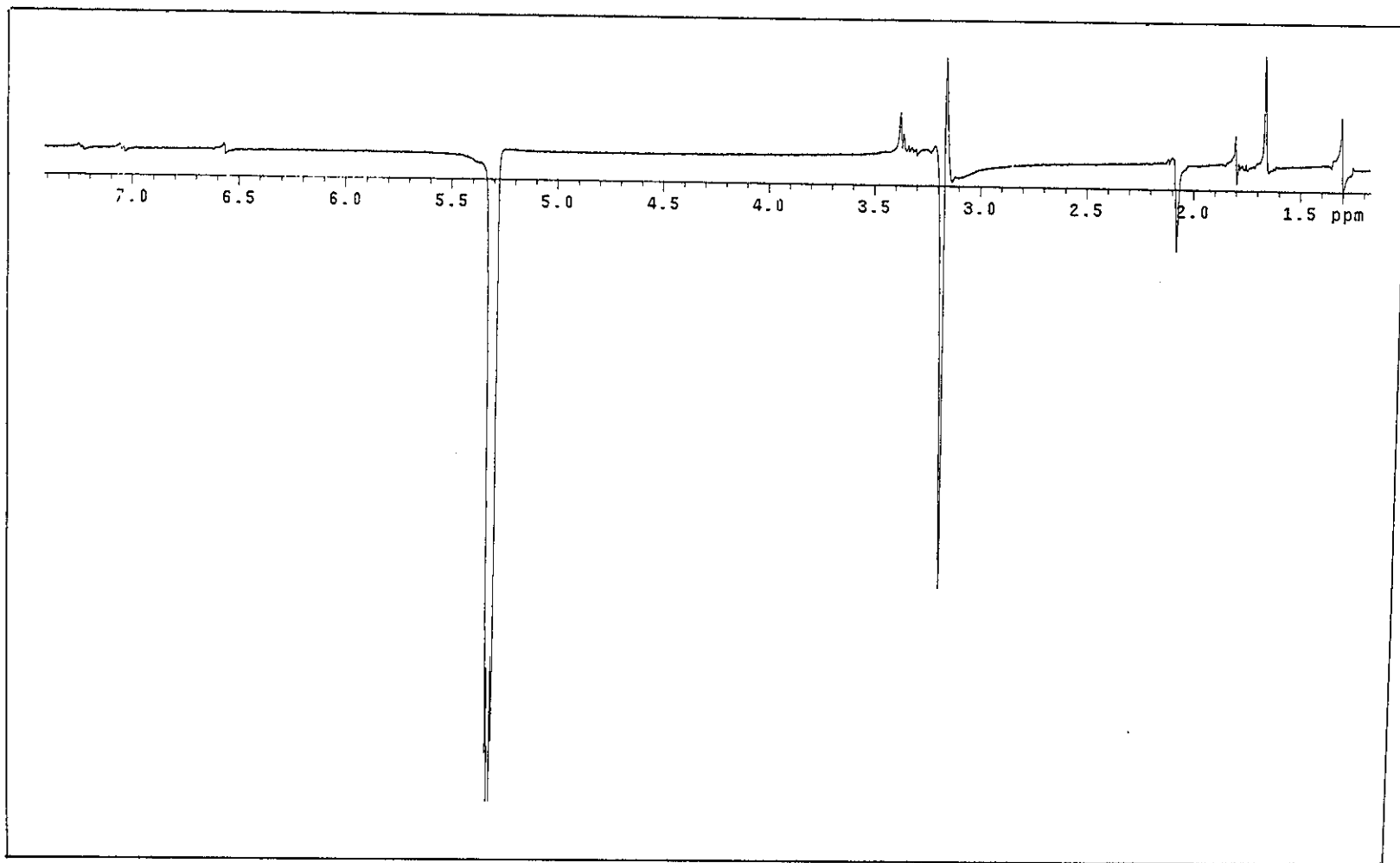


Figure 40 NOEDIFF spectrum of YU15 after irradiation at δ_{H} 5.29

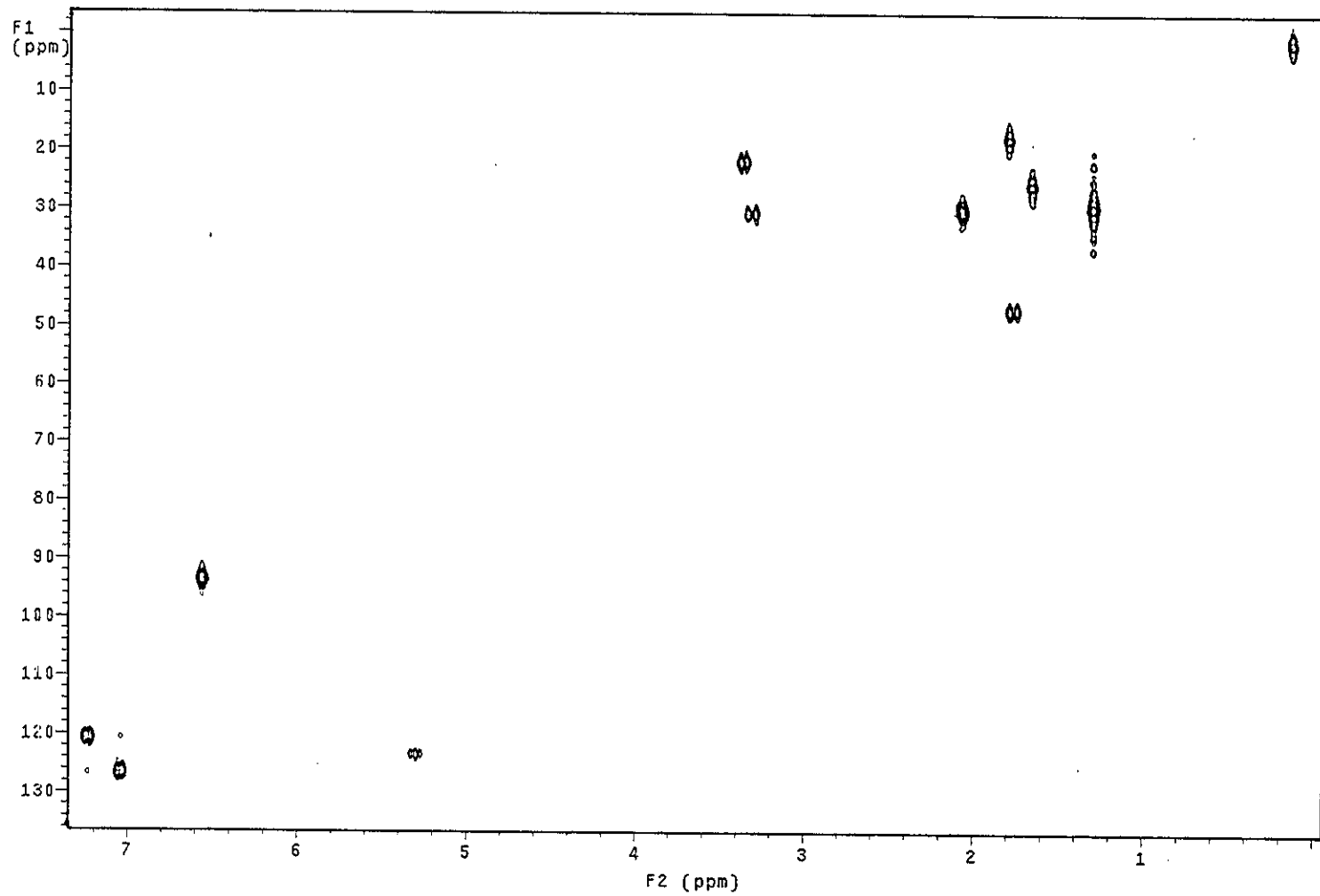


Figure 41 2D HMQC spectrum of YU15

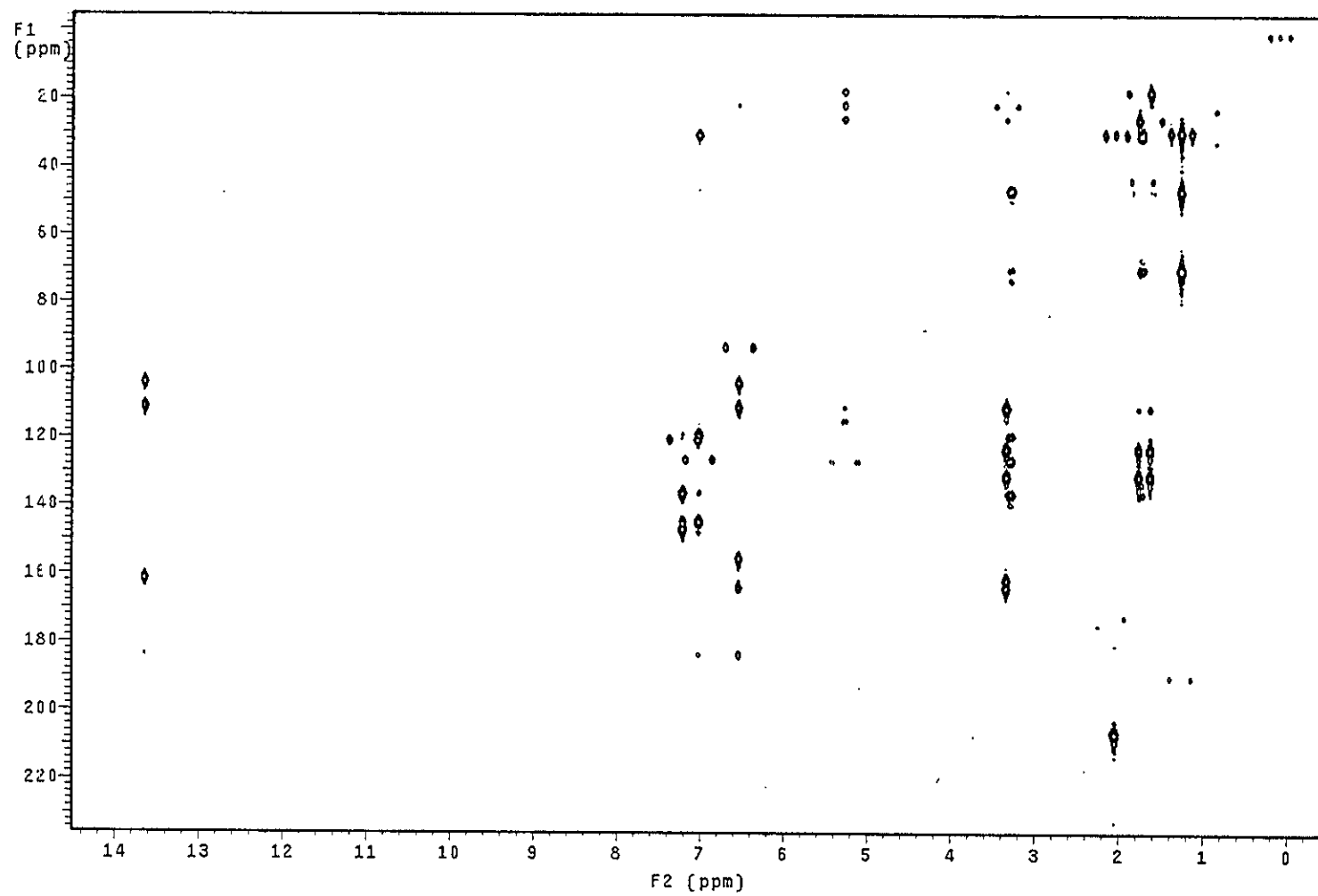


Figure 42 2D HMBC spectrum of YU15

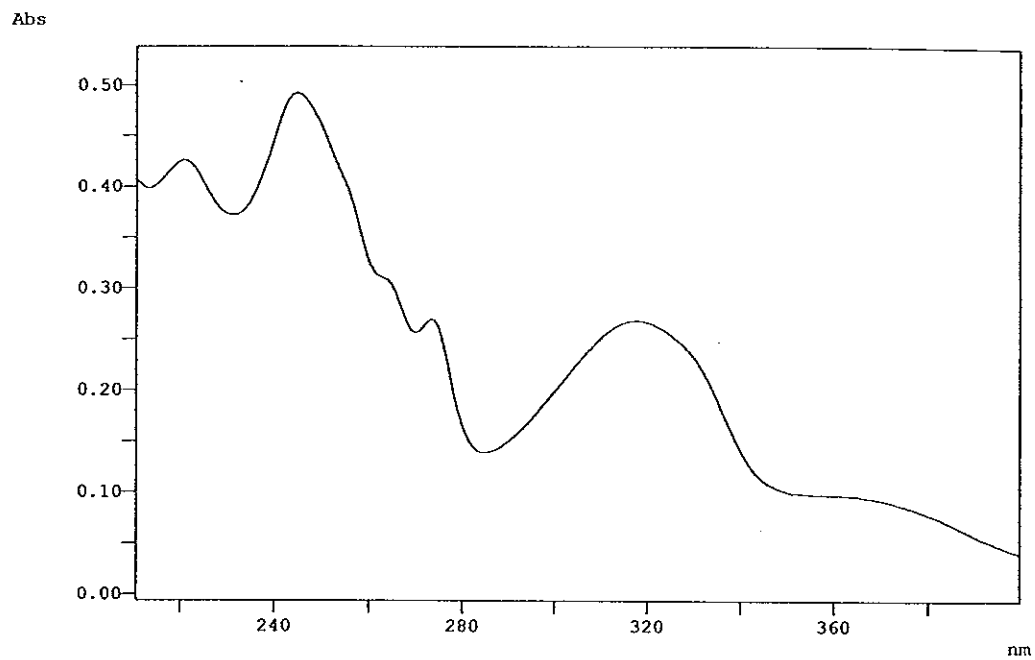


Figure 43 UV (MeOH) spectrum of YU14

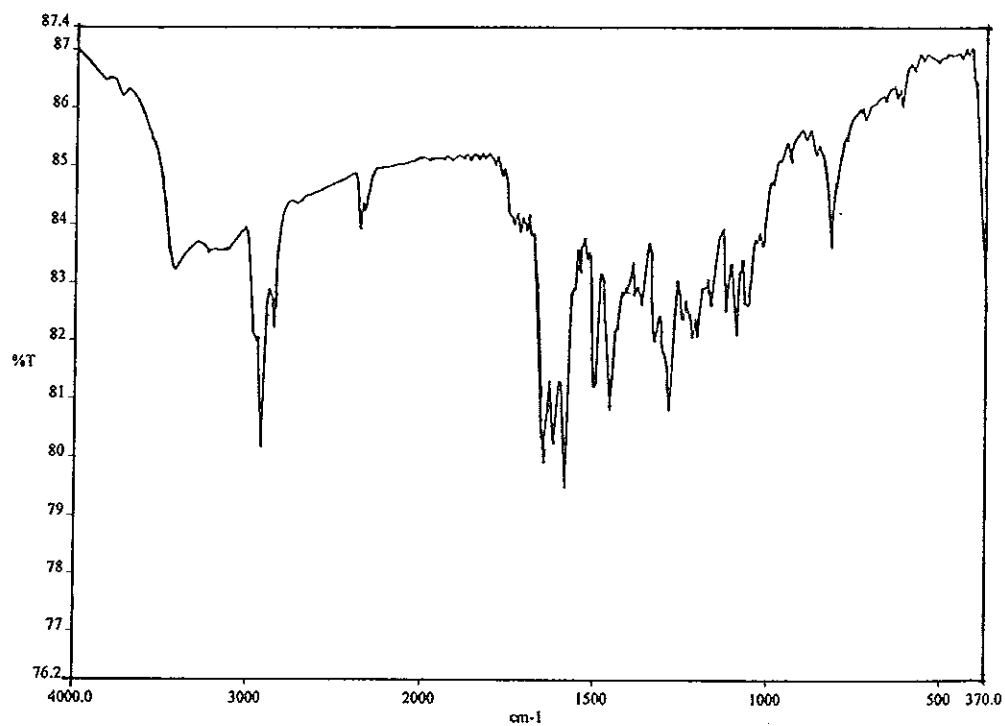


Figure 44 FT-IR (neat) spectrum of YU14

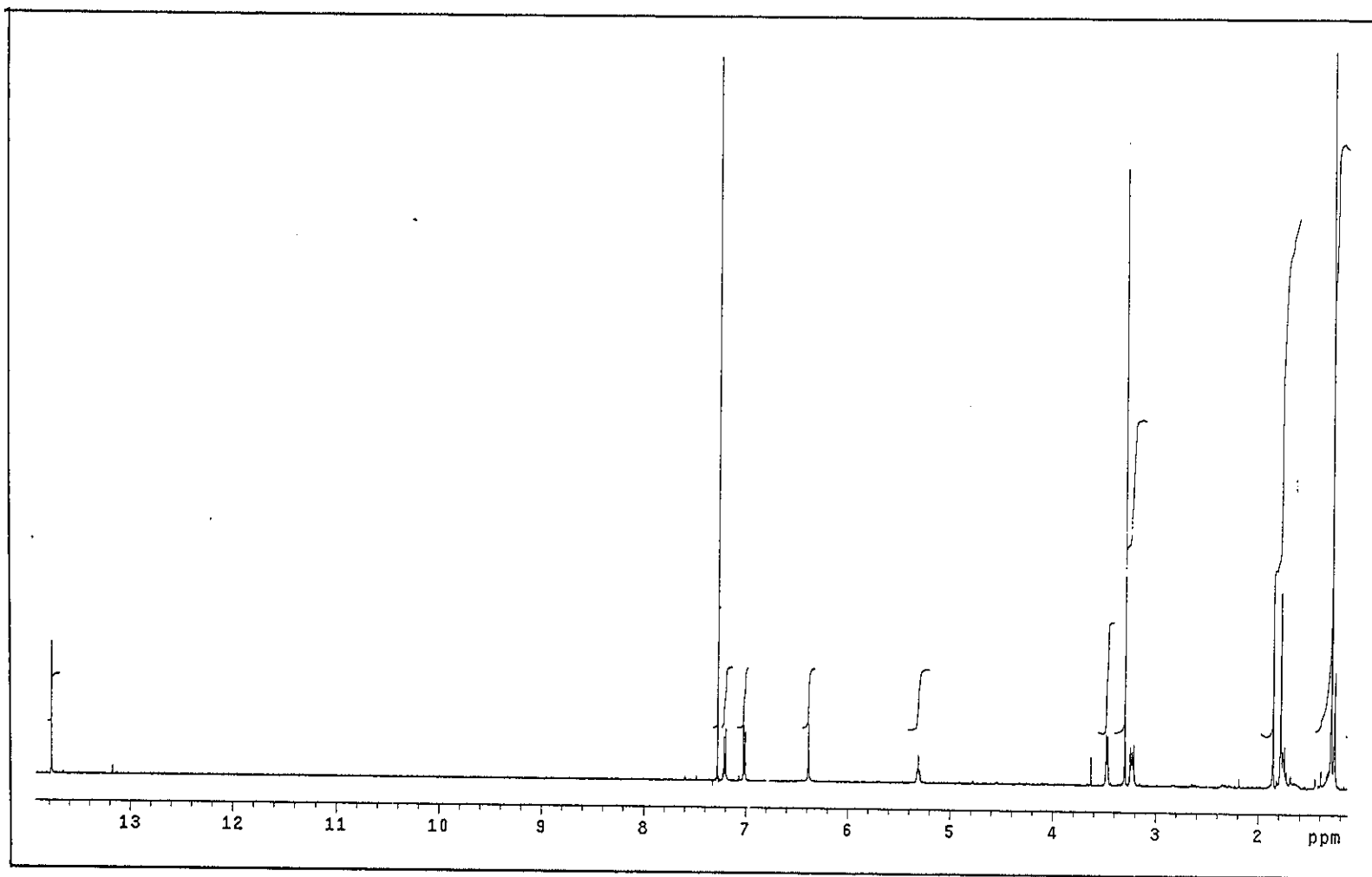


Figure 45 ^1H NMR (500 MHz) (CDCl_3) spectrum of YU14

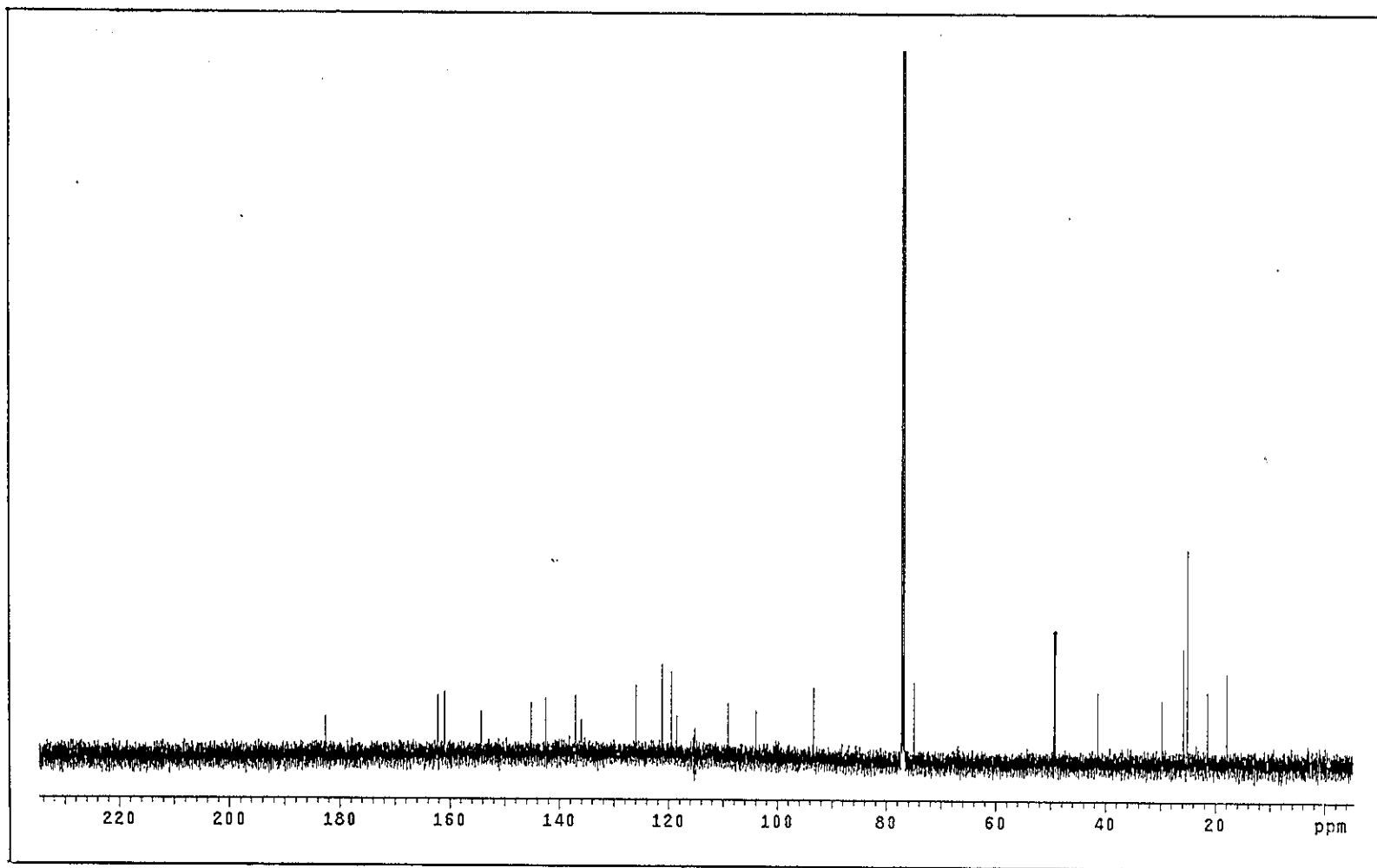


Figure 46 ^{13}C NMR (125 MHz) (CDCl_3) spectrum of YU14

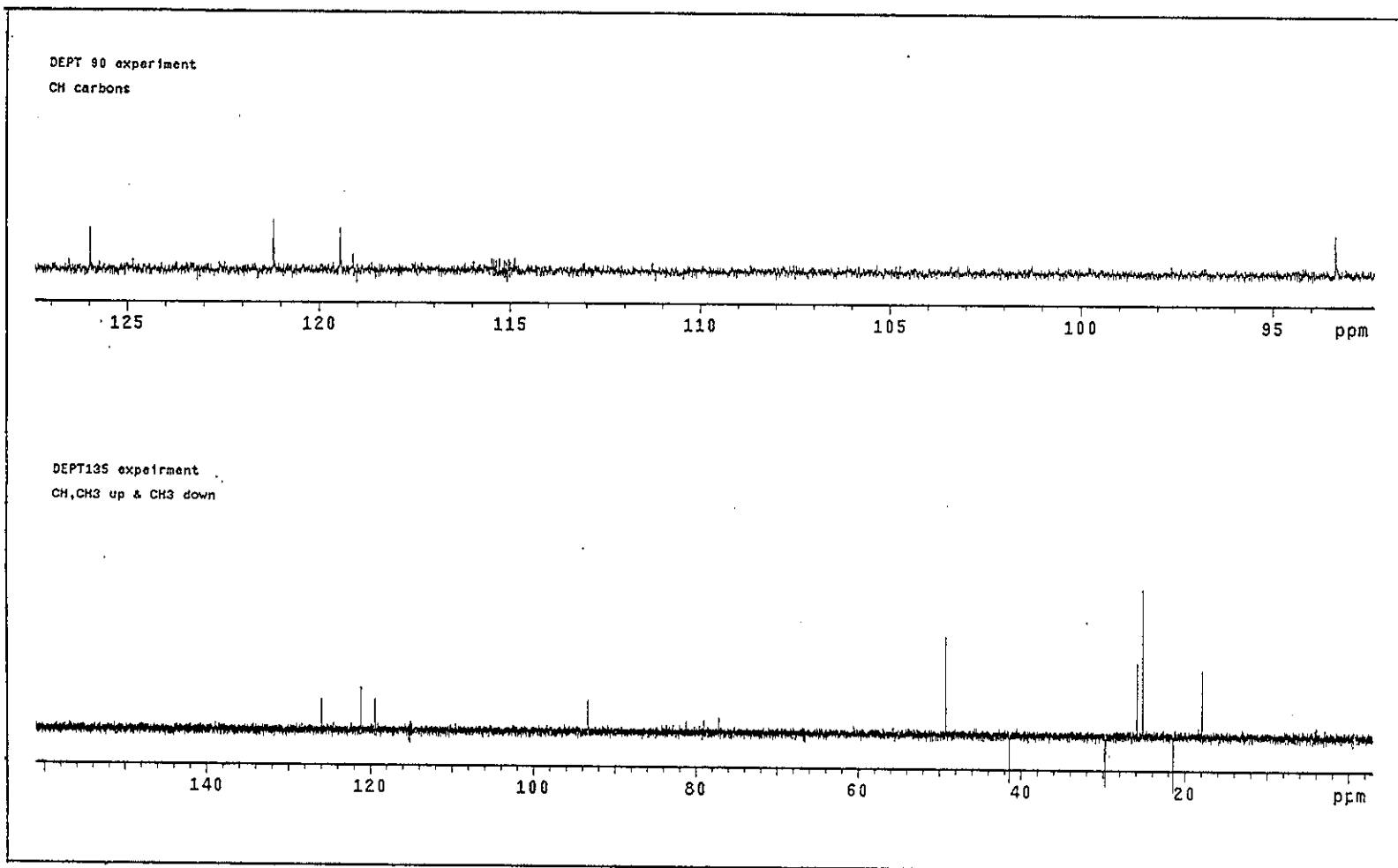


Figure 47 DEPT spectrum of YU14

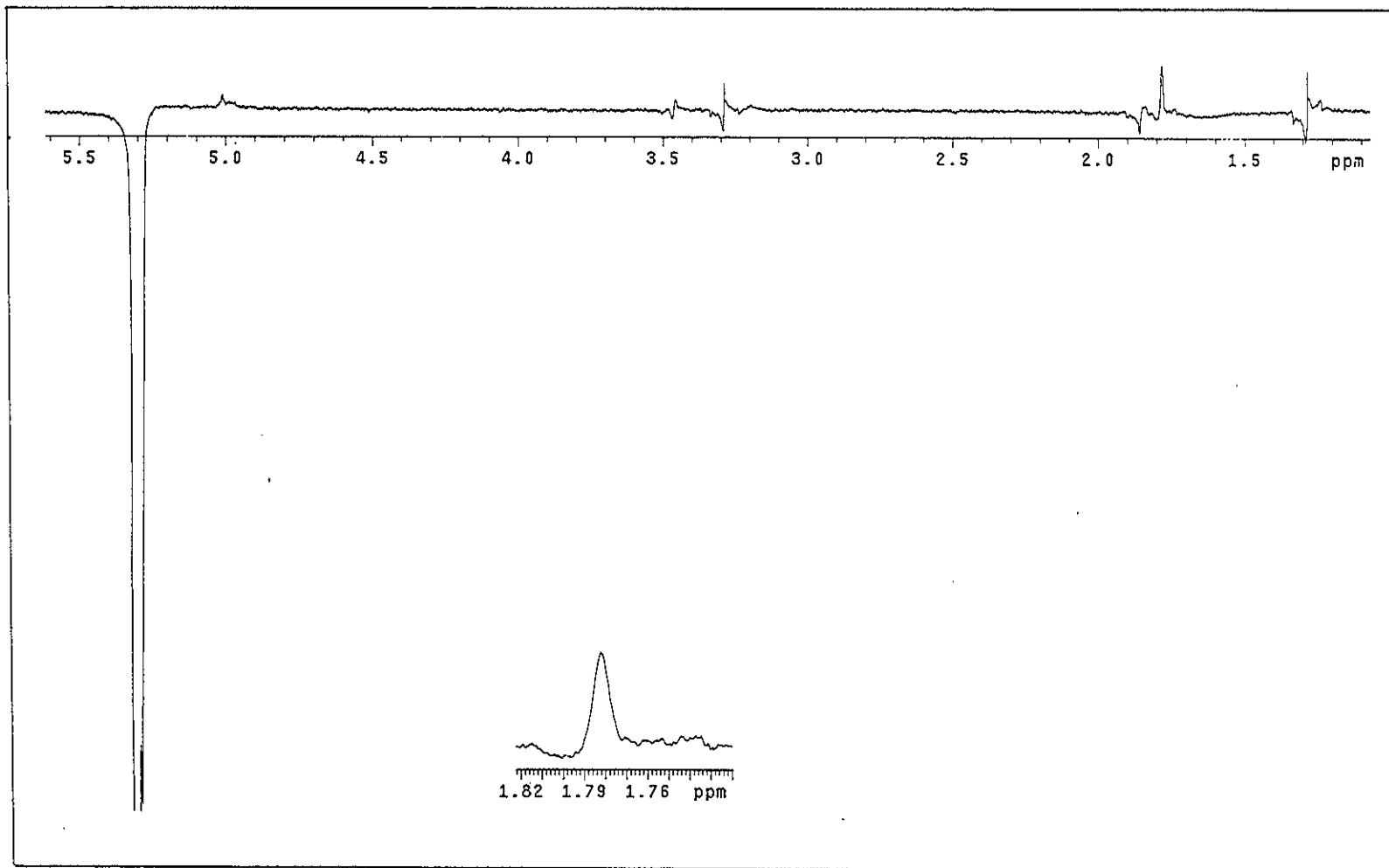


Figure 48 NOEDIFF spectrum of YU14 after irradiation at δ_{H} 5.31

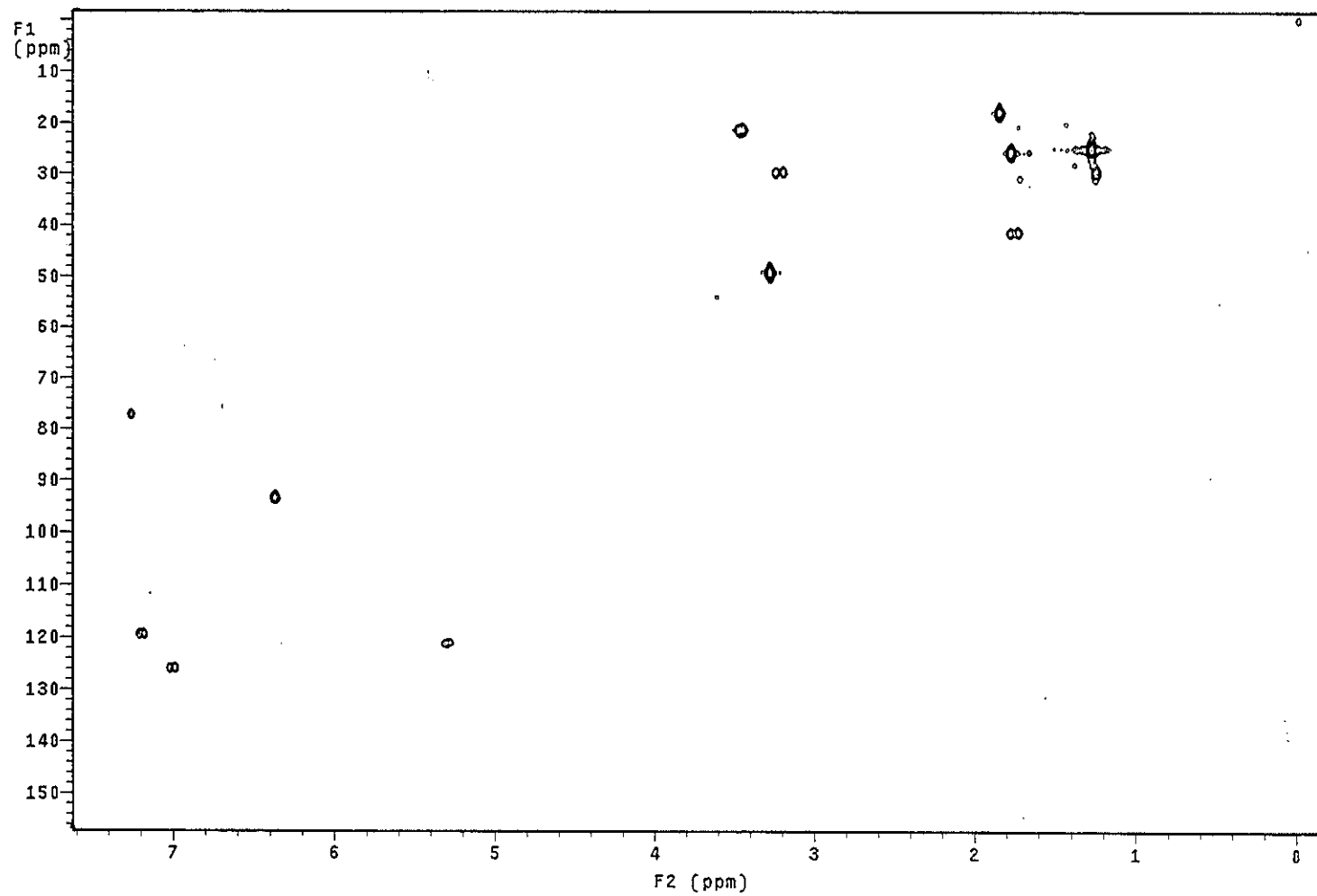


Figure 49 2D HMQC spectrum of YU14

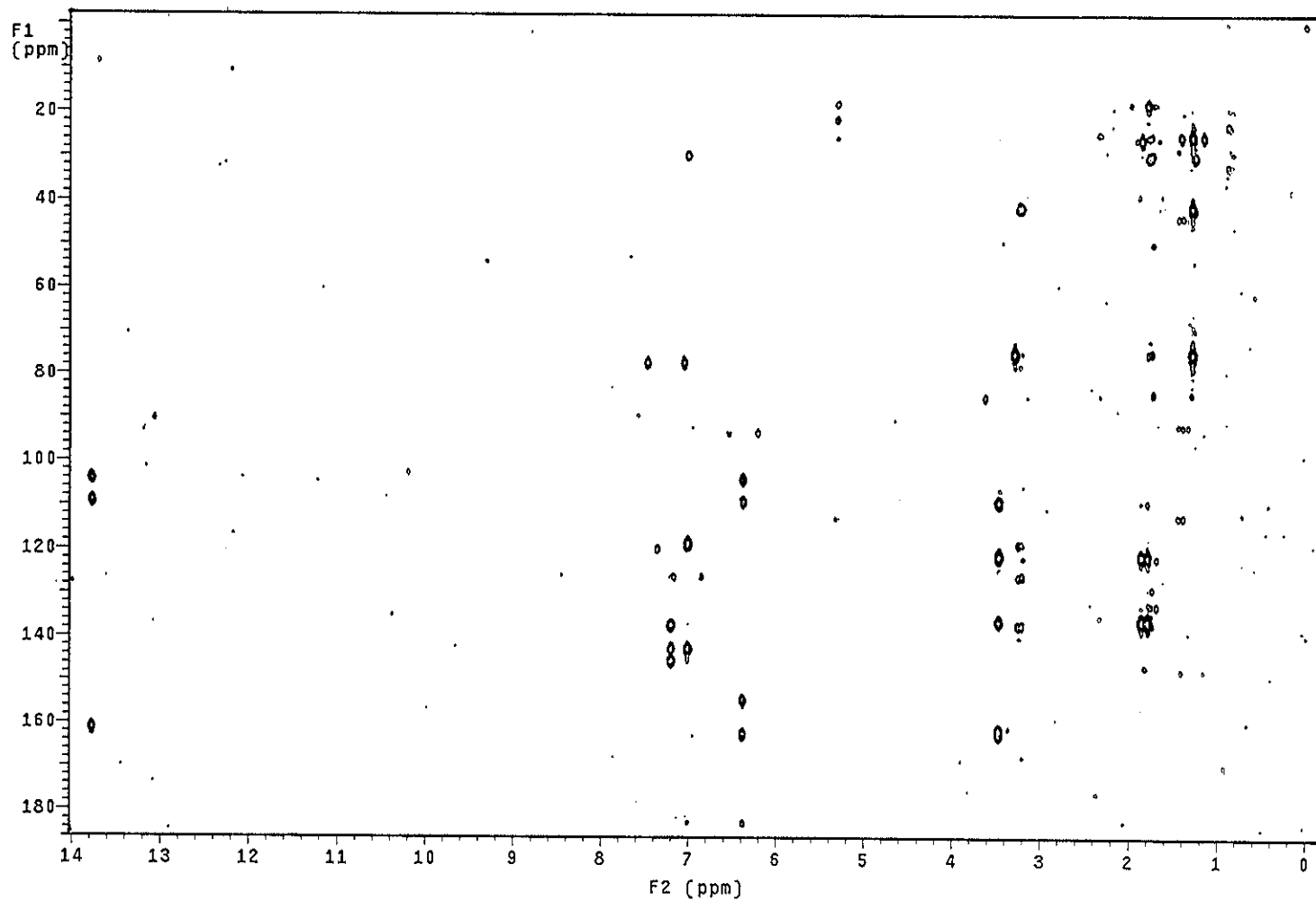


Figure 50 2D HMBC spectrum of YU14

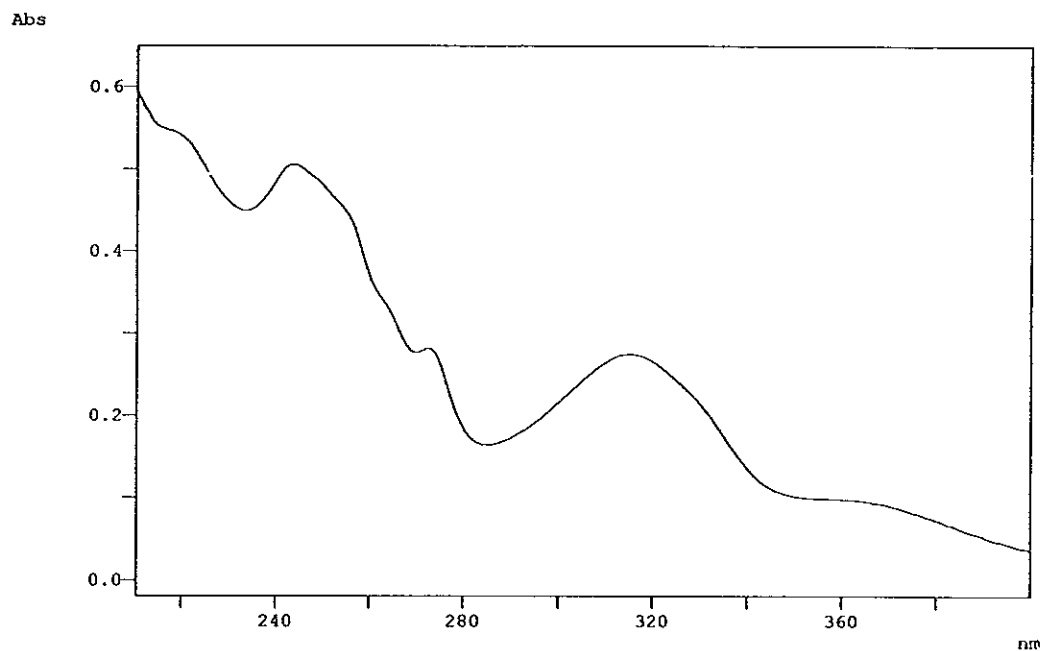


Figure 51 UV (MeOH) spectrum of YU17

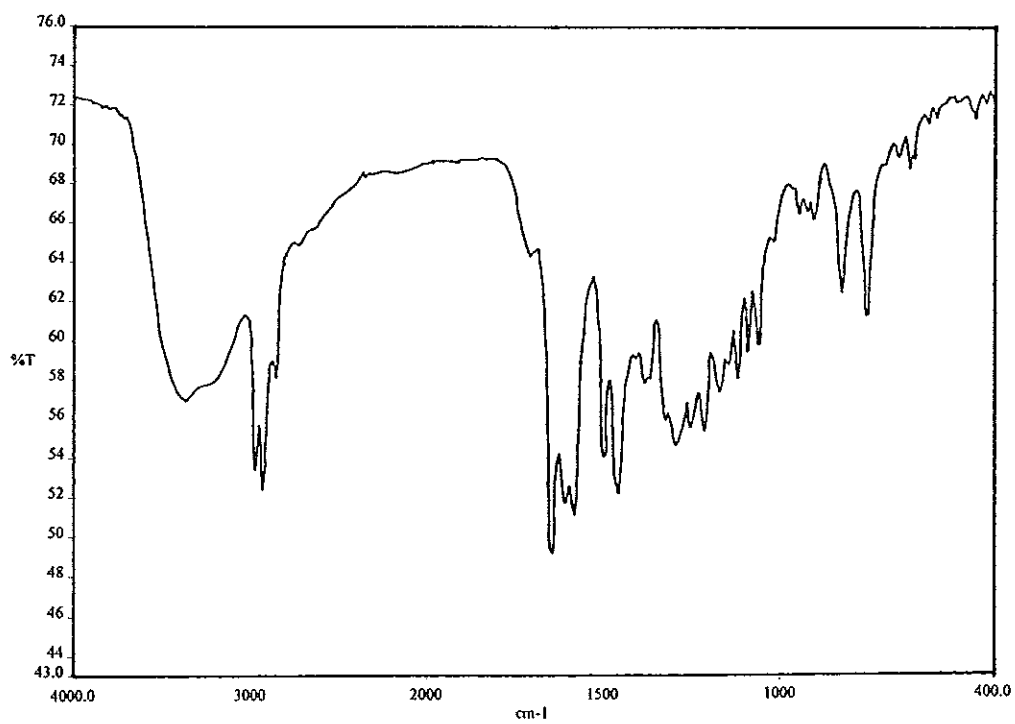


Figure 52 FT-IR (neat) spectrum of YU17

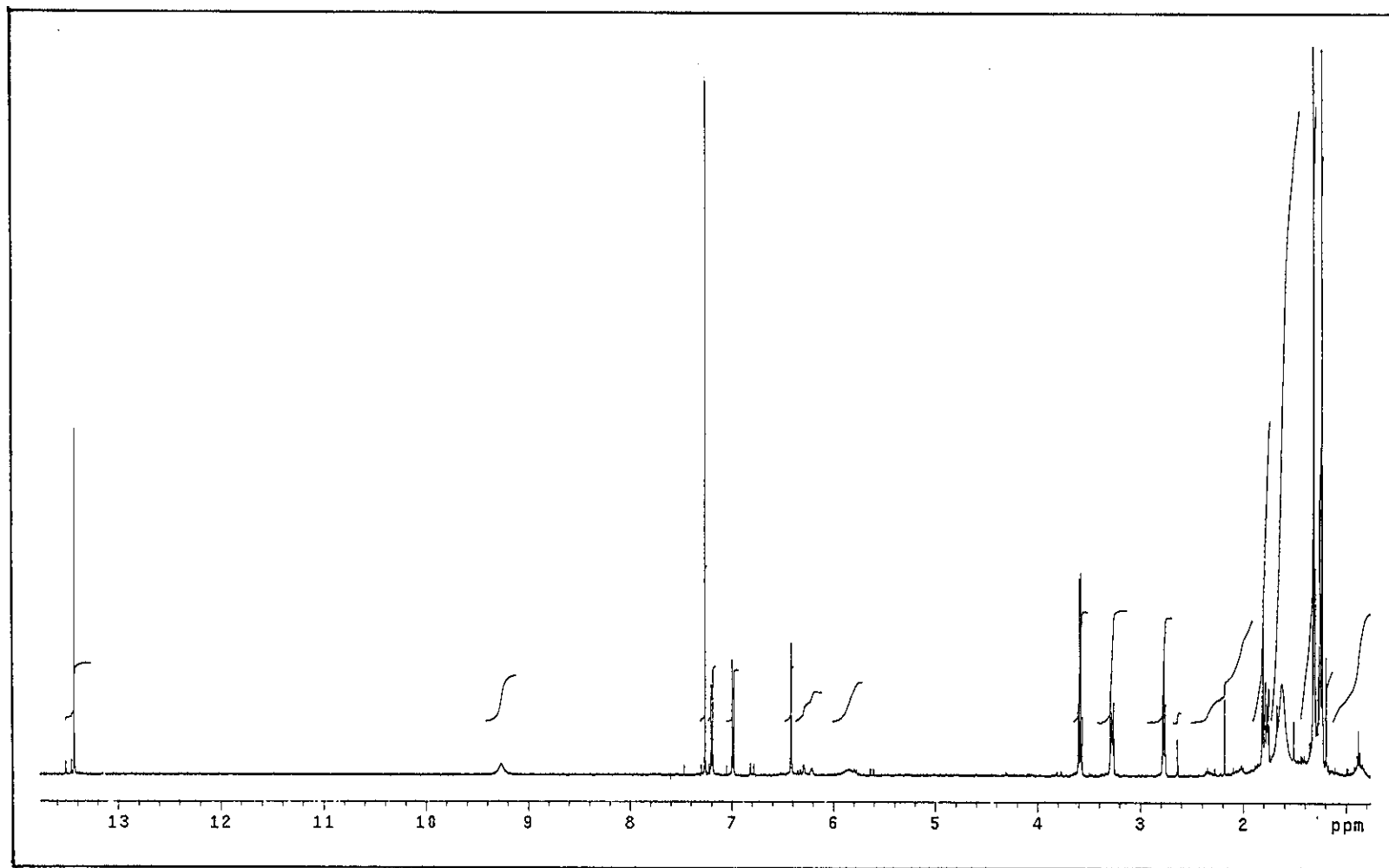


Figure 53 ^1H NMR (500 MHz) (CDCl_3) spectrum of YU17

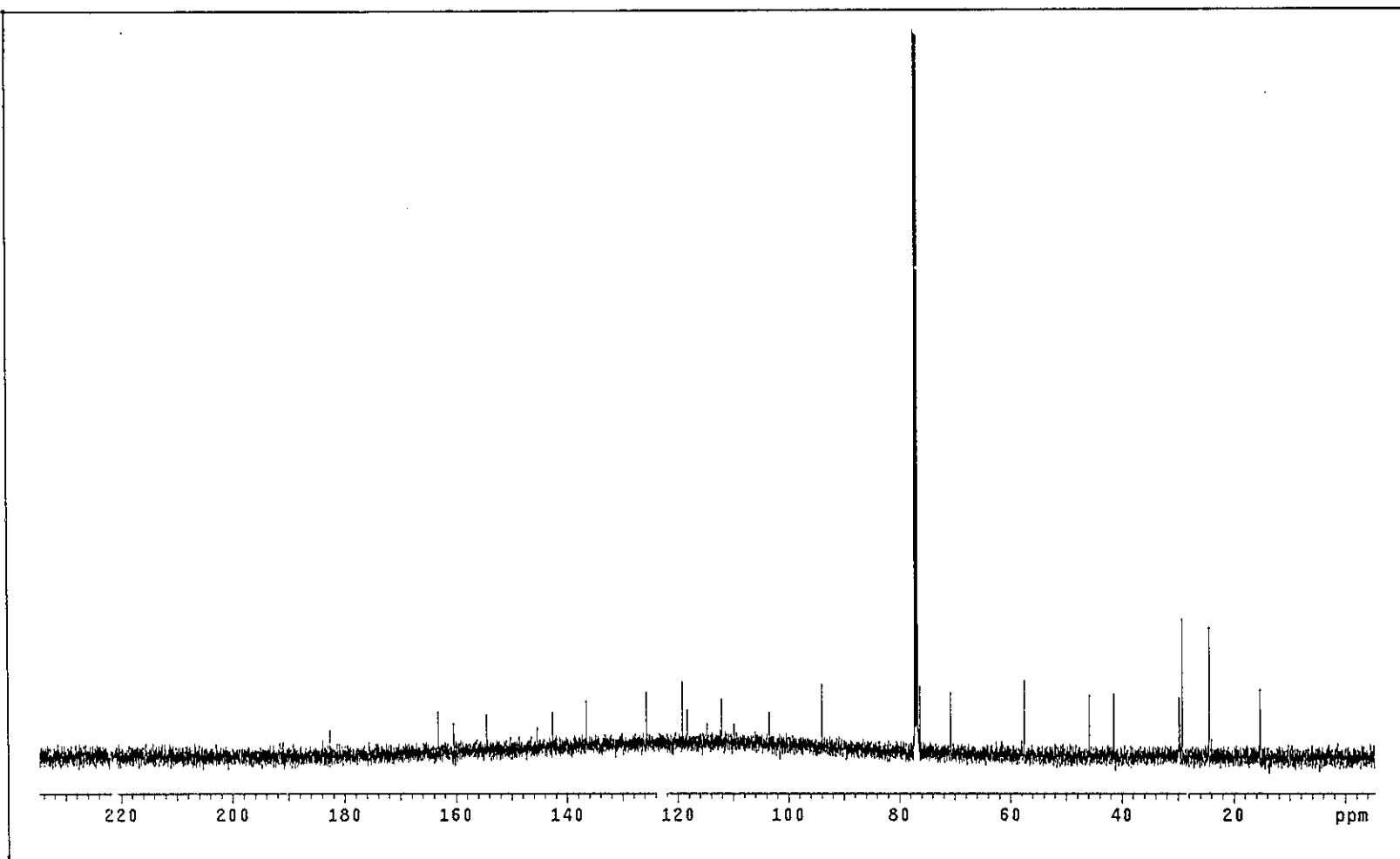


Figure 54 ^{13}C NMR (125 MHz) (CDCl_3) spectrum of YU17

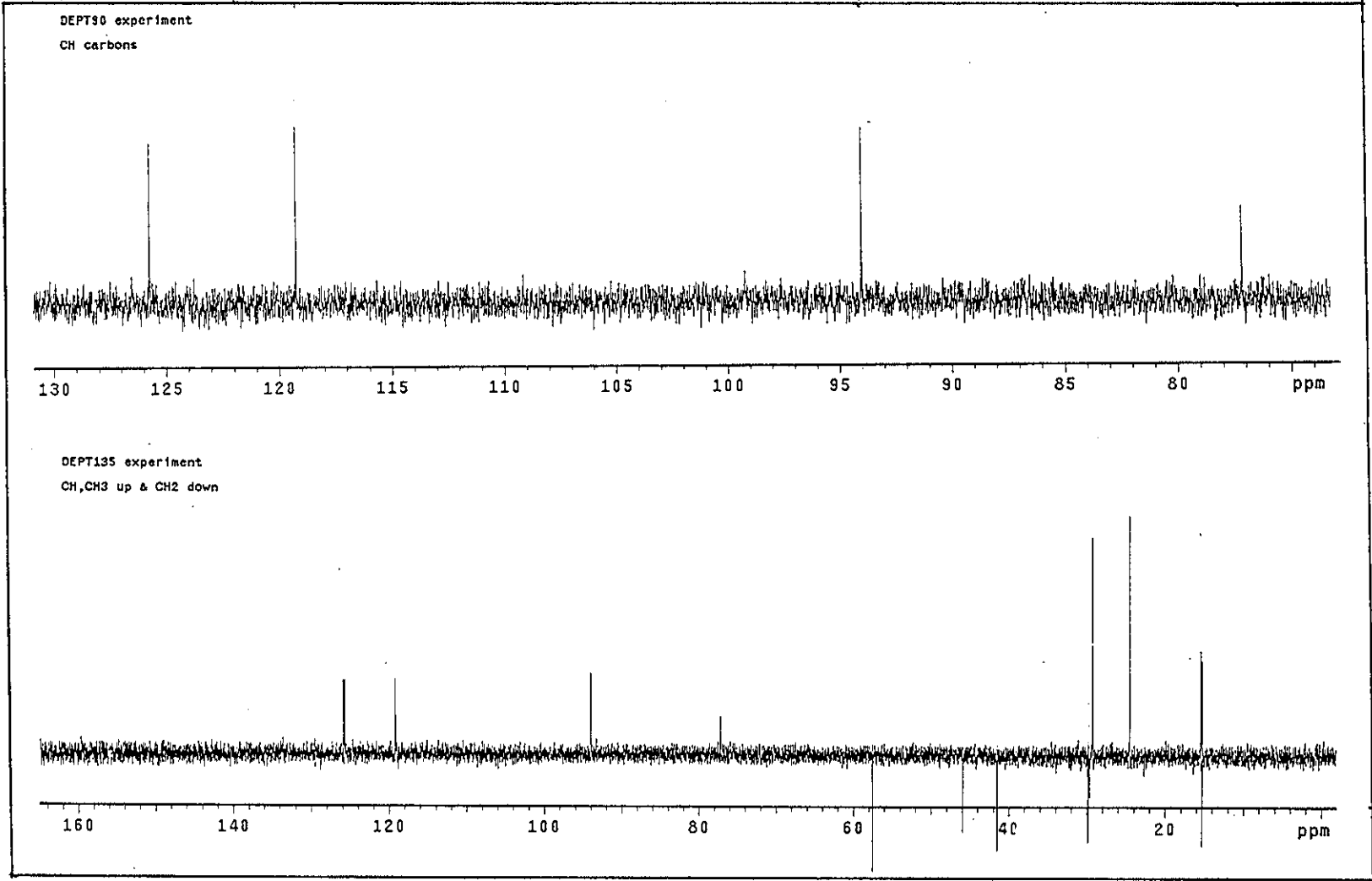


Figure 55 DEPT spectrum of YU17

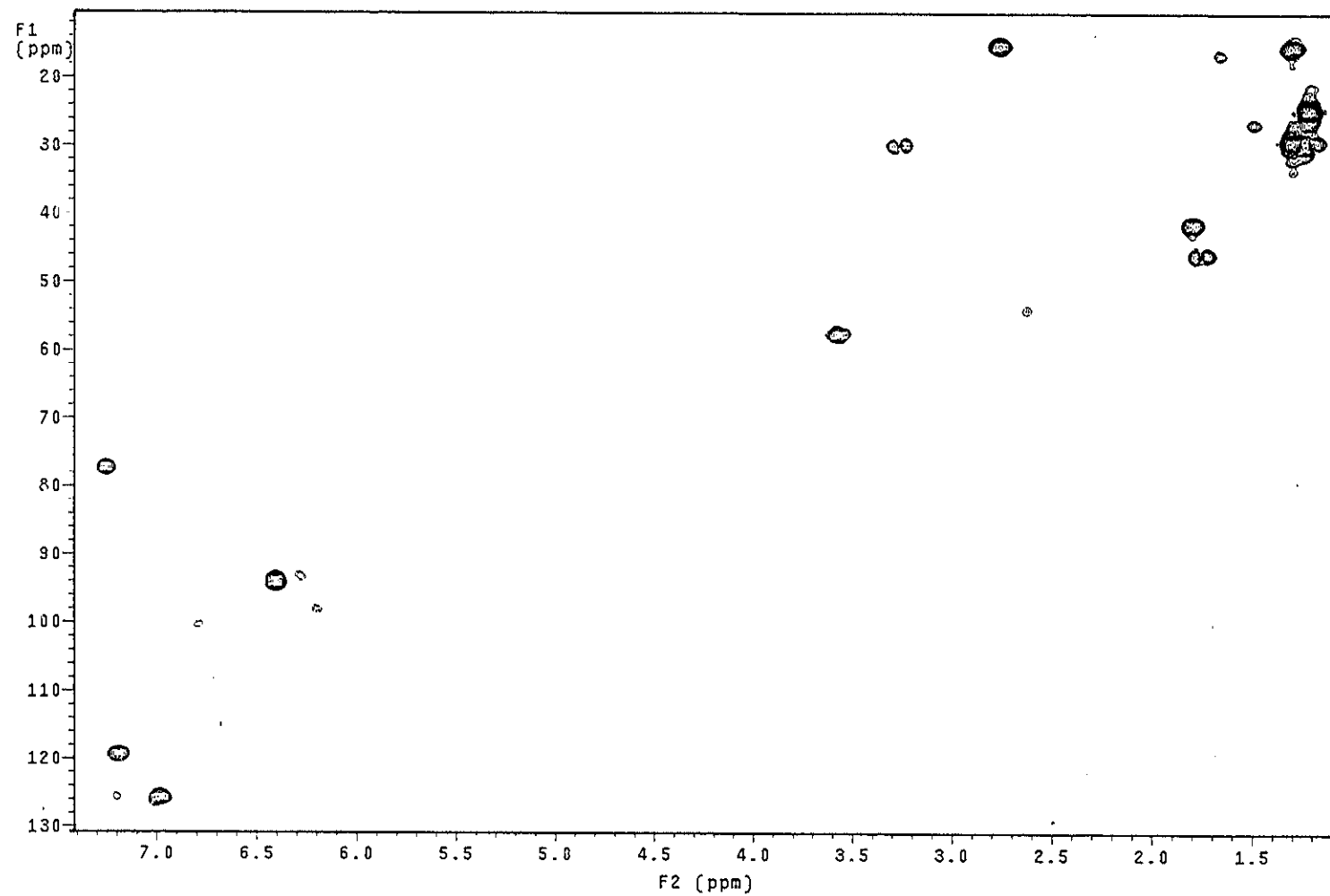


Figure 56 2D HMQC spectrum of YU17

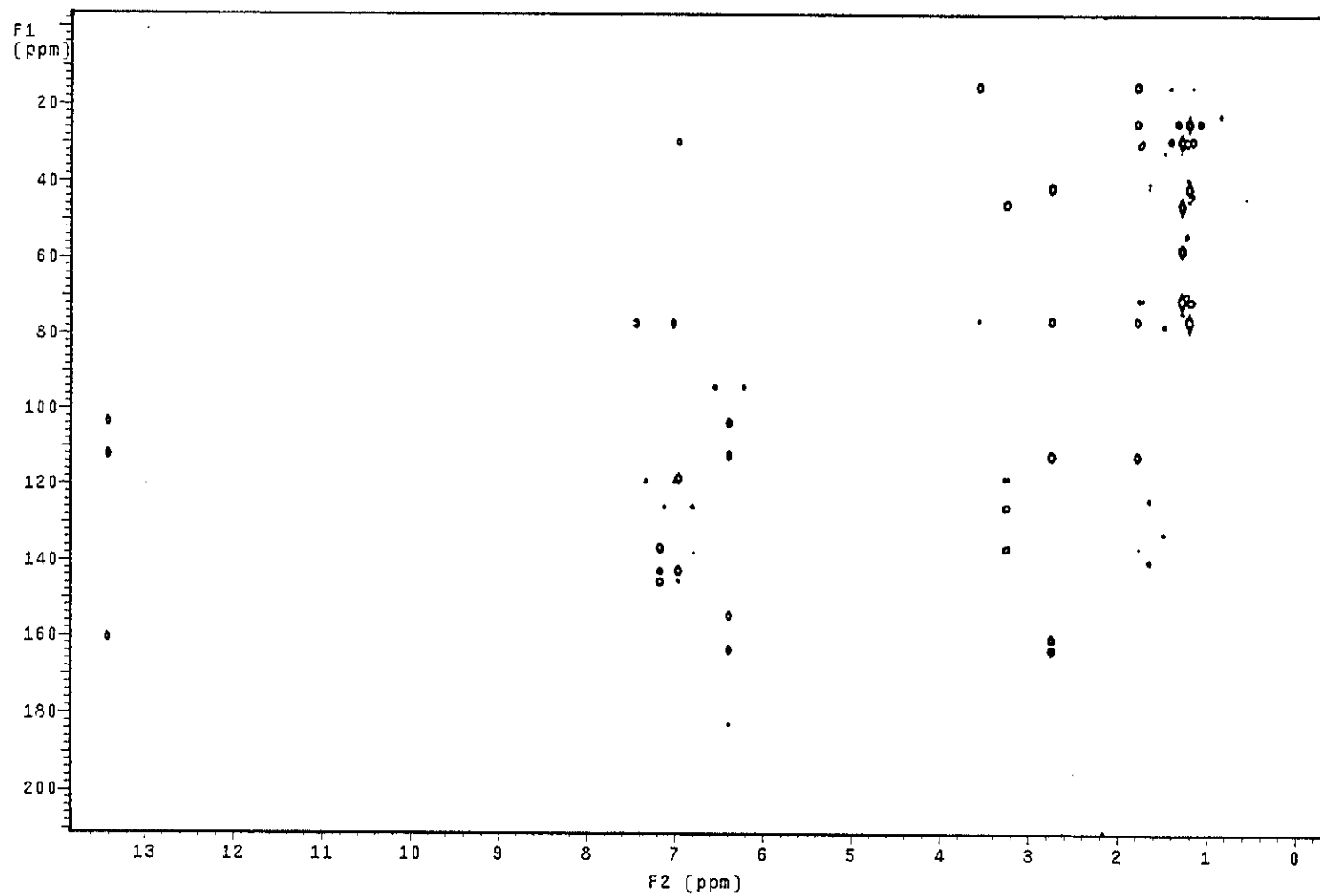


Figure 57 2D HMBC spectrum of YU17

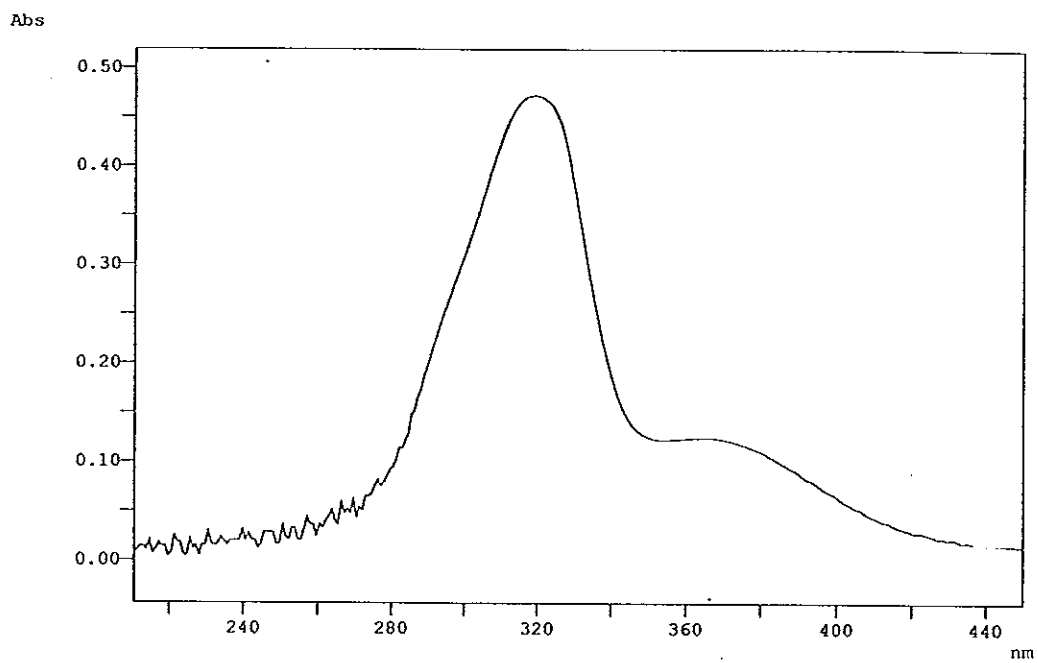


Figure 58 UV (MeOH) spectrum of YU4

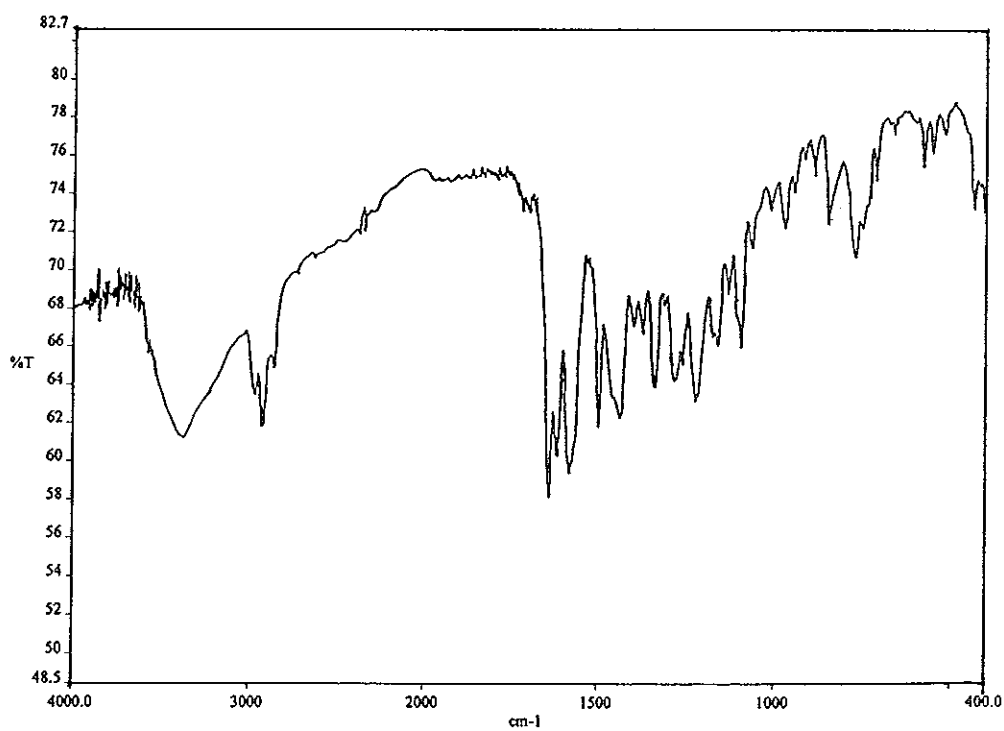


Figure 59 FT-IR (neat) spectrum of YU4

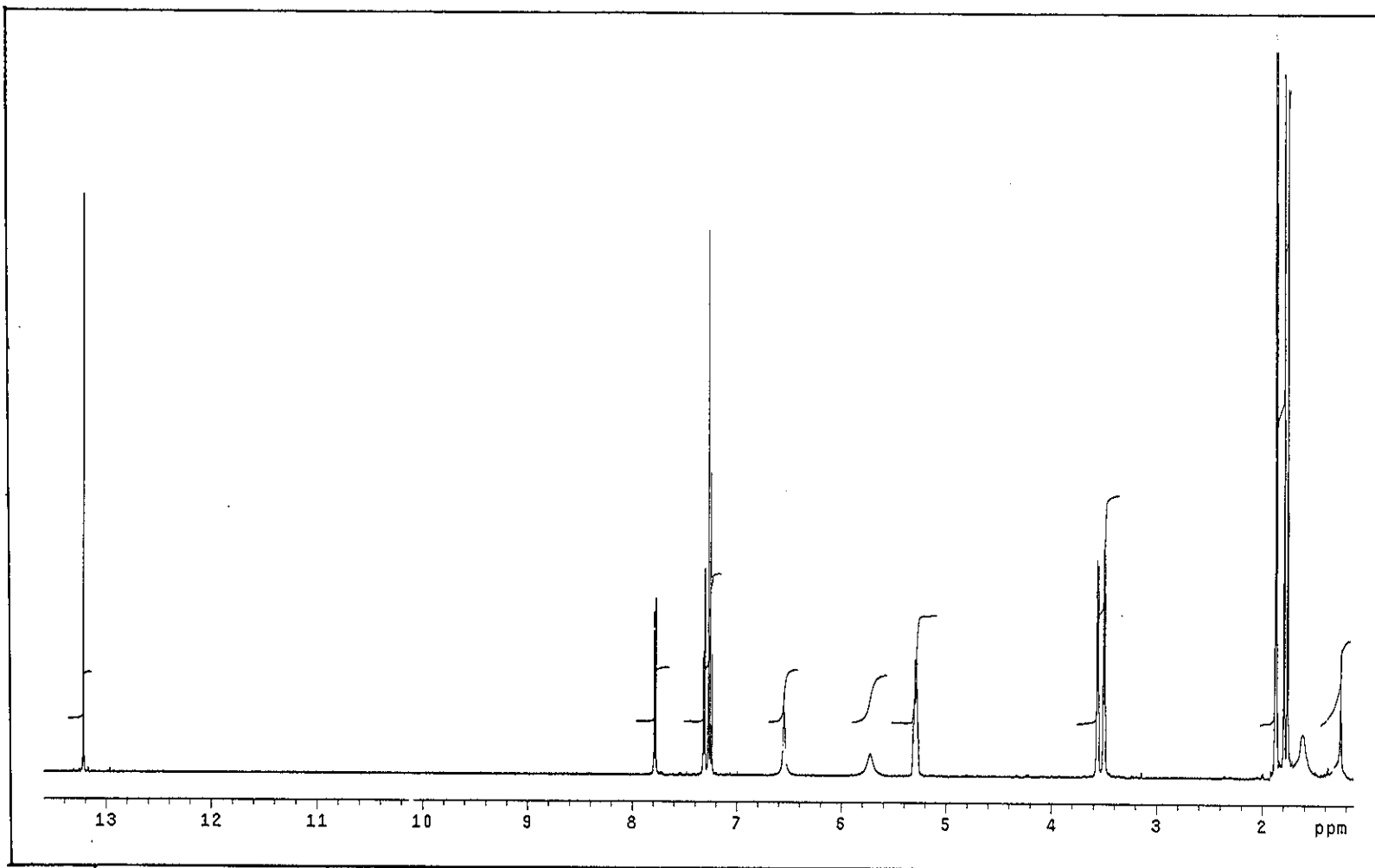


Figure 60 ^1H NMR (500 MHz) (CDCl_3) spectrum of YU4

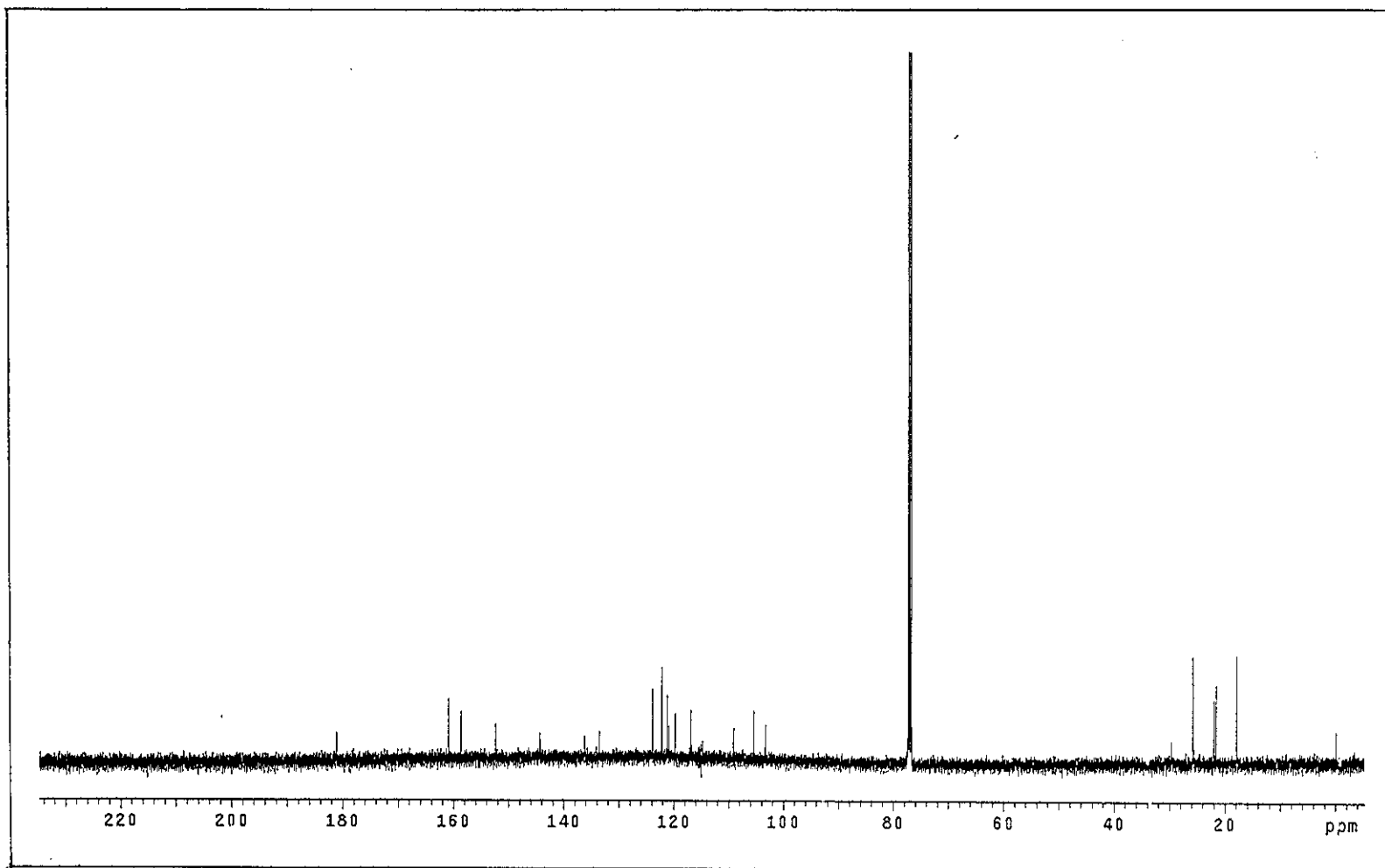


Figure 61 ^{13}C NMR (125 MHz) (CDCl_3) spectrum of YU4

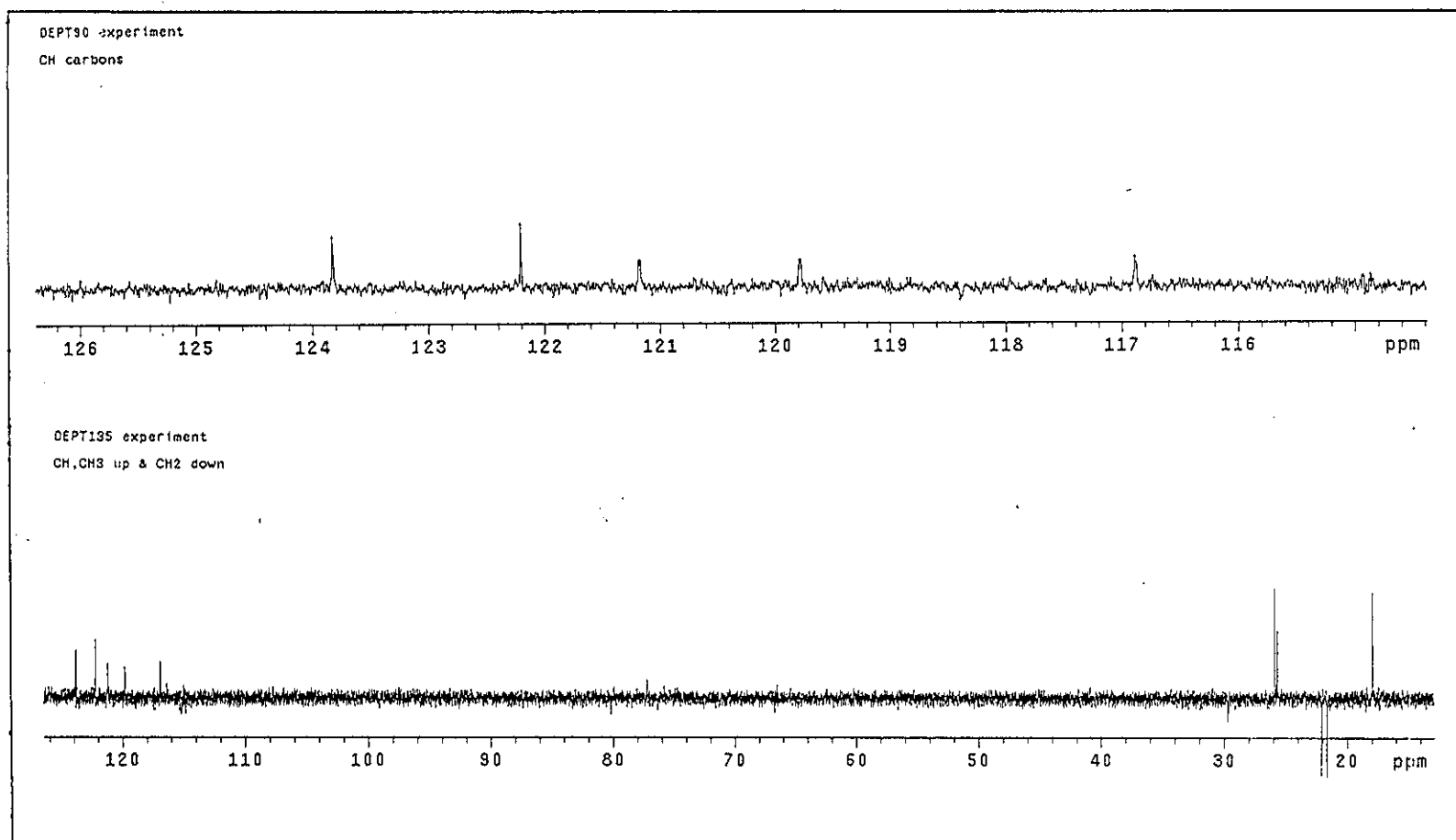


Figure 62 DEPT spectrum of YU4

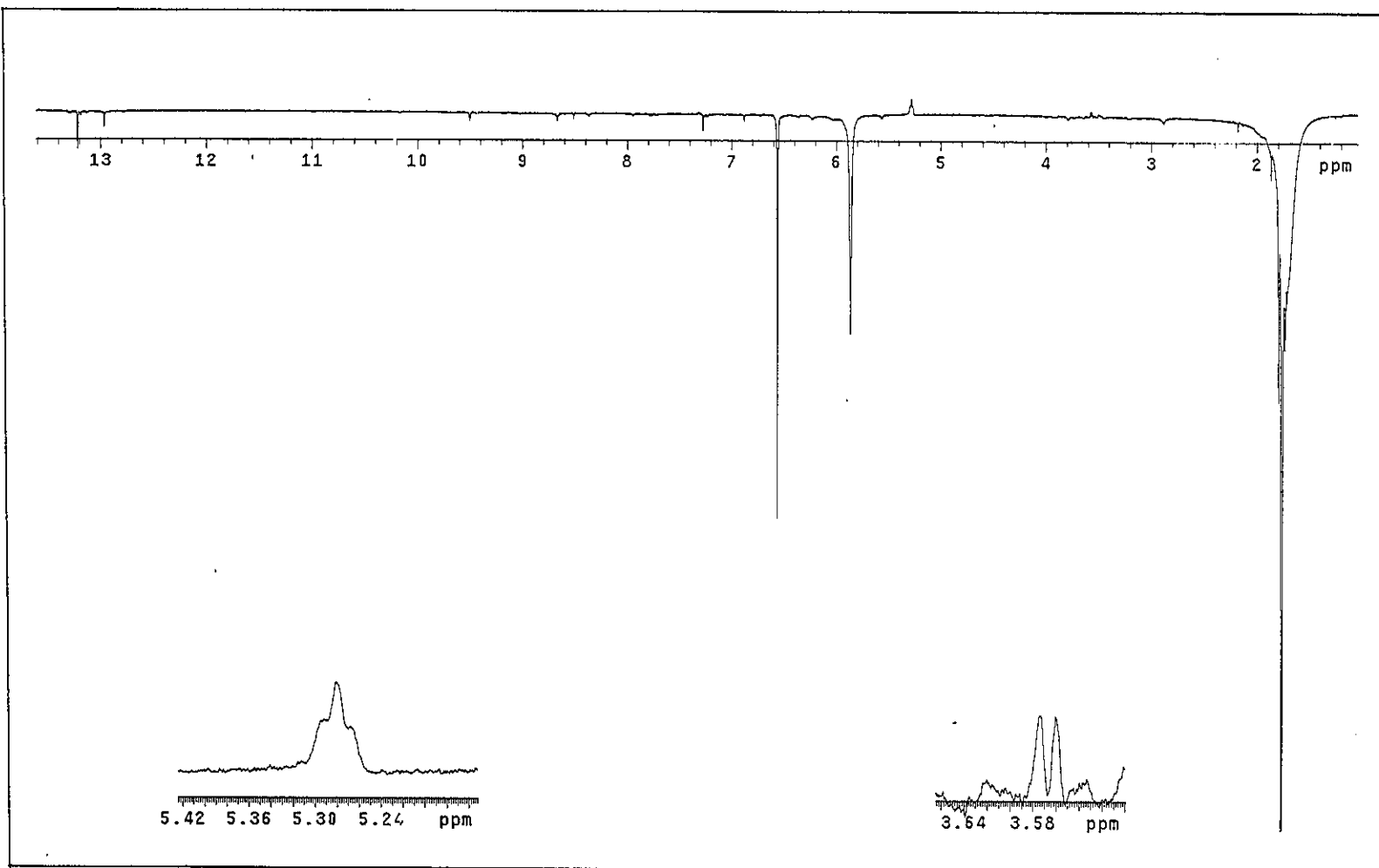


Figure 63 NOEDIFF spectrum of YU4 after irradiation at δ_H 1.76

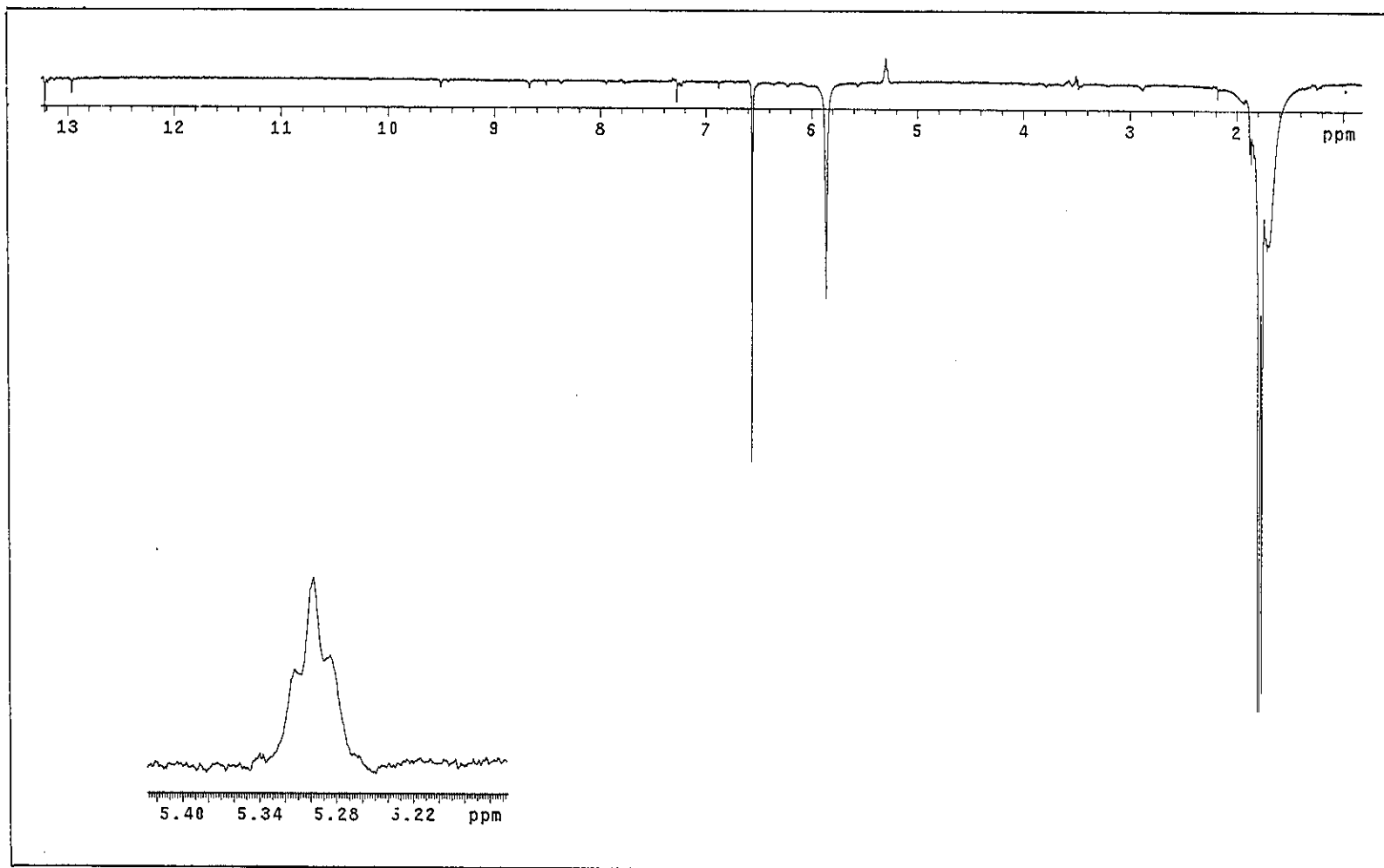


Figure 64 NOEDIFF spectrum of YU4 after irradiation at δ_H 1.79

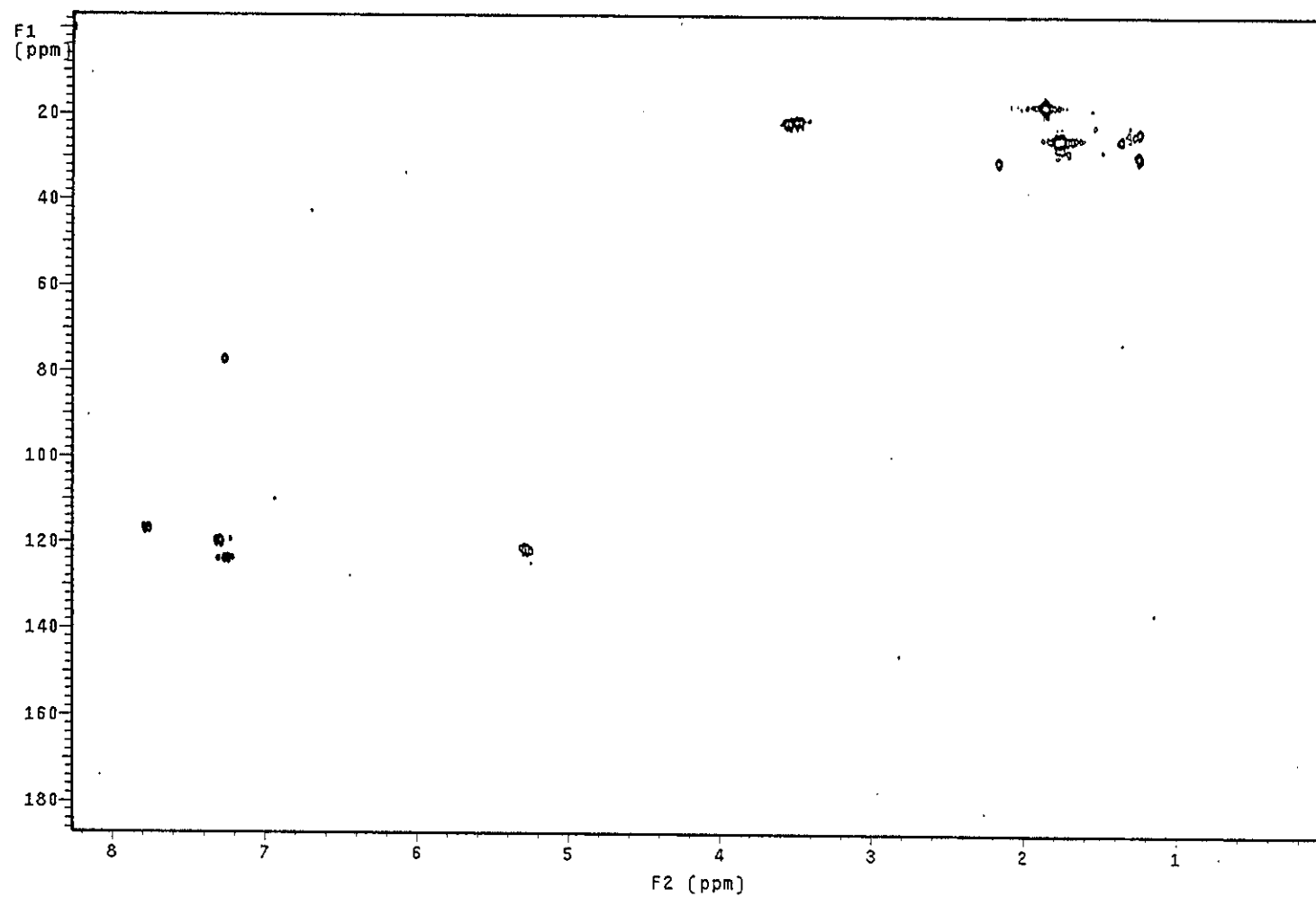


Figure 65 2D HMQC spectrum of YU4

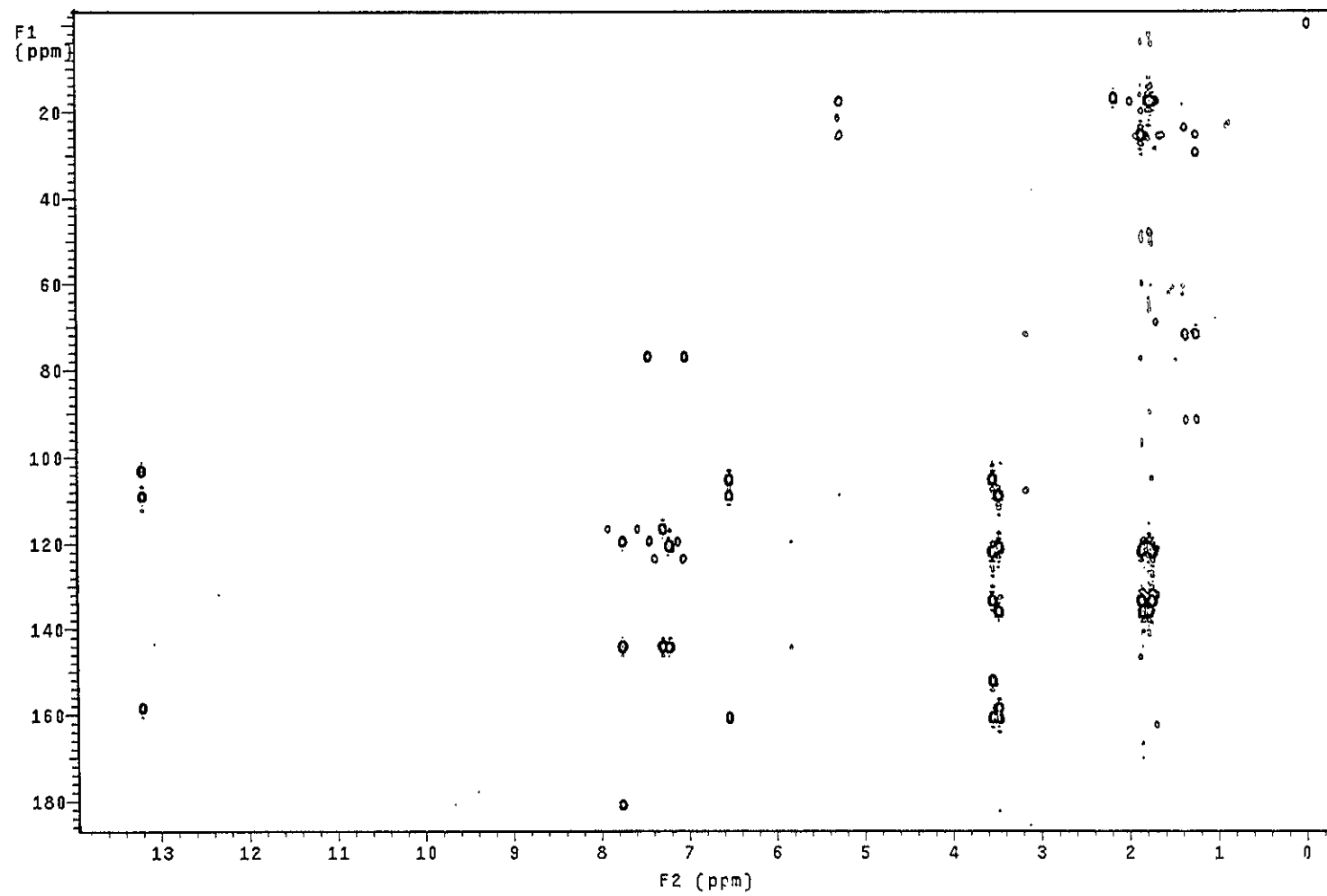


Figure 66 2D HMBC spectrum of YU4

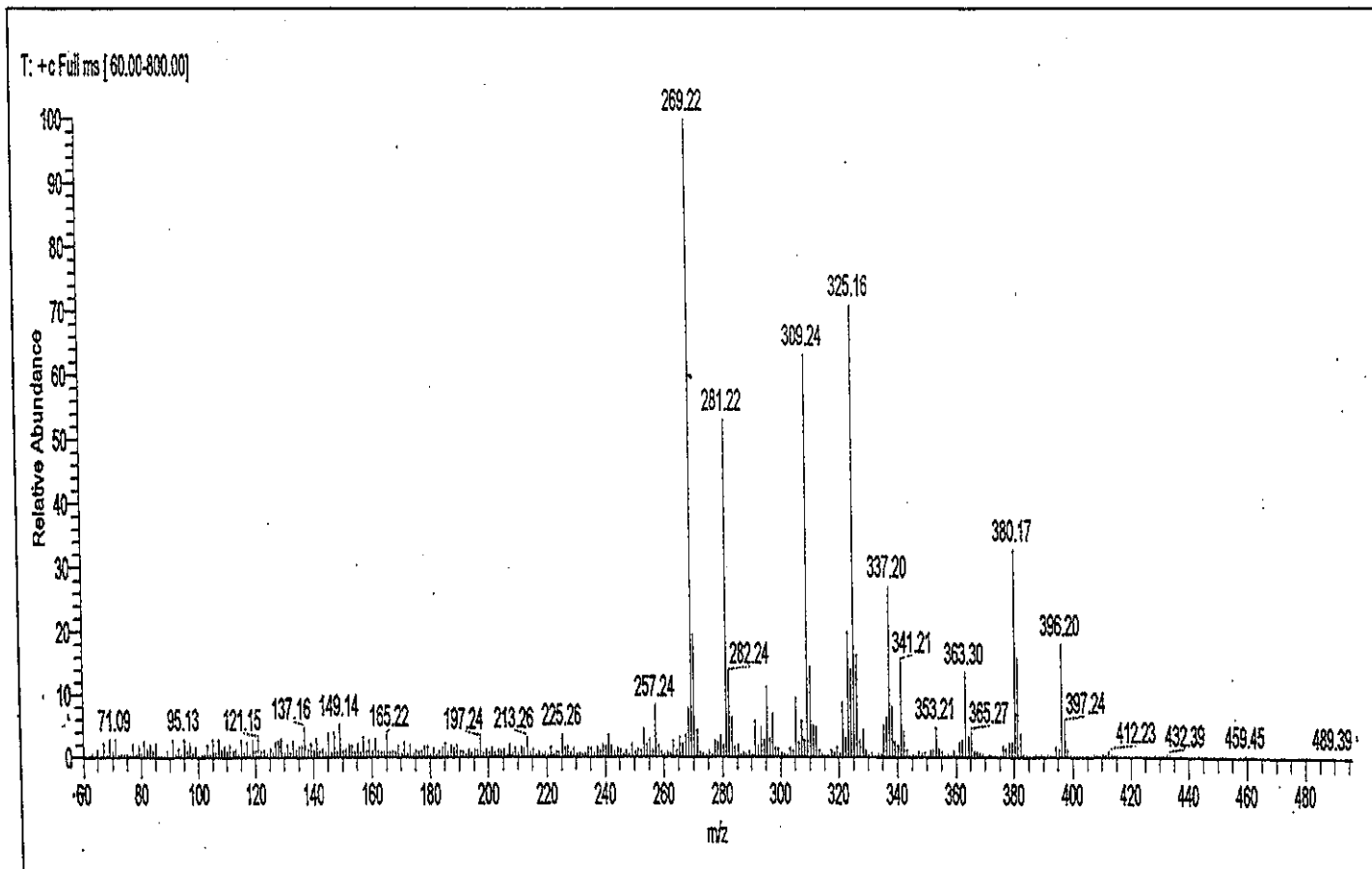


Figure 67 Mass spectrum of YU4

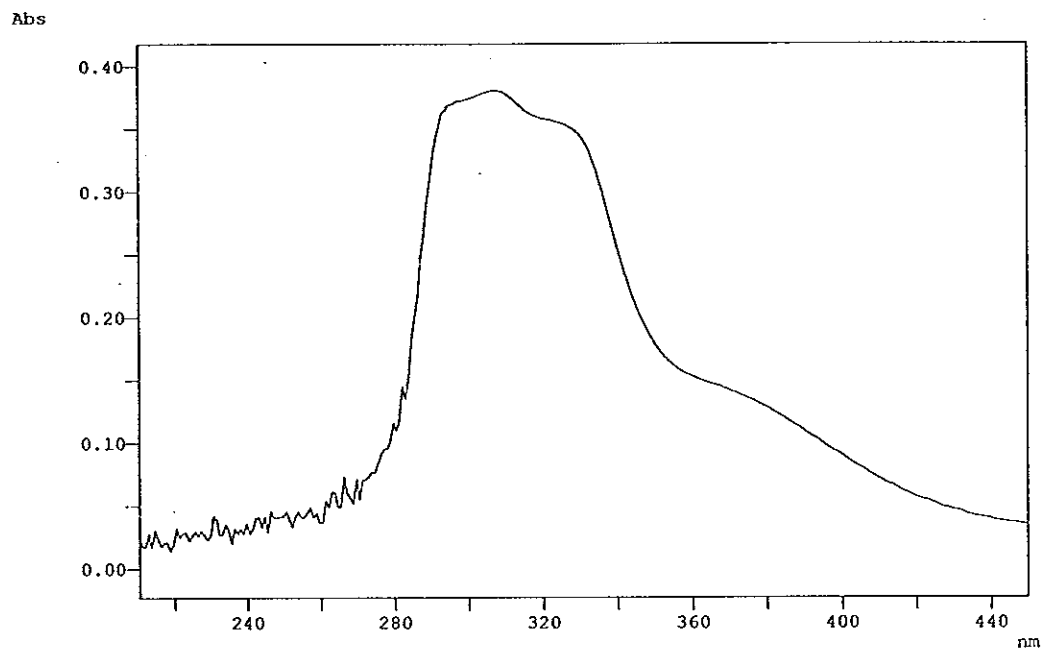


Figure 68 UV (MeOH) spectrum of YU3

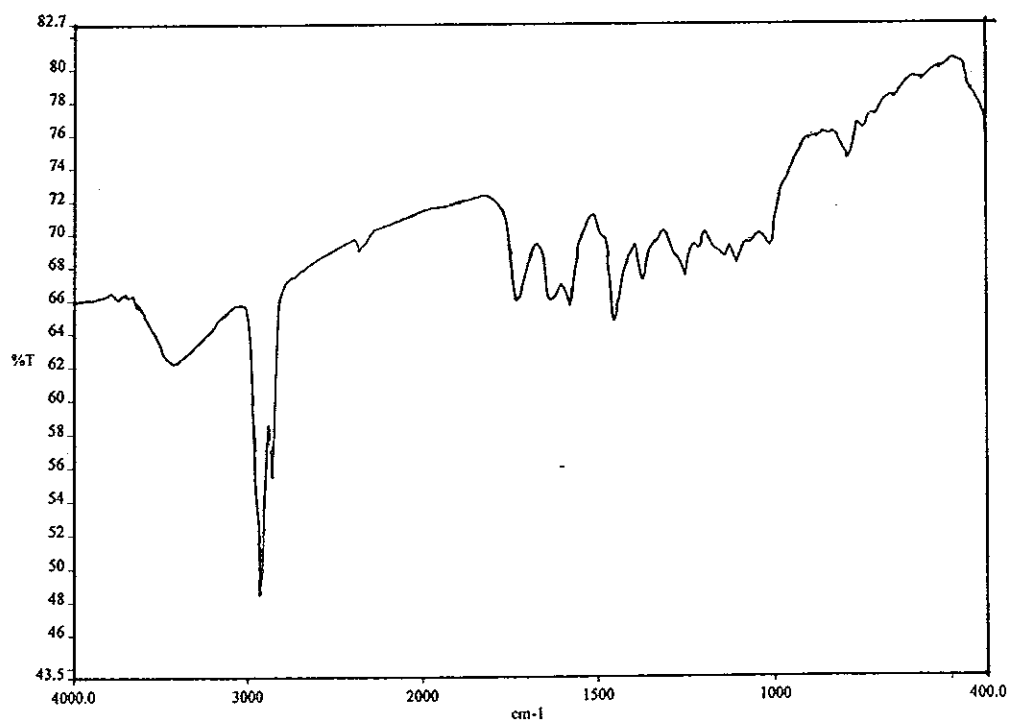


Figure 69 FT-IR (neat) spectrum of YU3

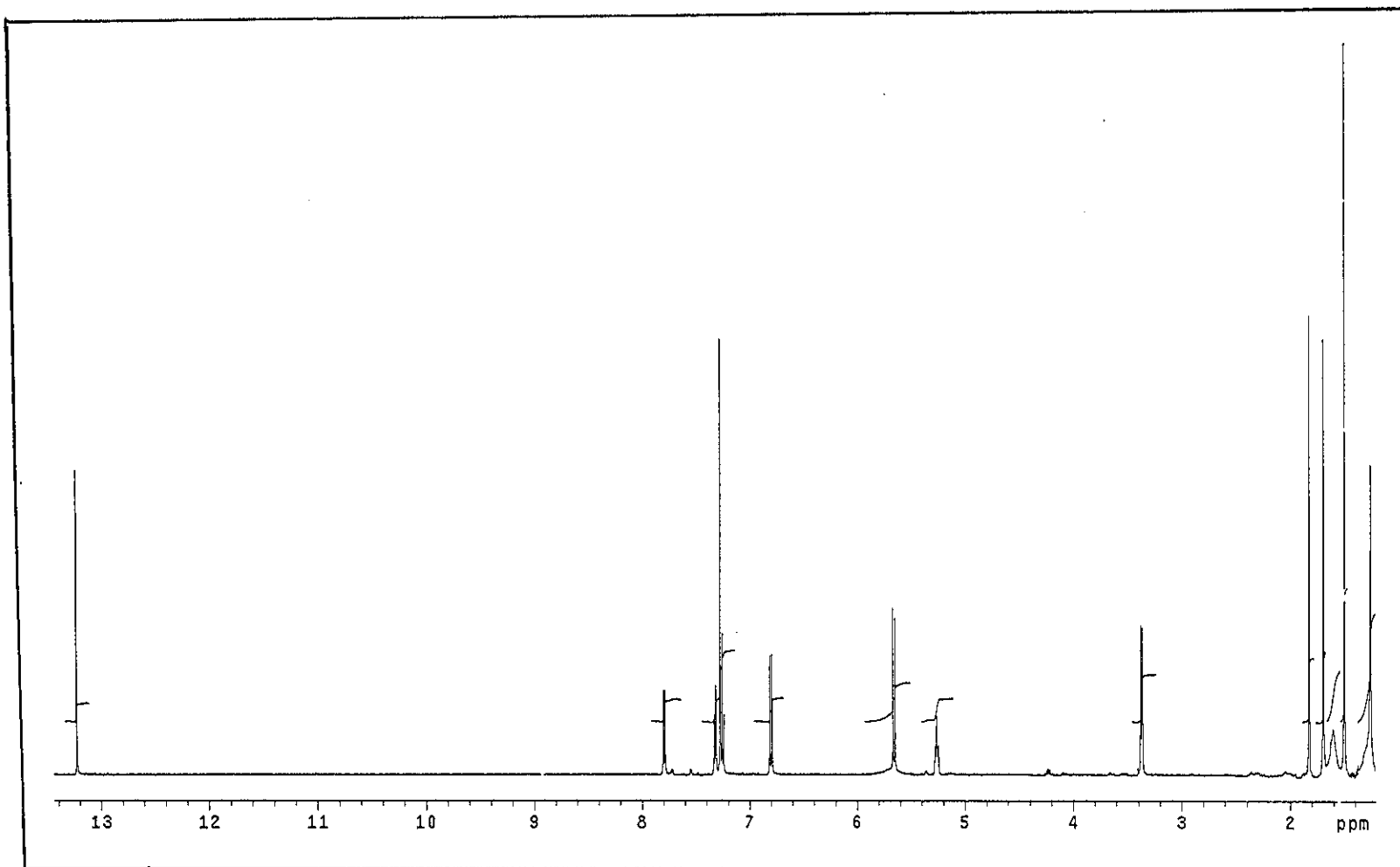


Figure 70 ^1H NMR (500 MHz) (CDCl_3) spectrum of YU3

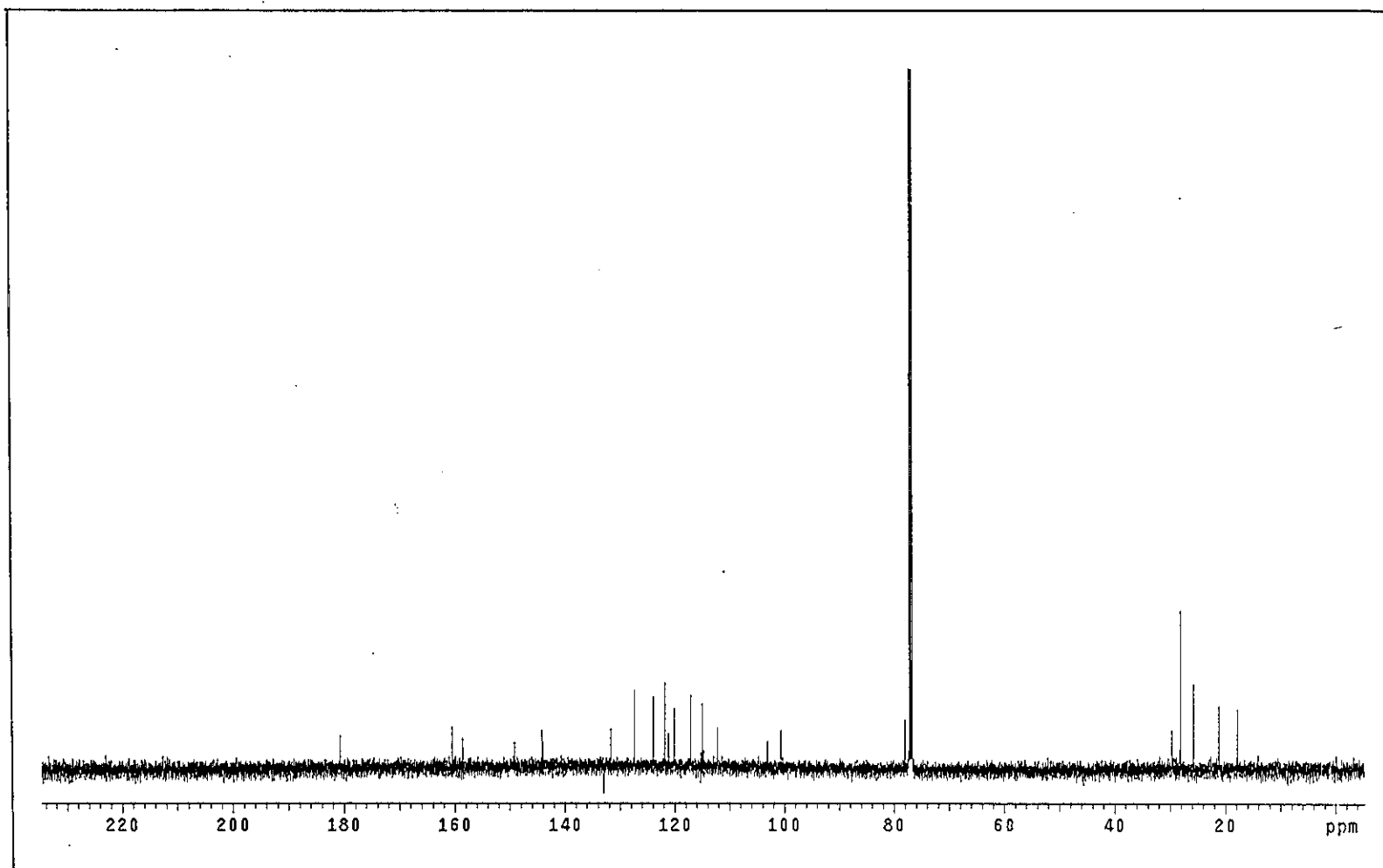


Figure 71 ^{13}C NMR (125 MHz) (CDCl_3) spectrum of YU3

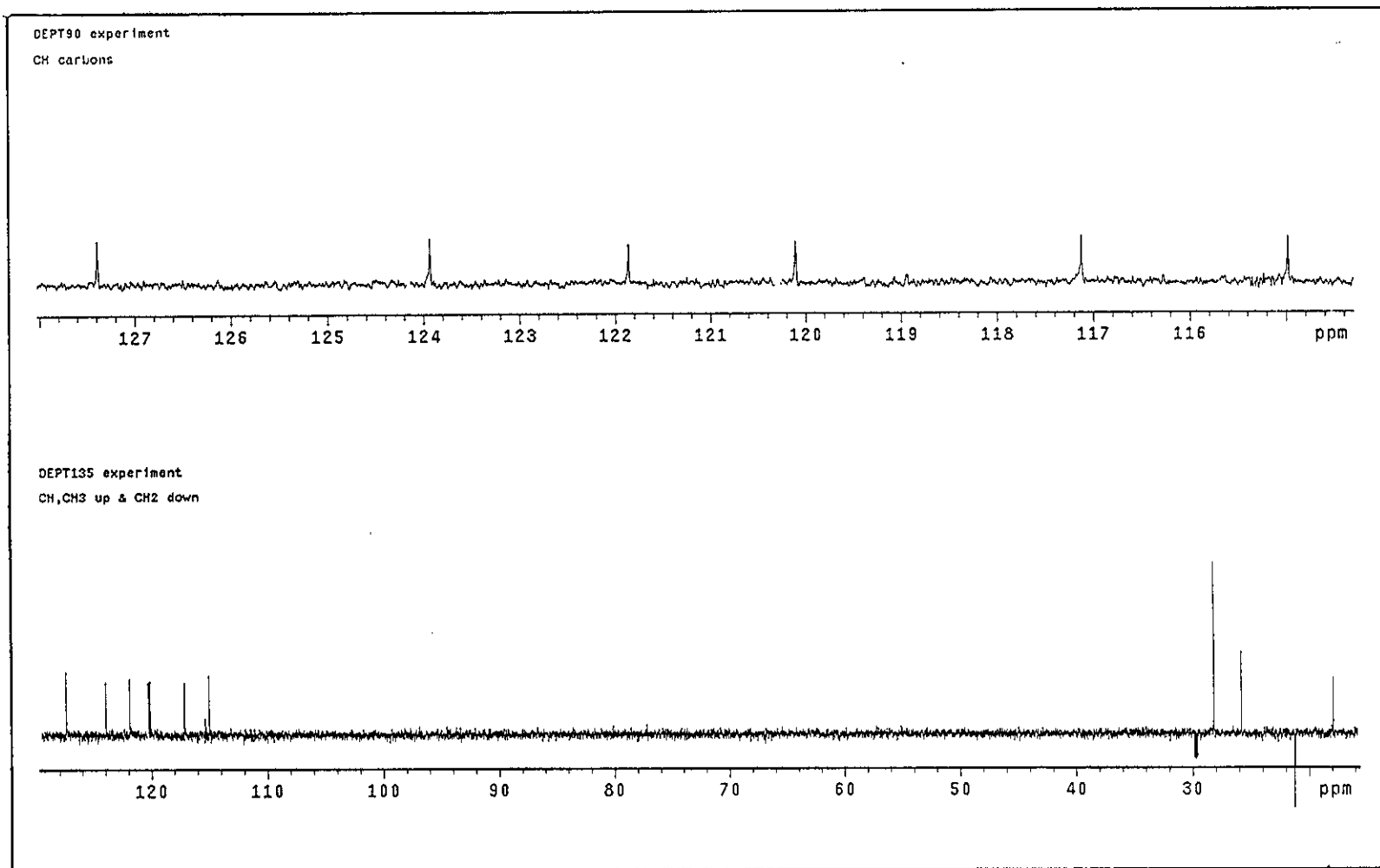


Figure 72 DEPT spectrum of YU3

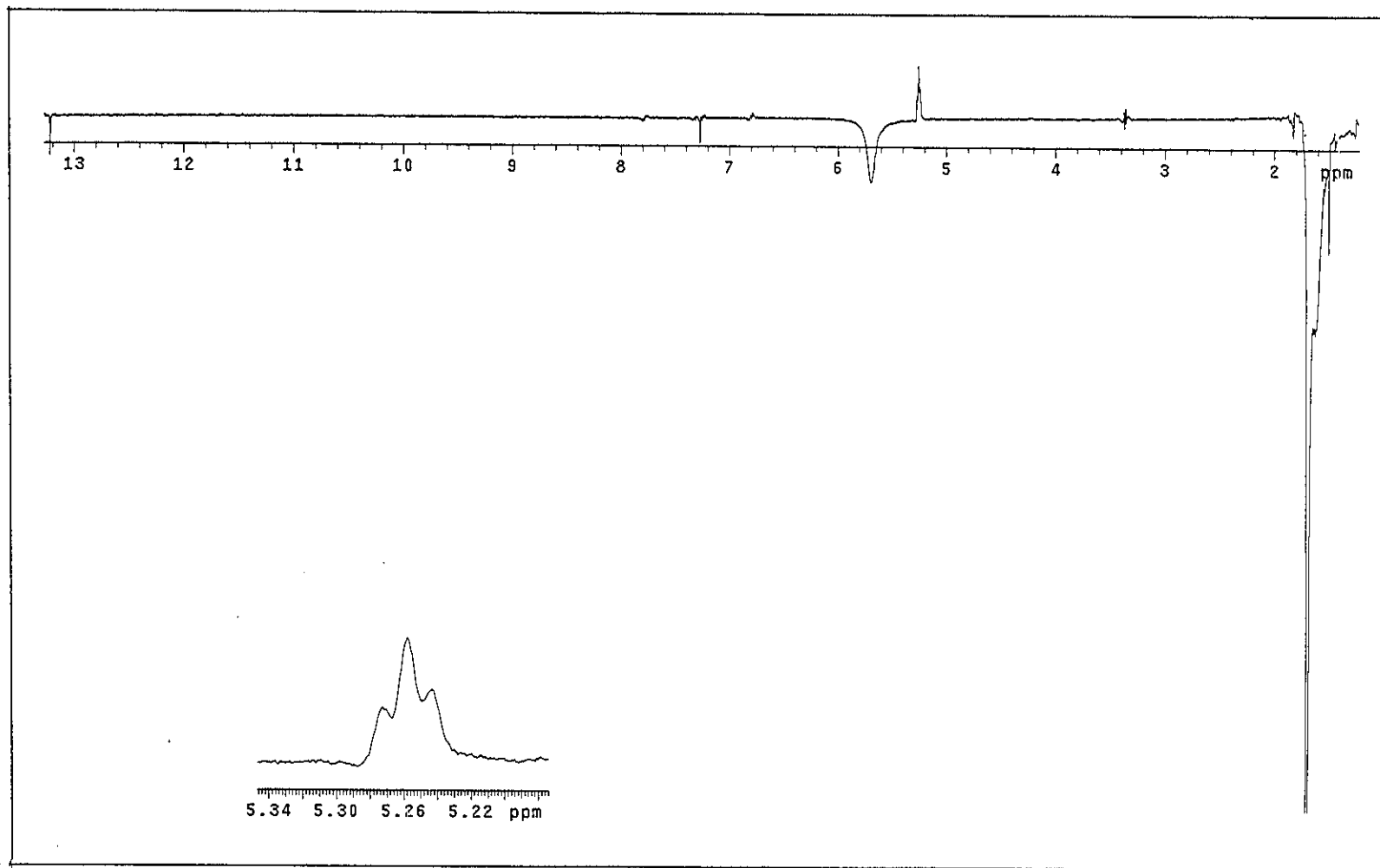


Figure 73 NOEDIFF spectrum of YU3 after irradiation at δ_H 1.70

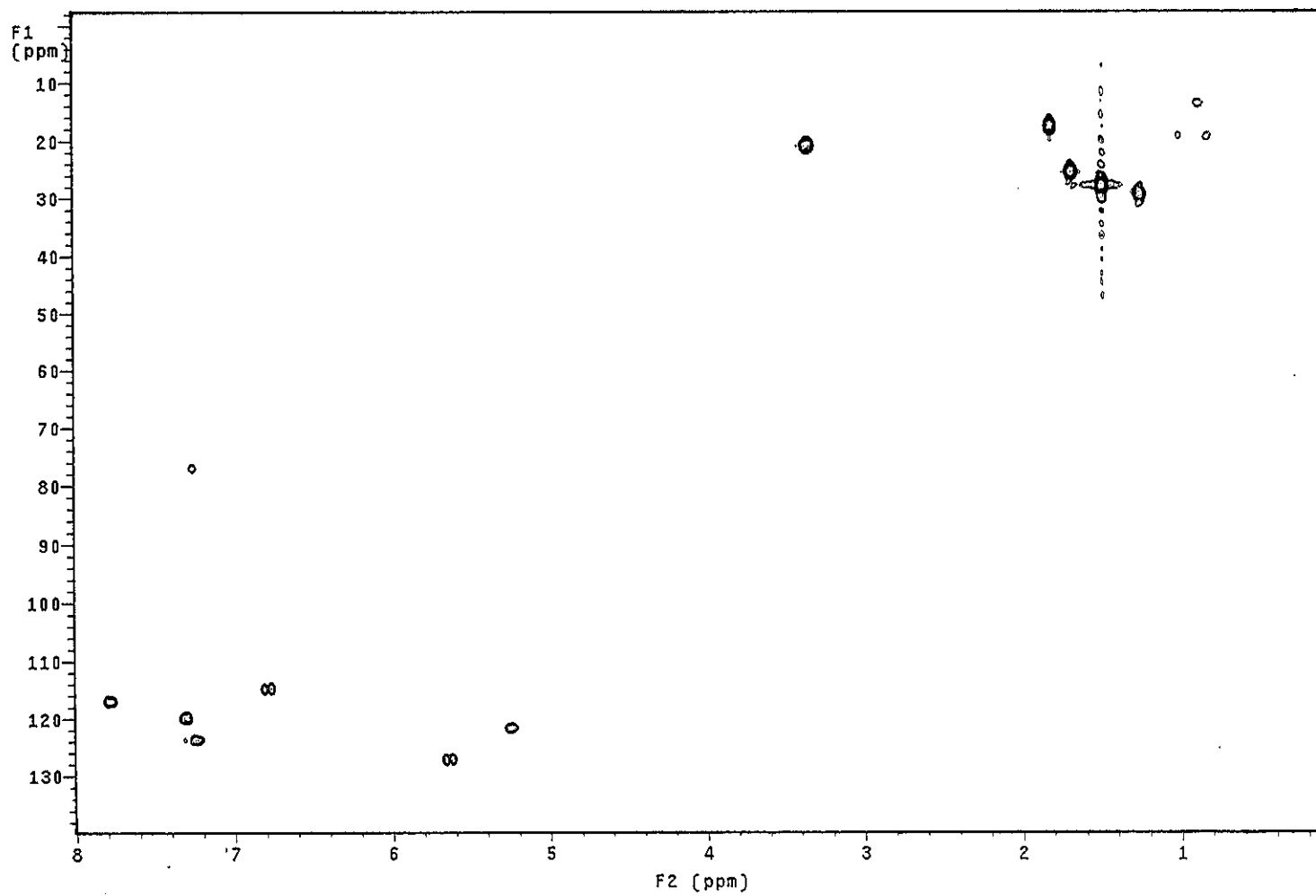


Figure 74 2D HMQC spectrum of YU3

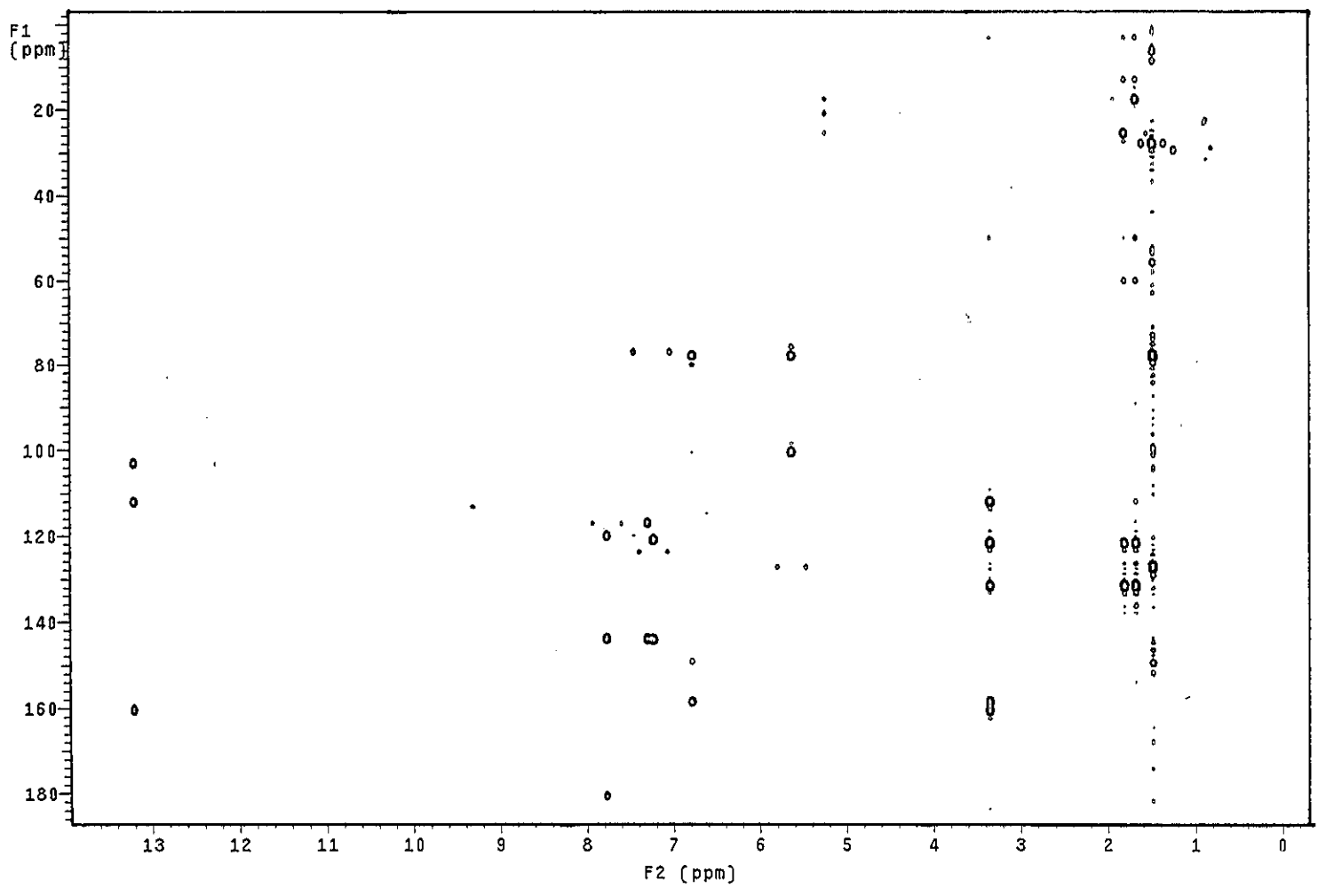


Figure 75 2D HMBC spectrum of YU3

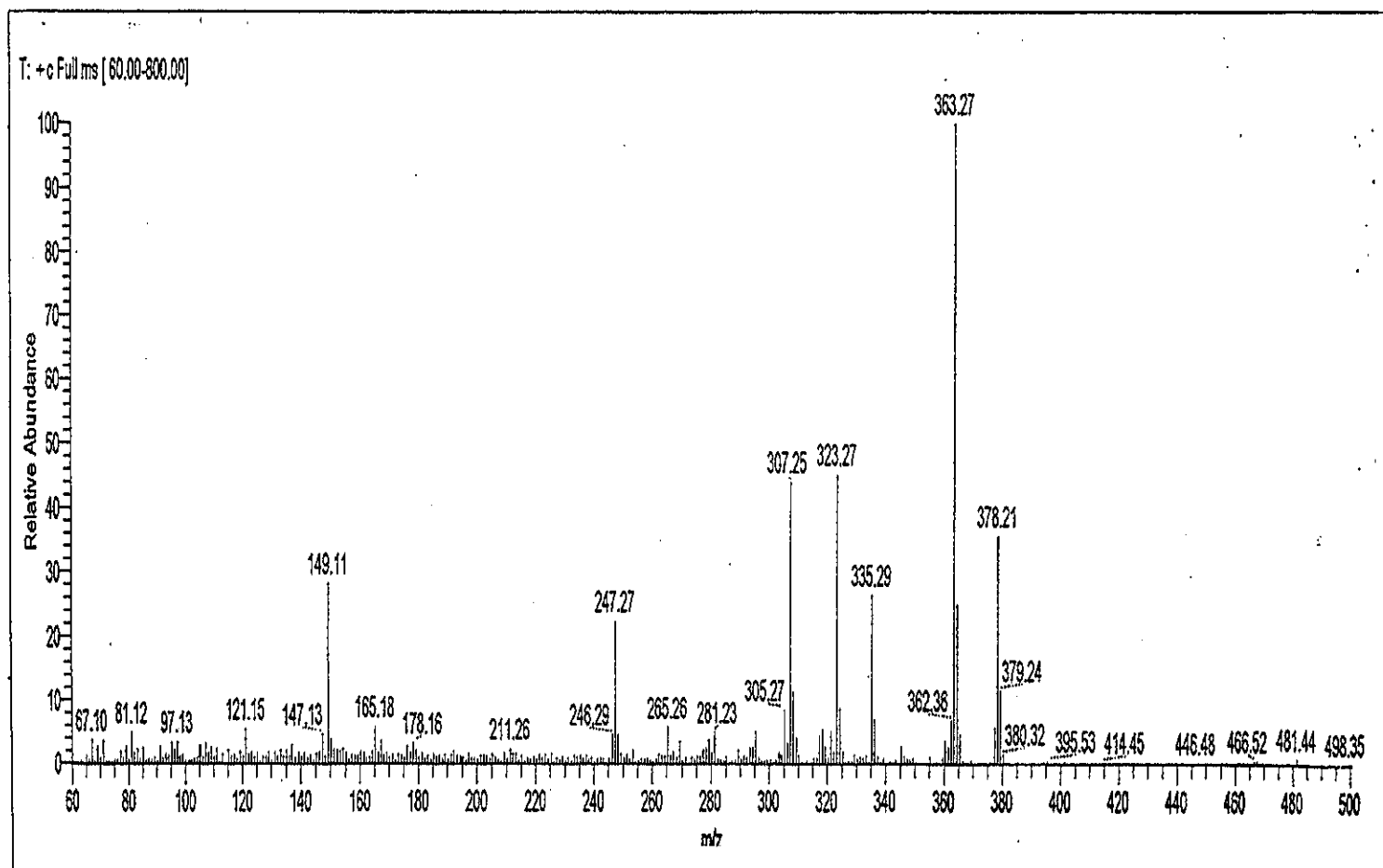


Figure 76 Mass spectrum of YU3

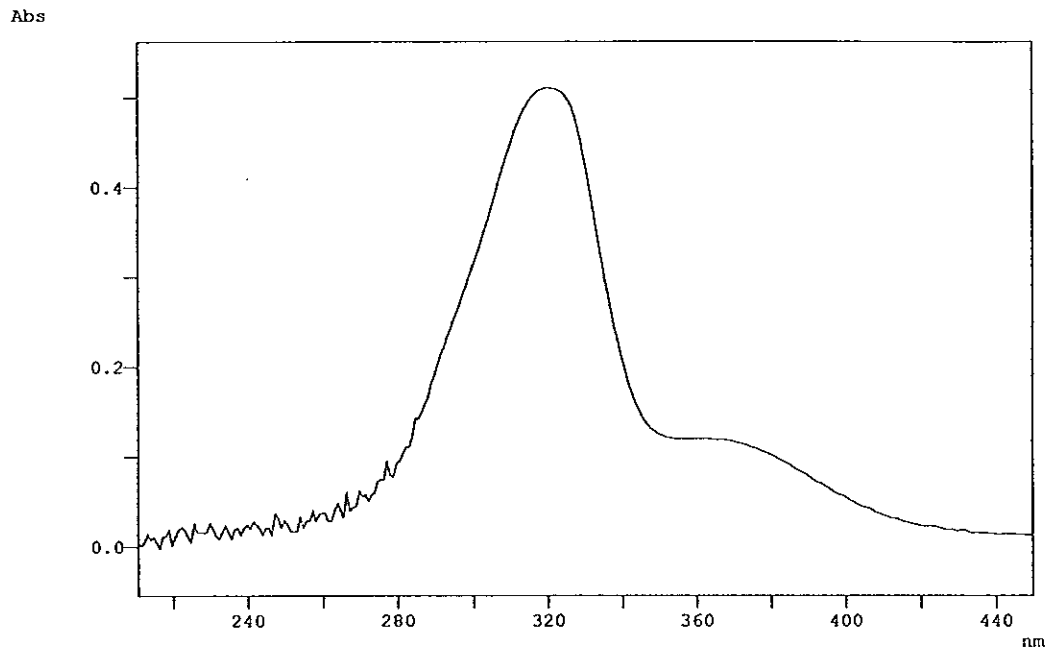


Figure 77 UV (MeOH) spectrum of YU6

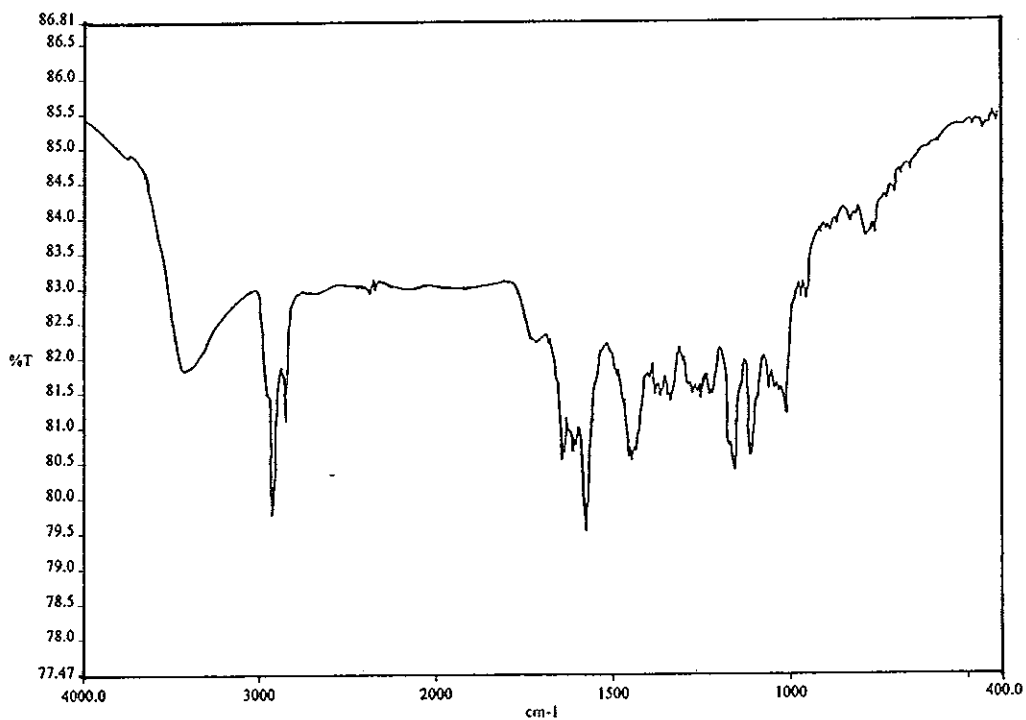


Figure 78 FT-IR (neat) spectrum of YU6

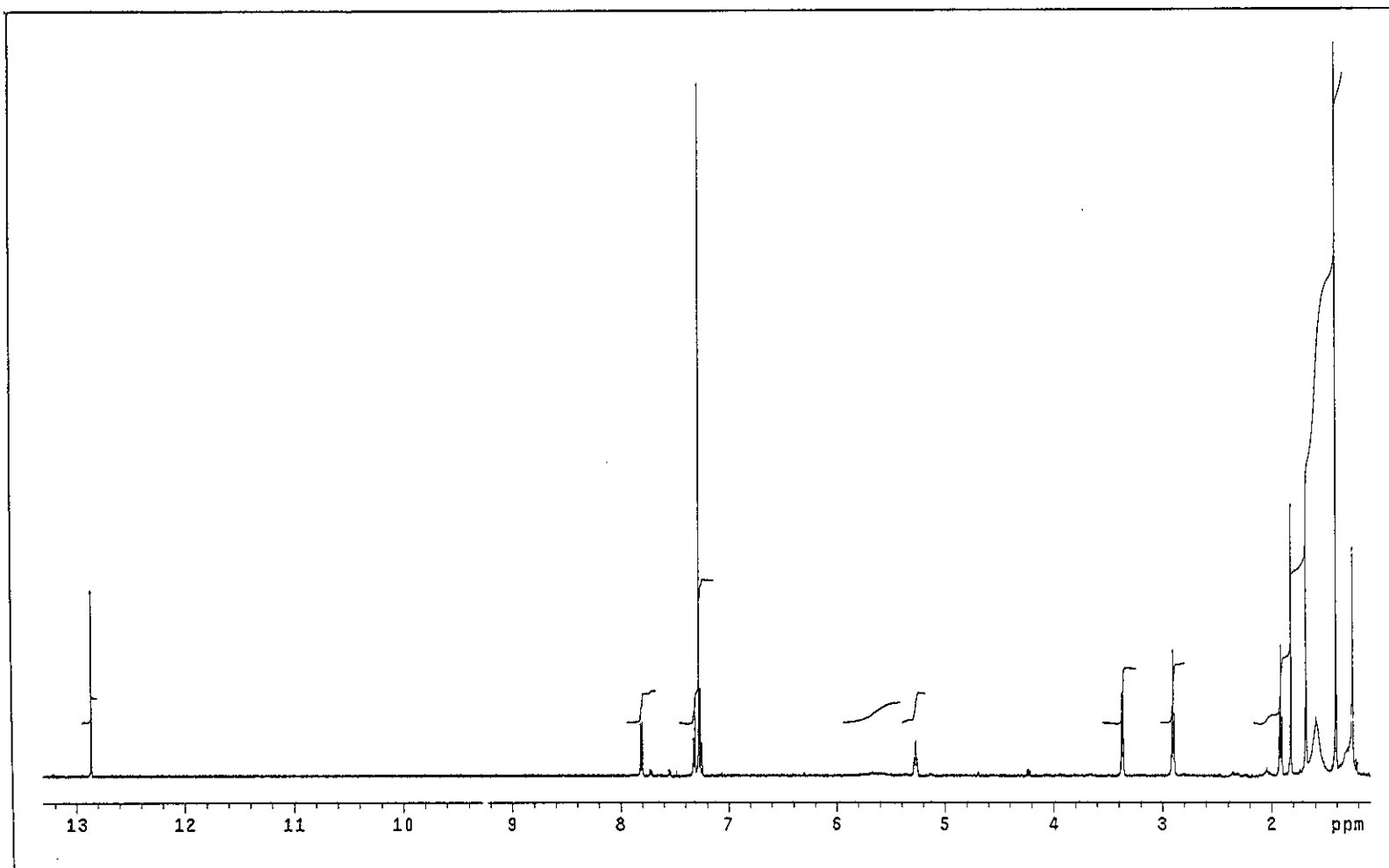


Figure 79 ^1H NMR (500 MHz) (CDCl_3) spectrum of YU6

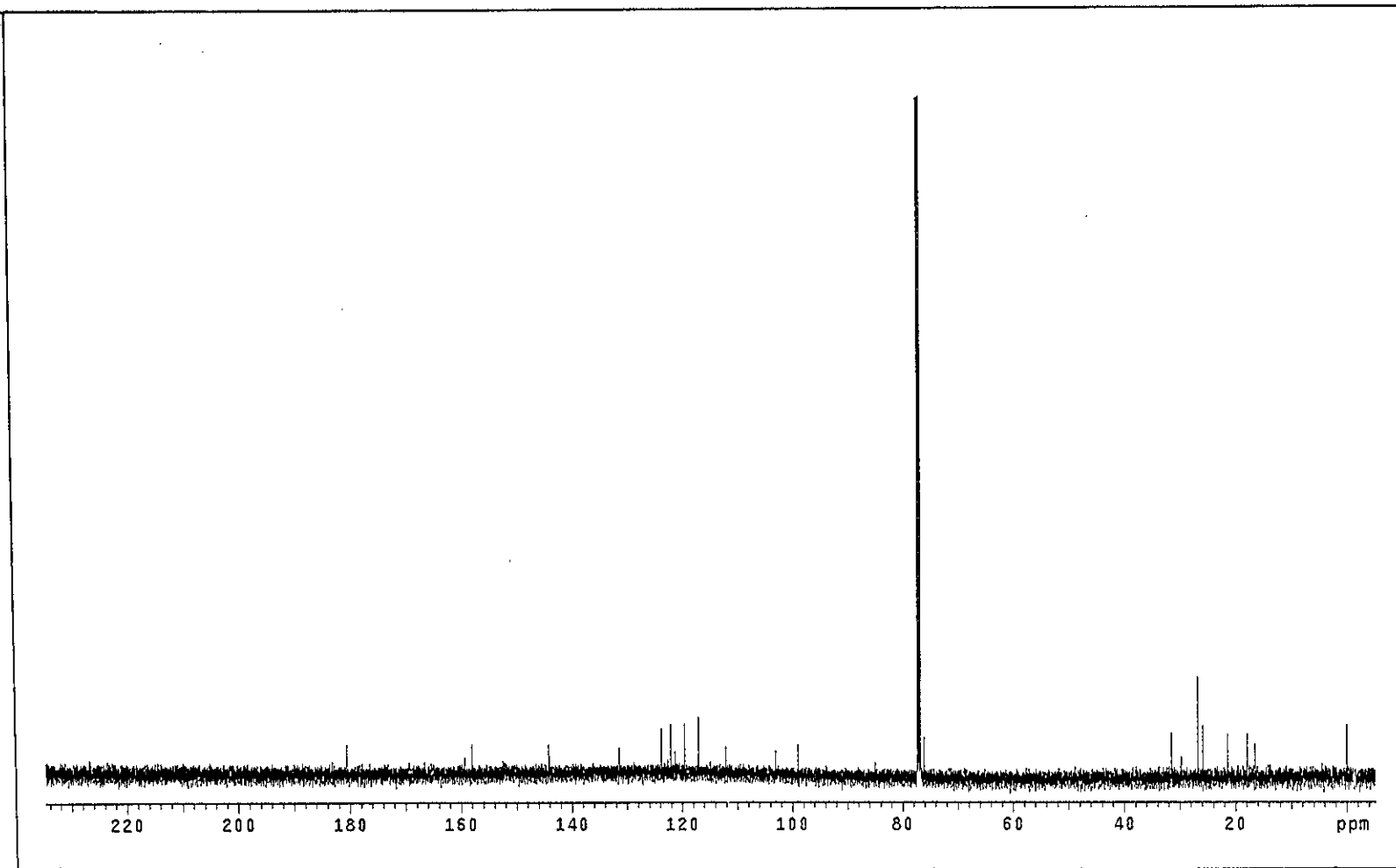


Figure 80 ^{13}C NMR (125 MHz) (CDCl_3) spectrum of YU6

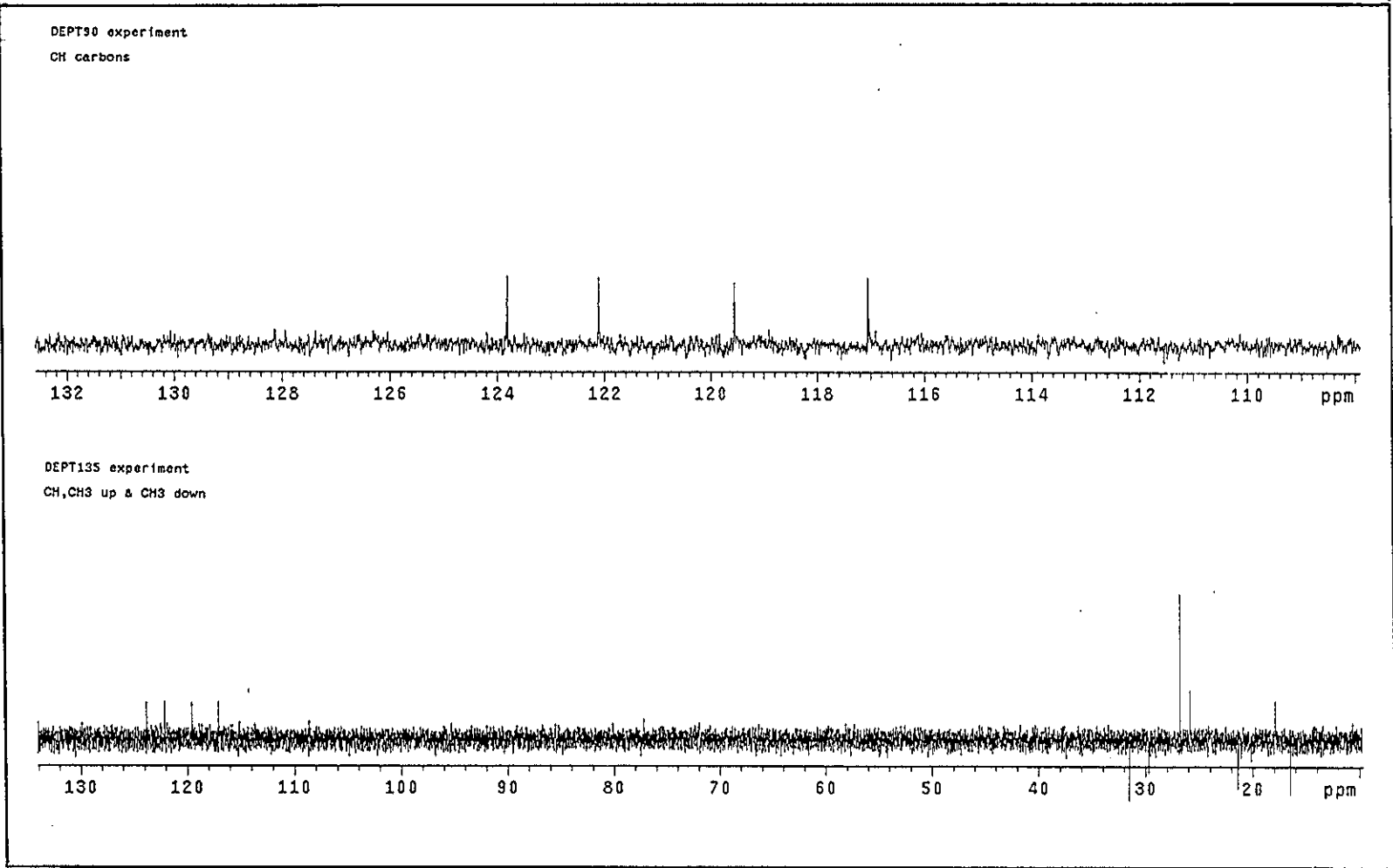


Figure 81 DEPT spectrum of YU6

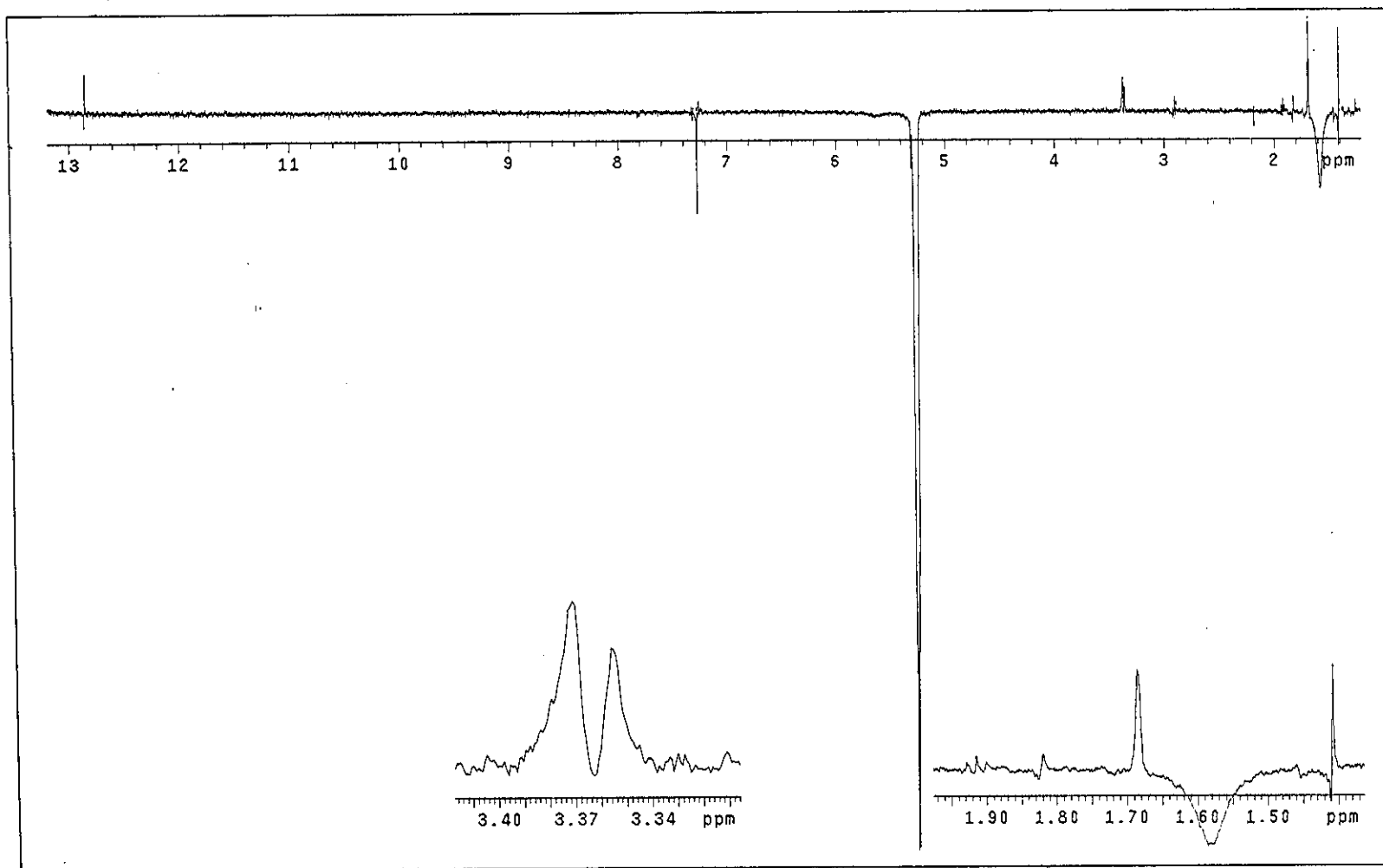


Figure 82 NOEDIFF spectrum of YU6 after irradiation at δ_H 5.27

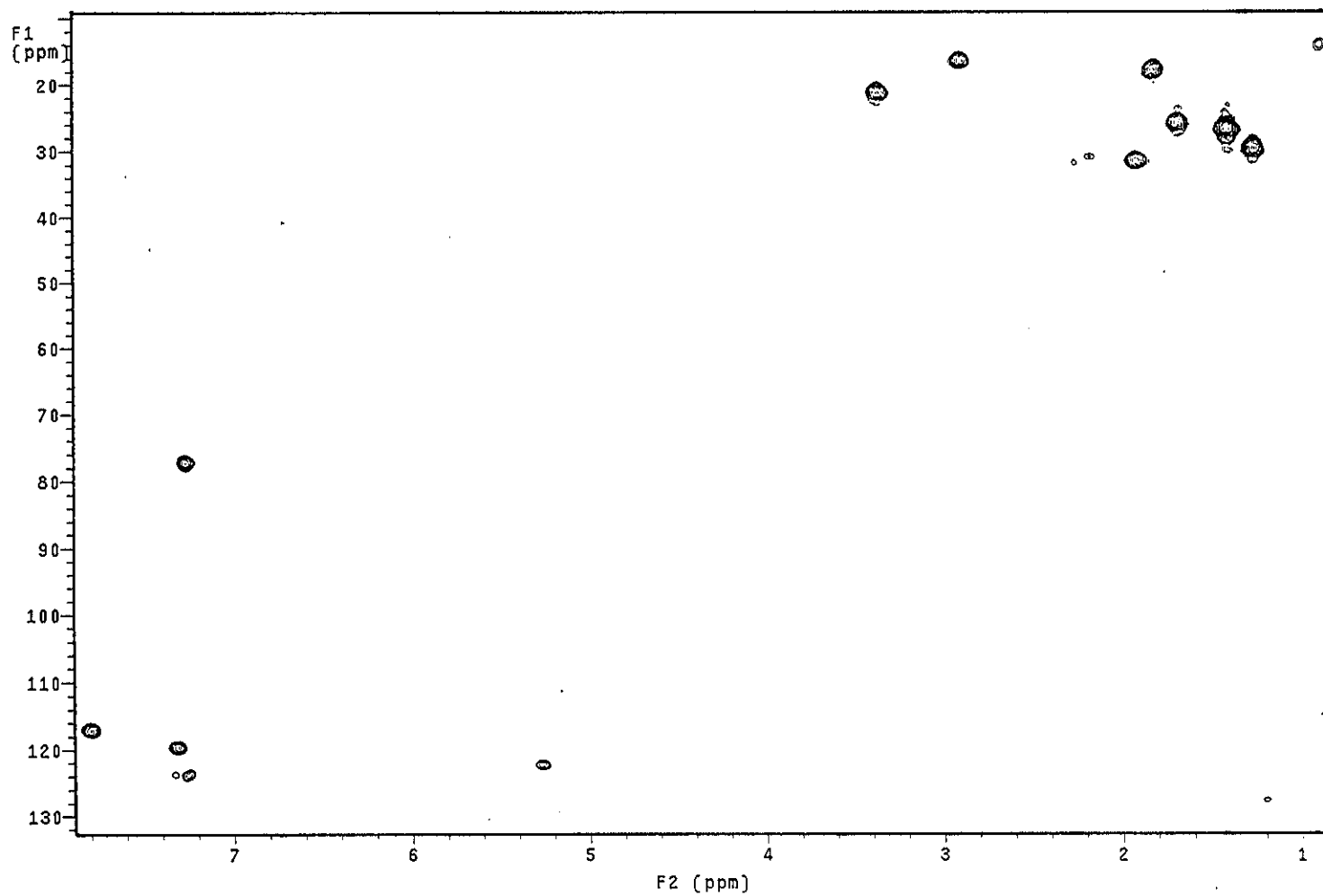


Figure 83 2D HMQC spectrum of YU6

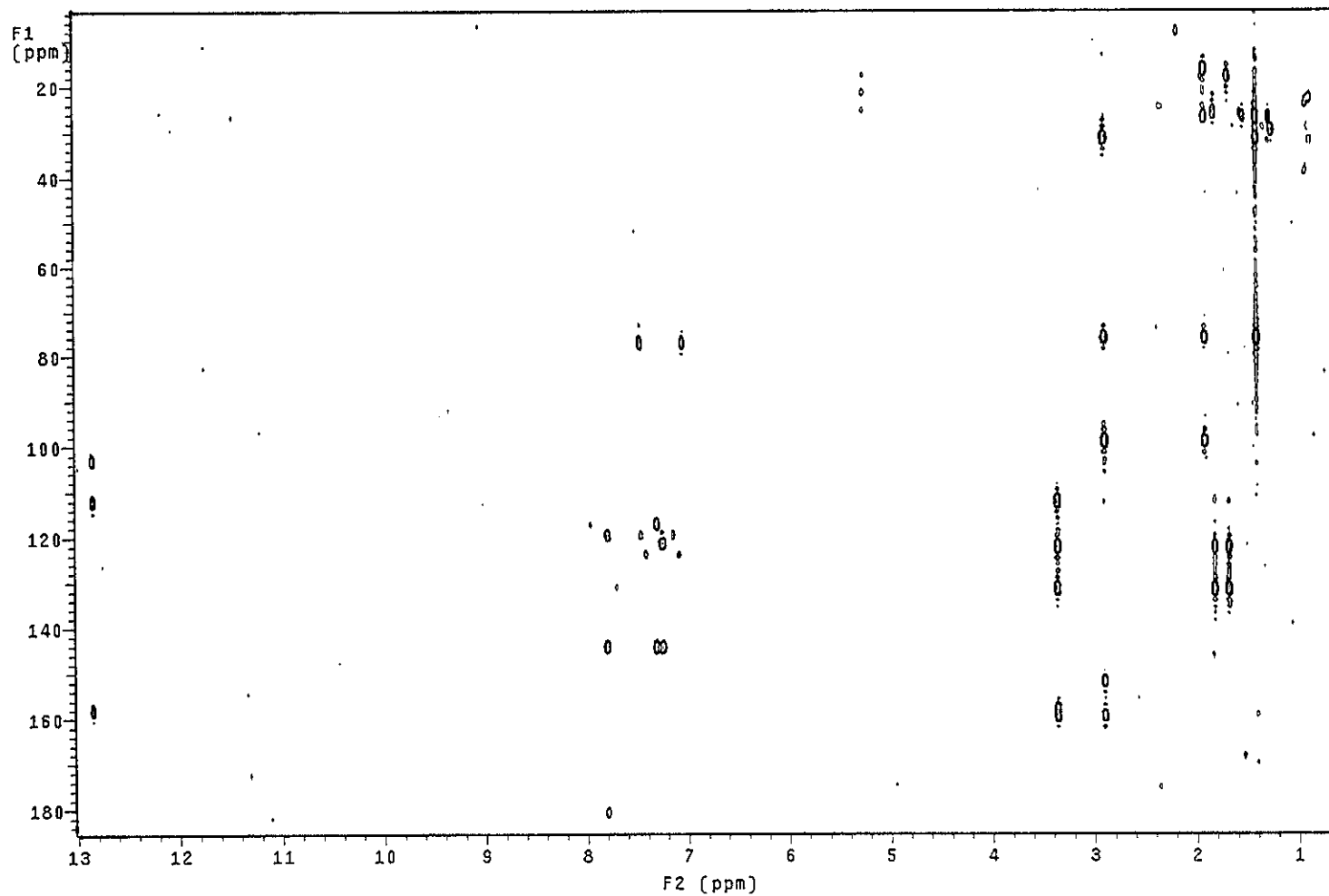


Figure 84 2D HMBC spectrum of YU6

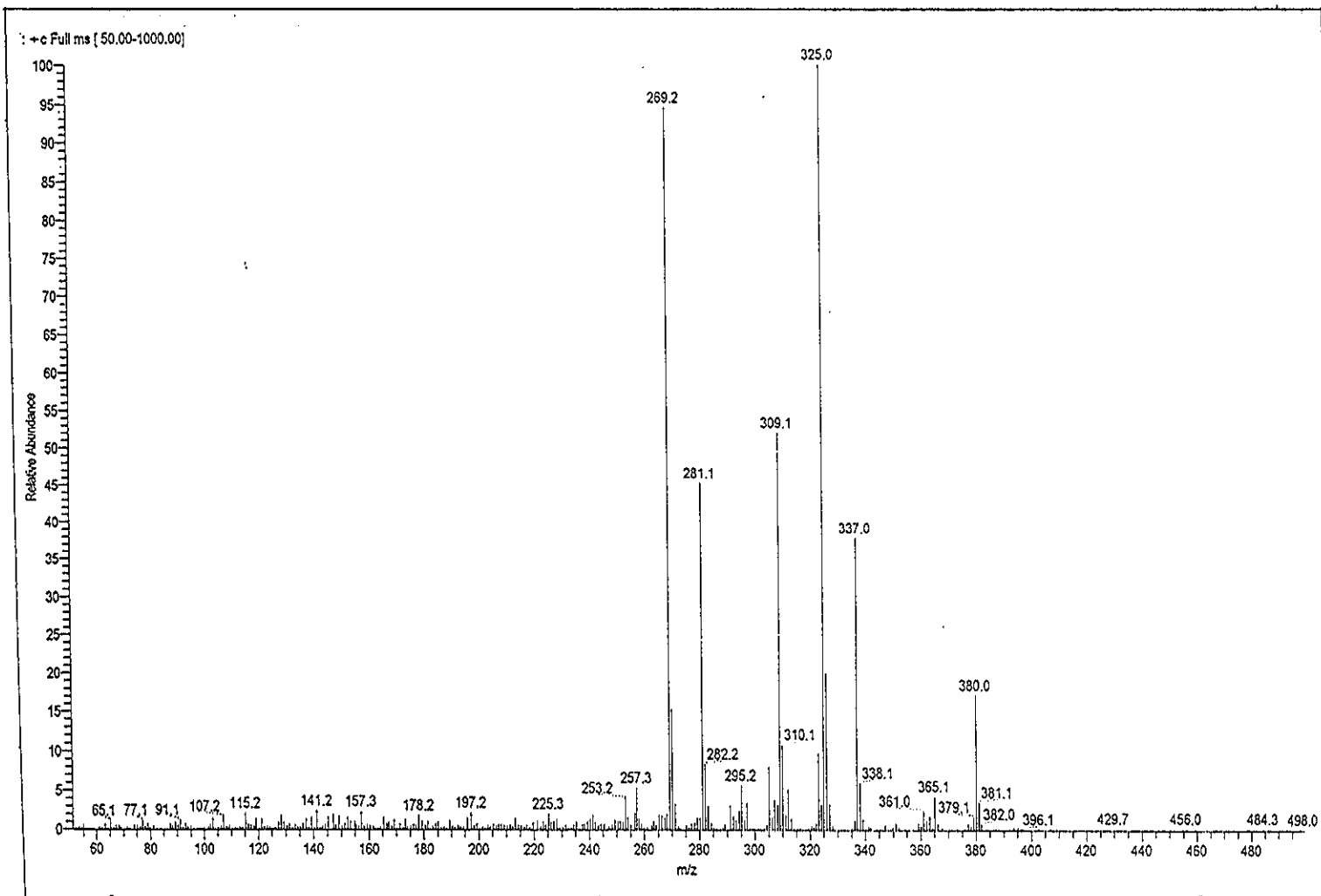


Figure 85 Mass spectrum of YU6

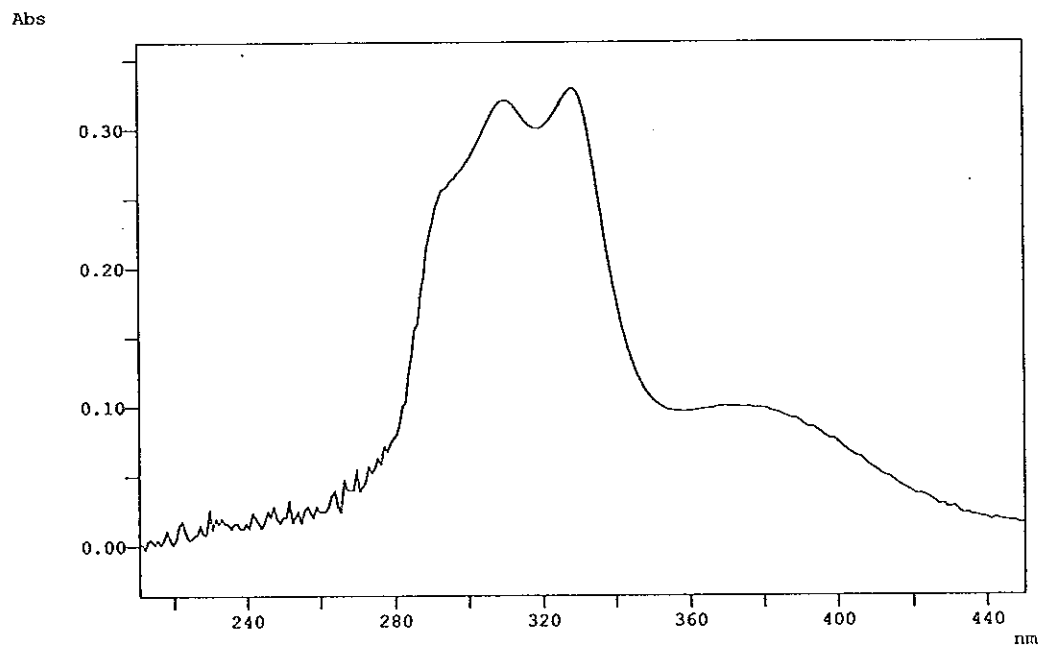


Figure 86 UV (MeOH) spectrum of YU11

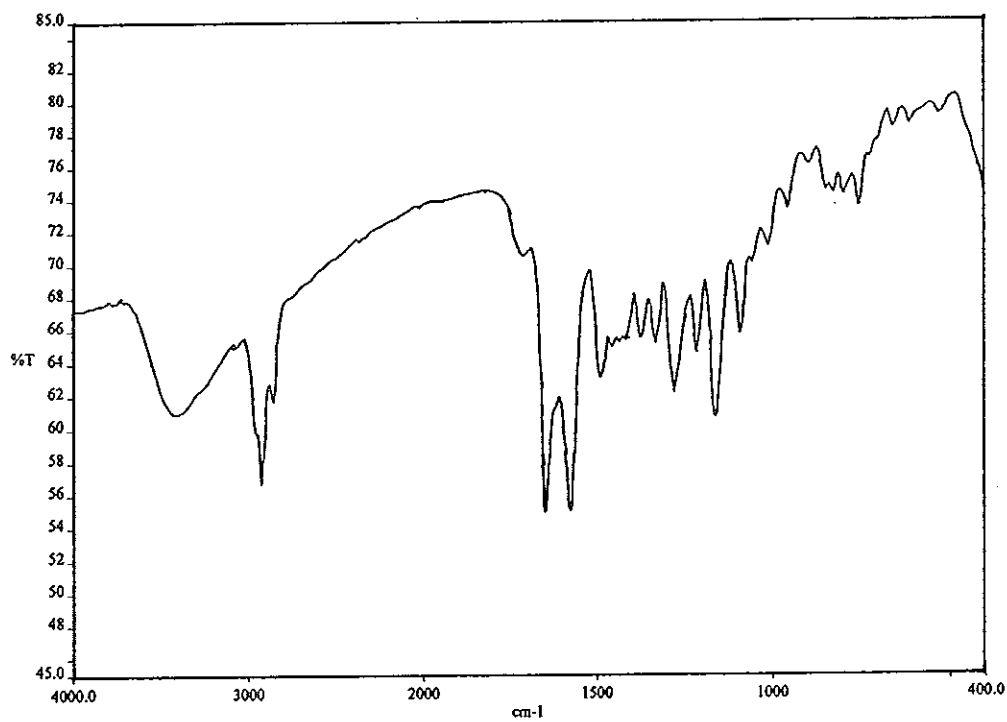


Figure 87 FT-IR (neat) spectrum of YU11

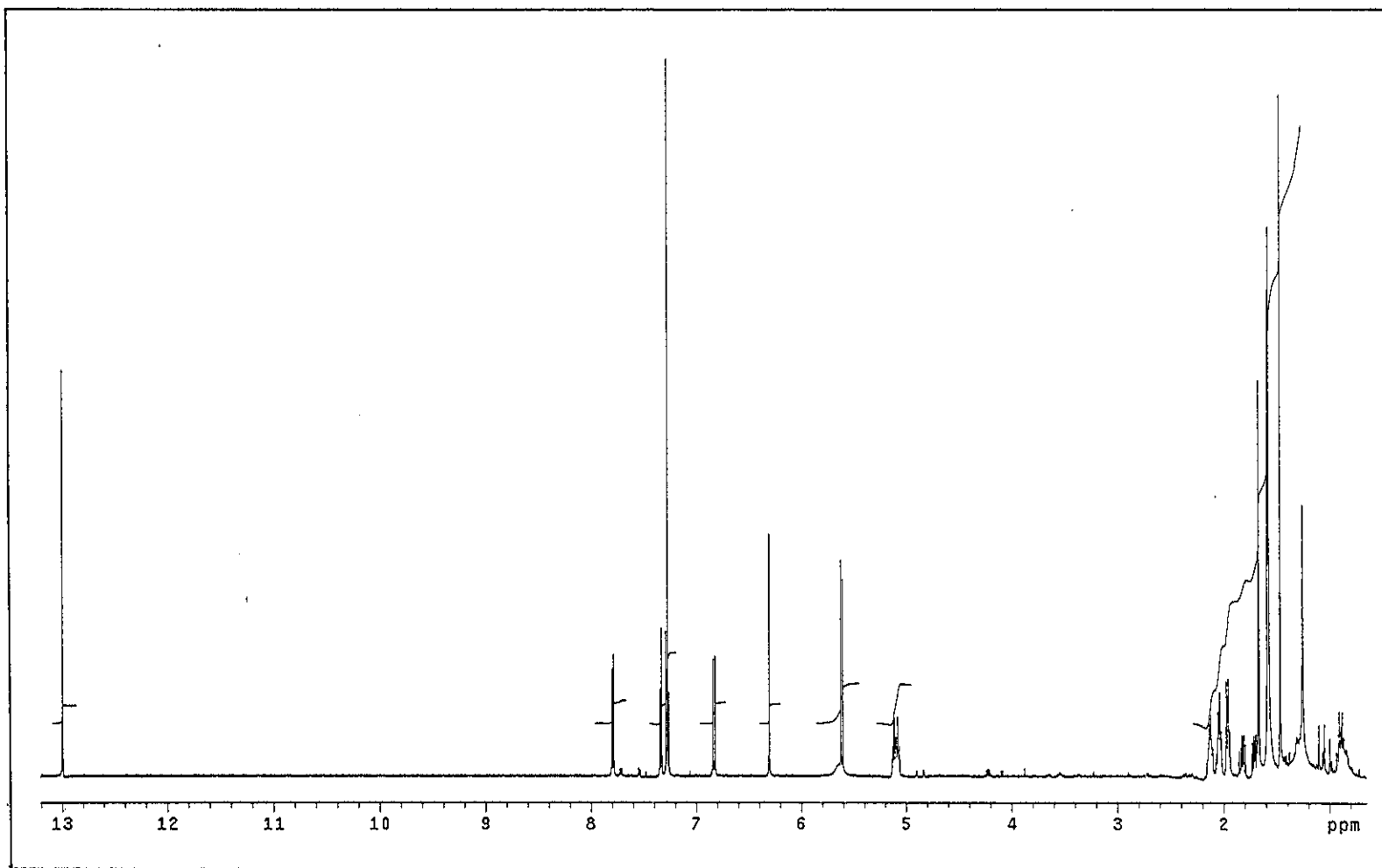


Figure 88 ^1H NMR (500 MHz) (CDCl_3) spectrum of YU11

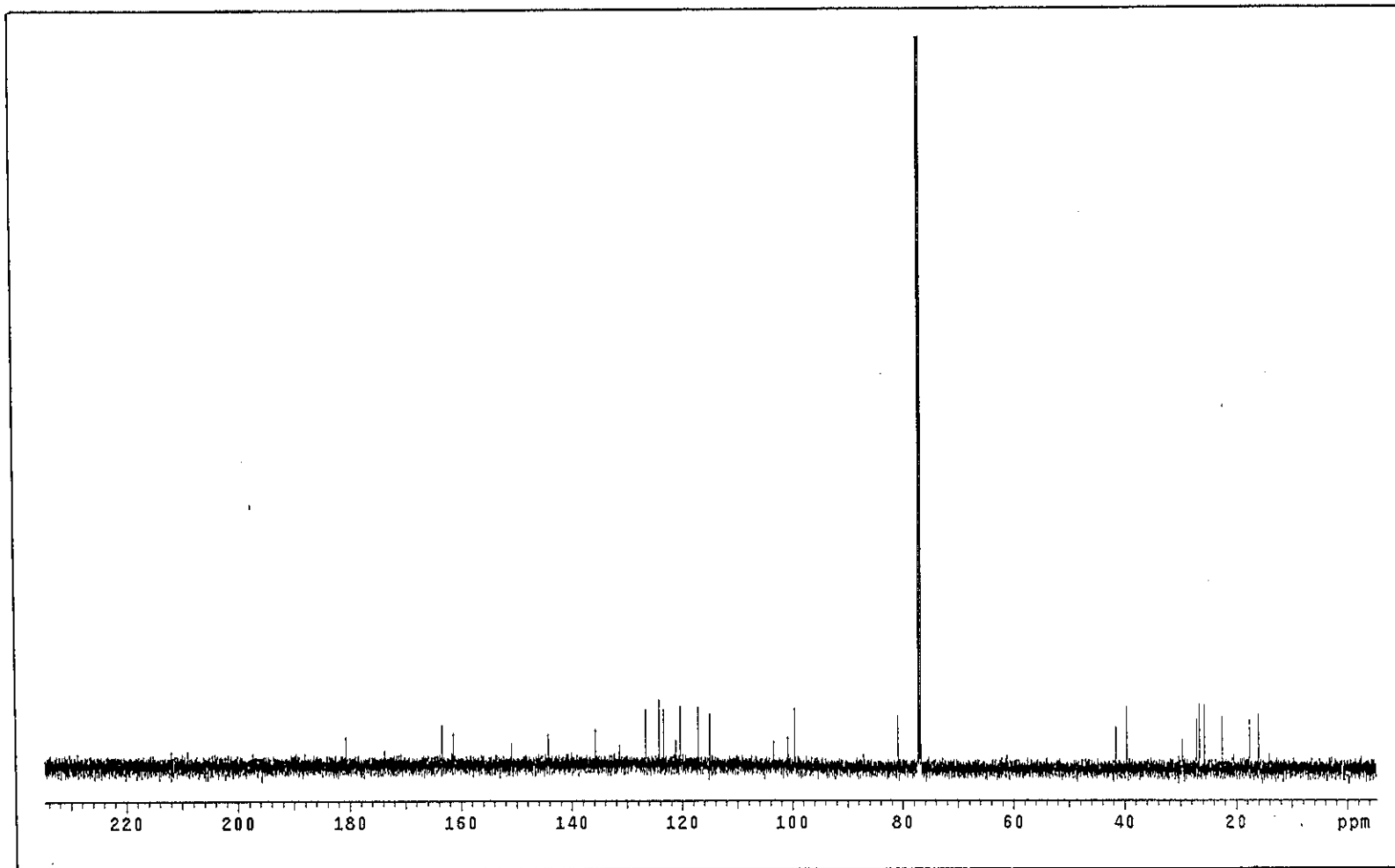


Figure 89 ^{13}C NMR (125 MHz) (CDCl_3) spectrum of YU11

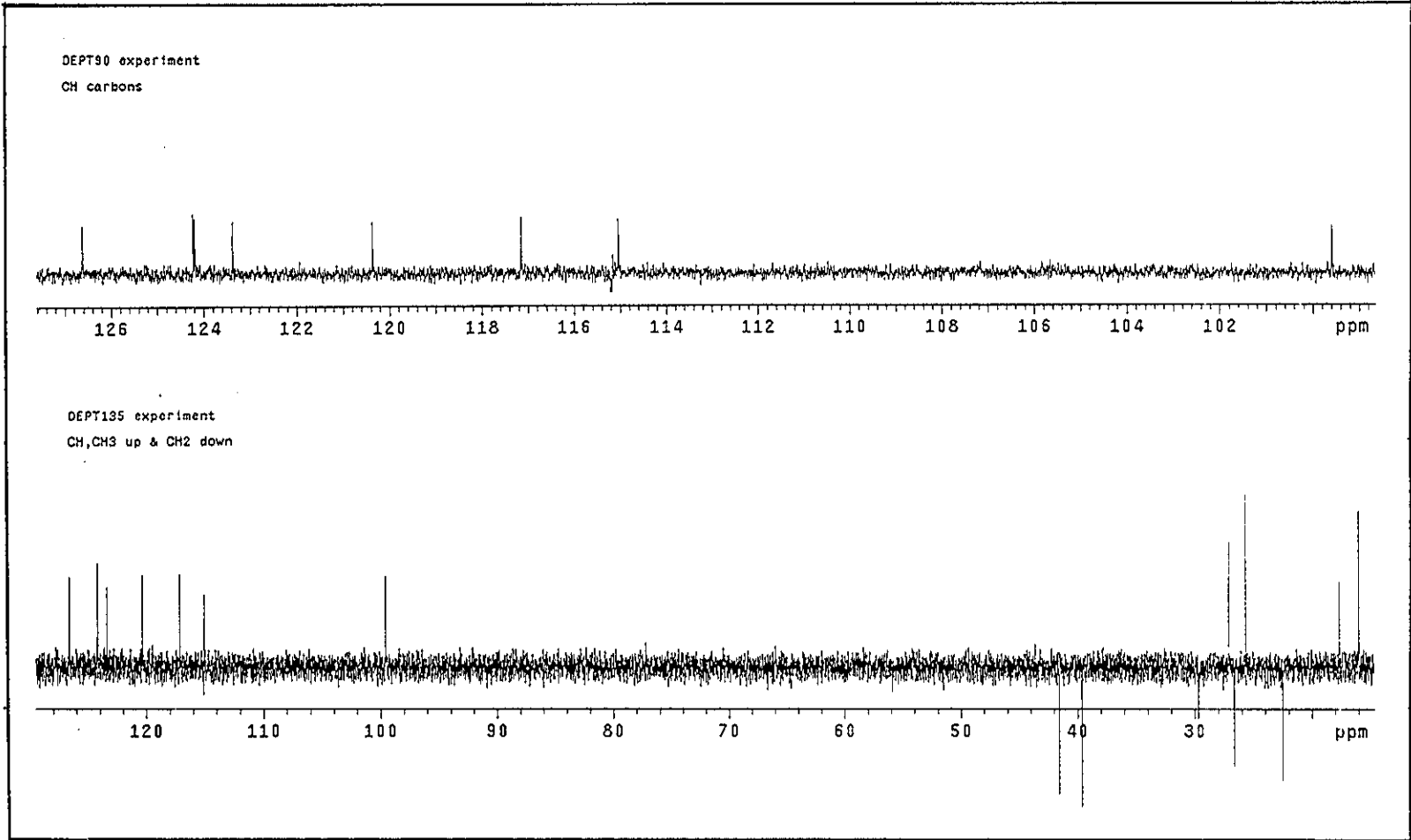


Figure 90 DEPT spectrum of YU11

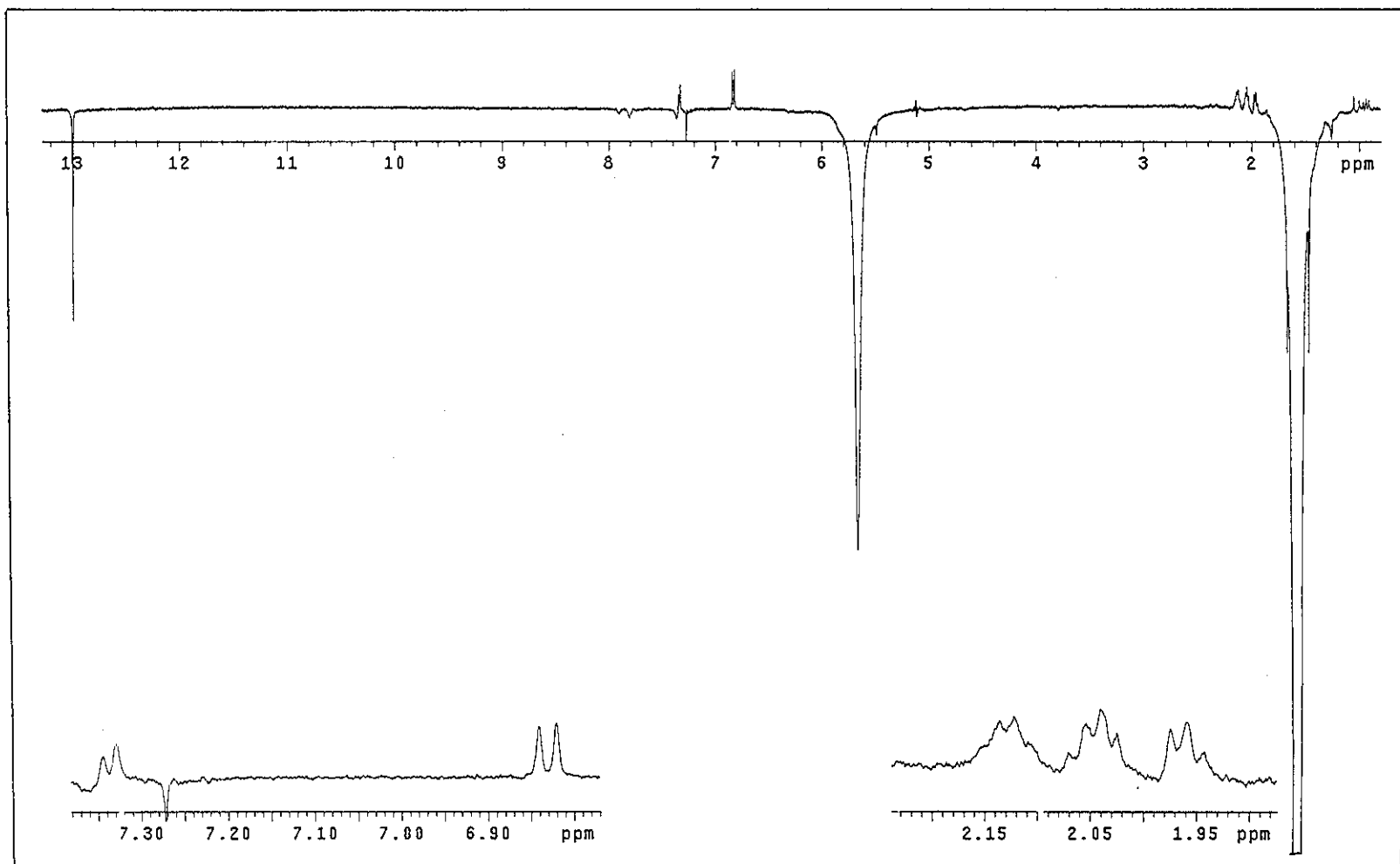


Figure 91 NOEDIFF spectrum of YU11 after irradiation at δ_H 1.58

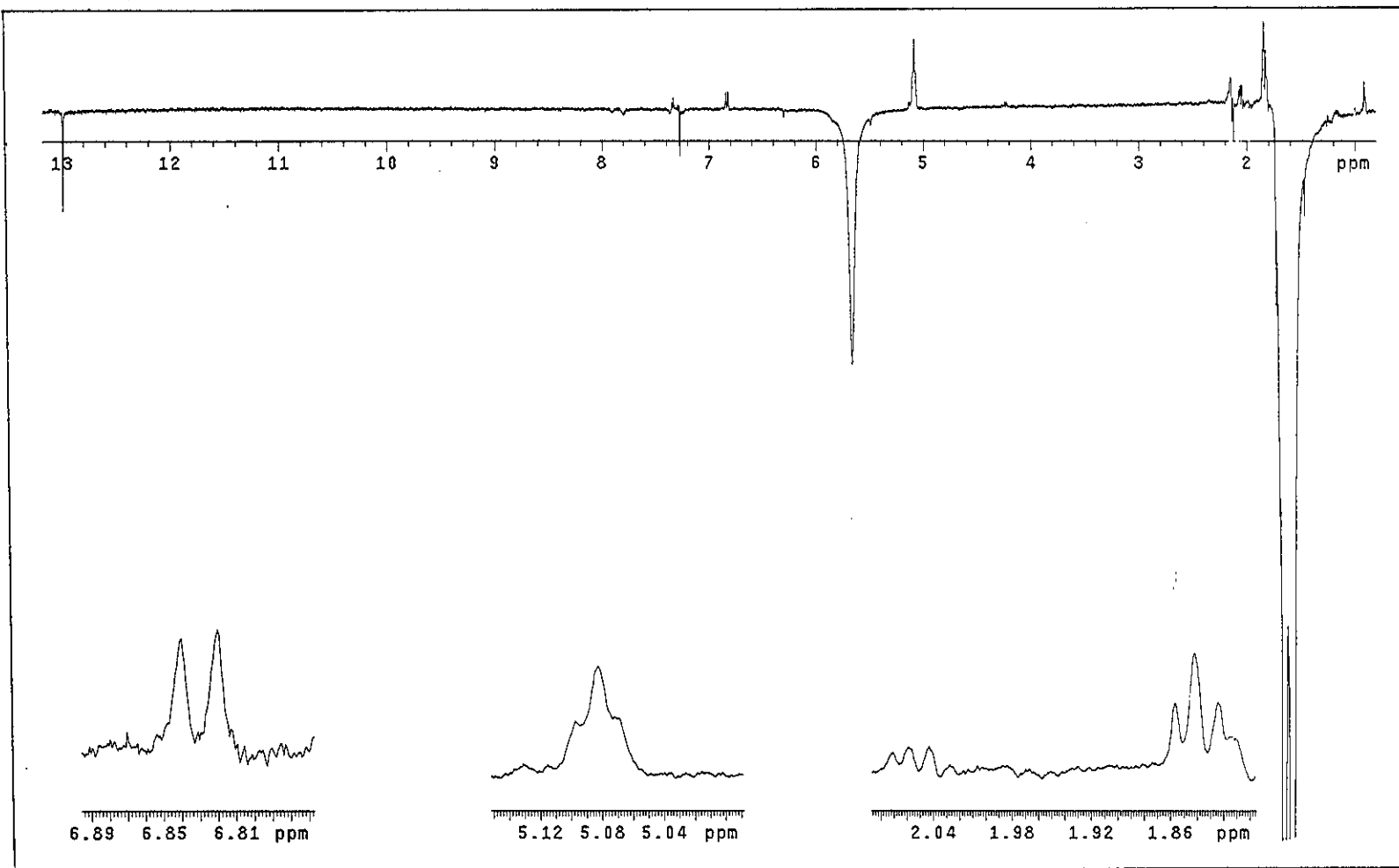


Figure 92 NOEDIFF spectrum of YU11 after irradiation at δ_H 1.67

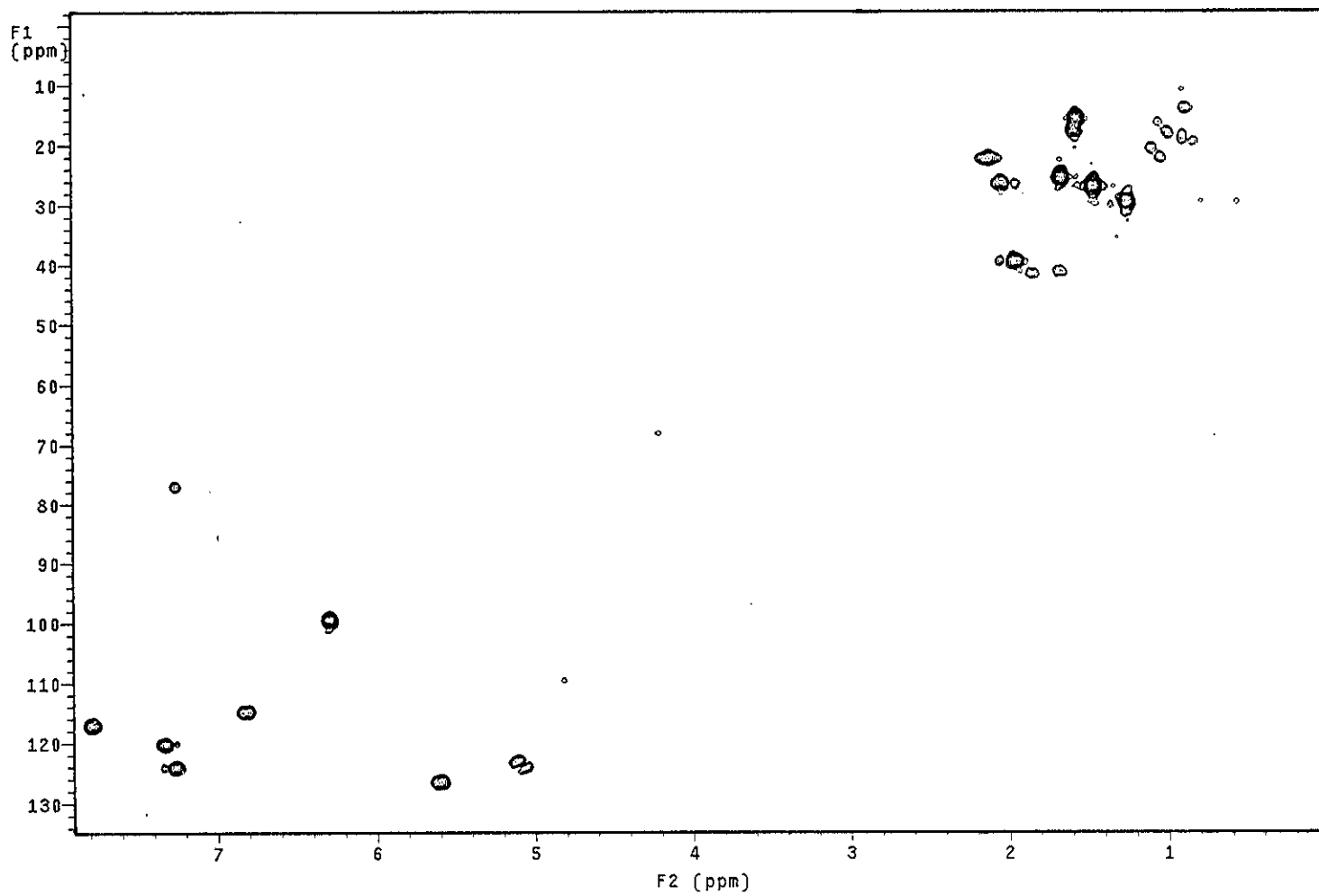


Figure 93 2D HMQC spectrum of YU11

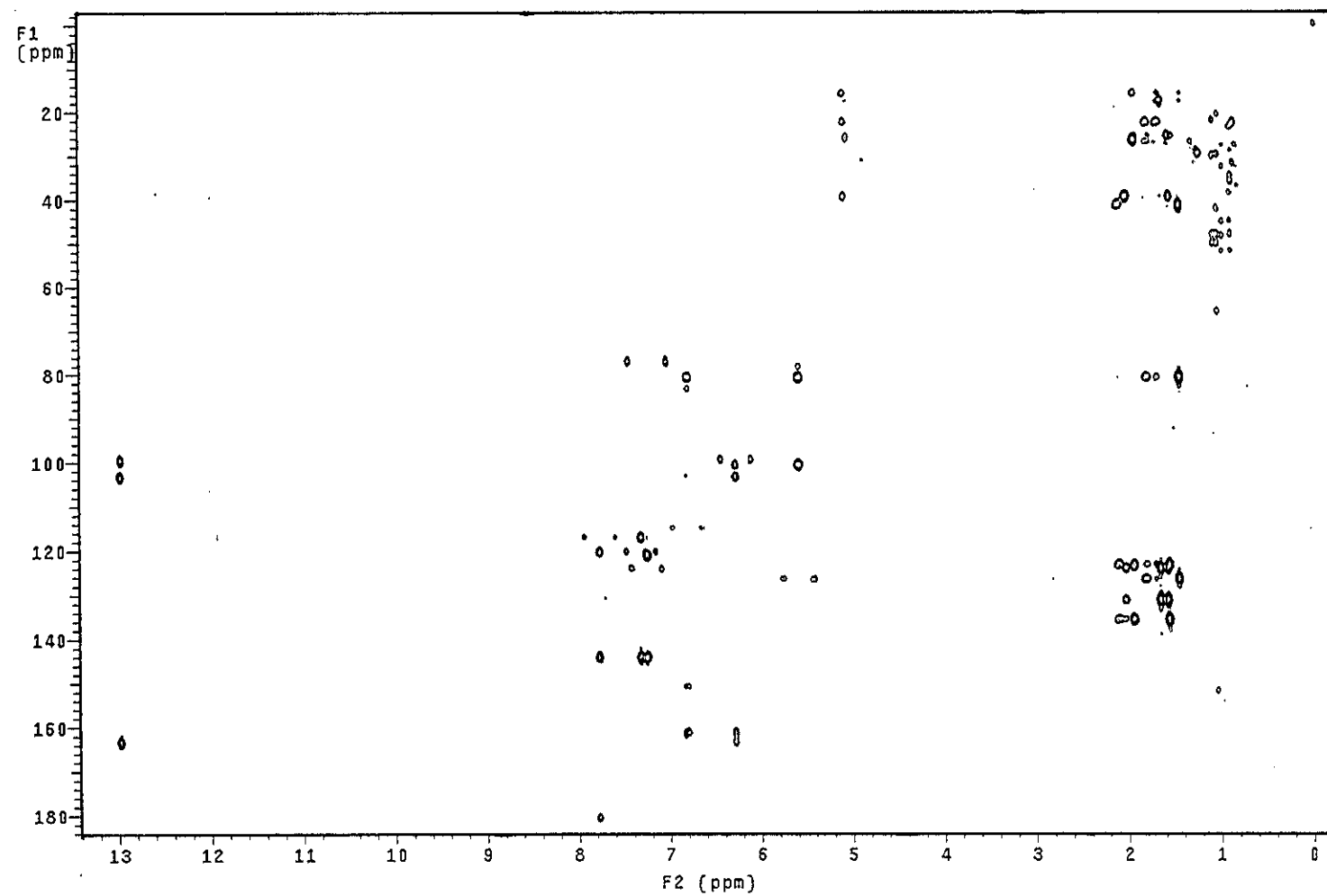


Figure 94 2D HMBC spectrum of YU11

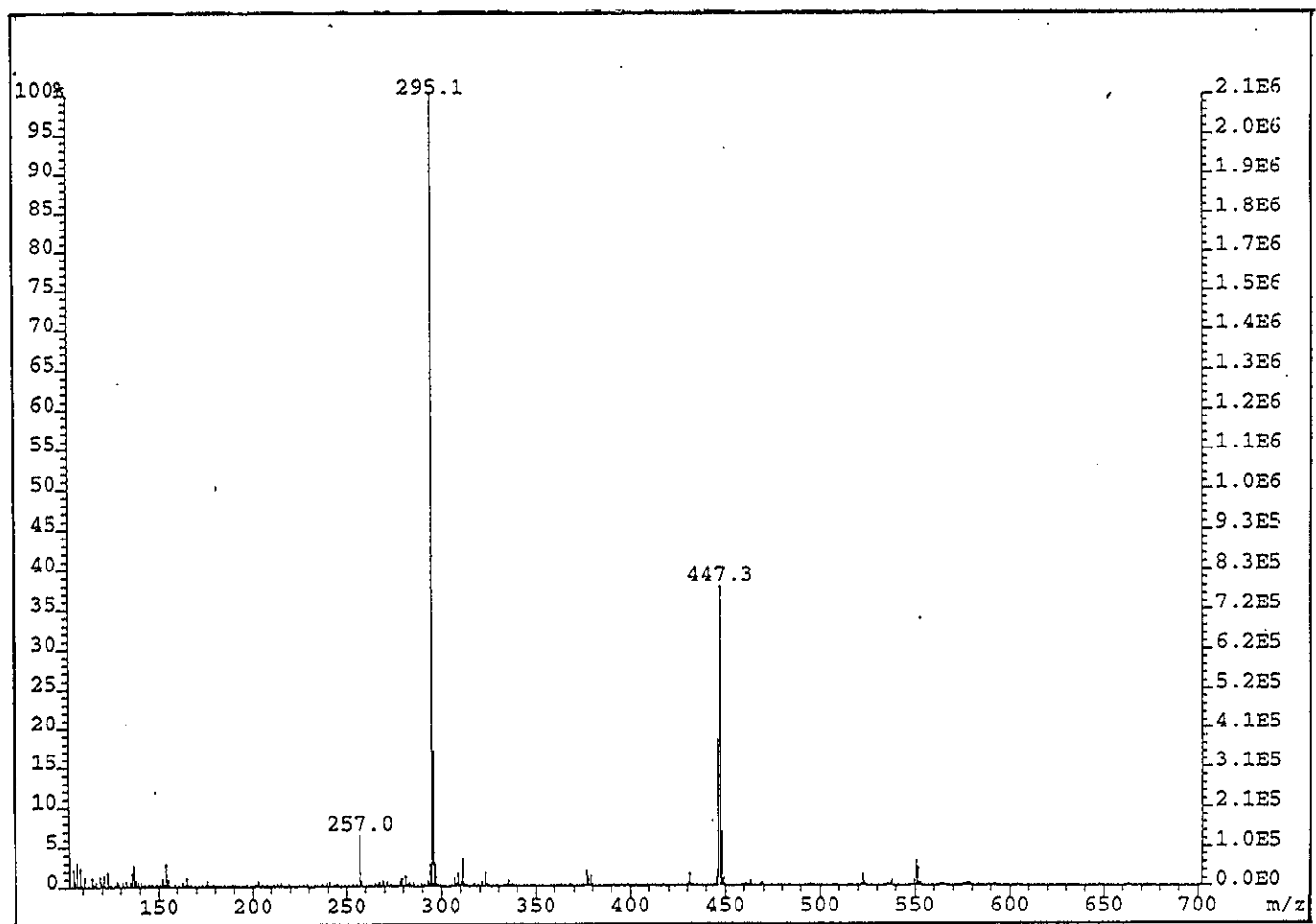


Figure 95 Mass spectrum of YU11

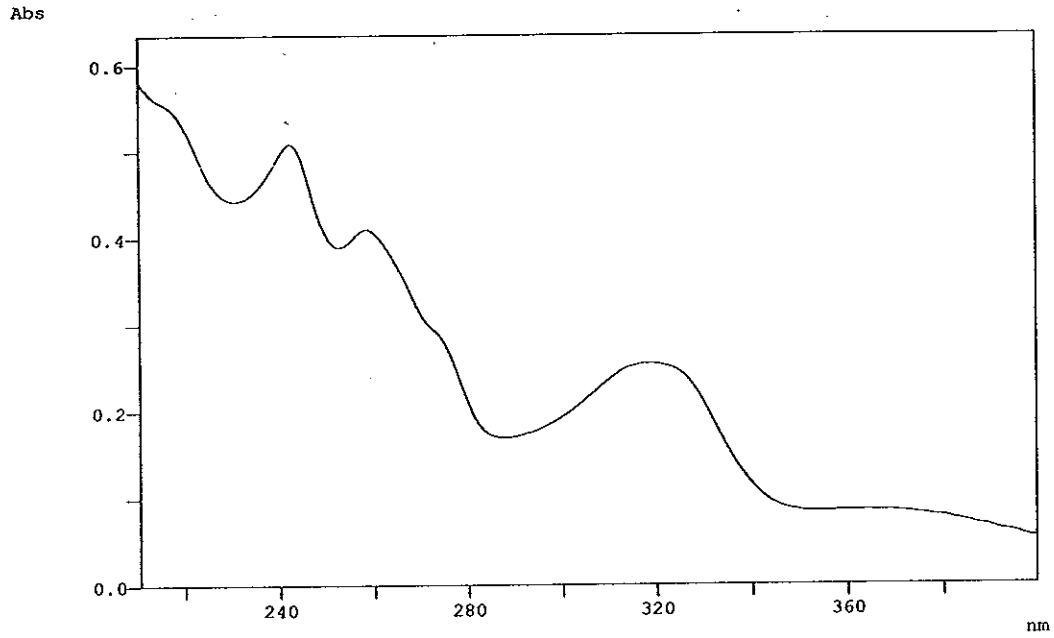


Figure 96 UV (MeOH) spectrum of YU16

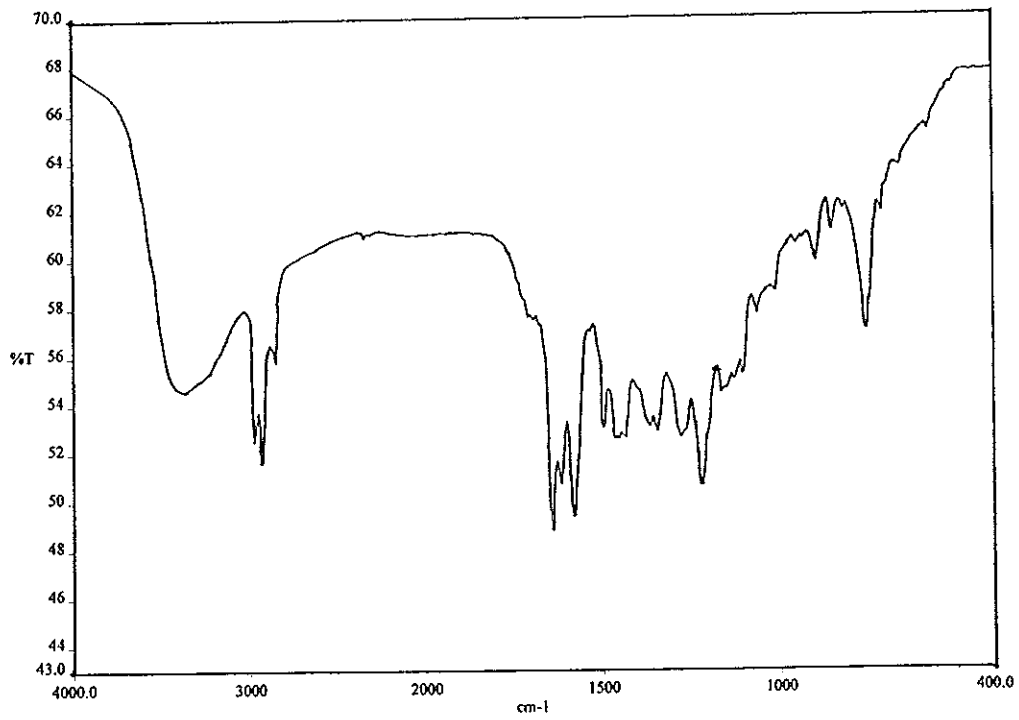


Figure 97 FT-IR (neat) spectrum of YU16

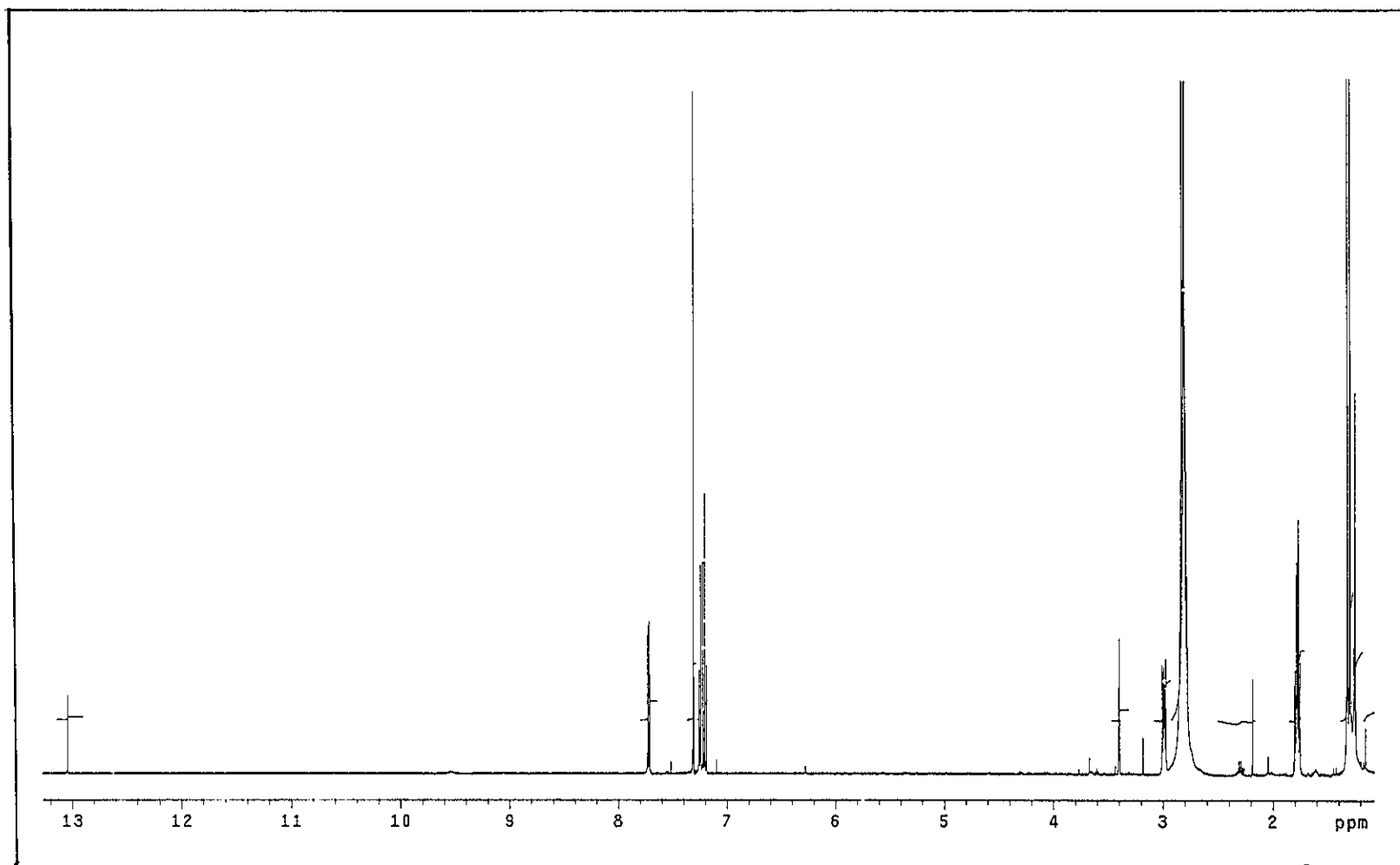


Figure 98 ^1H NMR (500 MHz) ($\text{CDCl}_3/\text{CD}_3\text{OD}$) spectrum of YU16

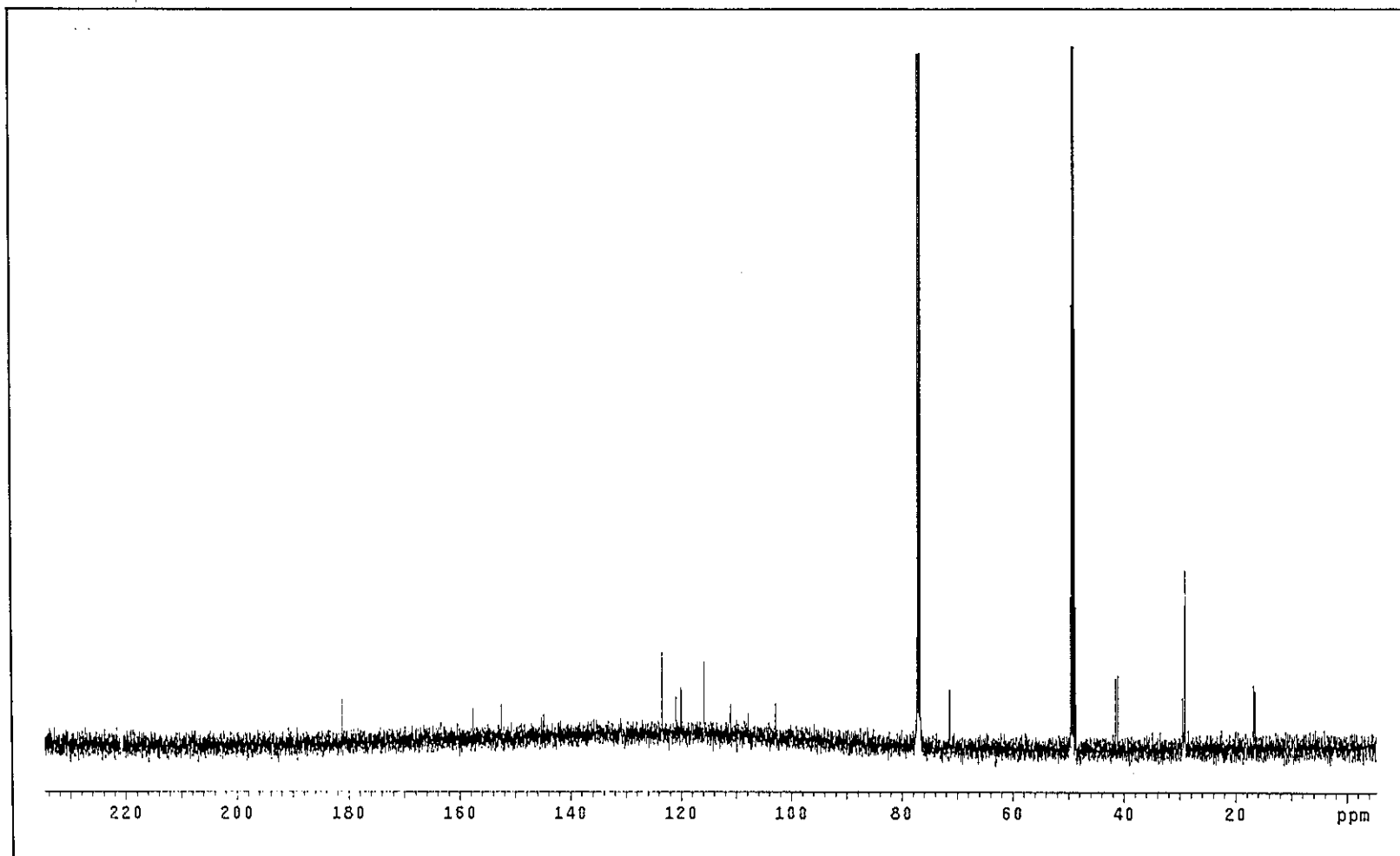


Figure 99 ^{13}C NMR (125 MHz) ($\text{CDCl}_3/\text{CD}_3\text{OD}$) spectrum of YU16

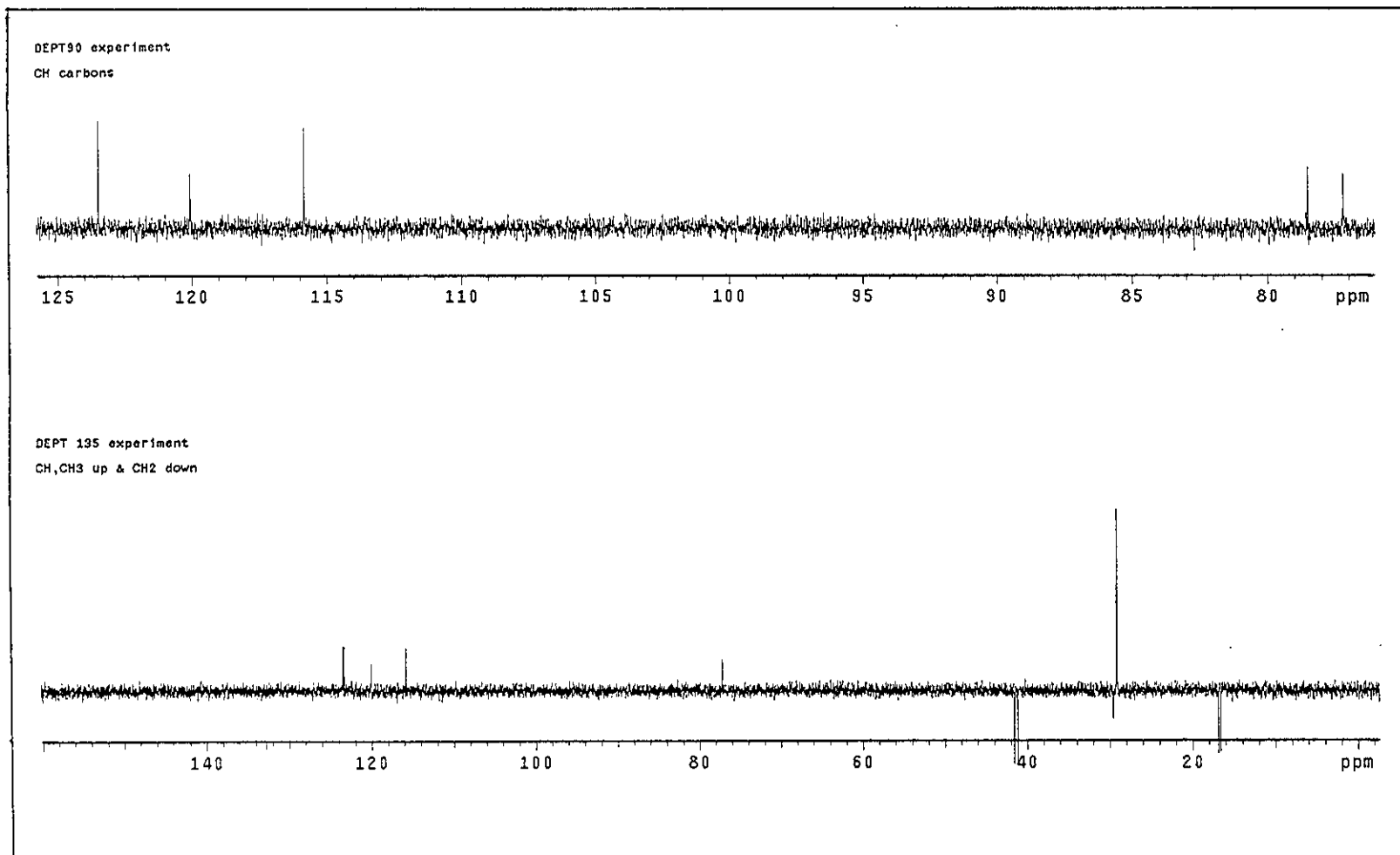


Figure 100 DEPT spectrum of YU16

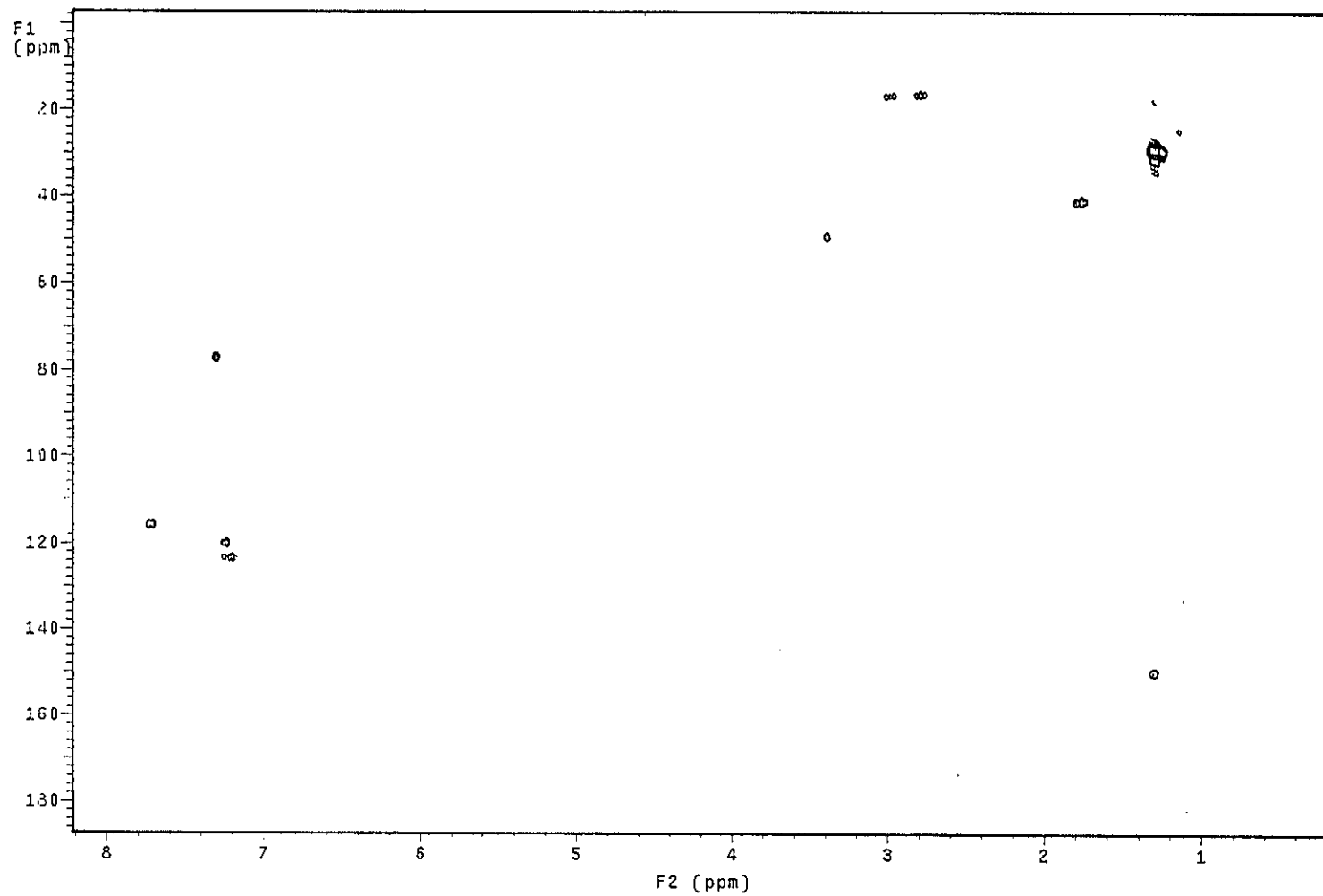


Figure 101 2D HMQC spectrum of YU16

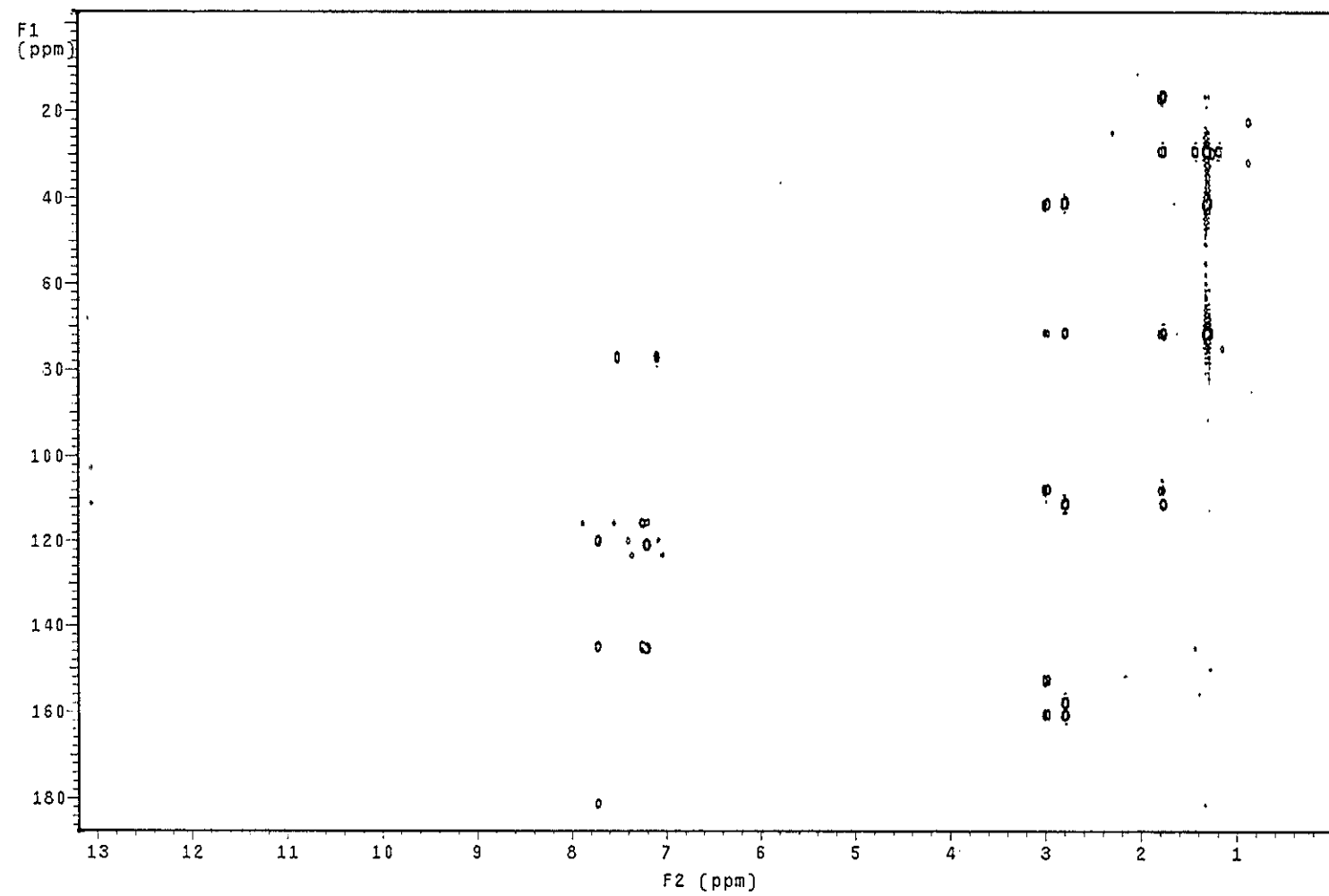


Figure 102 2D HMBC spectrum of YU16

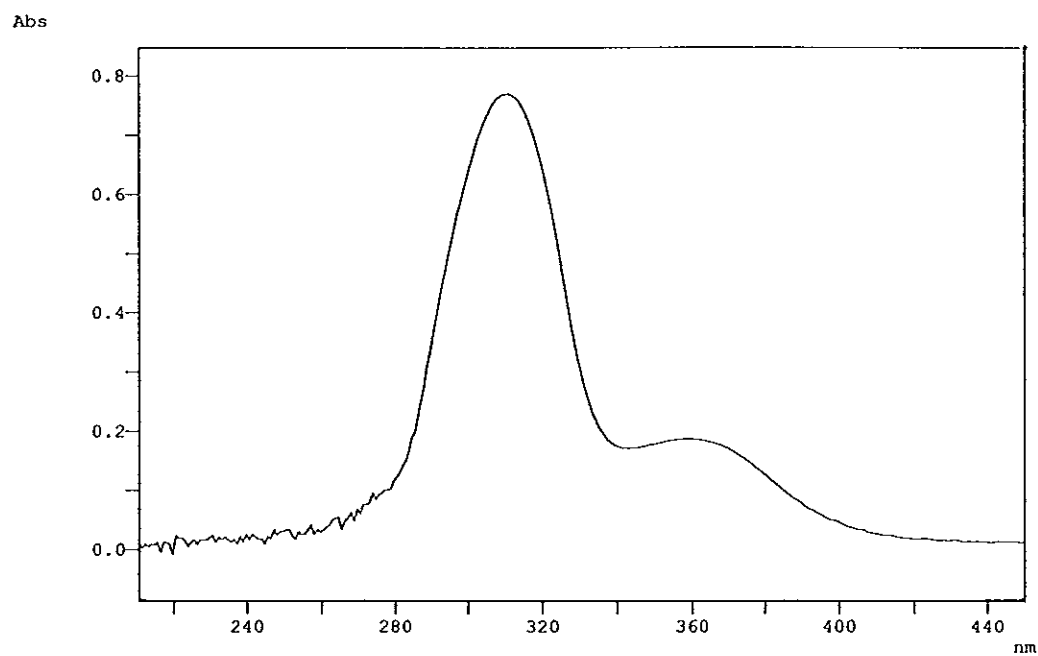


Figure 103 UV (MeOH) spectrum of YU7

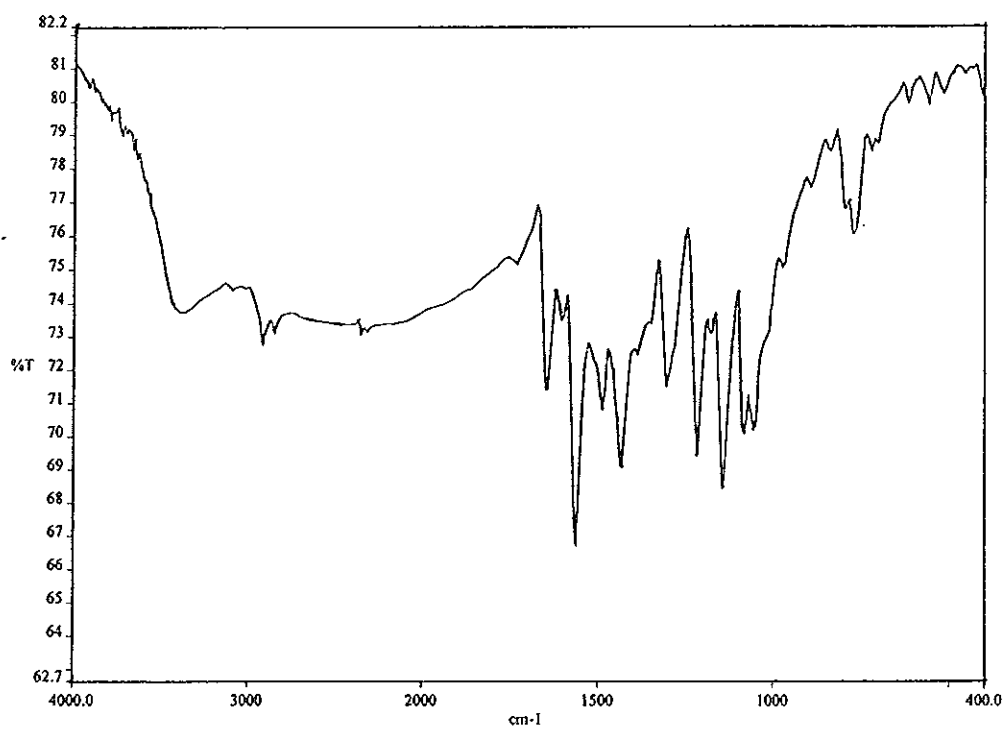


Figure 104 FT-IR (neat) spectrum of YU7

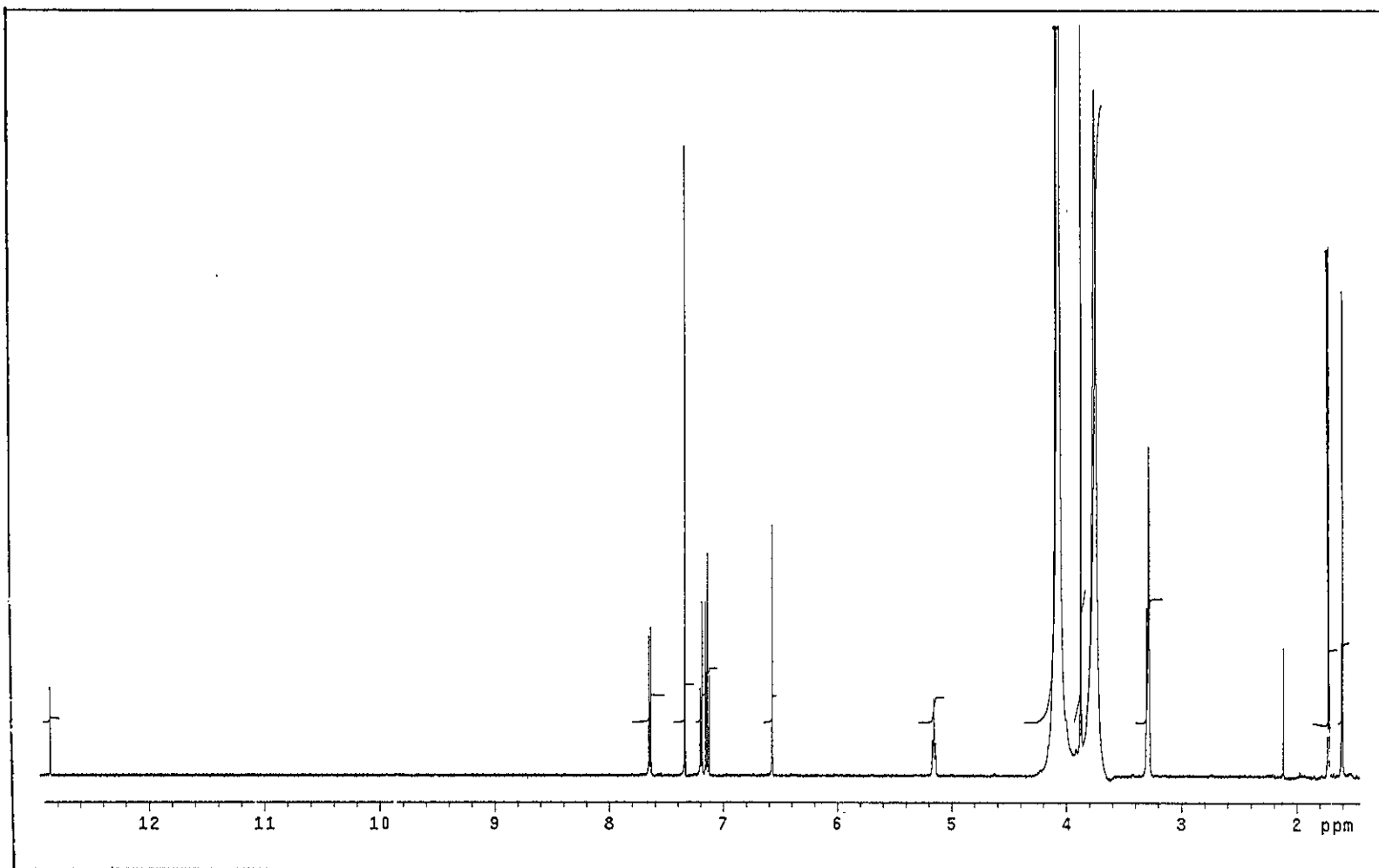


Figure 105 ^1H NMR (500 MHz) ($\text{CDCl}_3/\text{CD}_3\text{OD}$) spectrum of YU7

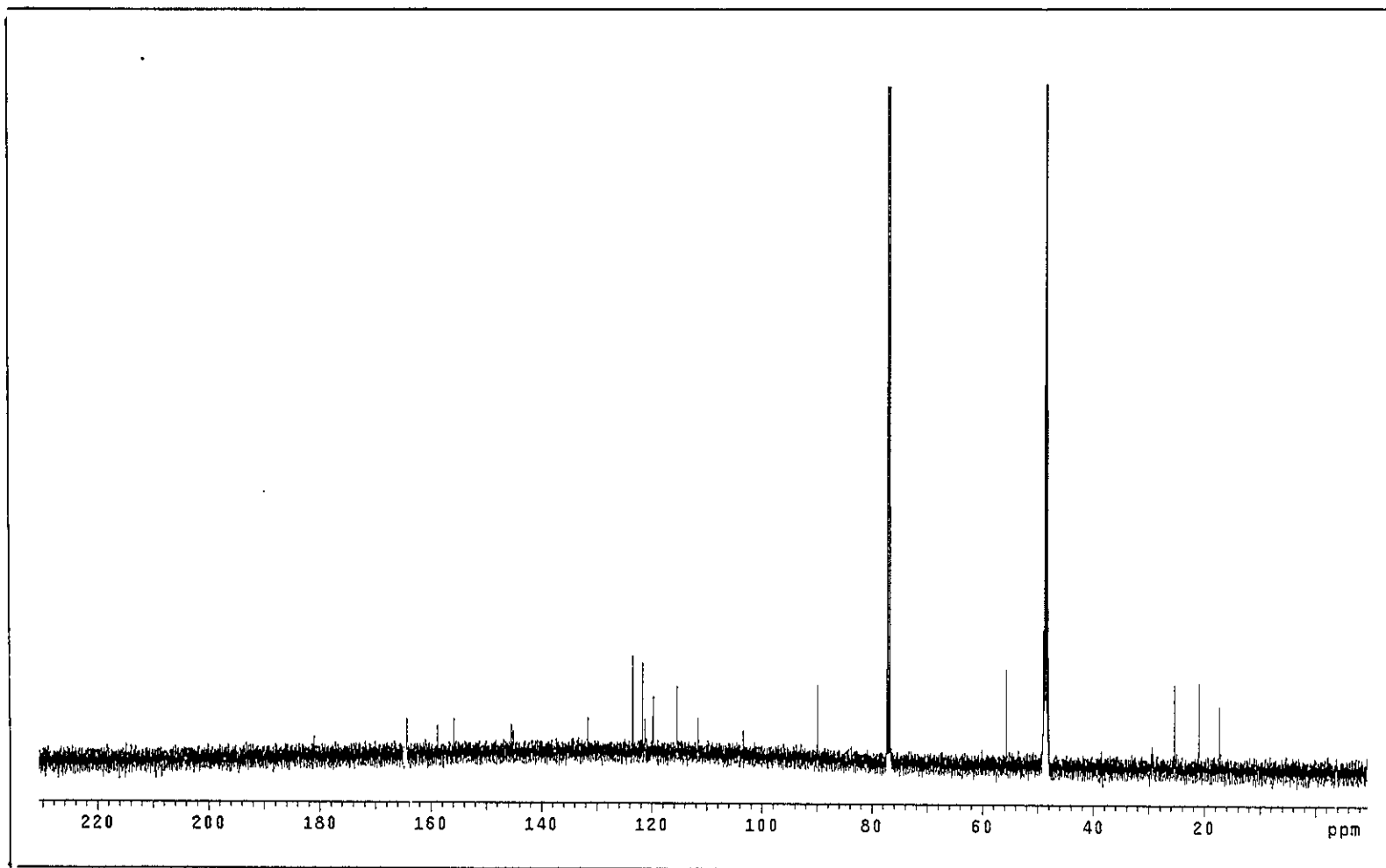


Figure 106 ^{13}C NMR (125 MHz) ($\text{CDCl}_3/\text{CD}_3\text{OD}$) spectrum of YU7

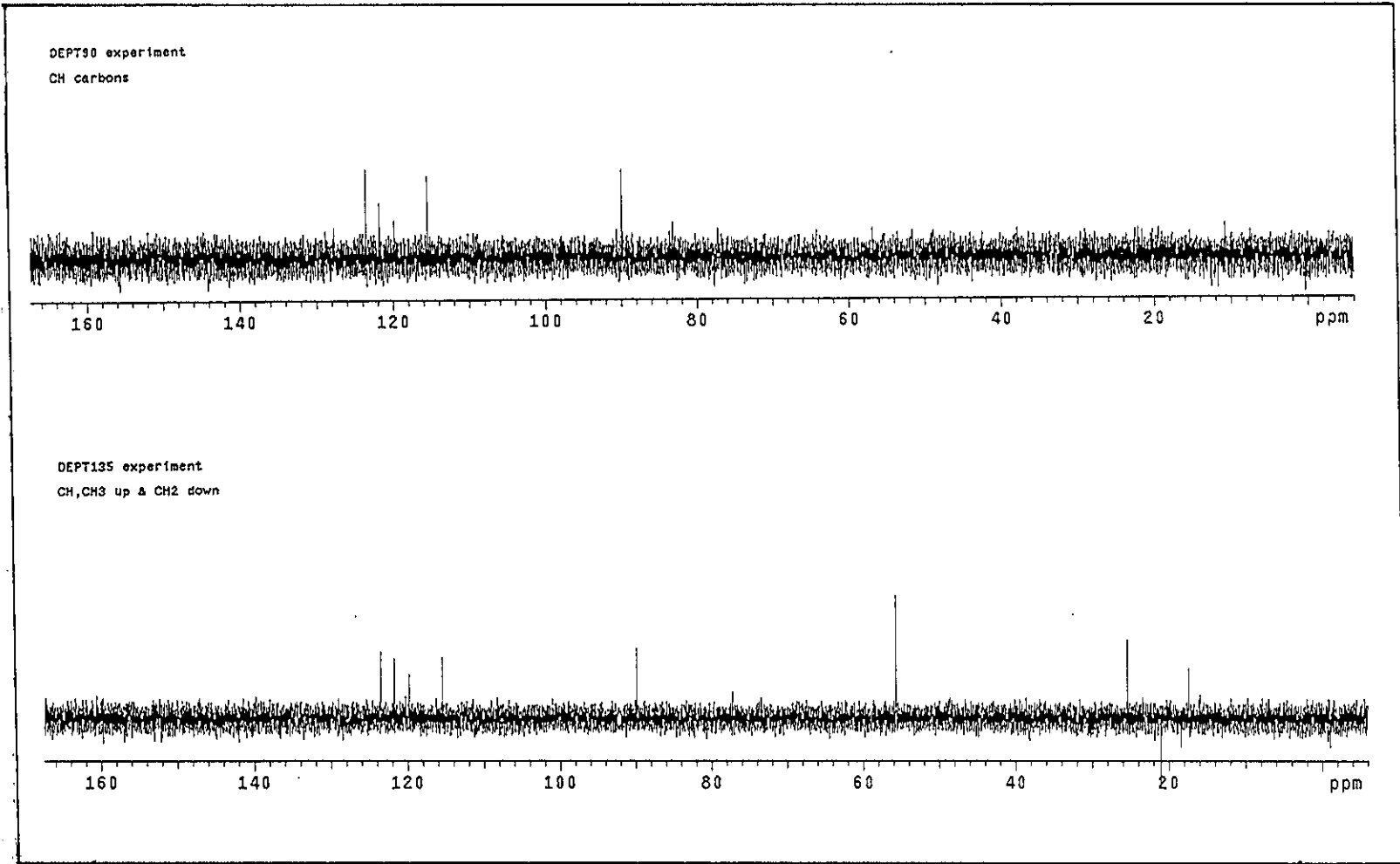


Figure 107 DEPT spectrum of YU7

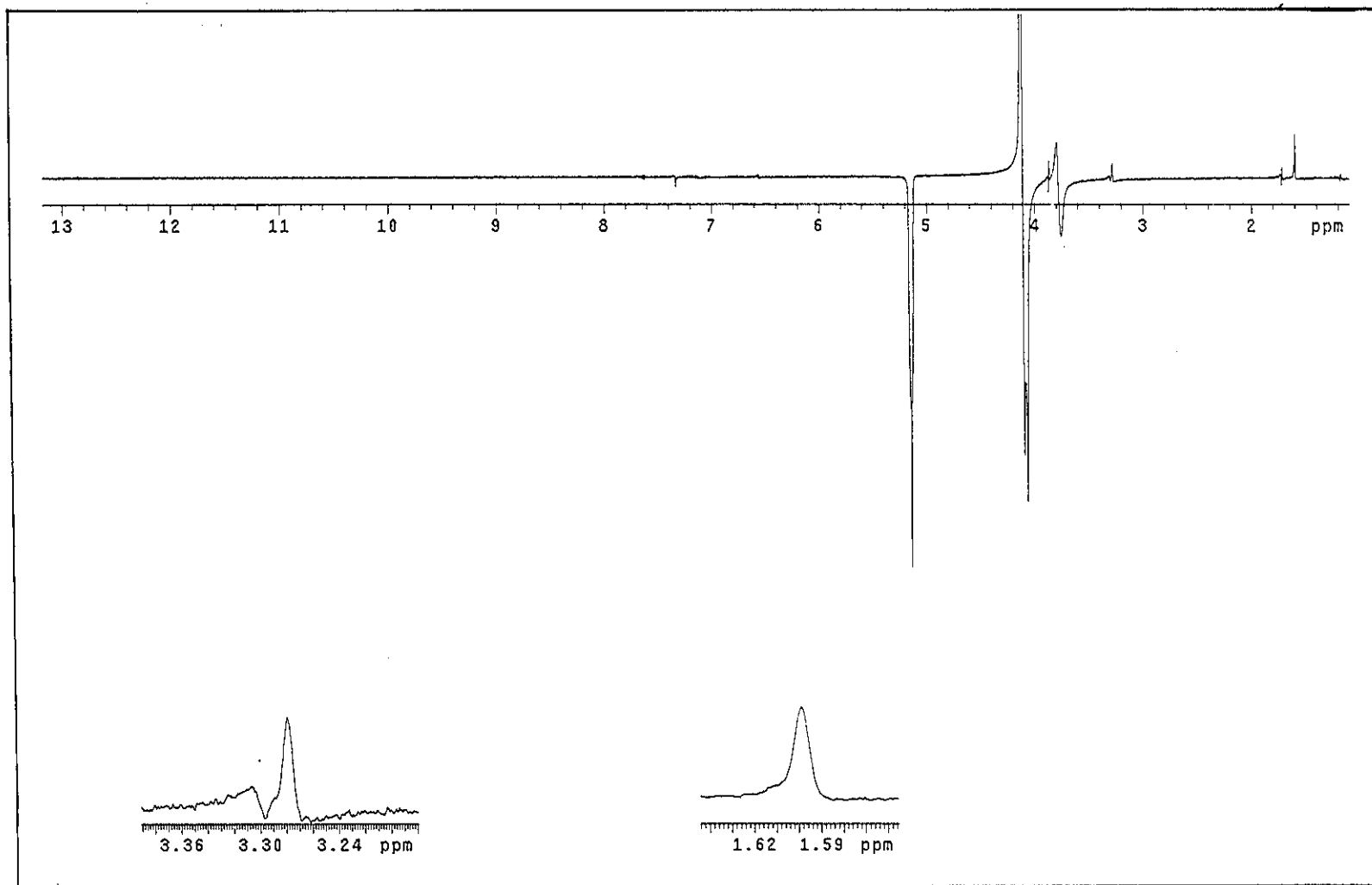


Figure 108 NOEDIFF spectrum of YU7 after irradiation at δ_H 5.15

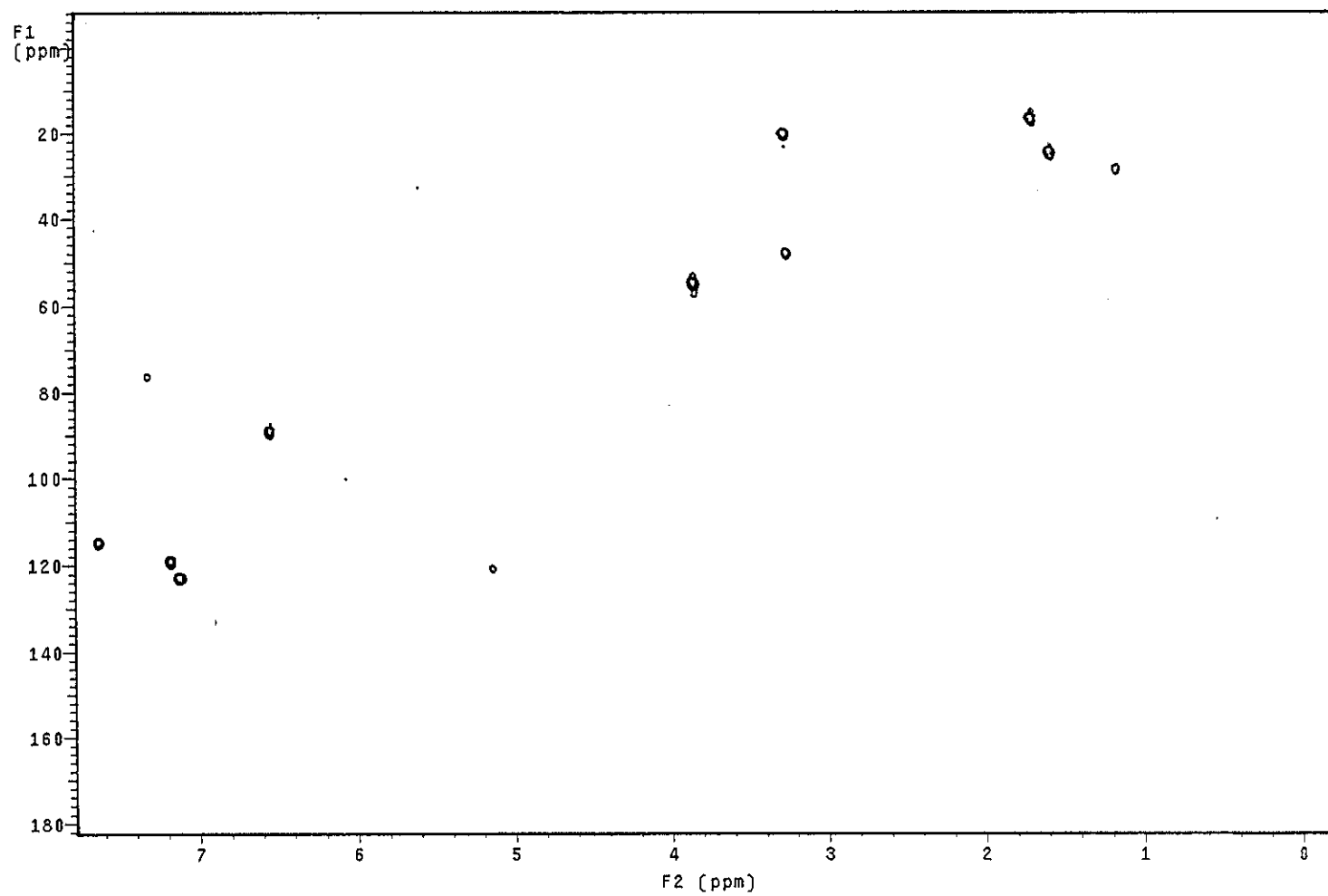


Figure 109 2D HMQC spectrum of YU7

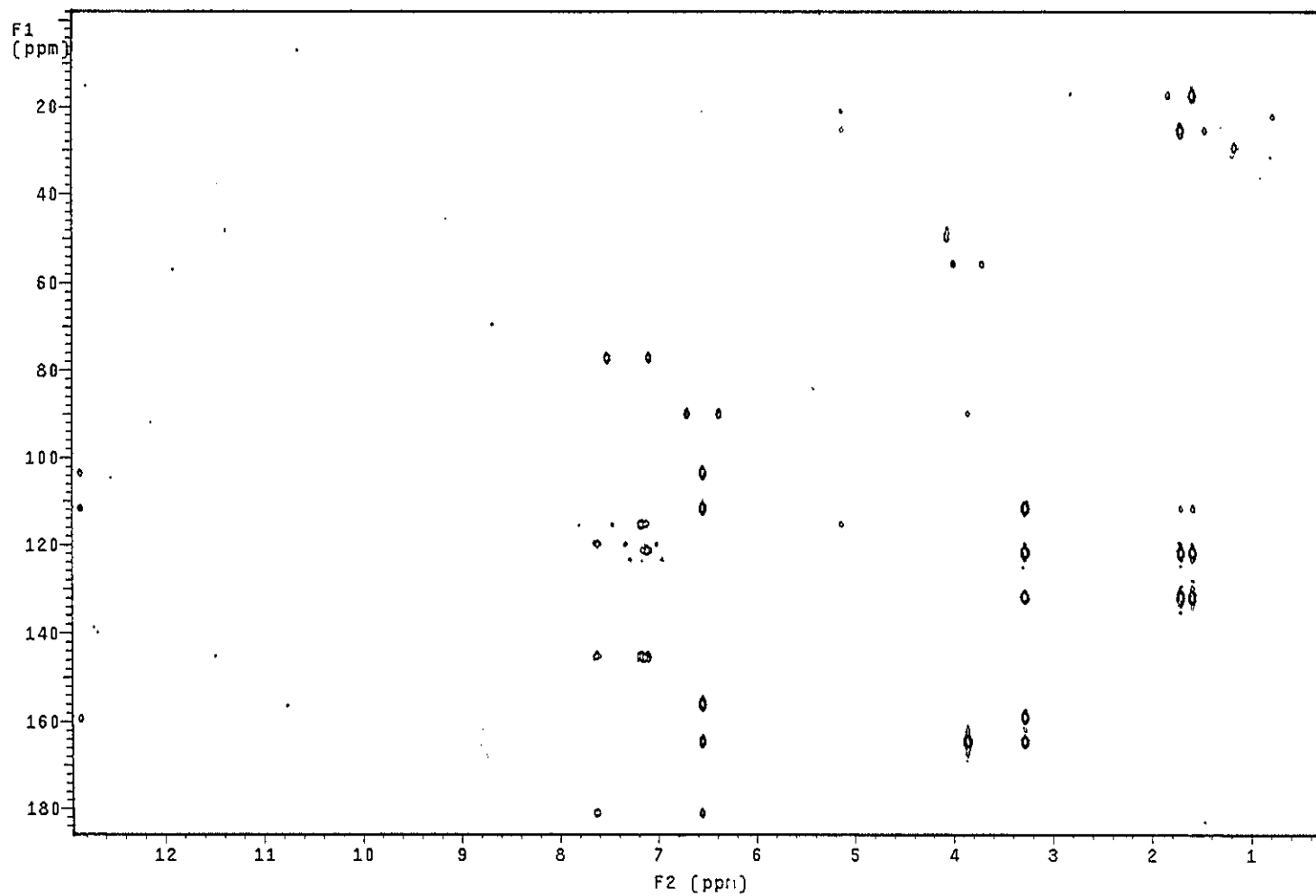


Figure 110 2D HMBC spectrum of YU7

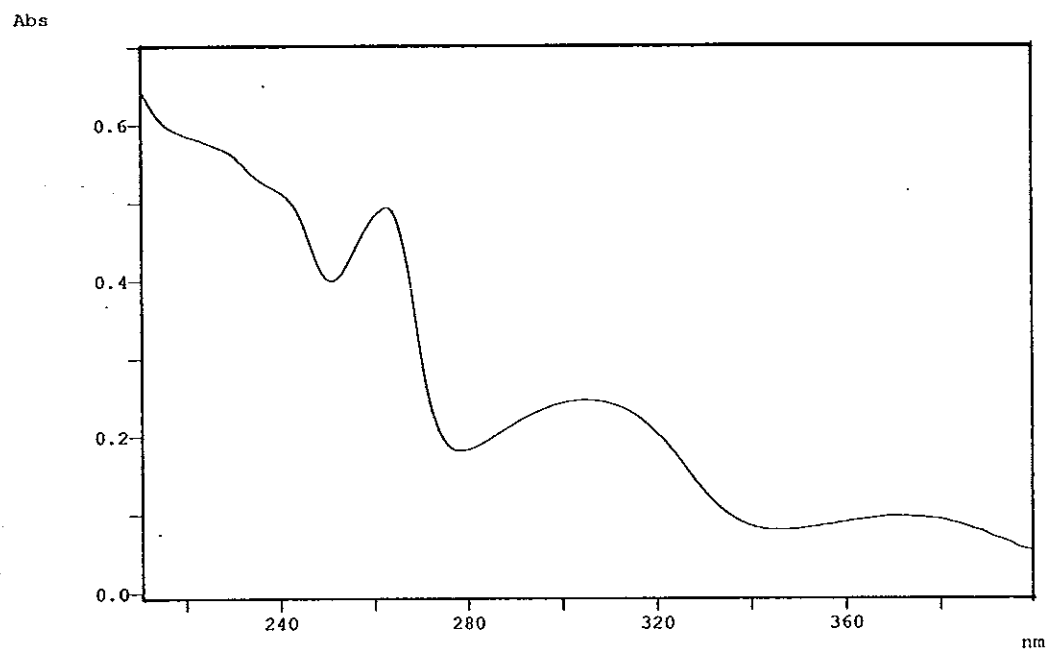


Figure 111 UV (MeOH) spectrum of YU12

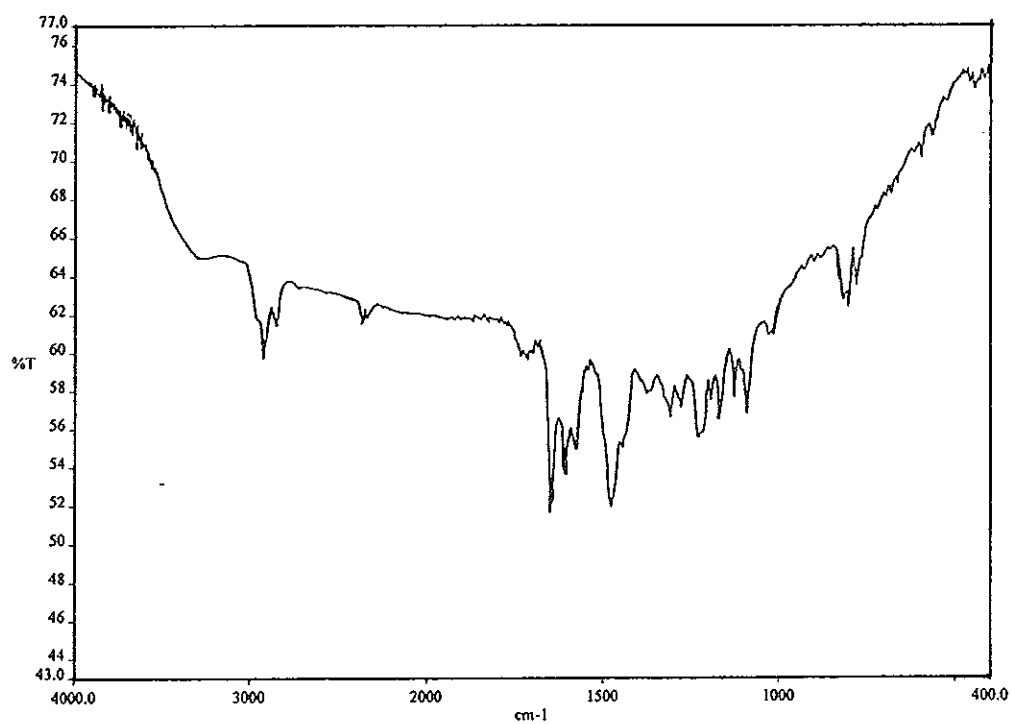


Figure 112 FT-IR (neat) spectrum of YU12

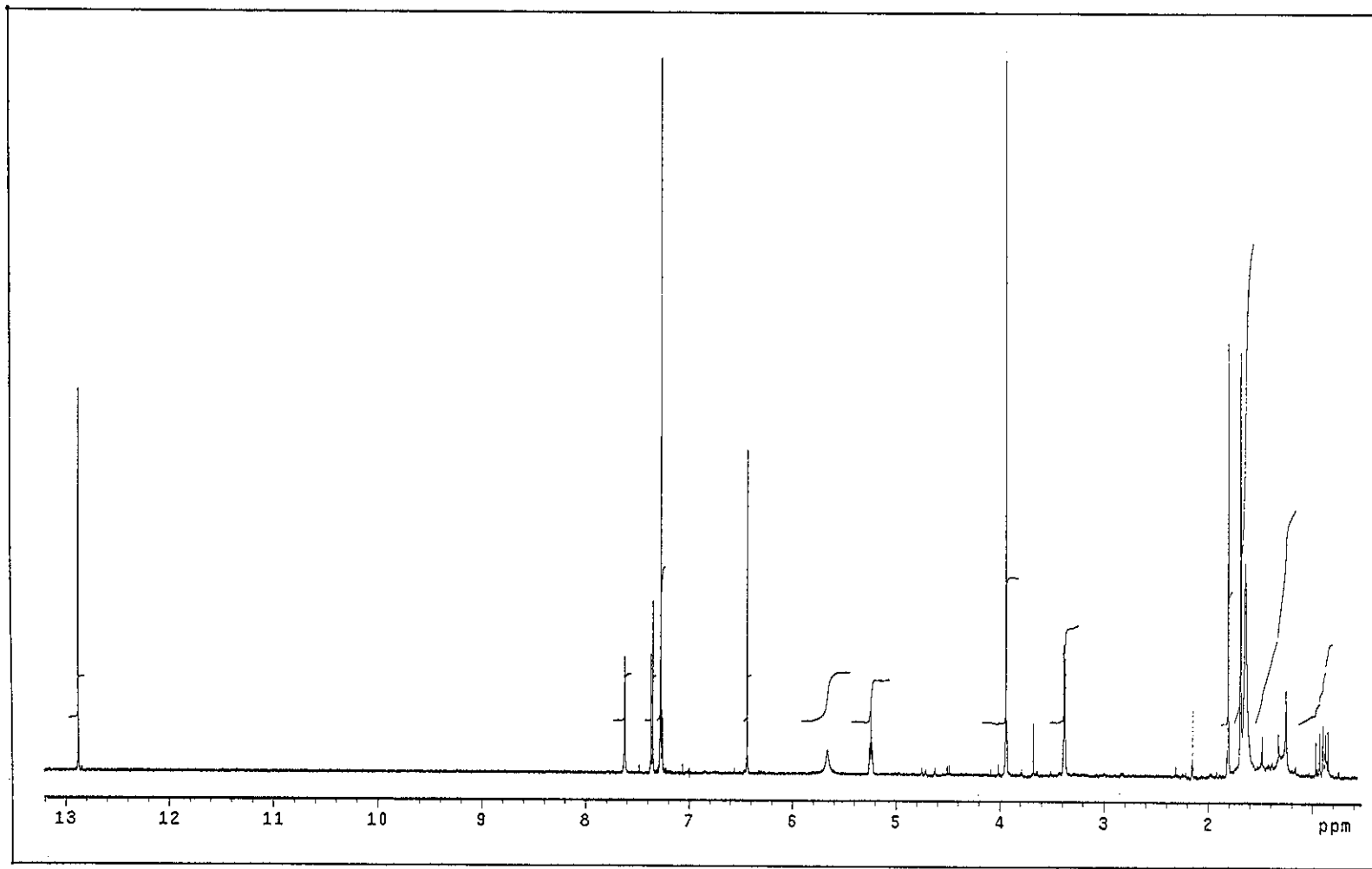


Figure 113 ^1H NMR (500 MHz) (CDCl_3) spectrum of YU12

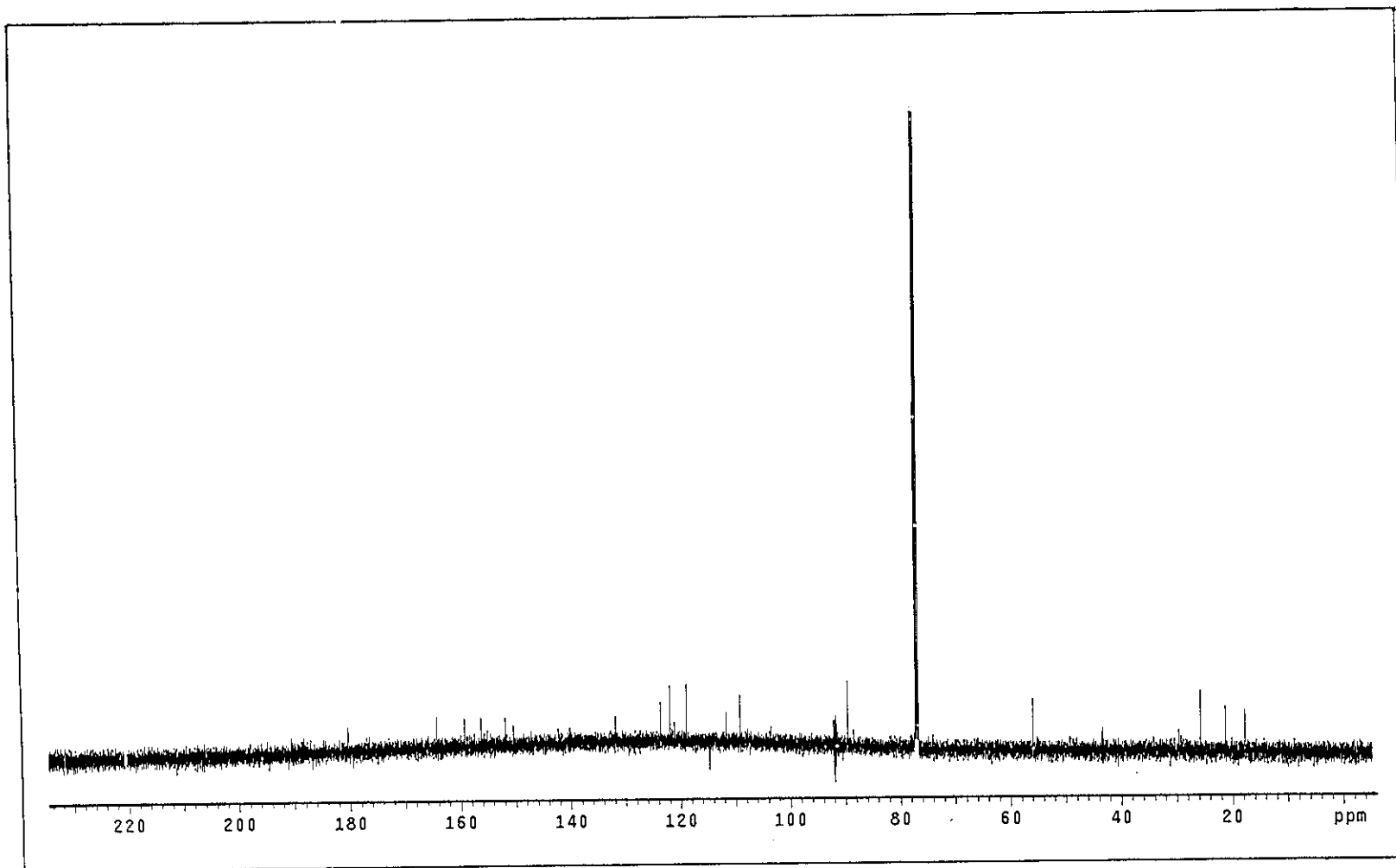


Figure 114 ^{13}C NMR (125 MHz) (CDCl_3) spectrum of YU12

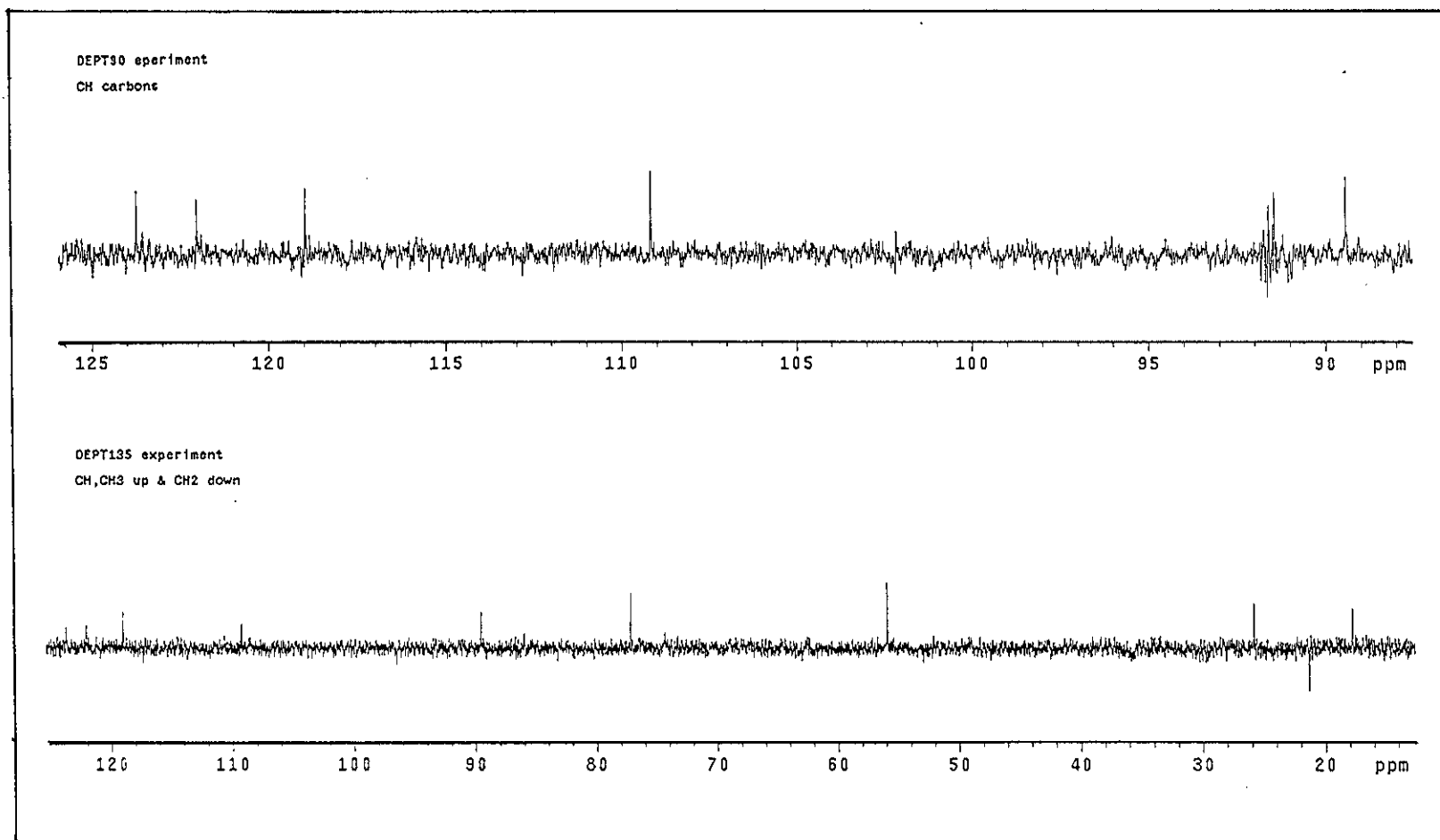


Figure 115 DEPT spectrum of YU12

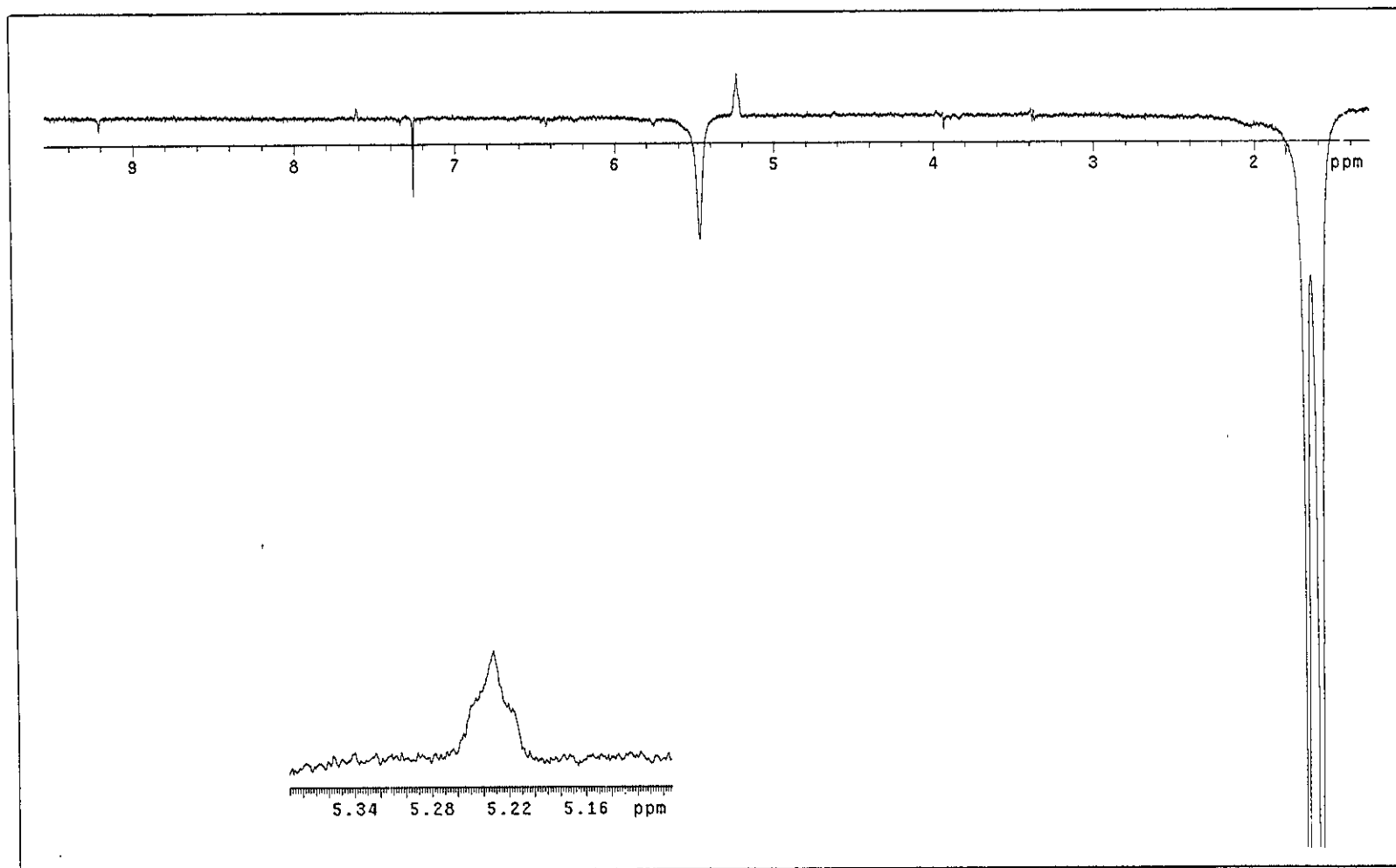


Figure 116 NOEDIFF spectrum of YU12 after irradiation at δ_{H} 1.69

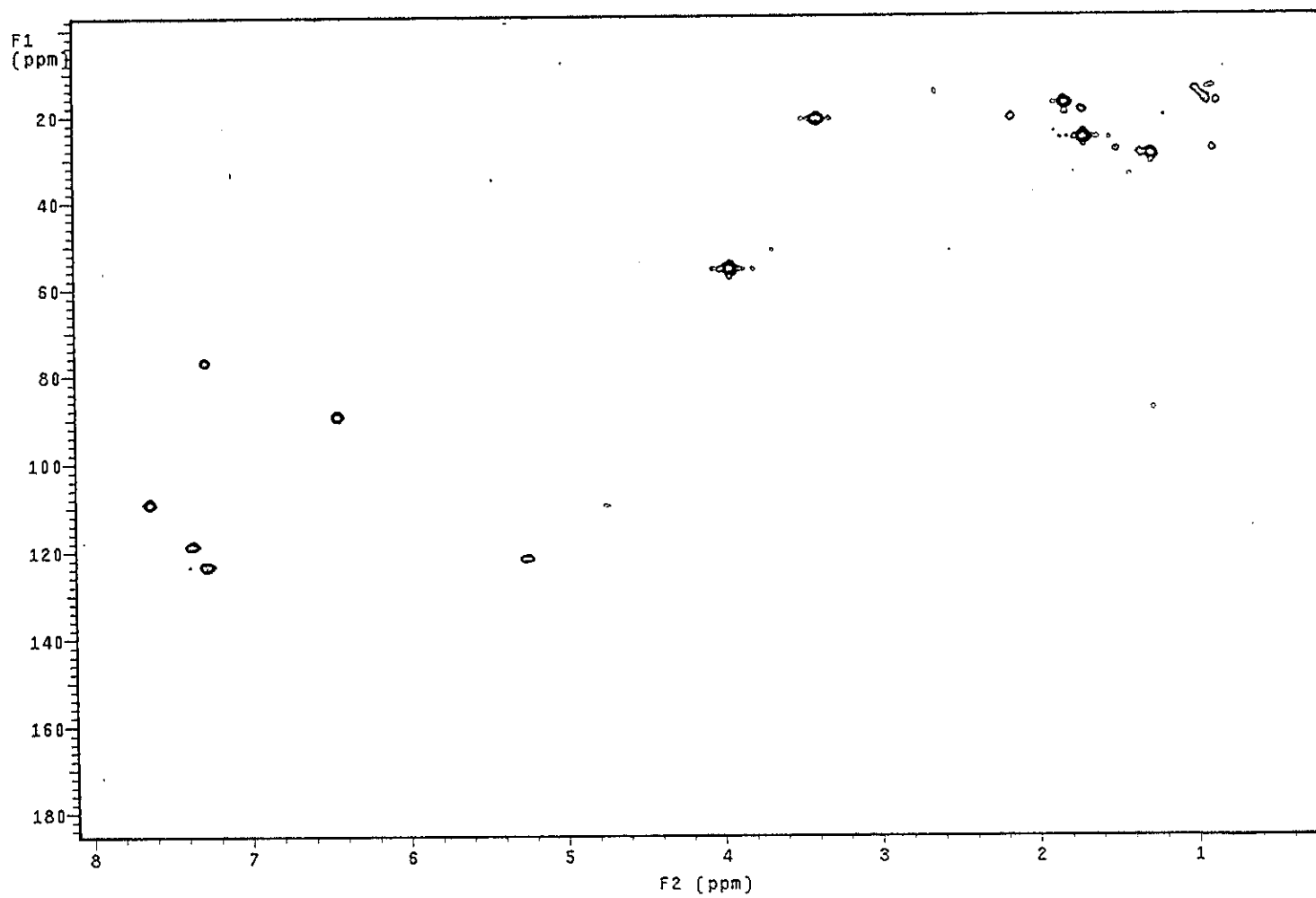


Figure 117 2D HMQC spectrum of YU12

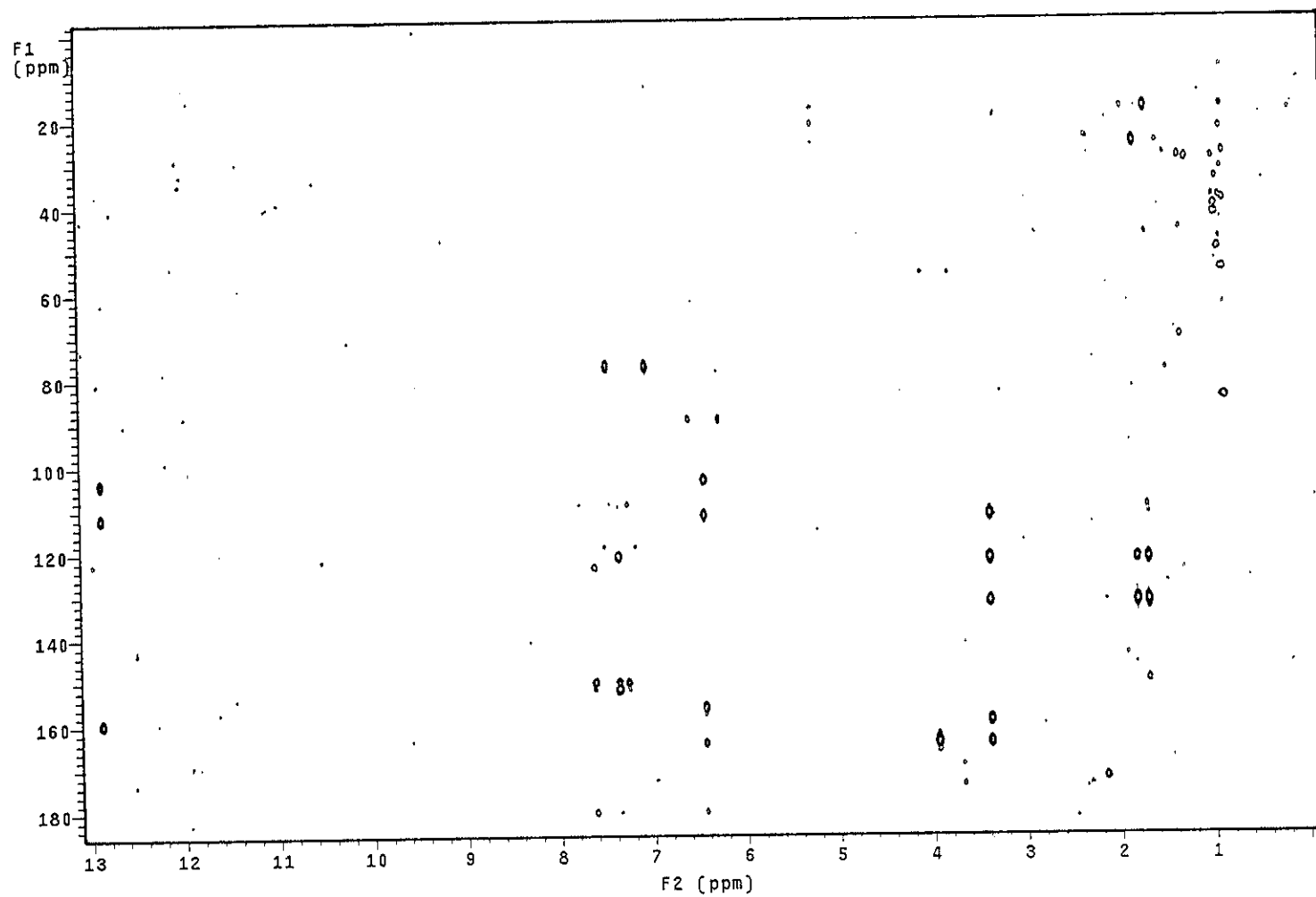


Figure 118 2D HMBC spectrum of YU12

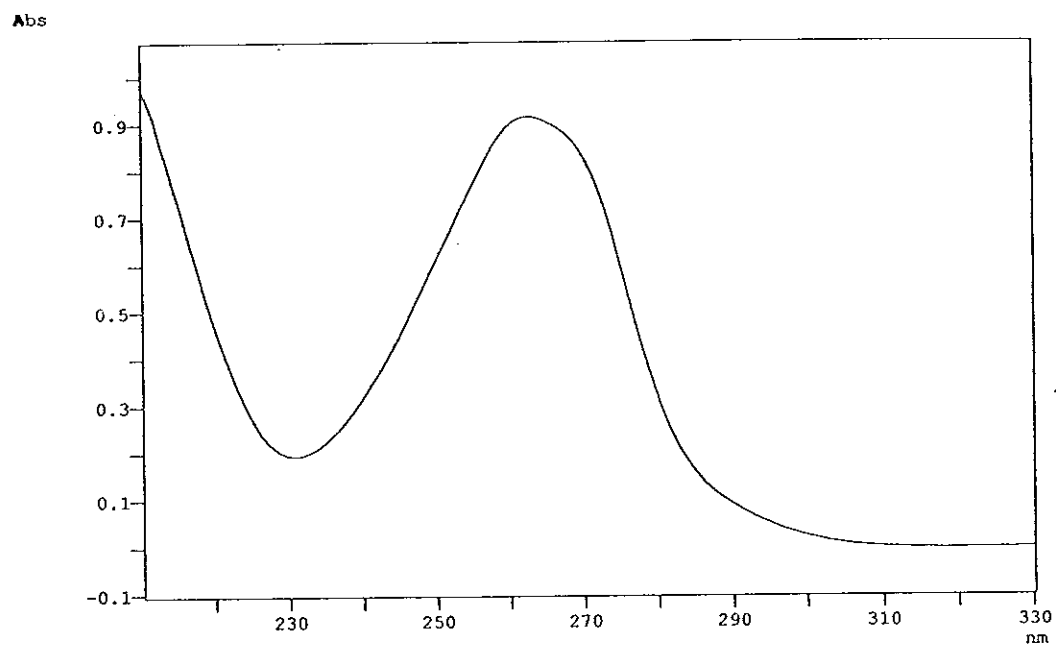


Figure 119 UV (MeOH) spectrum of YU5

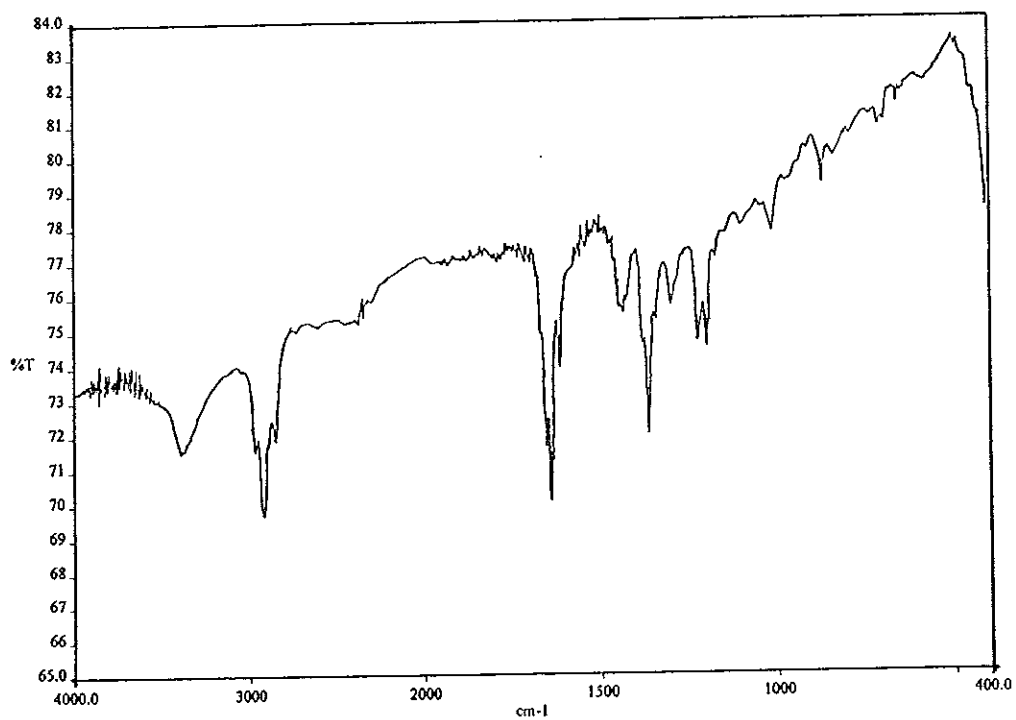


Figure 120 FT-IR (neat) spectrum of YU5

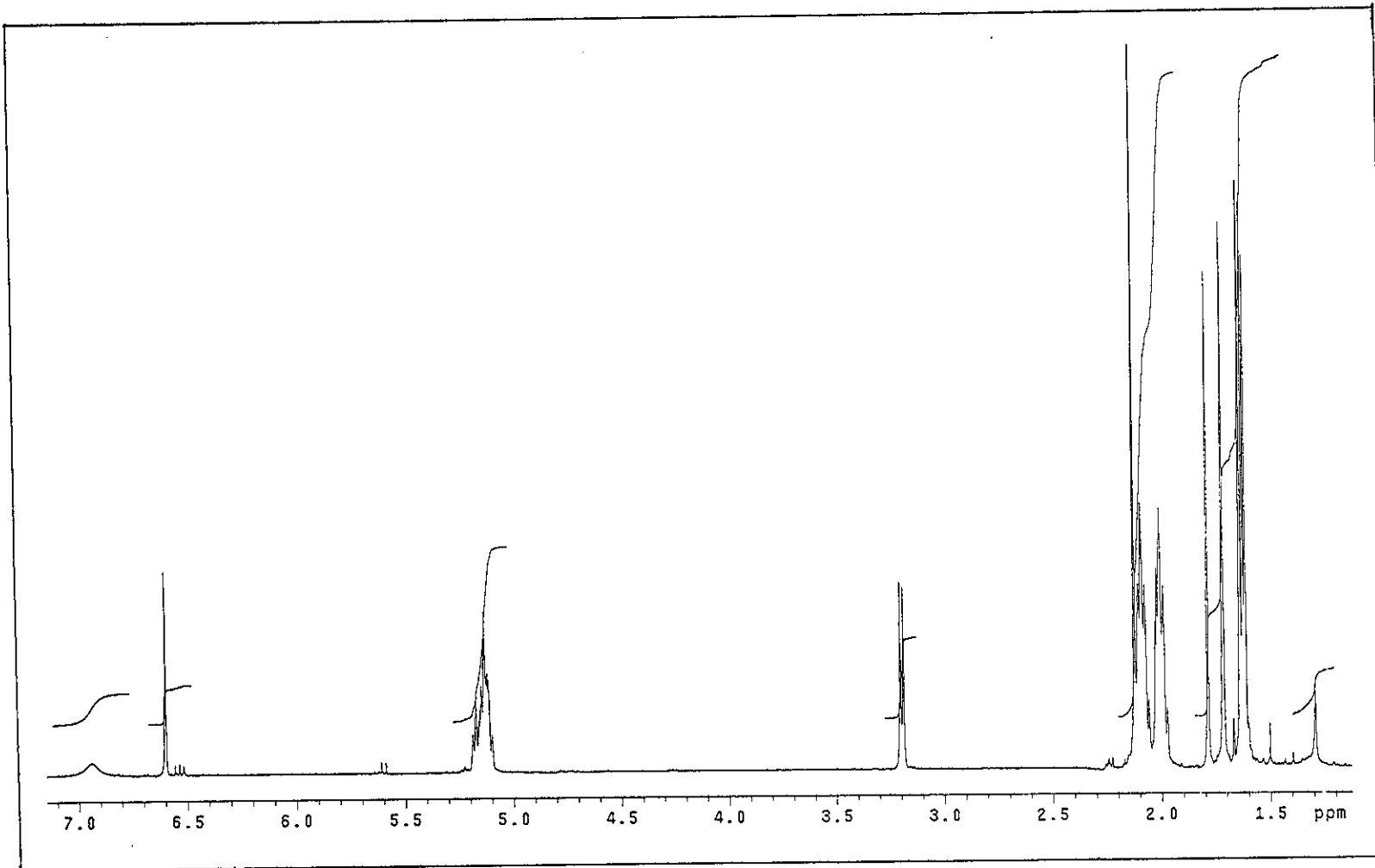


Figure 121 ¹H NMR (500 MHz) (CDCl₃) spectrum of YU5

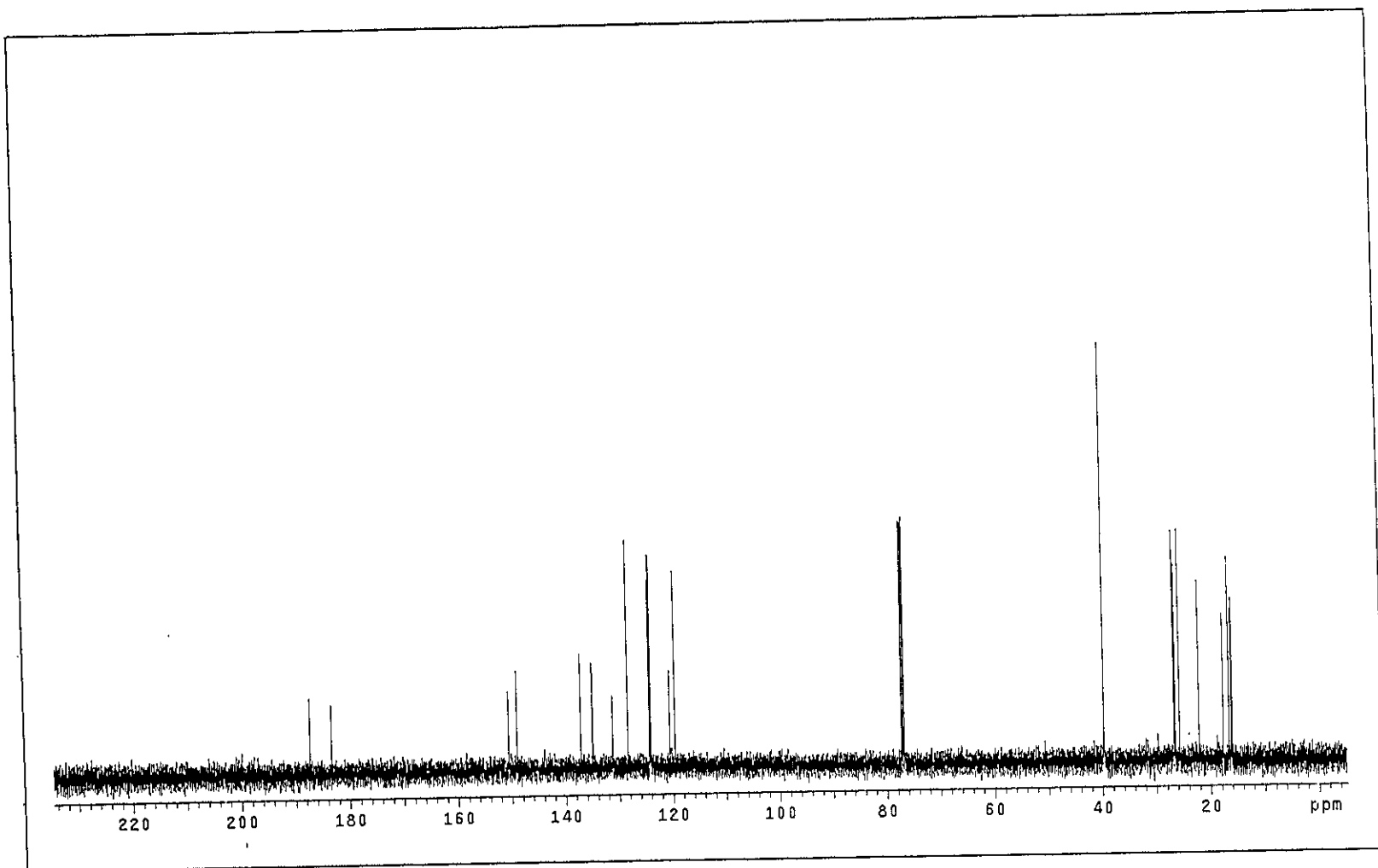


Figure 122 ^{13}C NMR (125 MHz) (CDCl_3) spectrum of YU5

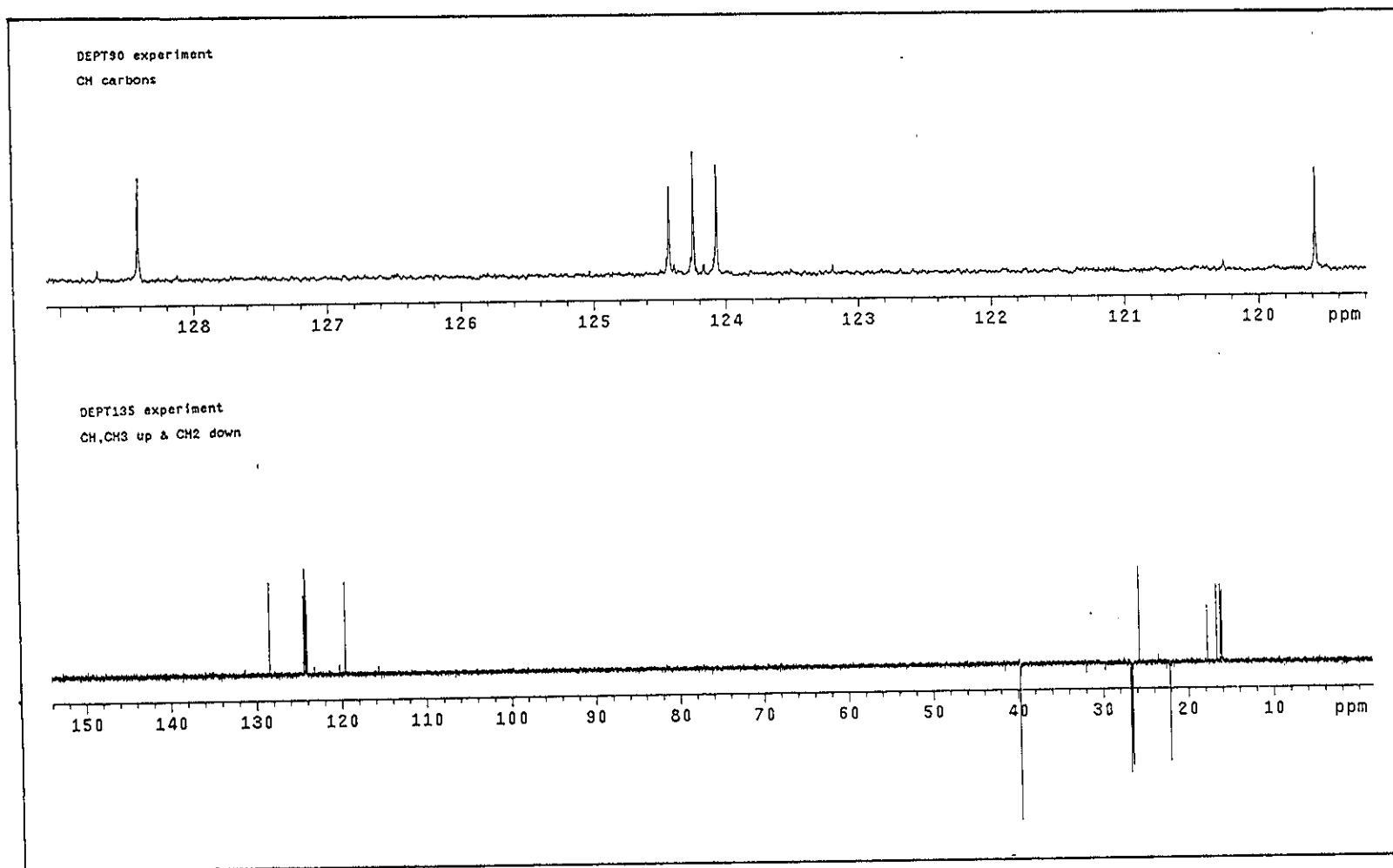


Figure 123 DEPT spectrum of YU5

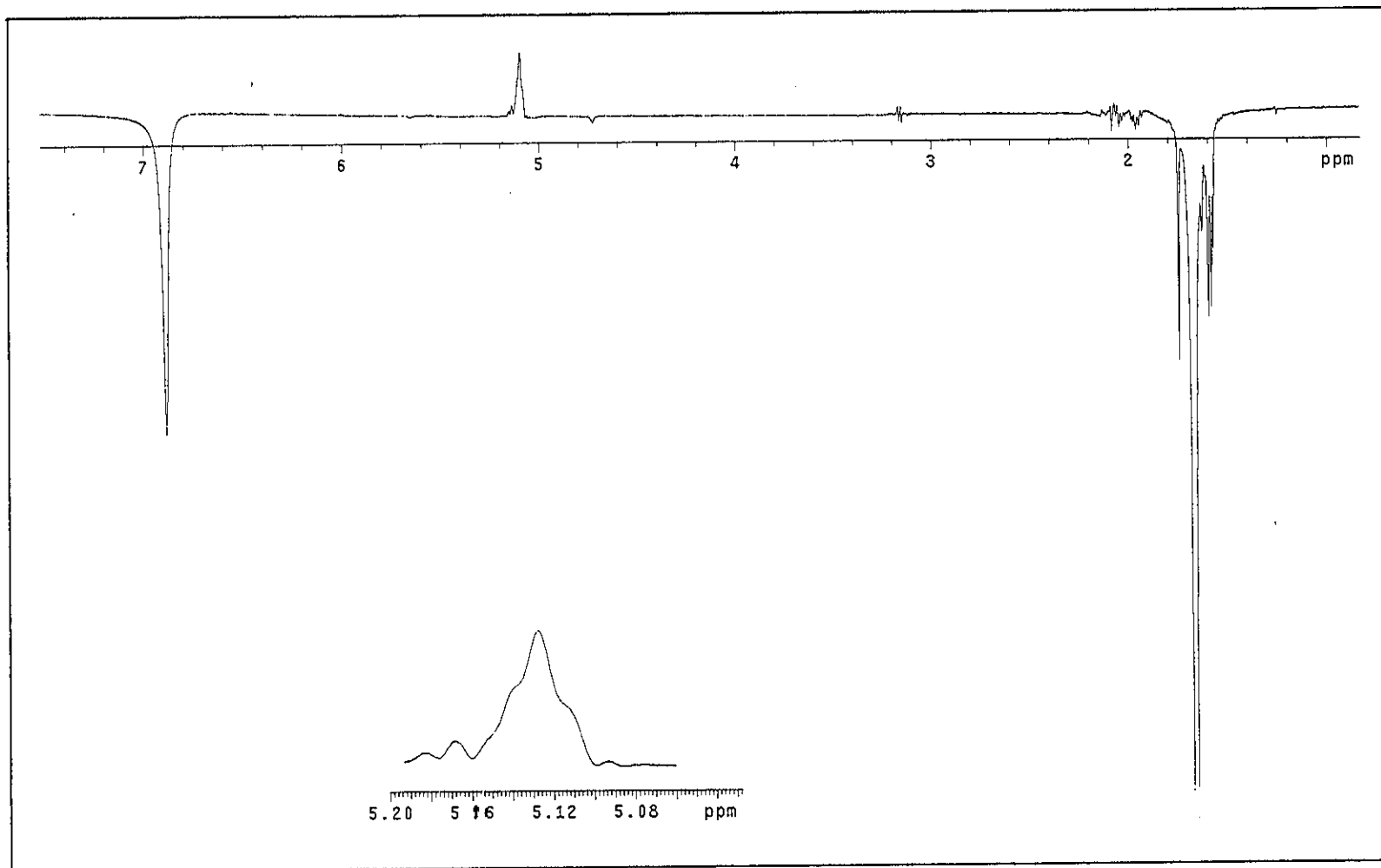


Figure 124 NOEDIFF spectrum of YU5 after irradiation at δ_H 1.71

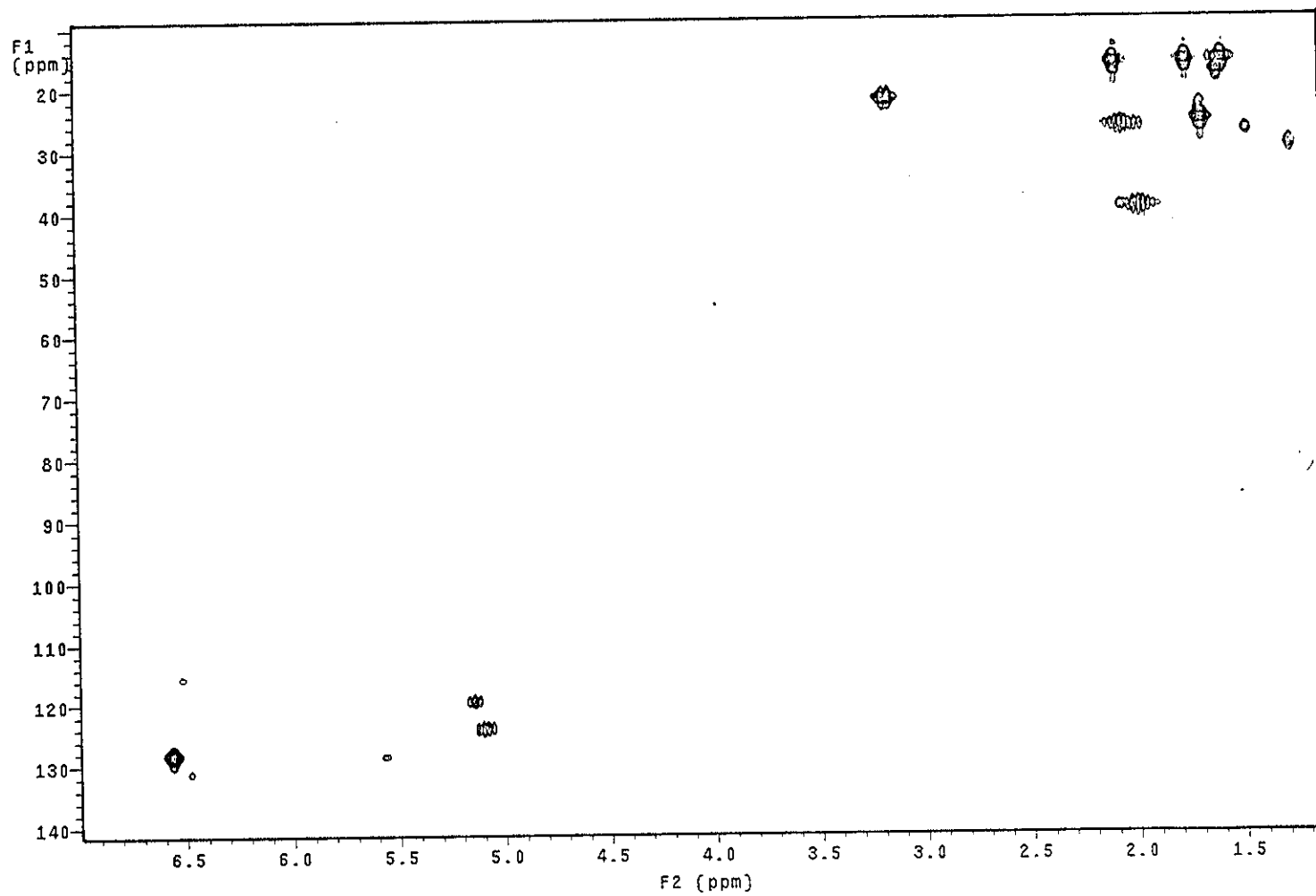


Figure 125 2D HMQC spectrum of YU5

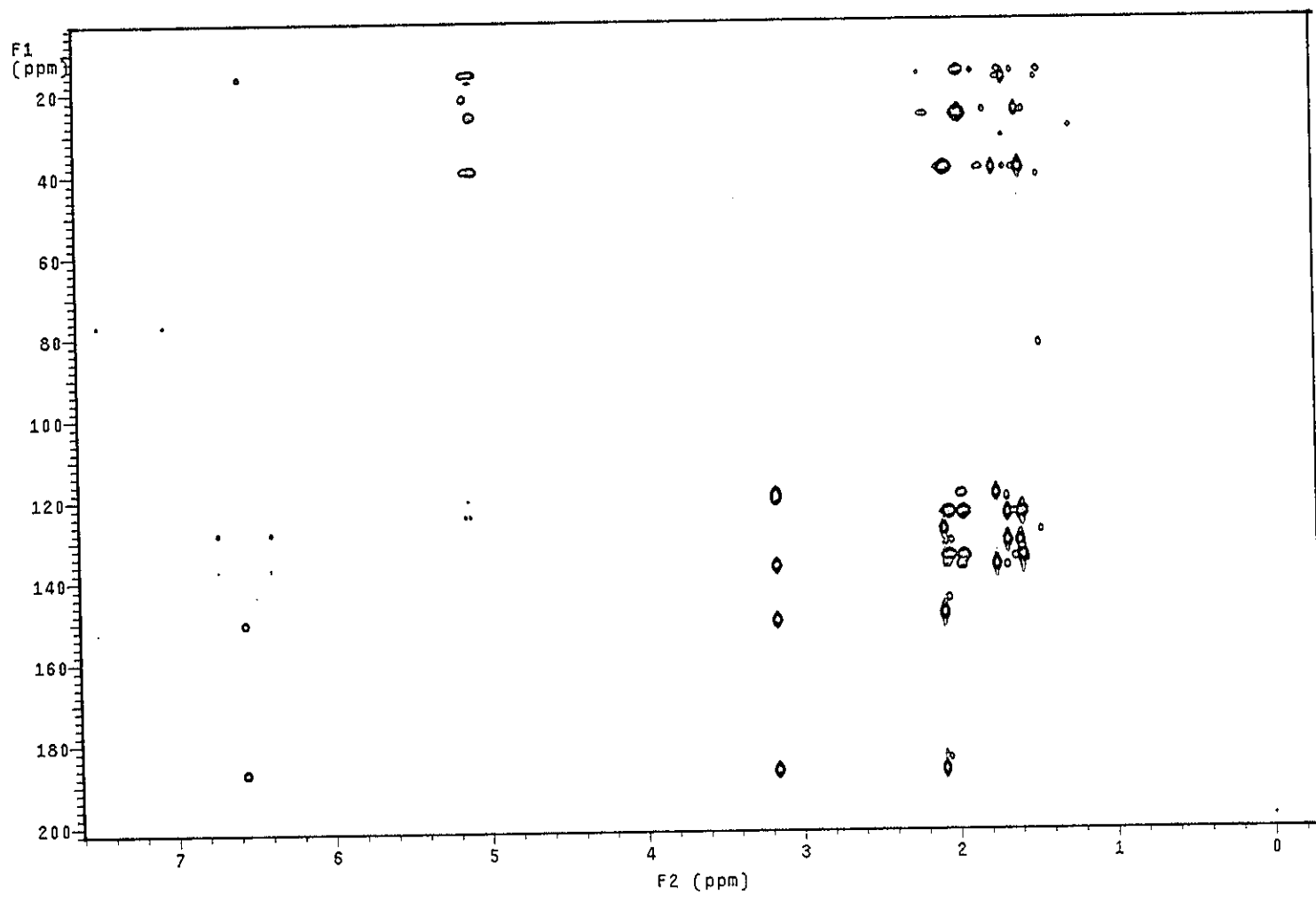


Figure 126 2D HMBC spectrum of YU5

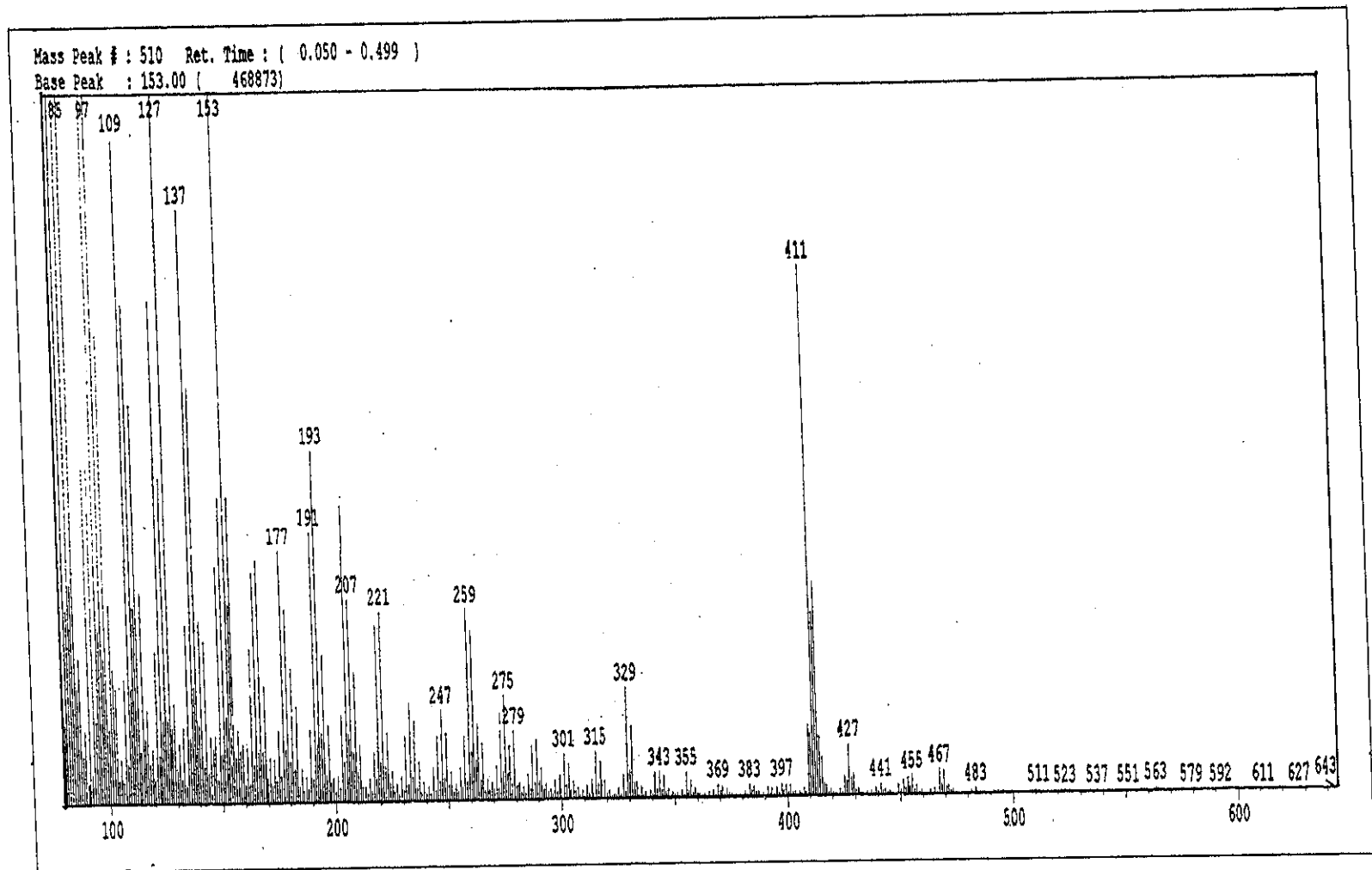


Figure 127 Mass spectrum of YU5

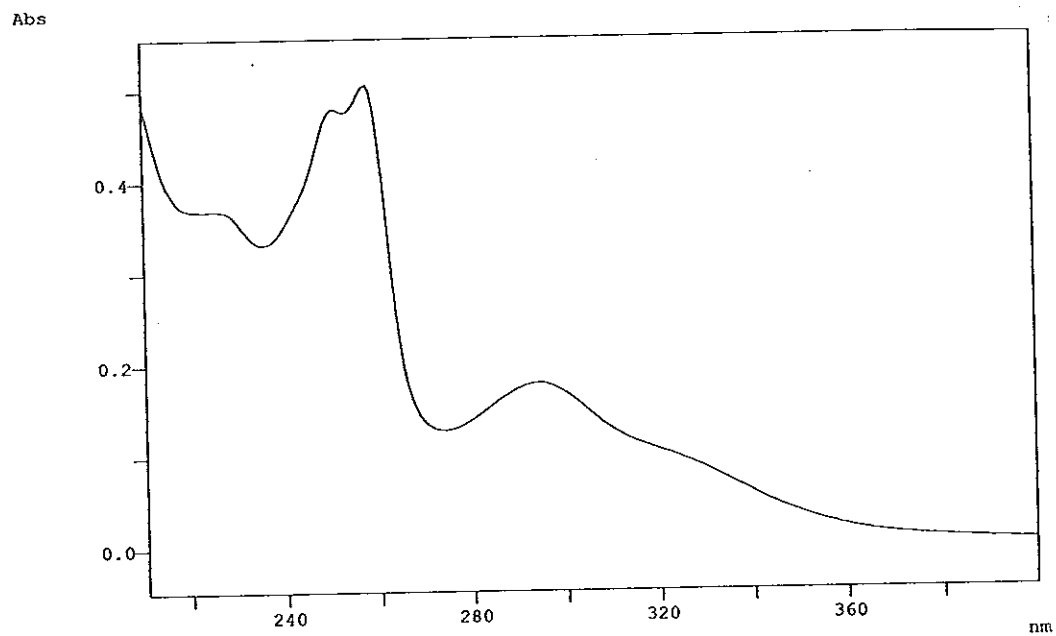


Figure 128 UV (MeOH) spectrum of YU13

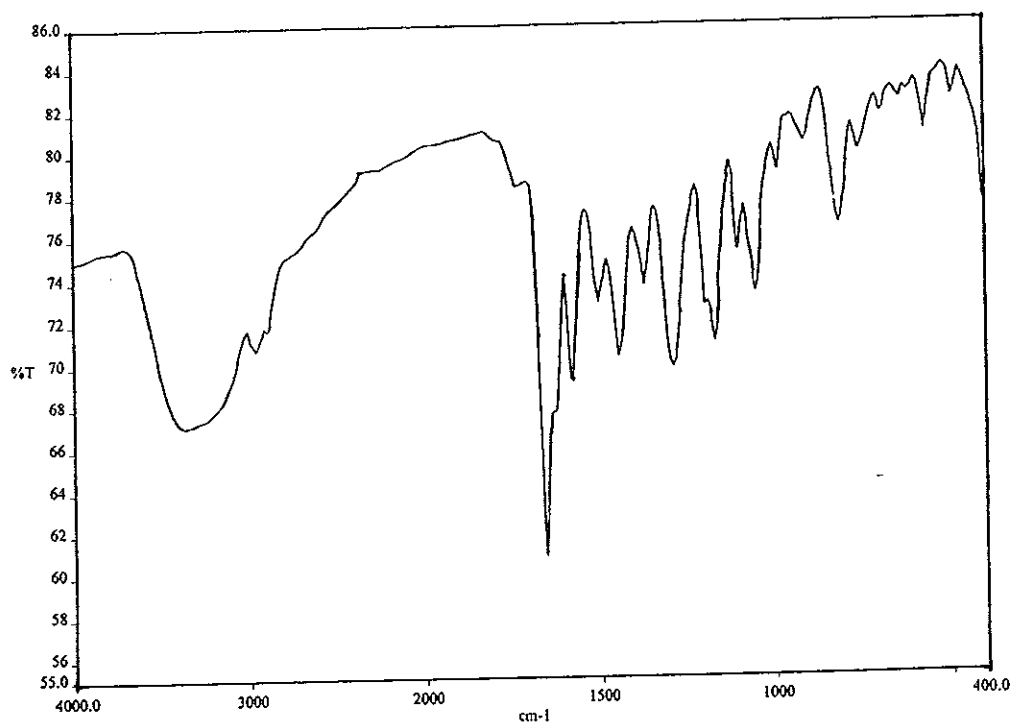


Figure 129 FT-IR (neat) spectrum of YU13

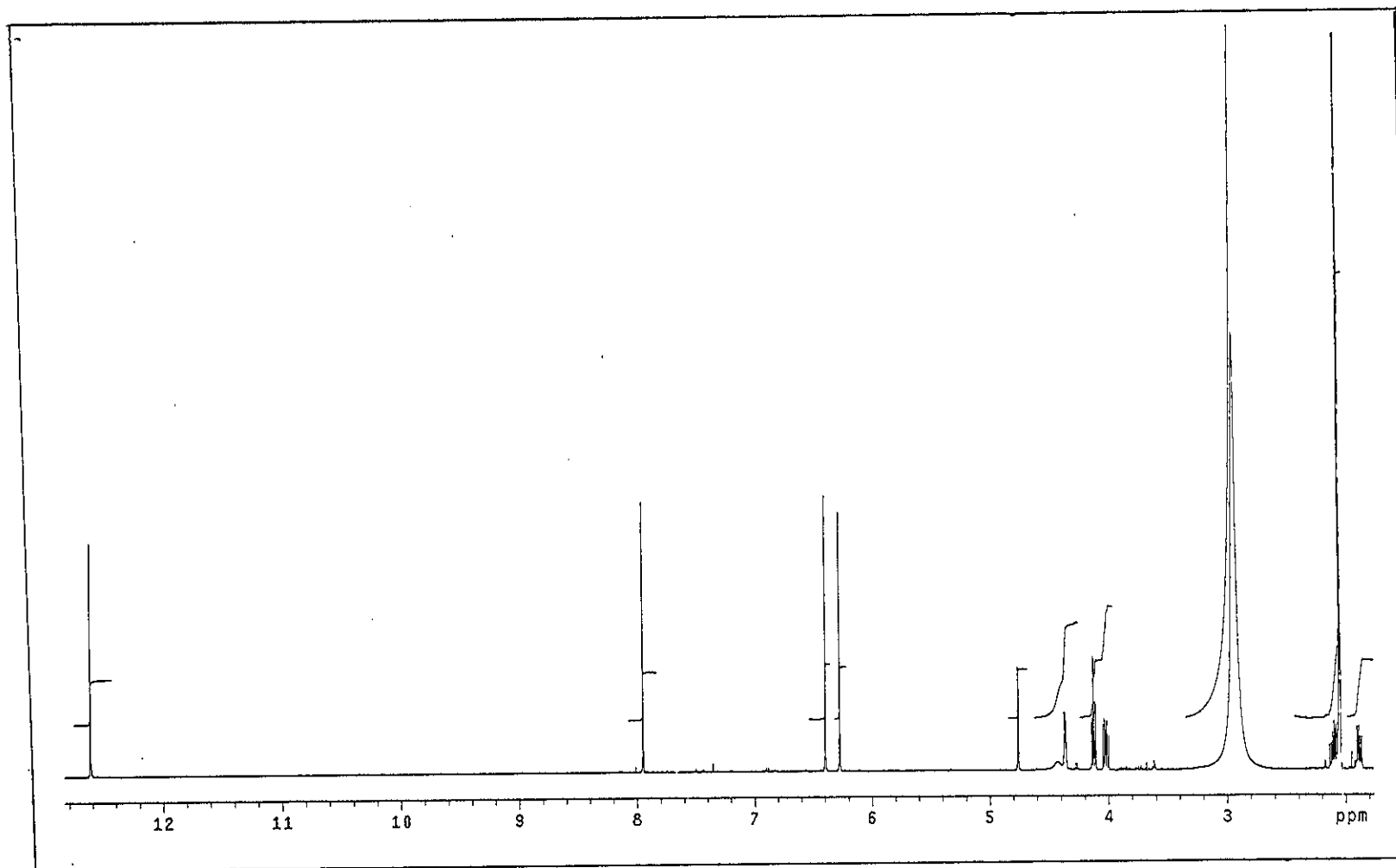


Figure 130 ^1H NMR (500 MHz) (Acetone- d_6) spectrum of YU13

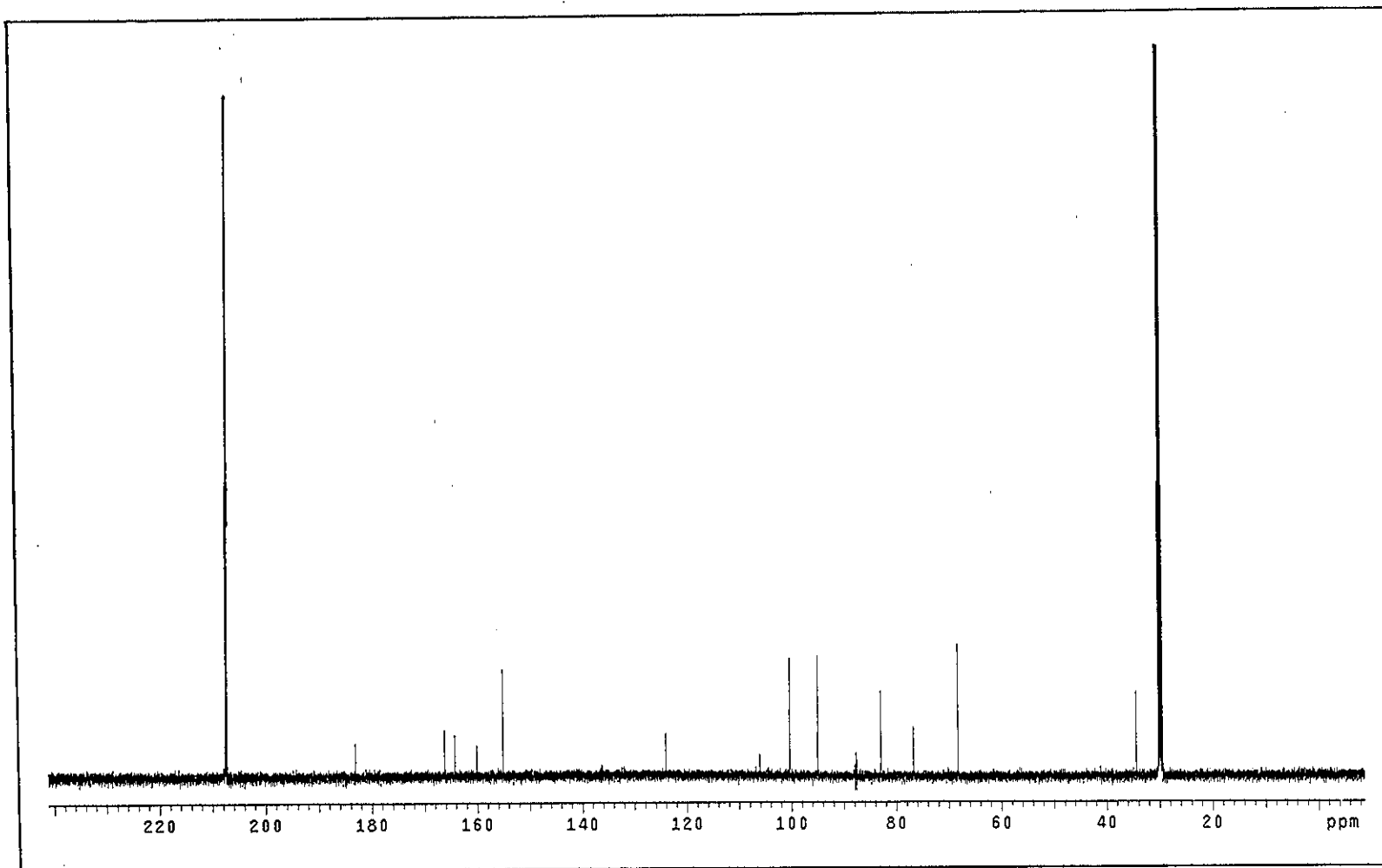


Figure 131 ^{13}C NMR (125 MHz) (Acetone- d_6) spectrum of YU13

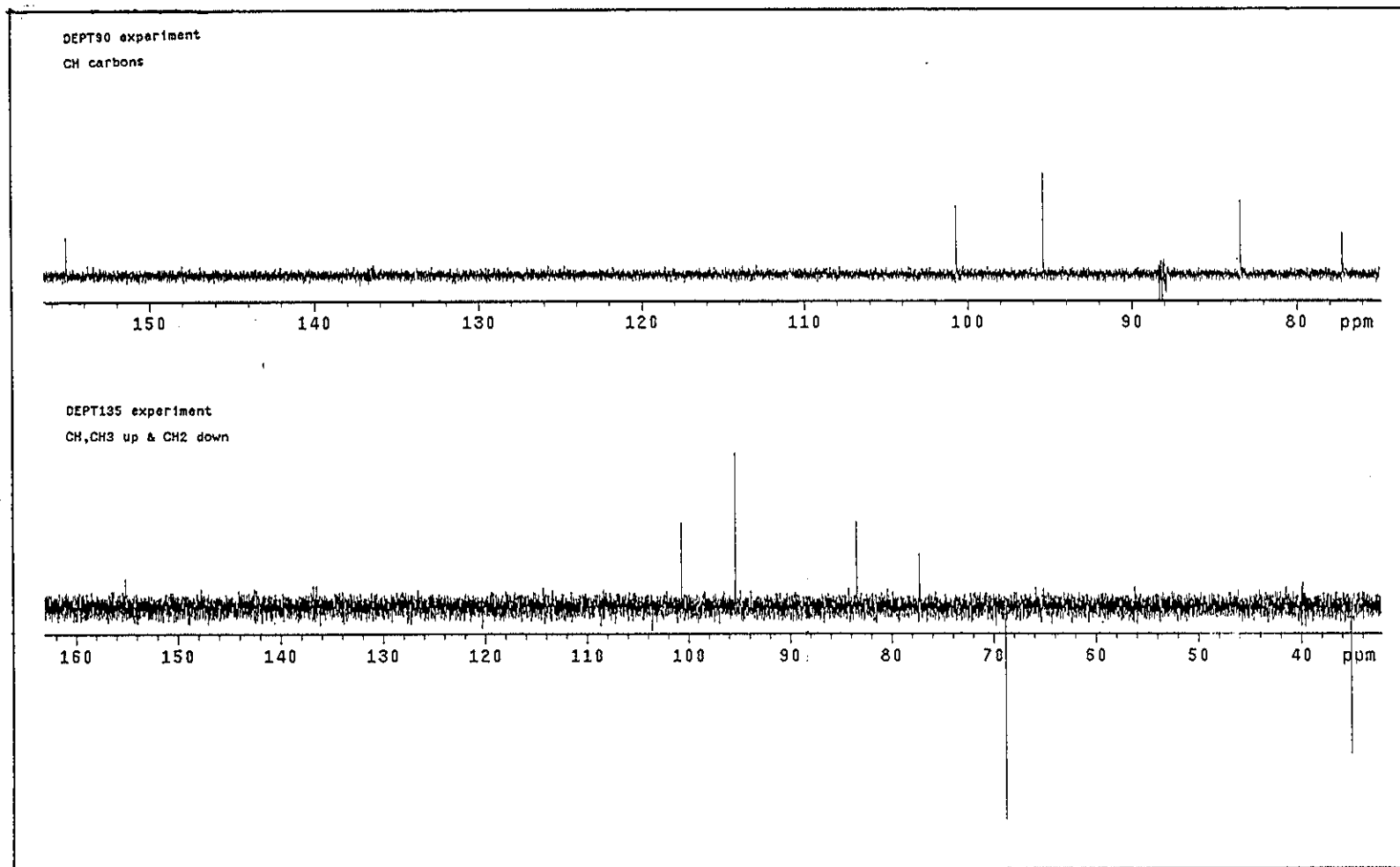


Figure 132 DEPT spectrum of YU13

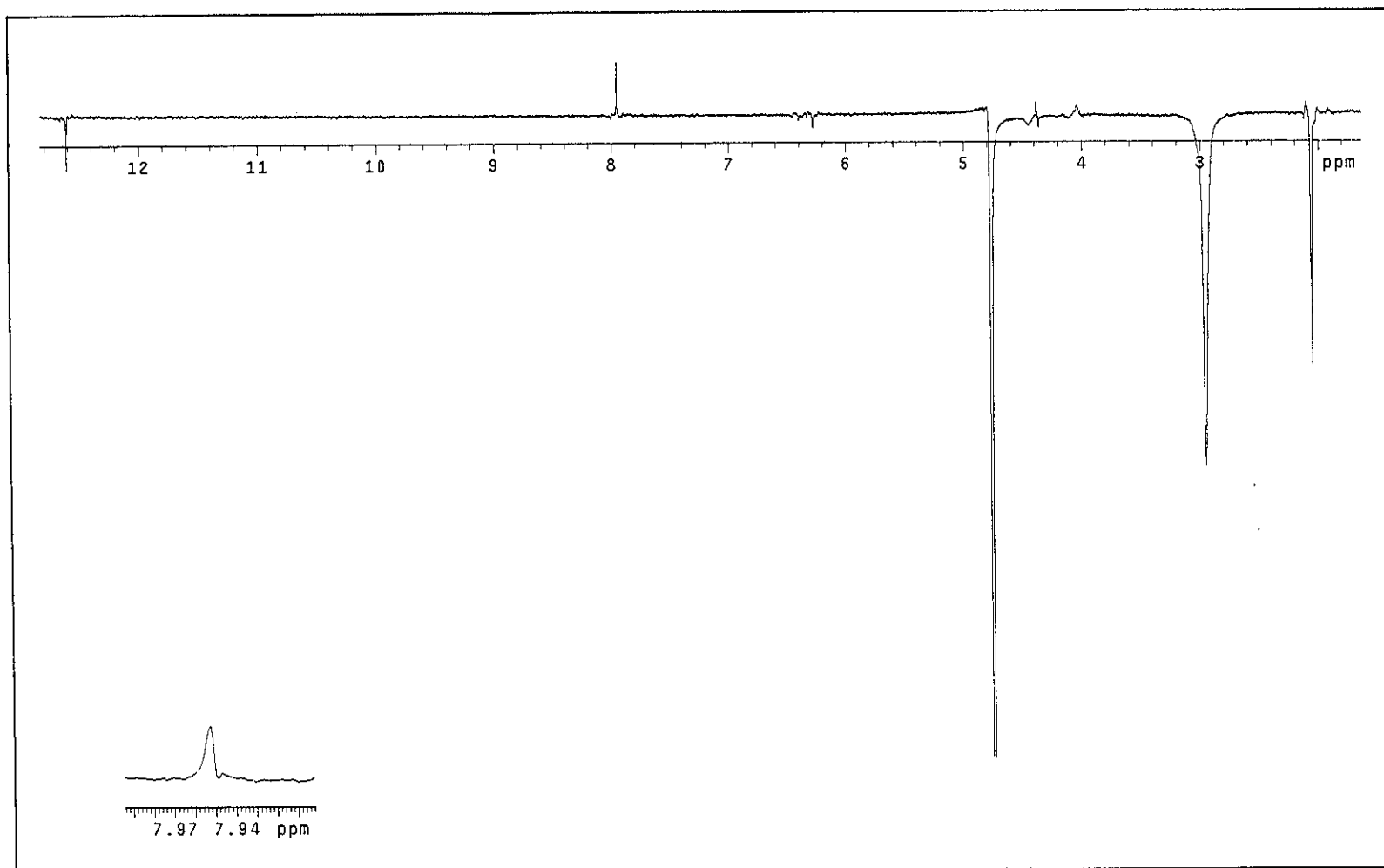


Figure 133 NOEDIFF spectrum of YU13 after irradiation at δ_{H} 4.76

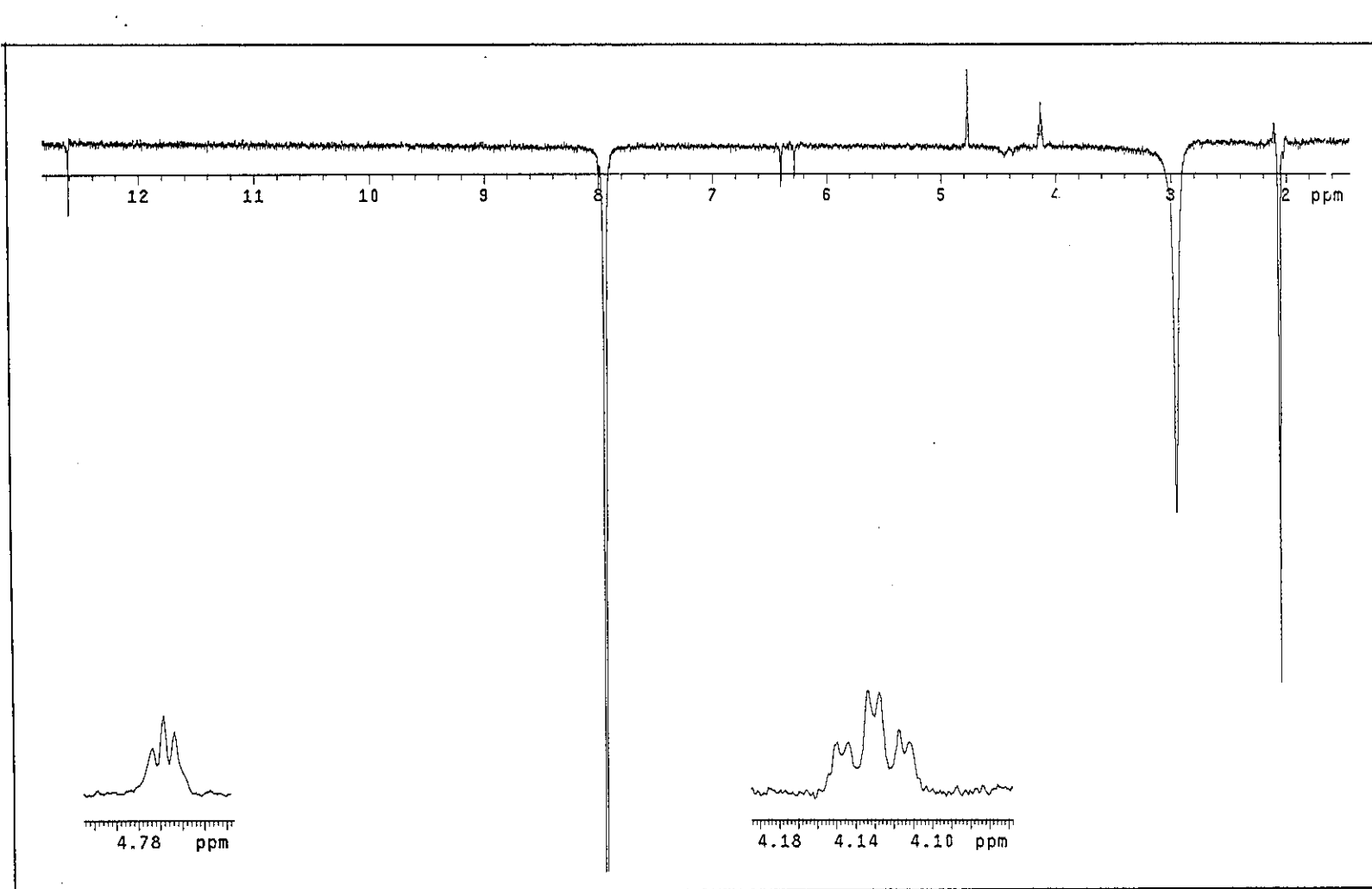


Figure 134 NOEDIFF spectrum of YU13 after irradiation at δ_{H} 7.95

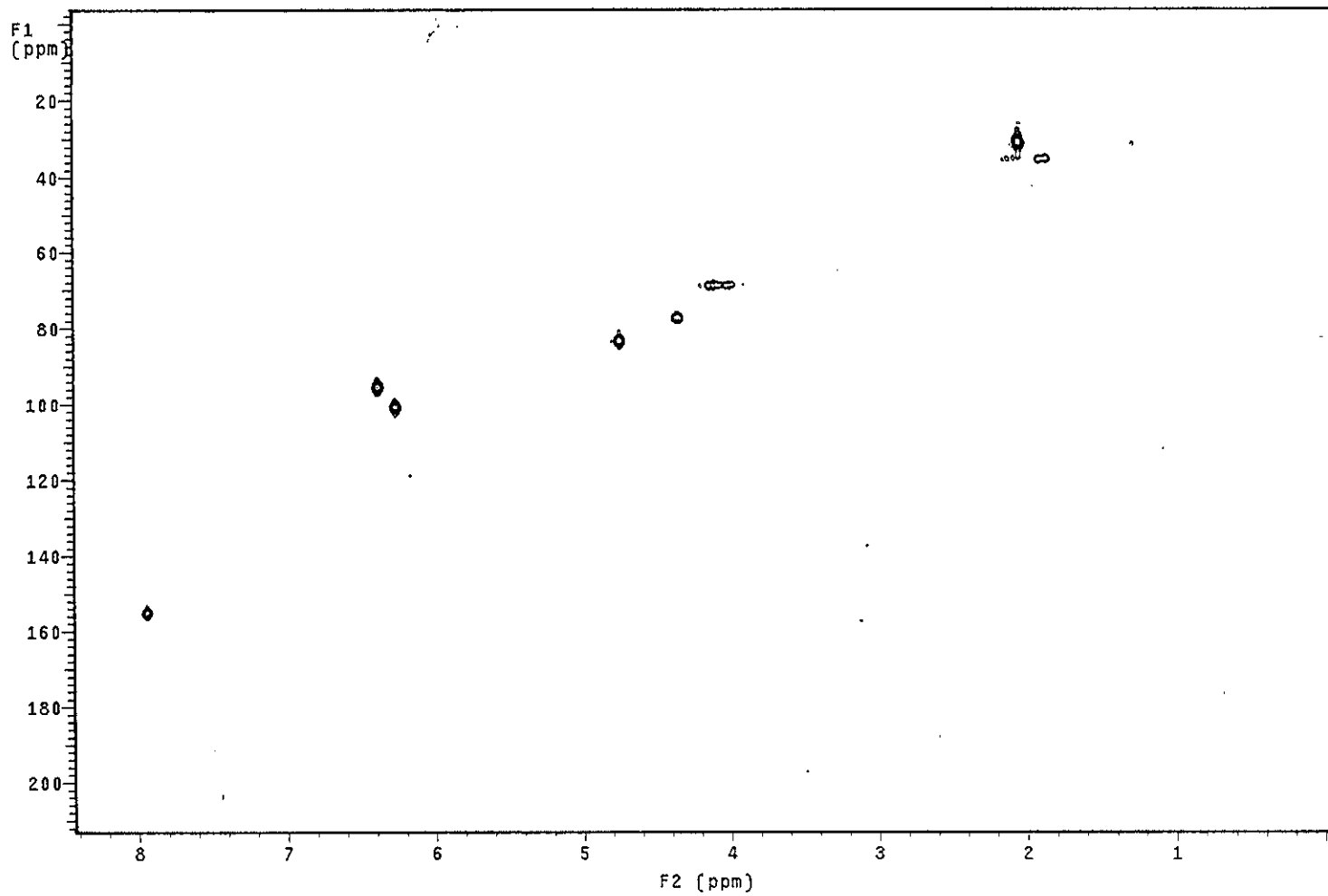


Figure 135 2D HMQC spectrum of YU13

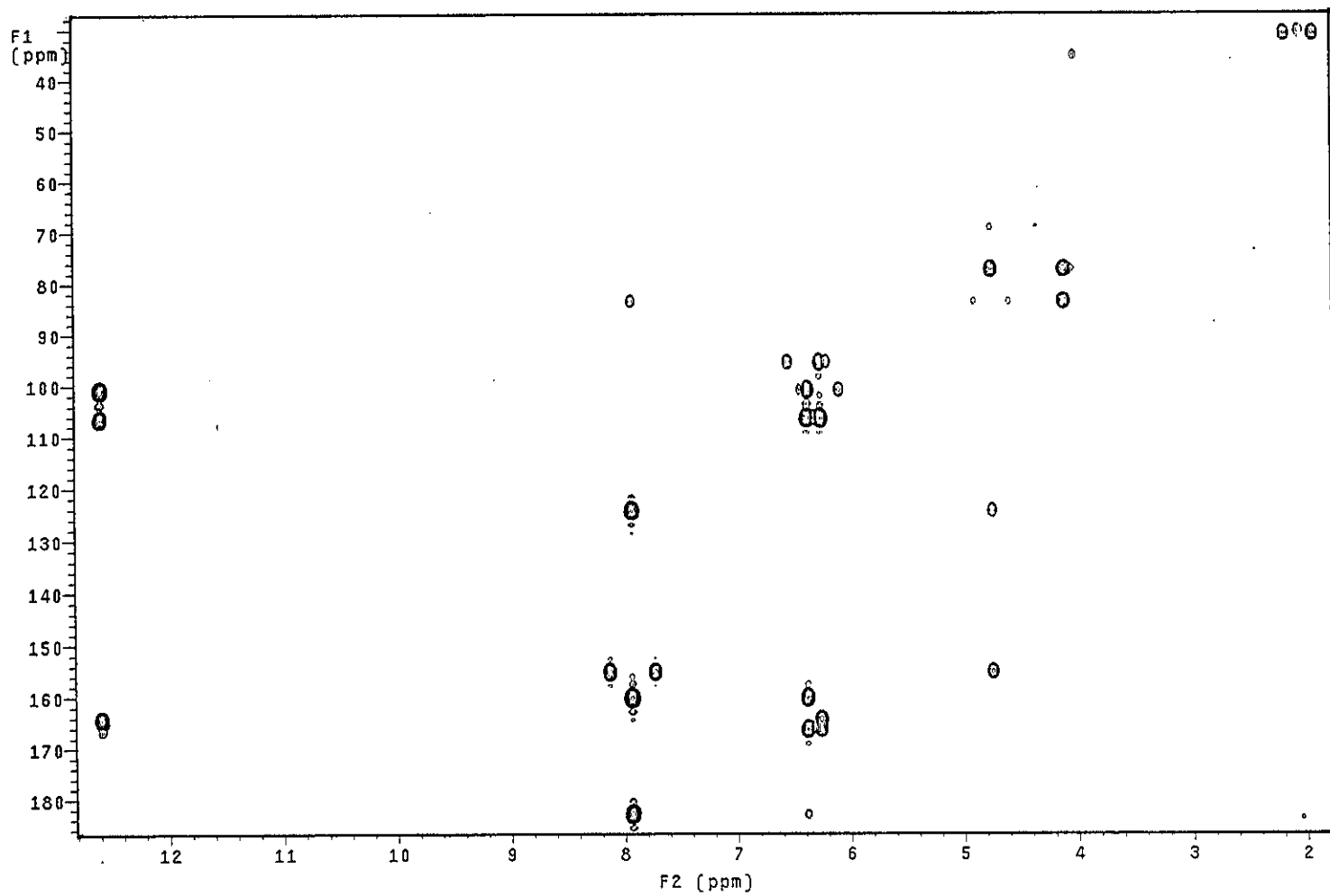


Figure 136 2D HMBC spectrum of YU13

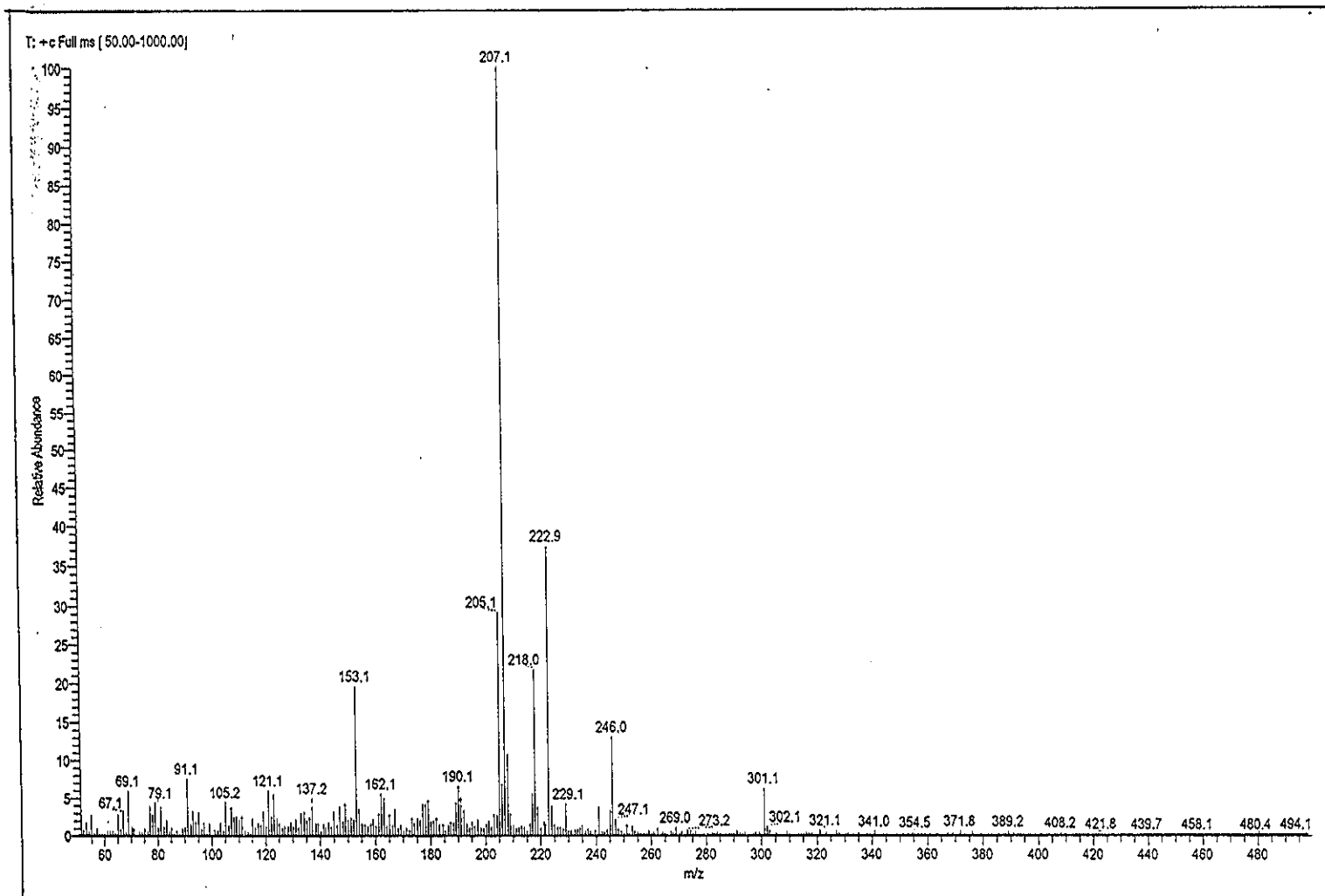


Figure 137 Mass spectrum of YU13

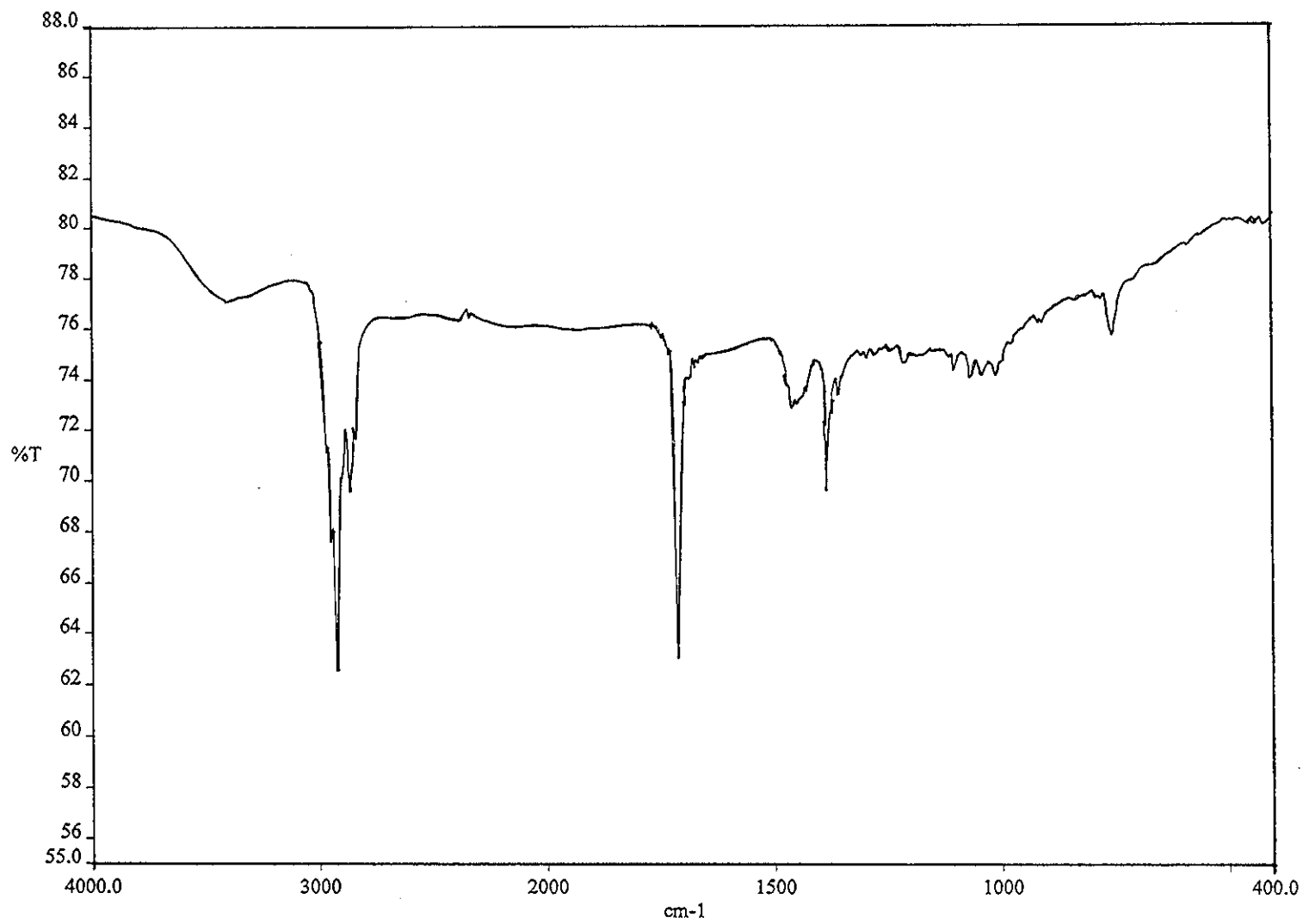


Figure 138 FT-IR (neat) spectrum of YU8

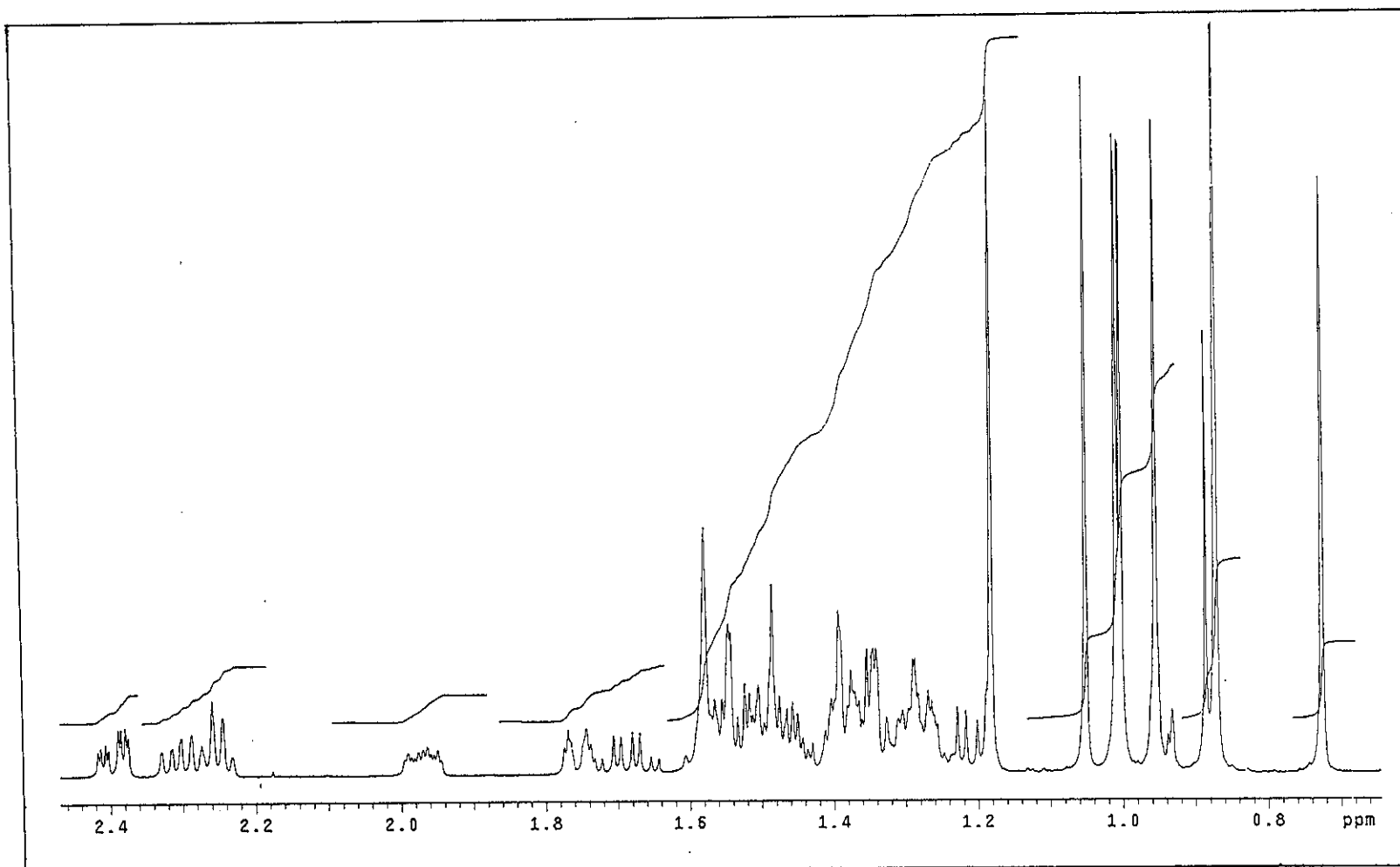


Figure 139 ^1H NMR (500 MHz) (CDCl_3) spectrum of YU8

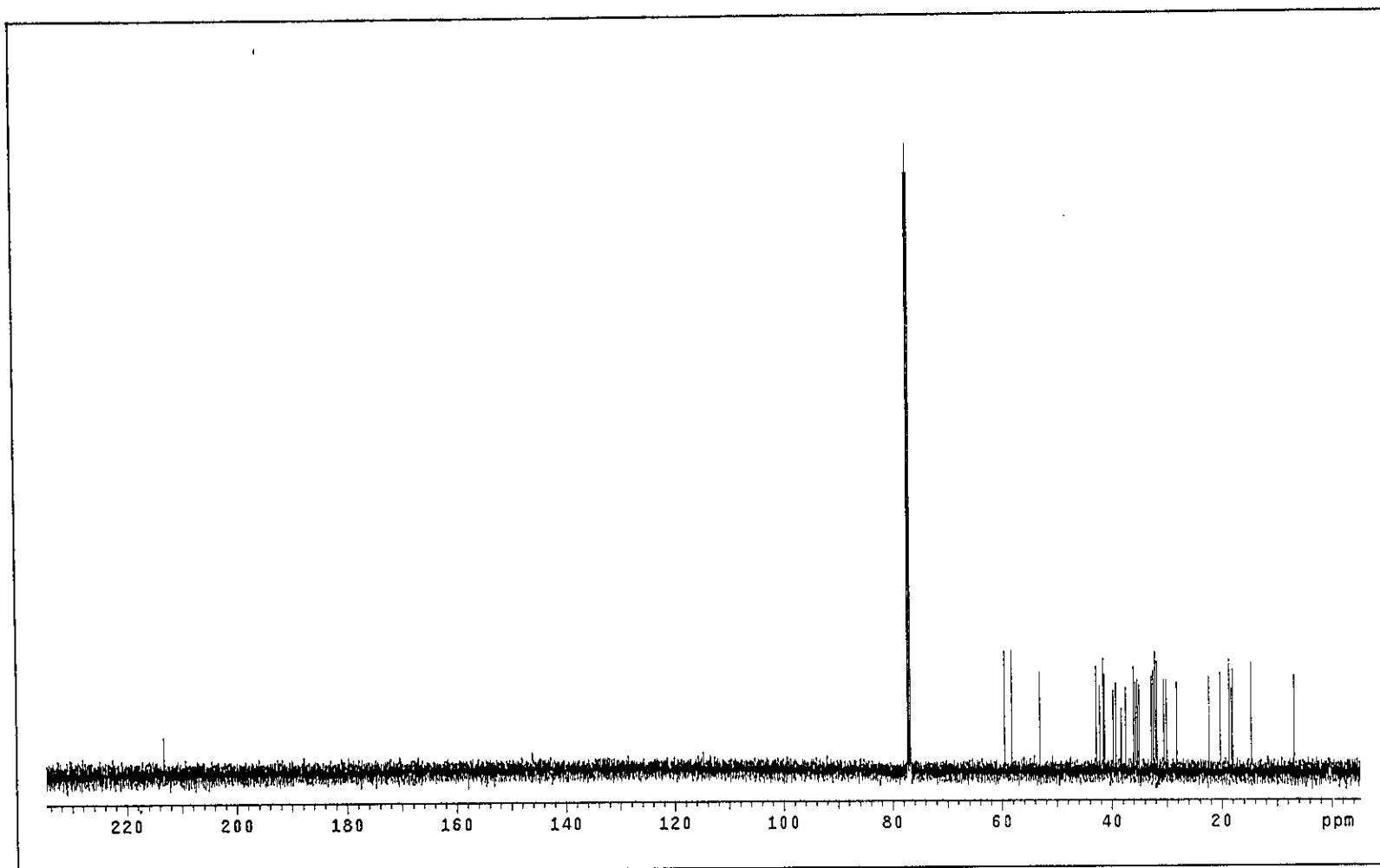


Figure 140 ^{13}C NMR (125 MHz) (CDCl_3) spectrum of YU8

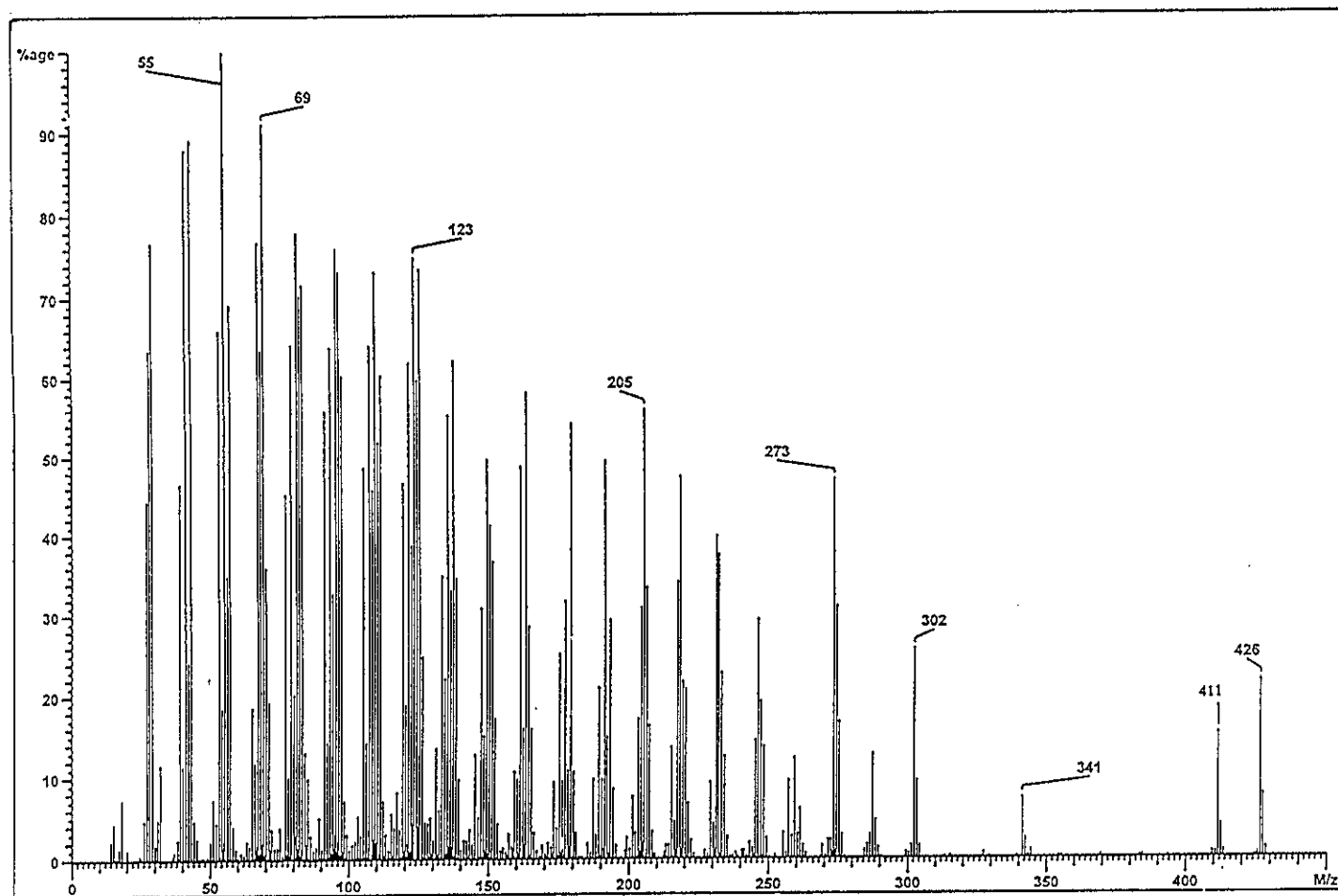


Figure 141 Mass spectrum of YU8

BIBLIOGRAPHY

- เต็ม สมิตินันท์. 2523. “ชื่อพันธุ์ไม้แห่งประเทศไทย (ชื่อพฤกษศาสตร์-ชื่อพื้นเมือง)”, กรมป่าไม้ กรุงเทพฯ : พันธุ์พลับพลึงชิง.
- Ali, S., Goundar, R., Sotheeswaran, S., Beaulieu, C. and Spino, C. 2000. “Benzophenones of *Garcinia pseudoguttifera* (Clusiaceae)”, *Phytochemistry*. 53, 281-284.
- Bayma, J. C., Arruda, M. S. P. and Neto, M. S. 1998. “A prenylated xanthone from the bark of *Symphonia globulifera*”, *Phytochemistry*. 49(4), 1159-1160.
- Bilia, A. R., Yusuf, A. W., Braca, A., Keita, A. and Morelli, I. 2000. “New Prenylated anthraquinones and xanthenes from *Vismia guineensis*”, *J. Nat. Prod.* 63, 16-21.
- Cao, S-G., Wu, X-H., Sim, K-Y., Tan, B. K. H., Pereira, J. T., Wong, W. H., Hew, N. F. and Goh, S. H. 1998a. “Cytotoxic caged tetraprenylated xanthonoids from *Garcinia gaudichaudii* (Guttiferae)”, *Tetrahedron Lett.* 39, 3353-3356.
- Cao, S-G., Sng, H. L. V., Wu, X-H., Sim, K. Y., Tan, B. K. H., Pereira, J. T. and Goh, S. H. 1998b. “Novel cytotoxic polyprenylated xanthonoids from *Garcinia gaudichaudii* (Guttiferae)”, *Tetrahedron*. 54(36), 10915-10924.
- Chairungrilerd, N., Takeuchi, K., Ohizumi, Y., Nozoe, S. and Ohta, T. 1996. “Mangostanol, a prenyl xanthone from *Garcinia mangostana*.”, *Phytochemistry*. 43(5), 1099-1102.

- Chung, M-I., Weng, J-R., Lai, M-H., Yen, M-H. and Lin, C-N. 1999. "A new chalcone, xanthenes, and a xanthonolignoid from *Hypericum geminiflorum*", *J. Nat. Prod.* 62, 1033-1035.
- Cortez, D. A. G., Young, M. C. M., Marston, A., Wolfender, J-L. and Hostettmann, K. 1998. "Xanthenes, triterpenes and a biphenyl from *Kielmeyera coriacea*", *Phytochemistry.* 47(7), 1367-1374.
- Cuesta Rubio, O., Padron, A., Velez Castro, H., Pizza, C. and Rastrelli, L. 2001. "Aristophenones A and B. A new tautomeric pair of polyisoprenylated benzophenones from *Garcinia aristata*", *J. Nat. Prod.* 64(7), 973-975.
- Dharmaratne, H. R. W. and Wanigasekera, W. M. A. P. 1996. "Xanthenes from root bark of *Calophyllum thwaitesii*", *Phytochemistry.* 42(1), 249-250.
- Fukuyama, Y., Kaneshi, A., Tani, N. and Kodama, M. 1993. "Subellinone, a polyisoprenylated phloroglucinol derivative from *Garcinia subelliptica*", *Phytochemistry.* 33(2), 483-485.
- Goh, S. H., Jantan, I., Gray, A. I. and Waterman, P. G. 1992. "Prenylated xanthenes from *Garcinia opaca*", *Phytochemistry.* 31(4), 1383-1386.
- Gonda, R., Takeda, T. and Akiyama, T. 2000. "Studies on the constituents of *Anaxagorea luzonensis* A. GRAY", *Chem. Pharm. Bull.* 48(8), 1219-1222.

- Gopalakrishnan, G., Banumathi, B. and Suresh, G. 1997. "Evaluation of the antifungal activity of natural xanthenes from *Garcinia mangostana* and their synthetic derivatives", *J. Nat. Prod.* 60(5), 519-524.
- Govindachari, T. R., Kalyanaraman, P. S., Muthukumaraswamy, N. and Pai, B. R. 1971. "Xanthenes of *Garcinia mangostana* Linn." *Tetrahedron.* 27, 3919-3926.
- Groweiss, A., Cardellina, J. H. and Boyd, M. R. 2000. "HIV-inhibitory prenylated xanthenes and flavones from *Maclura tinctoria*", *J. Nat. Prod.* 63, 1537-1539.
- Gunatilaka, A. A. L., Sriyani, H. T. B., Sotheeswaran, S. and Waight, E. S. 1983. "2,5-dihydroxy-1,6-dimethoxyxanthone and biflavonoids of *Garcinia thwaitesii*", *Phytochemistry.* 22(1), 233-235.
- Gustafson, K. R., Blunt, J. W., Munro, M. H. G., Fuller, R. W., McKee, T. C., Cardellina II, J. H., McMahon, J. B., Cragg, M. C. and Boyd, M. R. 1992. "The guttiferones, HIV-inhibitory benzophenones from *Symphonia globulifera*, *Garcinia livingstonei*, *Garcinia ovalifolia* and *Clusia rosea*", *Tetrahedron.* 48(46), 10093-10102.
- Hou, A-J., Fukai, T., Shimazaki, M., Sakagami, H., Sun, H-D. and Nomura, T. 2001. "Benzophenones and xanthenes with isoprenoid groups from *Cudrania cochinchinensis*", *J. Nat. Prod.* 64, 65-70.
- Huang, Y-L., Chen, C-C., Chen, Y-J., Huang, R-L. and Shieh, B-J. 2001. "Three xanthenes and a benzophenone from *Garcinia mangostana*, *J. Nat. Prod.* 64(7), 903-906.

- Ilyas, M., Kamil, M., Parveen, M. and Khan, M. S. 1994. "Isoflavones from *Garcinia nervosa*", *Phytochemistry*. 36(3), 807-809.
- Iinuma, M., Tosa, H., Tanaka, T. and Riswant, S., 1996a. "Two furanoxanthones from *Mammea acuminata*", *Phytochemistry*. 42(1), 245-247.
- Iinuma, M., Tosa, H. Ito, T., Tanaka, T. and Madulid, D. A. 1996b. " Two xanthones from roots of *Cratoxylum formosanum*", *Phytochemistry*. 42(4), 1195-1198.
- Iinuma, M., Tosa, H., Ito, T., Tanaka, T. and Riswan, S. 1996c. "Three new benzophenone-xanthone dimers from the root of *Garcinia dulcis*", *Chem. Pharm. Bull.* 44(9), 1744-1747.
- Iinuma, M., Tosa, H., Ito, T., Tanaka, T. and Riswan, S. 1996d. "Garciduols A and B, new benzophenone-xanthone dimers, from *Garcinia dulcis*", *Heterocycles*. 43 (3), 535-538.
- Iinuma, M., Tosa, H., Tanaka, T. and Riswan, S. 1996e. "Three new xanthones from the bark of *Garcinia dioica*", *Chem Pharm. Bull.* 44(1), 232-234.
- Iinuma, M., Tosa, H., Tanaka, T., Kanamaru, S., Asai, F., Kobayashi, Y., Miyauchi, K. and Shimano, R. 1996f. "Antibacterial activity of some *Garcinia* benzophenone derivatives against Methicillin-Resistant *Staphylococcus aureus*", *Bio. Pharm. Bull.* 19(2), 311-314.

- Iinuma, M., Ito, T., Tosa, H. Tanaka, T. Miyake, R. and Chelladurai, V. 1997. "Prenylated xanthonoids from *Calophyllum apetalum*", *Phytochemistry*. 46(8), 1423-1429.
- Ito, C., Miyamoto, Y., Nakayama, M., Kawai, Y., Rao, K.S and Furukawa, H. 1997. "A novel depsidone and some new xanthenes from *Garcinia Species*", *Chem. Pharm. Bull.* 45(9), 1403-1413.
- Ito, C., Itoigawa, M., Furukawa, H., Rao, K. S., Enjo, F., Bu, P., Takayasu, J., Tokuda, H. and Nishino, H. 1998. "Xanthenes as inhibitors of Epstein-Barr virus activation", *Cancer letters*. 132, 113-117.
- Ito, C., Mishina, Y., Litaudon, M., Cosson, J-P. and Furukawa, H. 2000. "Xanthone and dihydroisocoumarin from *Montrouzierra sphaeroidea*", *Phytochemistry*. 53, 1043-1046.
- Ito, C., Itoigawa, M., Mishina, Y., Filho, V. C., Mukainaka, T. Tokuda, H., Nishino, H. and Furukawa, H. 2002. "Chemical constituents of *Calophyllum brasiliensis*: structure elucidation of seven new xanthenes and their cancer chemopreventive activity", *J. Nat. Prod.* 65, 267-272.
- Kaewnok, W. 2000. "Chemical constituents from twigs of *Garcinia scortechinii*", M. Sc. Thesis. Prince of Songkla University, Thailand.
- Kijjoa, A., José, M., Gonzalez, T. G., Pinto, M. M. M., Damas, A. M., Mondranondra, I., Silva, A, M. S., and Herz, W. 1998. "Xanthenes from *Cratoxylum maingayi*", *Phytochemistry*. 49(7), 2159-2162.

- Kijjoo, A., Gonzalez, M. J., Afonso, C. M., Pinto, M. M. M., Anantackoke, C. and Herz, W. 2000a. "Xanthonenes from *Calophyllum teysmannii* var. *inophylloide*", *Phytochemistry*. 53, 1021-1024.
- Kijjoo, A., Gonzalez, M. J., Pinto, M. M. M., Silva, A. M. S., Anantachoke, C. and Herz, W. 2000b. "Xanthonenes from *Calophyllum teysmannii* var. *inophylloide*", *Phytochemistry*. 55, 833-836.
- Kosela, S., Hu, L-H., Yip, S-C., Rachmatia, T., Sukri, T., Daulay, T. S., Tan, G-K., Vittial, J.J. and Sim, K-Y. 1999. "Dulxanthone E: a pyranoxanthone from leaves of *Garcinia dulcis*", *Phytochemistry*. 52, 1375-1377.
- Kosela, S., Hu, L-H., Rachmatia, T., Hanafi, M. and Sim, K-Y. 2000. "Dulxanthonenes F-H, three new pyranoxanthonenes from *Garcinia dulcis*", *J. Nat. Prod.* 63(3), 406-407.
- Li, W., Chan, C-L., Leung, H-W., Yeung, H-W. and Xiao, P. 1999. "Xanthonenes from *Polygala caudata*", *Phytochemistry*. 51, 953-958.
- Likhitwitayawuid, K., Phadungcharoen, T. and Krungkrai, J. 1998a. "Antimalarial xanthonenes from *Garcinia cowa*", *Planta Medica*. 64(1), 70-72.
- Likhitwitayawuid, K., Chanmahasathien, W., Ruangrunsi, N. and Krungkrai, J. 1998b. "Xanthonenes with antimalarial activity from *Garcinia dulcis*", *Planta Medica*. 64 (3), 281-282.

- Lin, Y-M., Anderson, H., Flavin, M.T., Pai, Y-H. S., Mata-Greenwood, E., Pengsuparp, T., Pezzuto, M.J., Schinazi, R. F., Hughes, S. H. and Chen, F-C. 1997. "In vitro anti-HIV activity of biflavonoids isolated from *Rhus succedanea* and *Garcinia multiflora*", *J. Nat. Prod.* 60(9), 884-888.
- Mahabusarakam, W. and Wiriyaচিত্রা, P. 1987. "Chemical constituents of *Garcinia mangostana*", *J. Nat. Prod.* 50(3), 474-478.
- Minami, H., Kuwayama, A., Yoshizawa, T. and Fukuyama, Y. 1996. "Novel prenylated xanthenes with antioxidant property from the wood of *Garcinia subelliptica*", *Chem. Pharm. Bull.* 44(11), 2103-2106.
- Miyase, T., Noguchi, H. and Chen, X-M. 1999. "Sucrose esters and xanthone C-glycosides from the roots of *Polygala sibirica*", *J. Nat. Prod.* 62, 993-996.
- Monte, F. J. Q., Soares, F. P. and Braz-Filho, R. 2001. "A xanthone from *Shultesia guianensis*", *Fitoterapia.* 72, 715-716.
- Morel, C., Séraphin, D., Oger, J-M. Litaudon, M., Sévenet, T., Richomme, P. and Bruneton, J. 2000. "New xanthenes from *Calophyllum caledonicum*", *J. Nat. Prod.* 63, 1471-1474.
- Naito, T., Niitsu, K., Ikeya, Y., Okada, M. and Mitsuhashi, H. 1992. "A phthalide and 2-farnesyl-6-methyl benzoquinone from *Ligusticum chuangxiong*", *Phytochemistry.* 31(5), 1787-1789.

- Nilar and Harrison, L. J. 2002. "Xanthenes from the heartwood of *Garcinia mangostana*" *Phytochemistry*. 60, 541-548.
- Nguyen, L. H. D. and Harrison, L. J. 1998. "Triterpenoid and xanthone constituents of *Cratoxylum cochinchinense*", *Phytochemistry*. 50, 471-476.
- Nguyen, L. H. D. and Harrison, L. J. 2000. "Xanthenes and triterpenoids from the bark of *Garcinia vilersiana*", *Phytochemistry*. 53, 111-114.
- Nkengfack, A. E., Azebaze, G. A., Vardamides, J. C., Fomum, Z. T. and Heerden, F. R. 2002a. "A prenylated xanthone from *Allanblackia floribunda*", *Phytochemistry*. 60(4), 381-384.
- Nkengfack, A. E., Mkounga, P., Fomum, Z. T., Meyer, M. and Bodo, B. 2002b. "Globulixanthenes A and B, two new cytotoxic xanthenes with isoprenoid groups from the root bark of *Symphonia globulifera*", *J. Nat. Prod.* 65, 734-736.
- Nyemba, A-M., Mpondo, T. N., Connolly, J. D. and Rycroft, D. S. 1990. "Cycloartane derivatives from *Garcinia lucida*", *Phytochemistry*. 29(3), 994-997.
- Panthong, K. 1999. "Investigations of Bioactive Compounds from *Callophyllum teysmannii* var. *inophylloide* (Guttiferae), *Ventilago harmandiana* (Rhamnaceae) and *Anogeissus acuminata* var. *lanceolata* (Combretaceae)", Ph.D. Dissertation. Mahidol University, Thailand.
- Parveen, M., Khan, N. U., Achari, B. and Dutta, P. K. 1991. "A triterpene from *Garcinia mangostana*", *Phytochemistry*. 30(1), 361-362.

- Peres, V. and Nagem, T. J. 1997. "Trioxygenated naturally occurring xanthenes", *Phytochemistry*. 44(2), 191-214.
- Peres, V., Nagem, T. J. and Oliveira, F. F. 2000. "Tetraoxygenated naturally occurring xanthenes", *Phytochemistry*. 55, 683-710.
- Permana, D., Lajis, N. H., MacKeen, M. M., Ali, A. M., Aimi, N., Kitajima, M. and Takayama, H. 2001. "Isolation and bioactivities of constituents of the roots of *Garcinia atroviridis*", *J. Nat. Prod.* 64(7), 976-979.
- Pinheiro, T. R., Filho, V. C., Santos, A. R. S., Calixto, J. B., Monache, F. D., Pizzola, M. G. and Yunes, R. A. 1998. "Three xanthenes from *Polygala cyparissias*", *Phytochemistry*. 48(4), 725-728.
- Poobrasert, O., Constant, H. L., Beecher, C. W. W., Farnsworth, N. R., Kinghorn, A. D., Pezzuto, J. M., Cordell, G. A., Santisuk, T. and Reutrakul, V. 1998. "Xanthenes from the twigs of *Mammea siamensis*" *Phytochemistry*. 47(8), 1661-1663.
- Rath, G., Potterat, O., Mavi, S. and Hostettmann, K. 1996. "Xanthenes from *Hypericum roeperanum*", *Phytochemistry*,. 43(2), 513-520.
- Ritthiwigrom, T. 2002. "Xanthenes from the stem bark of *Garcinia nigrolineata*", M. Sc. Thesis. Prince of Songkla University, Thailand.
- Rukachaisirikul, V., Kaewnok, W., Koysomboon, S., Phongpaichit, S. and Taylor, W. C. 2000a. "Caged-tetraprenylated xanthenes from *Garcinia scortechinii*", *Tetrahedron*. 56, 8539-8543.

- Rukachaisirikul, V., Adiar, A., Dampawan, P., Taylor, W. C. and Turner, P. C. 2000b. "Lanostanes and friedolanostanes from the pericarp of *Garcinia hombroniana*", *Phytochemistry*. 55, 183-188.
- Sen, A. K., Sarkar, K. K., Majumder, P. C. and Banerji, N. 1981. "Minor xanthenes of *Garcinia mangostana*", *Phytochemistry*. 20, 183-185.
- Seo, E-K., Wall, M. E., Wani, M. C., Navarro, H., Mukherjee, R., Farnsworth, N. R. and Kinghorn, A. D. 1999. "Cytotoxic constituents from the roots of *Tovomita brevistaminea*", *Phytochemistry*. 52, 669-674.
- Seo, E-K., Kim, N-C., Wani, M. C., Wall, M. E., Navarro, H. A., Burgess, J. P., Kawanishi, K., Kardono, L. B. S., Riswan, S., Rose, W. C., Fairchild, C. R., Farnsworth, N. R. and Kinghorn, A. D. 2002. "Cytotoxic prenylated xanthenes and the unusual compounds anthraquinobenzophenones from *Cratoxylum sumatranum*", *J. Nat. Prod.* 65, 299-305.
- Spino, C., Lal, J., Sotheeswaran, S. and Aalbersberg, W. 1995. "Three prenylated phenolic benzophenones from *Garcinia myrtifolia*", *Phytochemistry*. 38(1), 233-236.
- Suksamrarn, S., Suwannapoch, N., Ratananukul, P., Aroonlerk, N., Suksamrarn, A. 2002. "Xanthenes from three fruit hulls of *Garcinia mangostana*", *J. Nat. Prod.* 65(5), 761-763.
- Thoison, O., Fahy, J., Dumontet, V., Chiaroni, A., Riche, C., Tri, M.V. and Sevenet, T. 2000. "Cytotoxic prenylxanthenes from *Garcinia bracteata*", *J. Nat. Prod.* 63(4), 441-446.

- Tosa, H. Iinuma, M., Murakami, K-I., Ito, T., Tanaka, T., Chelladurai, V. and Riswan, S. 1997. "Three xanthenes from *Poeciloneuron pauciflorum* and *Mammea acuminata*", *Phytochemistry*. 45(1), 133-136.
- Whitmore, M.A. 1973. "*Tree Flora of Malaya*", Malasia: Forest Department Ministry of Primary Industries, Longman, 218.
- Wu, Q-L., Wang, S-P., Du, L-J., Yang, J-S. and Xiao, P-G. 1998. "Xanthenes from *Hypericum japonicum* and *H. henryi*", *Phytochemistry*. 49(5), 1395-1402.
- Xu, Y-J., Chiang, P-Y., Lai, Y-H., Vittal, J. J., Wu, X-H., Tan, B. K. H., Imiyabir, Z. and Goh, S-H. 2000. "Cytotoxic prenylated depsidones from *Garcinia parvifolia*", *J. Nat. Prod.* 63(10), 1361-1363.
- Yang, X-D., Xu, L-Z. and Yang, S-L. 2001. "Xanthenes from the stems of *Securidaca inappendiculata*", *Phytochemistry*. 58, 1245-1249.
- Zhang, Z., Elsohly, H. N., Jacob, M. R., Pasco, D. S., Walker, L. A. and Clark, A. M. 2002. "Natural products inhibiting *Candida albicans* secreted aspartic proteases from *Tovomita krukovii*", *Planta Med.* 68, 49-54.

VITAE

Name Miss Mayuree Kamkaew

Birth Date 1 June 1977

Place of Birth Ang-Thong, Thailand

Educational Attainment

Degree	Name of Institution	Year of Graduation
Bachelor of Science (Chemistry)	Prince of Songkla University	1996-2000
Master of Science (Organic Chemistry)	Prince of Songkla University	2000-2002

Scholarship Awards during Enrolment

1. The partail support from Higher Education Development Project: Postgraduate Education and Research Program in Chemistry, funded by The Royal Thai Government.